

ResearchOnline@JCU

This file is part of the following reference:

Ryan, Emma Jean (2016) *Fringing reef growth on the central Great Barrier Reef: signatures of sea-level change, storms and sedimentation*. PhD thesis, James Cook University.

Access to this file is available from:

<http://researchonline.jcu.edu.au/46598/>

The author has certified to JCU that they have made a reasonable effort to gain permission and acknowledge the owner of any third party copyright material included in this document. If you believe that this is not the case, please contact

*ResearchOnline@jcu.edu.au and quote
<http://researchonline.jcu.edu.au/46598/>*

**Fringing Reef Growth on the Central Great
Barrier Reef: Signatures of Sea-level Change,
Storms and Sedimentation**

**Thesis submitted by
Emma Jean Ryan B.Sc. (Hons), M.Sc.**

**In March 2016
For the degree of Doctor of Philosophy
In the College of Marine and Environmental Sciences
James Cook University**

Statement of the Contribution of Others

Financial support

- National Environmental Research Program (Project 1.3 ‘Characterising the cumulative impacts of global, regional and local stressors on the present and past biodiversity of the Great Barrier Reef)
(Doctorate stipend, analytical and field support)
- Graduate Research School, James Cook University
(Post-graduate Research Scheme, field support)
- College of Marine and Environmental Sciences (formerly the School of Earth and Environmental Sciences), James Cook University
(Post-graduate Research Scheme, field support)
- Australian Institute of Nuclear Science and Engineering
(Research Award to Stephen Lewis, analytical support)
- Great Barrier Reef Marine Park Authority (GBRMPA)
(Science for Management Award, field support)

Thesis Committee

- Assoc. Prof. Scott Smithers, College of Marine and Environmental Sciences, James Cook University
- Dr. Stephen Lewis, The Centre for Tropical Water and Aquatic Ecosystem Research, James Cook University

Data collection/analysis

- Research Vessel James Kirby (field support)
- Volunteer field and laboratory helpers
- Dr. Tara Clark, Prof. Jian-xin Zhao and others, The Radiogenic Isotope Facility, The University of Queensland (analytical support)
- Dr. Christa Placzek, Advanced Analytical Centre, James Cook University (analytical support)
- Dr. Quan Hua, Australian Nuclear Science and Technology Organisation (analytical support)

Intellectual support

- Assoc. Prof. Scott Smithers, Dr. Stephen Lewis
- Dr. Tara Clark and Kimmie Riskas (editorial support)

Permits

- All field work was undertaken in accordance with GBRMPA permit number G12/34974.1 (granted to Prof. Jian-xin Zhao and Prof. John Pandolfi)

Inclusion of Published Papers in this Thesis

Chapter 2: Ryan, E.J., Smithers, S.G., Lewis, S.E., Clark, T.R. and Zhao, J.X. 2016 Chronostratigraphy of Bramston Reef reveals a long-term record of fringing reef growth under muddy conditions in the central Great Barrier Reef, *Palaeogeography, Palaeoclimatology, Palaeoecology*, 441: 734-747.

Chapter 4: Ryan, E.J., Smithers, S.G., Lewis, S.E., Clark, T.R. and Zhao, J.X. 2016 The influence of sea level and cyclones on Holocene reef flat development: Middle Island, central Great Barrier Reef, *Coral Reefs*, DOI 10.1007/s00338-016-1453-9.

Inclusion of Manuscripts ‘In Review’ in this Thesis

Chapter 3: Ryan, E.J., Lewis, S.E., Smithers, S.G., Clark, T.R. and Zhao, J.X. Multi-scale records of reef development and condition provide context for contemporary changes on inshore reefs, *Global and Planetary Change*, in review.

The nature and extent of the intellectual input of each author, including the candidate: (applies to all published or ‘in review’ manuscripts)

The authors co-developed the research questions. Ryan collected the data with assistance from Smithers and Lewis. Ryan conducted the majority of analytical work, with assistance from Clark and Zhao in U-Th dating. Ryan wrote the manuscripts with editorial revisions from Smithers, Lewis and Clark. Ryan developed all figures and tables.

Acknowledgements

To my wonderful supervisors Scott and Steve, thank you for all the profound advice, support and encouragement that you have given me. Thank you for being so welcoming and for patiently teaching me so much about coral reef geomorphology. I am particularly grateful for the amount of time you gave up to help me with field work and to read many drafts of my thesis chapters, including so many public holidays and weekends. I feel very fortunate to have had such excellent supervisors and have thoroughly enjoyed working with you both.

Staff and students at the Radiogenic Isotope Facility were invaluable to this project. In particular I would like to express my gratitude to Dr. Tara Clark and Prof. Jian-xin Zhao for all their time and support in Brisbane in teaching me the process of U-Th sample preparation and chemistry. Also to Dr. Quan Hua at ANSTO, for carrying out radiocarbon dating. Thanks to the crew of the RV James Kirby and JCU technical staff (Clive Grant, Paul Givney, Rob Scott, Russell Warburton, Ralph Botting and Steve Moore) for your help in organising field trips. A special mention to everyone who willingly volunteered their time to help me in the field: Daniela Waltrick, Dean Thompson, Jamie Johnson, Sarah Ballard, James Daniell, Russel Warburton, Scott Stinson, Seb Hoepker, Alex Heid and Geoff Endo. I was also assisted in the lab occasionally by Daniela Waltrick, Elien Boogaerts, Emma Williams, Seb Hoepker, Kyle Morgan, Jamie Johnson and Jodie Kilpatrick; thank you for your help, company and hard work. I am further grateful to Assoc. Prof. Kevin Parnell for RTK GPS advice and trouble-shooting and to Dr. Christa Placzek for instructions in the clean laboratory at JCU. To the lovely administration ladies in the College of Marine and Environmental Science (formerly the School of Earth and Environmental Sciences), thank you for your support and chats.

To all the friends I have made in sunny Townsville, thanks for the adventures, your friendship and your part in making this an awesome place to live and study. Special thanks to dearest Qian and Kim, with whom I have shared all the highs and lows of PhD life! Thanks for all the laughs in the office Kim.

A huge thank you to Mum, Dad, Sophie, Sarah and my extended family who have encouraged me and supported me in so many ways, including coming to visit me so often. Despite missing you all so much, your support has meant a lot. Last but not least, to my partner Dean, thank you so much for making the move over the ditch to support me. Your endless patience, care and love have made this journey considerably more enjoyable and fun.

Abstract

Coral reefs globally are impacted by a range of natural and anthropogenic stressors. Inshore reefs on Australia's Great Barrier Reef (GBR) are widely argued as degraded following a decline in coral cover and diversity over the past few decades. Inshore reefs are located between the 20 m isobath and the coast, where they are exposed to a variety of natural stressors, including high turbidity and/or sedimentation, as well as episodic cyclones and associated freshwater flood events. The impacts of these natural stressors may have been amplified by anthropogenic factors since European settlement of coastal catchments along the GBR, both directly as a result of activities such as modified land use within the catchments, and indirectly via the effects of human-induced global climate change. Anthropogenic factors are commonly implicated as drivers of recent ecological changes on inshore reefs, though isolating the various effects of natural and anthropogenic stressors remains difficult and poorly understood, partly due to a paucity of long-term data on baseline reef condition and variability prior to European settlement. Long-term records from coral reefs have great potential to address this deficit, and to detail past variability in reef growth and ecology to improve our understanding of present and future reef condition. However, such records are rare.

The main aim of this research was to investigate in detail the Holocene development of fringing reefs over a cross-shelf transect in the central GBR, as baseline context for understanding present reef condition. In particular, the objectives of this research were to: 1) determine reef initiation ages and antecedent substrates; 2) reconstruct the chronostratigraphy of the fringing reefs along this transect to establish past rates and styles of reef development and any variability over time, including detailed examinations of the palaeo-ecological coral community compositions; 3) investigate the influence of Holocene sea-level change and cyclones on reef development; 4) describe and quantify the contemporary ecological community composition and structure and determine whether this has changed since European settlement; and 5) investigate Holocene reef development and present reef condition across the shelf, to identify variability and similarities across this gradient, and to examine how such patterns reflect the influence of key environmental parameters. This research focused on fringing reefs at four sites in the central GBR near Bowen that extend across a 40 km gradient from the mainland coast to the mid-shelf. The fringing reefs were located at: a) the mainland-attached Bramston Reef; b) Stone Island, ~3 km further offshore; c) Middle Island, ~10 km offshore; and d) Holbourne Island, ~40 km north of Bramston Reef. These sites were chosen because they provide a unique opportunity to examine Holocene fringing reef development across a mainland to mid-shelf transect within the central GBR where valuable historical records of reef condition are also available that extend back to the end of the 19th Century.

In total, 42 reef cores were collected across the four sites. Sedimentological and palaeo-ecological analyses, coupled with uranium-thorium (U-Th) dating were used to develop chronostratigraphic records of reef growth. In addition, the ages and elevations (measured very precisely using a Real Time Kinematic Global Positioning System) of un-moated fossil *Porites* microatolls were used as a proxy for past sea level and documented the minimum age for reef flat development. Contemporary reef geomorphology and ecological community structure were quantified using a variety of techniques, including precise topographic surveying, underwater videography and photo quadrat surveys.

The chronostratigraphic records of reef growth revealed that all of the reefs examined in this study initiated in the early- to mid-Holocene, between $5,396 \pm 51$ yBP (Bramston Reef) and $7,873 \pm 17$ yBP (Middle Island). Generally, initiation occurred earlier at the further offshore sites, probably as a result of the pre-reefal foundations being flooded earlier during the post-glacial transgression. The reefs established over a variety of substrates, including unconsolidated transgressive sands and gravels (Bramston Reef), compacted regolith (Middle Island), and last interglacial reef (Holbourne Island). The mode of reef development varied subtly between sites and was affected by the shape of the underlying pre-Holocene surface, variations in sedimentation, the degree of exposure to cyclones, and Holocene sea-level instability. All reefs rapidly accreted vertically and began to form a reef flat at sea level within ~1,000 years of initiation, regardless of the reef start-up time. Average rates of vertical reef accretion were highest at the inshore locations (up to 9.5 mm/yr), where the non-framework reef matrix sediments include a high proportion of mud (up to $53.8 \pm 17.4\%$ on average). The high mud content contributed to rapid net reef accretion by burying the reef framework, enhancing coral framework preservation, limiting the impacts of bioerosion and contributing to reef structure volume. Reef flat development began in the mid-Holocene when sea levels were up to 1.0 m higher than present, as recorded by back reef fossil microatolls at Stone Island and Bramston Reef, and accretion continued as sea-level fell and stabilised at the present level. This late-Holocene sea-level fall is reflected in the slowing of reef accretion at most sites after the majority of the reef flat was emplaced. At Stone Island, the reef flat was entirely emplaced by ~5,000 yBP and little reef accretion has occurred since. Similar patterns were observed at other locations where relatively little reef growth occurred over the past 5,000 years (Middle Island and Holbourne Island) to 2,000 years (Bramston Reef). Palaeo-ecological analyses of the coral framework within the cores revealed the inshore sites were comprised of a diverse coral assemblage that persisted throughout the Holocene. Twenty-five and 28 coral genera were firmly identified in the cores from Bramston Reef and Stone Island, respectively, while 15 and 10 genera were identified in the cores from Middle and Holbourne Island, respectively. These

estimates of diversity are likely to be conservative, as a considerable proportion of the material in most cores, particularly from Middle and Holbourne Islands, was comprised of detrital material, which was hard to confidently identify to genera.

The geomorphological impacts of cyclones on past reef development were most evident at the two locations furthest offshore (Holbourne and Middle Islands). Chronological gaps in the internal reef structure during the mid-Holocene of 3,500 or 5,000 years at Holbourne Island and Middle Island, respectively, are attributed to stripping of the outer reef flat and upper reef slope by cyclones. Geomorphological features on the reef flats and islands at these locations, including shingle ridges and basset edges, provide complementary depositional evidence to support the hypothesis that the outer reef framework was stripped by cyclones. Radiometric dating of fossil microatolls on the reef flat at these two sites indicates that the fossil microatolls are relatively young (<600 yBP), which together with their elevations above modern open-water microatolls indicates that they were most likely moated on the reef flat by storm-deposited shingle ridges. The moated fossil microatoll ages, along with other contemporary geomorphological features, provide insights into the effects of storms/cyclones over the past ~600 years at Holbourne and Middle Islands.

Despite limited reef development since the mid-Holocene at most sites, contemporary ecological surveys revealed that most sites displayed high live coral cover on some areas of the reef flat and slope (e.g., $63.1 \pm 20.2\%$ average cover on Middle Island outer reef flat). This finding challenges previous conclusions that inshore reefs in this region are in poor ecological condition. These conclusions were made on the basis of comparisons between historical photographs of the reef flat at Stone Island showing high coral cover and structural diversity and reports of its contemporary condition, in which both cover and diversity are reduced. While very few live corals were surveyed on Stone Island reef flats, which were dominated by macroalgae and sediment, coral cover was high on nearby reef flats ($63.1 \pm 20.2\%$ cover at Middle Island reef flat) and on Stone Island's reef slopes ($46.0 \pm 36.2\%$ cover). This spatial variability in reef condition within a small geographic area suggests that the current poor condition of Stone Island reef flats may more likely reflect localised reef-scale stressors rather than regional environmental or water quality conditions within Edgumbe Bay.

This research provides the first records of long-term reef growth from Edgumbe Bay in the central GBR, developed using high-precision dating and topographic survey techniques. Cross-shelf variations in the timing and mode of Holocene reef development are identified and discussed and the influences of sea-level change and exposure to cyclones and sedimentation are examined. This research emphasises the value of combining data over various temporal

scales (millennial-scale core records, centennial-scale historical records and contemporary ecological data) to provide a more detailed understanding of present reef condition and recent changes in reef environments. This examination of five fringing reefs revealed some consistencies in reef development through time, which were comparable with other fringing reefs in the GBR and globally, but also revealed diversity in modes of development, palaeo-ecology and present condition.

Table of Contents

Fringing Reef Growth on the Central Great Barrier Reef: Signatures of Sea-level Change, Storms and Sedimentation	i
1 Introduction	1
1.1 Global decline of coral reef condition	2
1.2 Types of coral reefs.....	2
1.3 The Great Barrier Reef	3
1.4 Background	5
1.4.1 Holocene reef development.....	5
1.4.2 Holocene sea level.....	6
1.5 Tropical cyclones.....	7
1.6 Aims and objectives	8
1.7 Significance of research	9
1.8 Study location	10
1.9 Methodology	12
1.9.1 Topography and contemporary ecology	12
1.9.2 Holocene reef growth	14
1.9.3 Palaeo-ecology.....	16
1.9.4 Fossil microatolls.....	16
1.9.5 U-Th dating.....	17
1.10 Thesis structure	18
2 Chronostratigraphy of Bramston Reef reveals a long-term record of fringing reef growth under muddy conditions in the central Great Barrier Reef.....	21
2.1 Abstract.....	22
2.2 Introduction	22
2.3 Study site and environment.....	24
2.4 Materials and methods.....	26
2.5 Results.....	27
2.5.1 Present morphology and ecology.....	27
2.5.2 Palaeo-ecology.....	28
2.5.3 Reef growth and variability	29
2.6 Discussion	30
2.6.1 Comparing past and present ecology.....	31

2.6.2	Holocene reef evolution.....	34
2.6.3	Considerations for future research.....	40
2.7	Conclusions.....	41
3	Multi-scale records of reef development and condition provide context for contemporary changes on inshore reefs	43
3.1	Abstract.....	44
3.2	Introduction	44
3.3	Regional setting	47
3.4	Materials and methods.....	49
3.4.1	Past reef development.....	50
3.4.2	Present geomorphology and benthic cover	50
3.5	Results.....	51
3.5.1	Holocene reef development at Stone Island	51
3.5.2	Contemporary eco-geomorphology	53
3.6	Discussion	62
3.6.1	Stone Island reef condition – temporal variability	63
3.6.2	Local versus regional effect.....	68
3.7	Conclusion.....	72
4	The influence of sea level and cyclones on Holocene reef flat development: Middle Island, central Great Barrier Reef.....	74
4.1	Abstract.....	75
4.2	Introduction	75
4.3	Materials and methods.....	77
4.3.1	Study site.....	77
4.3.2	Core recovery, logging and analysis	80
4.3.3	Fossil microatolls.....	81
4.4	Results.....	81
4.4.1	Holocene reef growth	82
4.4.2	Fossil microatolls.....	85
4.5	Discussion	86
4.5.1	Early-Holocene – and the role of sea level.....	86
4.5.2	Mid- to late-Holocene – the role of cyclones.....	89
4.6	Conclusions.....	92

5	Fringing reef growth over a shallow last interglacial reef foundation at a mid-shelf high island: Holbourne Island, central Great Barrier Reef.....	93
5.1	Abstract.....	94
5.2	Introduction	94
5.3	Regional setting	96
5.4	Materials and methods.....	99
5.5	Results.....	100
5.5.1	Holocene reef development	100
5.5.2	Contemporary geomorphology	102
5.6	Discussion	110
5.6.1	Last interglacial reef foundation.....	110
5.6.2	The Holocene reef chronostratigraphy	112
5.6.3	The role of cyclones over centennial scales	115
5.7	Conclusions.....	116
6	General discussion: Fringing reef development along a cross-shelf transect	117
6.1	Introduction	118
6.2	Variations in reef growth across the shelf.....	120
6.2.1	Timing of reef initiation upon antecedent foundations.....	120
6.2.2	Holocene reef development.....	125
6.3	Contemporary reef ecology and geomorphology – cross-shelf variations	135
7	Conclusions.....	142
7.1	Summary of research findings and future directions	142
7.2	Concluding remarks	147
	References	149
	Appendices	163

List of Figures

- Figure 1.1 Summary of Holocene sea-level data relative to present mean sea level (msl) for the Queensland region modified after Lewis et al. (2013). Sea-level indicators include corals, coral microatolls, foraminifera, mangrove and oyster beds and these data are presented in Lewis et al. (2013) and references therein. 7
- Figure 1.2 Location of study sites and Edgumbe Bay (EB) in Queensland, Australia. The approximate extent of the inner-, mid-, and outer-shelf regions are shown. 12
- Figure 1.3 (a) Trimble RTK GPS set up, with base station set up on the tripod and rover attached to the backpack; (b) measuring co-ordinates and elevation of the fossil *Porites* microatoll (shown exposed above water level) and taking a coral sample using a hand drill shown in (c) along with retrieved coral core..... 13
- Figure 1.4 (a) Percussion coring on the reef flat at Middle Island; (b) rotary drill rig set up on a fossil microatoll at Holbourne Island flat..... 15
- Figure 1.5 Schematic diagram of the overview of this thesis by chapter. 20
- Figure 2.1 Location of a) Edgumbe Bay in Australia, b) Bramston Reef in Edgumbe Bay and c) Bramston Reef flat transect (solid line) indicating percussion core locations (white circles) and drop camera transect (dashed line). 25
- Figure 2.2 Photograph of *Porites* colonies at Bramston Reef, showing upper surfaces colonised with macroalgae, hard corals and soft corals, with Stone Island (SI), Gloucester Island (GI) and Cape Gloucester (CG) in the background. The approximate location of this photograph is shown in Figure 2.1 and the elevation is given in Appendix 10. 25
- Figure 2.3 Bramston Reef flat profile extending seaward, with reef age indicated by the uranium-thorium (U-Th) ages ($yBP \pm 2\sigma$) from percussion cores (core locations shown by black rectangles) and microatolls. Vertical and horizontal arrows show average reef growth rates. Benthic composition of each eco-geomorphological zone on the present reef flat (numbered 1 – 10) is indicated by the shaded pie charts. Elevation is relative to lowest astronomical tide (LAT)..... 31
- Figure 2.4 Composite core logs showing (left to right) sedimentary facies, carbonate and terrigenous mud content of the matrix, grain size content and palaeo-ecology data. Palaeo-ecology data are shown as percent abundance of the total carbonate content >1 cm in size. Dominant coral genera (comprising >25% of each segment) are labelled for each 20 cm downcore segment..... 33
- Figure 2.5 Downcore abundance of major coral genera (comprising >10% of total composition in more than one percussion core). Each core is represented individually within each group; PC1 at the start of the group through to PC8 at the end of the group. Time is

indicated by dashed lines (older than 3,000 yBP) and solid lines (younger than 3,000 yBP). A thick line represents coral genera contributing to $\geq 50\%$ of the total coral composition, while a thin line represents a contribution $< 50\%$ 35

Figure 2.6 Photographs of the various live coral morphologies at Bramston Reef. Massive colonies of *Galaxea* (a) and *Goniopora* (b), plate colony of *Acropora* (c), massive *Porites* colony (d), foliaceous *Turbinaria* (e), free-living *Fungia* and encrusting coral (f), plate *Acropora* and *Turbinaria* (g) and branching *Montipora* on the reef flat (h). See Appendix 10 for elevation of (h). 36

Figure 2.7 Conceptual model of reef development at Bramston Reef in two morphological phases (growth phase 1: 1 – 3, growth phase 2: 4 – 6). Late Holocene sea-level fall is represented by a palaeo-lowest astronomical tide (LAT) envelope at each time period. Reef matrix composition is indicated by the shading (diagonal lines: muddy matrix, dots: sand matrix) and was approximated based on the core facies in Figure 2.4. 38

Figure 3.1 Photographs of the Stone Island reef flat: (a) taken by Saville-Kent (1893) in 1883, (b) taken in 1915 by unknown photographer, (c) and (d) taken by E. Ryan during spring low tides (0.13 and 0.23 m above lowest astronomical tide on 22 [c] and 21 July [d] 2013, respectively). Note the high standing fossil microatolls at the waters edge in (c). For elevations of (c) and (d) see Appendix 10 and for additional photographs see Appendix 3. 47

Figure 3.2 (a) Location of Stone Island, Middle Island and Bramston Reef in Edgcumbe Bay, Australia; (b) the reef flat and transects one (MI-1) and two (MI-2) at Middle Island; (c) the reef flats at Stone Island South (SI-S) and Stone Island North (SI-N). Fossil microatolls (numbered 1 – 16) are shown by black dots and living open-water microatolls are shown by white dots. The approximate location of the photographs taken by Saville-Kent (1893) and Wachenfeld (1997) is shown by the white X; (d) the location of percussion cores (white squares) on the transect at SI-S; and (e) the location of percussion cores (white squares) on the transect at SI-N. 49

Figure 3.3 Profiles of the reef at (a) Stone Island South and (b) Stone Island North extending seaward, with reef age indicated by the uranium-thorium (U-Th) ages on the fossil microatolls and in the percussion cores (labelled grey rectangles). The arrows indicate average vertical accretion rates (mm/yr). Elevation is relative to lowest astronomical tide (LAT). Benthic composition of each contemporary eco-geomorphological zone (numbered Z1 – Z8) is indicated by the shaded pie charts. 56

Figure 3.4 Composite core logs of the uranium-thorium dated percussion cores (PC) from Stone Island South (S) and Stone Island North (N) showing (left to right) sedimentary facies, carbonate and mud content of the matrix, grain size of the matrix, and palaeo-ecology data (shown as % relative abundance of the total carbonate content >1 cm in size). Dominant

coral genera (comprising >25% of each segment) are labelled for each 20 cm downcore segment. Unlabelled white bars represent coral genera <25%. Grey bars represent the % contribution of the remaining un-identified carbonate fraction. 57

Figure 3.5 Upper photographs are from the quadrat and drop camera surveys, illustrating the differences in benthic cover across the reef at Stone Island South (SI-S), Stone Island North (SI-N) and Middle Island (MI). Eco-geomorphological zone numbers indicated in top left corner of each photograph. Lower photographs are of the outer reef flat at lowest astronomical tide (LAT). See Appendix 10 for elevations of the reef flat photographs.... 58

Figure 3.6 Profiles of transects MI-1 and MI-2 at Middle Island extending seaward where elevation is relative to lowest astronomical tide (LAT). Benthic composition of each eco-geomorphological zone (numbered Z1 – Z8) is indicated by the shaded pie charts. Note that the depth of slope is roughly estimated. The fossil microatoll ages are derived from Chapter 4 and are presented in Appendix 2. 61

Figure 4.1 Location of (a) Middle Island in the central Great Barrier Reef, Australia; (b) core transect at Middle Island; (c) percussion cores (P), drill core (D), fossil microatolls (FMA) on the reef flat. The approximate locations of previously reported radiocarbon (¹⁴C) ages (Hopley, 1975) from Middle Island are shown; (d) reef flat profile extending seaward with major morphological zones labelled. Elevation is relative to lowest astronomical tide (LAT) at the Abbot Point tide gauge..... 78

Figure 4.2 Photograph of basset edges at the backreef flat, Middle Island. 79

Figure 4.3 Middle Island reef flat profile extending seaward, with reef age indicated by the coral uranium-thorium (U-Th) ages (yBP ± 2σ) from within the percussion cores (core locations shown by thick black lines) and fossil microatolls on the reef flat. Vertical arrows show the average reef growth rates. Elevation is relative to lowest astronomical tide (LAT). 83

Figure 4.4 Composite core logs showing (left to right) sedimentary facies and uranium-thorium (U-Th) ages (yBP ± 2σ), carbonate and mud content of the matrix and palaeo-ecology data. Palaeo-ecology data are shown as % abundance of the total carbonate content >1 cm in size. Dominant coral genera (>25% of each segment) are labelled for each 20 cm downcore segment in the percussion cores. Arrows indicate average vertical reef accretion rates. 84

Figure 4.5 Middle Island fossil microatoll (FMA) ages (yBP with 2σ error bars) and elevations above lowest astronomical tide (LAT), excluding FMA-1 due to the comparatively old age (6,895 ± 19 yBP; Appendix 2). 85

Figure 4.6 Conceptual model of reef development at Middle Island. Late Holocene sea-level fall is represented by a lowest astronomical tide (LAT) envelope at each time period, based on the sea-level curve presented in Lewis et al. (2013). 87

- Figure 5.1 (a) Location of Holbourne Island, central Great Barrier Reef, Australia; (b) aerial image of Holbourne Island showing reef core sites on the reef flat; (c) geomorphological map of Holbourne Island and reef flat, using survey data augmented with a previous map presented by Hopley (1975), showing important zones across the reef flat, transect locations (A – B: Transect 1; C – D: Transect 2; E – F: Transect 3), and surveyed fossil microatolls and storm deposits (reef flat shingle ridges numbered 1 – 4). 97
- Figure 5.2 Photographs of some of the geomorphological features or zones on the reef flat at Holbourne Island. a) moated backreef zone with living *Porites* microatolls; b) moated backreef zone with high fossil microatolls; c) landward edge of a coral shingle ridge on the reef flat; d) basset edges (photo looking towards the north-west); e) outer reef flat algal turf zone; f) outer reef flat living coral zone showing live branching, massive and plate coral morphologies. See Appendix 10 for the elevations of the reef flat and features shown. 104
- Figure 5.3 Profile of transect 2 at Holbourne Island reef flat extending seaward, with reef age indicated by the uranium-thorium (U-Th) ages ($yBP \pm 2\sigma$) from the percussion cores (P1 – P5; core locations shown by black rectangles) and drill cores (D1 – D4). Percussion core logs are shown in the inset below the profile, indicating the reef facies and the carbonate and mud content of the sediment matrix. Vertical arrows indicate average reef growth rates. Elevation is relative to lowest astronomical tide (LAT)..... 105
- Figure 5.4 a) photograph of the lower section of core D-2 showing the last interglacial reef material and the Holocene reef branching rubble material above it, and b) photograph of the last interglacial reef material. 106
- Figure 5.5 Profiles of transects 1, 2 and 3 at Holbourne Island extending seaward showing elevation of the reef flat surface relative to lowest astronomical tide (LAT) and the benthic composition for each eco-geomorphological zone (numbered) in pie charts. TOB: Toe of beach. The upper surfaces of high, moated fossil microatolls (FMA) are shown. Letters A – F represent the transect locations shown in Figure 5.1 for reference. Examples of the high FMA, reef flat shingle ridges and basset edges are shown in Figure 5.2b, c, d, respectively. Note that the depth of the reef slope on transect 2 is estimated..... 108
- Figure 5.6 Microatoll ages (note that ages are presented as calendar years AD) and elevations (relative to lowest astronomical tide [LAT]). Triangles represent radiocarbon ages and squares represent uranium-thorium ages. 2σ age errors shown by bars..... 110
- Figure 6.1 (a) Millennial-scale timeline showing the main period of Holocene reef development for the four study sites. Uranium-thorium (U-Th) ages are those obtained in this thesis from cores and fossil microatolls. Re-calibrated radiocarbon ages from other sources are also presented with 2σ age errors (ages initially presented in Chappell et al. [1983]; Hopley, [1975] and re-calibrated using Calib 7.0 [Stuiver and Reimer, 1993]). Note age

errors are too small to warrant inclusion for the U-Th ages. The period since European settlement of the Queensland coast is highlighted in the grey box and blown up in (b), showing estimated reef ‘condition’ (+ equals good condition [high coral cover and structural diversity] and – equals poor condition [low coral cover and limited structural diversity]) over time based on historical photographs (Saville-Kent, 1893; Clark et al., 2016), accounts (Hedley, 1925; Marshall et al., 1925; Rainford, 1925; Stanley, 1928; Steers, 1937; Richards, 1938; Stephenson et al., 1953; Hopley, 1975) contemporary photographs (Wachenfeld, 1997; Ryan et al., 2016; Clark et al., 2016) and available modern ecological data from this thesis and Ryan et al. (2016); Clark et al. (2016)..... 122

Figure 6.2 Schematic diagrams showing (a) cross-section through the inner- and mid-shelf Great Barrier Reef extending seaward from the coast at Edgecumbe Bay; (b) the cross-shelf relative influence of environmental parameters; and (c) scaled conceptual reef growth models for each site based on the chronostratigraphies present in Chapter 2 (Bramston Reef), Chapter 3 (Stone Island South and North), Chapter 4 (Middle Island) and Chapter 5 (Holbourne Island). Elevations are relative to lowest astronomical tide (LAT). In the key, * denotes where features are not to scale..... 127

Figure 6.3 Estimated vertical reef accretion rates (based on uranium-thorium ages of coral material within reef cores) and the mean mud content (<63 microns) of the sediment that contributed to the reef matrix during the time period for which each growth rate was estimated. Vertical error bars show one standard deviation for the mud content. SI-S is Stone Island South reef and SI-N is Stone Island North reef..... 132

Figure 6.4 Average vertical accretion rates (estimated based on uranium-thorium ages of coral material within reef cores) for each reef over time. Time is grouped into thousands of years before present (k yBP) where present is 1950 AD. SI-S is Stone Island South and SI-N is Stone Island North. 134

List of Tables

Table 2.1 Details of percussion cores (total length, penetration and compaction rates) collected from the Bramston Reef flat.....	27
Table 2.2 Eco-geomorphological zones on the transect at Bramston Reef. Oldest known surficial ages are based on uranium-thorium ages obtained from (Figure 2.3) and Appendix 2. Elevations are relative to lowest astronomical tide (LAT).....	29
Table 2.3 Core facies descriptions and matrix components including percent (mean $\pm 1\sigma$) sand vs. mud, percent (mean $\pm 1\sigma$) carbonate content, and mean grain size (mgs) of the sand fraction.	32
Table 3.1 Core facies descriptions and matrix components including percent sand, mud and carbonate (CaCO_3) content (mean and 1σ standard deviation [SD]).	53
Table 3.2 Contemporary eco-geomorphological zones at Stone Island and Middle Island. Elevation is relative to lowest astronomical tide (LAT).	59
Table 3.3 Reef condition in Edgecumbe Bay over millennia based on reef cores. Time is thousands of years before present (k yBP).....	70
Table 3.4 Statements of reef condition in Edgecumbe Bay over the past ~150 years derived from various sources.	71
Table 4.1 Core facies descriptions and matrix components including percent sand, mud and carbonate (CaCO_3) content (mean and 1σ standard deviation [SD]).	83
Table 5.1 Reef core facies descriptions with average percent mud and carbonate (CaCO_3) values of the sediment matrix. Standard deviations (SD) are 1σ	102
Table 5.2 Details of the eco-geomorphological zones on the reef flat at Holbourne Island, across transect 1 (T1), transect 2 (T2) and transect 3 (T3). Elevations are relative to lowest astronomical tide (LAT).....	109
Table 5.3 Fossil microatoll groups on the Holbourne Island reef flat differentiated according to the age of the sample (note that ages are presented as calendar years AD) the elevation of the fossil microatoll upper surface (relative to lowest astronomical tide [LAT]), and the diameter of the fossil microatoll.	109
Table 6.1 Summary of Holocene reef growth attributes at the study reefs. uranium-thorium (U-Th) ages are presented as years before present (1950 AD).....	121
Table 6.2 A comparison of average ($\pm 1\sigma$) mud content (<63 microns) and carbonate content (CaCO_3) of the sediment matrix within upper facies (A – B) and lower facies (C – E) in the percussion cores from each study site.	128
Table 6.3 Descriptions of reef flat ecological/geomorphological condition at each study site. Elevations are relative to lowest astronomical tide (LAT).	128

List of Plates

Plate 1. Outer reef flat at Middle Island exposed during spring low tide, showing high live coral cover with Gloucester Island visible on the horizon.	1
Plate 2. Part of a percussion core from Bramston Reef, looking downcore and showing the excellent preservation of <i>in situ</i> coral material among a muddy sediment matrix.....	21
Plate 3. Live faviid and <i>Porites</i> corals growing among macroalgae at Stone Island outer reef flat. See Appendix 10 for elevation of these corals.	43
Plate 4. View across Middle Island looking to the west showing from left to right: part of the exposed reef flat at low tide, beach, shingle ridges, large vegetated shingle ridge (centre) extending to the enclosed ephemeral lake (far right).	74
Plate 5. Photograph of (a) a <i>Porites</i> microatoll (living edges and dead upper surface) growing in ponded water on the Holbourne Island reef flat and (b) fossil microatolls previously moated at a higher level.	93

1 Introduction



Plate 1. Outer reef flat at Middle Island exposed during spring low tide, showing high live coral cover with Gloucester Island visible on the horizon.

This chapter provides background information and a brief review of the literature relevant to fringing reef development in the Great Barrier Reef, identifying key gaps in knowledge. The aims and objectives of this thesis are stated, followed by a description of the study setting and the methodologies used. An overview of the thesis structure is presented to show the connections between chapters.

1.1 Global decline of coral reef condition

Coral reef ecosystems worldwide have reportedly experienced accelerated decline in coral cover and diversity over the past few decades, generating global concern for their long-term futures (Pandolfi et al., 2003; Bellwood et al., 2004; Bruno and Selig, 2007; Wilkinson, 2008; De'ath et al., 2012). Reported indicators of deteriorating reef condition include: 'phase-shifts' characterised by a transition from coral dominance to macroalgal dominance (Done, 1992; Hughes, 1994; Bellwood et al., 2004); declines in live coral cover (Bruno and Selig, 2007; De'ath et al., 2012); and reduced coral species diversity (Hughes, 1994; Pandolfi and Jackson, 2006). Natural stressors affecting reefs that can cause declines in coral cover and diversity include: cyclones/hurricanes (Done, 1992); crowns-of-thorns starfish (COTS) outbreaks (Pratchett et al., 2014); and terrestrial sedimentation (Risk, 2014). Human pressures may exacerbate the impacts of these naturally occurring stressors. For example, human-induced global climate change, including elevated ocean surface temperatures (Baker et al., 2008) and ocean acidification (Hoegh-Guldberg et al., 2007) may lead to increased frequency and intensity of disturbance events (Bruno and Selig, 2007; Wilkinson, 2008; Thompson and Dolman, 2010). Additionally, disruptions to natural reef ecosystem function may occur because of over-fishing (Jackson et al., 2001; Hughes et al., 2007), while elevated levels of sediment, nutrients and contaminants in runoff from modified coastal catchments may reduce reef recovery and coral recruitment rates (Fabricius, 2005; Bruno and Selig, 2007). Although human impacts have undoubtedly caused changes on some reefs, the regional or global extent of coral reef decline is unknown (Bruno et al., 2009), partly due to the lack of baseline, long-term knowledge about past reef condition and variability that can be preserved in geological, sedimentological and historical records of coral reefs (Pandolfi and Jackson, 2006; Kittinger et al., 2011; Reymond et al., 2013; Pandolfi, 2015). Furthermore, it is difficult to isolate the various anthropogenic and natural causes of changing reef condition, which may act collectively or solely. Nonetheless, such efforts are important for appropriate management of socially, environmentally and economically important reef ecosystems (Moberg and Folke, 1999; Burke et al., 2011).

1.2 Types of coral reefs

Coral reefs are structurally defined as "a tract of corals growing on a massive, wave-resistant structure and associated sediments" (Done, 2011 pp. 261) and have traditionally been characterised into three broad types: fringing reefs, barrier reefs and atolls (Darwin, 1842). Fringing reefs are coral reefs growing attached or very close to an adjacent land structure, while barrier reefs typically rise from greater depths and are significantly detached from a land structure by a lagoon (Guilcher, 1988; Kennedy and Woodroffe, 2002). Barrier reefs may be

continuous and relatively linear features. Atolls on the other hand are circular (often asymmetrical) reefs surrounding a central lagoon with a deep volcanic basement (Guilcher, 1988; Kennedy and Woodroffe, 2002). Fringing reefs can develop in a variety of ways and Chappell et al. (1983) were among the first researchers to realise this, showing that some reefs prograded from the shore seaward but others developed in more complex ways. Commonly referred to as growth 'modes' or 'styles', continued investigations over time have been expanded and refined to show that fringing reefs develop in many ways (Partain and Hopley, 1989; Kennedy and Woodroffe, 2002; Smithers et al., 2006). The size, shape and composition of the substrate underlying a coral reef can influence the mode and timing of fringing reef development (Woodroffe et al., 2000). Fringing reef development is also controlled by the available accommodation space, which is a function of relative sea level and the rate of reef growth (Kennedy and Woodroffe, 2002). Up to eight fringing reef growth modes have been identified, including vertical accretion followed by seaward reef flat progradation, episodic seaward reef crest advance, and offshore development followed by shoreline-reef coalescence (see Kennedy and Woodroffe [2002] and Smithers et al. [2006] for detailed descriptions of growth modes). Typically, vertical reef accretion occurs until the reef reaches sea level and all available vertical accommodation space is filled, forcing lateral accretion to prevail and, eventually, reef flat formation. A reef flat is simply defined as coral reef growth at sea level (Thornborough and Davies, 2011) and generally constitutes a cemented pavement incorporating detrital carbonate material, including sediment (Guilcher, 1988). Reef flats are typically sub-aerially exposed during low tidal stages (Guilcher, 1988; Kennedy and Woodroffe, 2002), often with lower elevation seaward edges (Hopley et al., 2007), which may be abrupt or more gently sloping. The living reef is generally confined to the outer (seaward) reef flat and reef crest, particularly on those fringing reef flats that are sub-aerially exposed during low tidal stages (Hopley et al., 2007).

1.3 The Great Barrier Reef

Australia's Great Barrier Reef (GBR) is the world's largest coral reef ecosystem, covering 15° of latitude and extending about 2,300 km along the north-eastern shelf of Queensland (Hopley et al., 2007). Despite the GBR's protected status as a World Heritage Area and being one of the most highly-managed reef systems in the world (Brodie and Waterhouse, 2012), the GBR's future is threatened by numerous stressors associated with human activities on the reef and in adjacent coastal catchments (GBRMPA, 2014). Since the onset of modern monitoring programs on the GBR in the early 1980s, declines in live coral cover and diversity (Thompson and Dolman, 2010; De'ath et al., 2012) and 'phase-shifts' from coral to macroalgal dominance (Cheal et al., 2010; Hughes et al., 2010) have been observed. Cyclones, COTS outbreaks and

coral bleaching have been implicated as drivers of these changes in some cases (De'ath et al., 2012), but human activities are argued to be responsible in others (Fabricius et al., 2005, 2010; Roff et al., 2012). Most studies that report a decline in reef condition are based on just a few decades at most of coral cover and diversity data. Comparisons of historical (late 1800s) and recent (1994 onwards) photographs of reef flats that show declines in coral cover and structural diversity have also been used as evidence of reef decline at some inshore sites (Wachenfeld, 1997). Despite providing a wealth of important information for management and science purposes, these decadal-scale data and centennial-scale photographic records span a relatively short time period in comparison to the growth history of many reefs on the GBR, which typically extends over several millennia (Smithers et al., 2006).

The GBR continental shelf can be separated into three general shelf-parallel zones: the inner-shelf (within the 20 m isobath and the coast), mid-shelf (between the 20 – 50 m isobaths) and outer-shelf (beyond the 50 m isobath) (Hopley et al., 2007). The GBR comprises 2904 named coral reefs, of which, more than 758 are fringing or nearshore reefs (Hopley et al., 2007), usually located on the inner-shelf (inshore) zone. Inshore reefs on the GBR develop in a variety of environmental settings, including as fringing reefs attached to the mainland coast or the shoreline of high continental islands, fringing reefs that develop within embayments, and as nearshore reefs or shoals which develop detached from the shoreline (Browne et al., 2012). Fringing reefs also occur on the mid-shelf GBR, usually attached to the shorelines of high continental or volcanic islands.

Inshore reefs, including those referred to as 'turbid zone reefs' that survive in high turbidity water, are perceived as particularly stressed or degraded on the GBR due to their close proximity to modified coastal catchments and exposure to anthropogenic threats (Fabricius et al., 2005; Browne et al., 2012). Since European settlement of the Queensland coast in the early-mid 1800s, sediment, nutrient and pollutant loads exported to the GBR lagoon in fluvial run-off have increased two- to ten-fold (McCulloch et al., 2003; Fabricius et al., 2005; Kroon et al., 2012; Waters et al., 2014). More frequent large floods have also been recorded for the period 1948 – 2011, compared to the century preceding European settlement (Lough et al., 2015). However, evidence of direct influences of anthropogenic factors on inshore reefs is lacking and contentious (see Sweatman et al., 2011; Hughes et al., 2011; and Sweatman and Syms, 2011). Researchers need to consider whether the decline in coral cover on the GBR measured over the past ~30 years (De'ath et al., 2012) represents enough of a long-term signal to make conclusions about future reef condition, especially because many GBR inshore reefs preserve several millennia of growth history in their internal structures (Smithers et al., 2006; Browne et al., 2012; Lewis et al., 2012). Thus, knowledge about past long-term variability in reef

condition and the stressors to reefs is required to better understand the recently observed changes in reef condition on the GBR.

1.4 Background

1.4.1 Holocene reef development

Long-term (millennial-scale) records of reef development derived from radiometrically dated reef cores reveal important insights about reef initiation, the timing, mode and rates of reef development, palaeo-ecology, sediment regimes and variations through time (Hopley, 1982; Kennedy and Woodroffe, 2002; Montaggioni, 2005; Hopley et al., 2007). Many fringing reefs initiated ~7,000 yBP, well before monitoring of the GBR began (Hopley et al., 2007). Over the past few decades investigations of Holocene reef development on the GBR have increased and become more detailed, as the value of long-term records becomes increasingly recognised and with advancements in coring and dating techniques (Kennedy and Woodroffe, 2002; Smithers et al., 2006; Clark et al., 2012) and geochemical reconstructions of environmental records from coral skeletons (Gagan et al., 1998; Fallon et al., 2003; Jupiter et al., 2008). In particular, investigations on inshore reefs have increased due to their perceived vulnerability to anthropogenic stressors (Perry and Smithers, 2011; Perry et al., 2012; Roff et al., 2012), but there are still many fringing reefs for which growth records are unknown. Mainland-attached fringing reefs (Roche et al., 2011) and mid-shelf fringing reefs (Kleypas, 1996) are particularly poorly known and are themselves rare in the central GBR. Smithers et al. (2006) provided a detailed review of the Holocene development of inshore reefs of the GBR, highlighting that many inshore reefs experience natural growth cycles, independent of anthropogenic forcing, whereby a period of rapid growth preceded a late evolutionary state characterised by low accretion potential (see also Perry and Smithers, 2011). An understanding of natural trajectories on coral reefs, which may be forced by factors such as accommodation space (Masse and Montaggioni, 2001) and exposure to and recovery from natural stressors (Roche et al., 2011), is required to understand the relative impacts of anthropogenic change. Furthermore, many inshore reefs have high coral cover and diversity (Browne et al., 2010) and are able to accrete rapidly in turbid settings (Palmer et al., 2010; Perry et al., 2012; Roff et al., 2015) challenging long-held notions that such conditions are antithetic to reef growth (Rogers, 1990; Fabricius, 2005). Recent studies have suggested that although inshore reefs are exposed to high turbidity and sedimentation that would be problematic for clear water or outer-shelf reefs (Pastorak and Bilyard, 1985; Larcombe and Woolfe, 1999a), they may be well adapted and resilient to such stressors (Browne et al., 2010). Identifying past variability in reef growth and understanding how past stressors have influenced reef development are required to further our understanding

of contemporary reef condition.

1.4.2 Holocene sea level

Relative sea level is an important control on reef development and morphology in the GBR, controlling the timing of reef initiation, the availability of accommodation space and the onset of reef flat development (Davies et al., 1985; Chappell et al., 1982, 1983; Kennedy and Woodroffe, 2002). An understanding of past relative sea-level fluctuations is required to correctly interpret present reef state and to isolate the influence of various forcing factors on reef growth (Woodroffe and Webster, 2014). Sea level may drive intrinsic shifts in coral community assemblages as reefs grow from depth and reach the sea surface (Perry and Smithers, 2011). Since the early 1970s, our understanding of Holocene sea-level movements on the GBR has increased (Larcombe et al., 1995a; Lewis et al., 2008, 2013). It is generally accepted that after the post-glacial marine transgression (PGMT) sea-level approached the present position around 8,000 yBP (Larcombe et al., 1995a; Lewis et al., 2008; Woodroffe, 2009), before rising to a mid-Holocene highstand where sea level was 1.0 – 1.5 m above present (Lewis et al., 2013) (Figure 1.1). While there is general consensus regarding when sea level attained its current position following the post-glacial rise, the timing and nature of late-Holocene sea-level fall remain contentious (Lewis et al., 2013). Whether sea level dropped smoothly (Chappell et al., 1983; Larcombe et al., 1995a), remained at a prolonged highstand before dropping rapidly (Lewis et al., 2015), or experienced oscillations (Lewis et al., 2008; Leonard et al., 2016) remains debated. Importantly, most sites from which GBR sea-level data have been produced are situated on the inner-shelf (within 10 – 20 km of the Queensland coast). The degree of late-Holocene relative sea-level fall is likely to be variable across the continental shelf and along the GBR coast, due to spatial variations in hydro-isostatic shelf deformation effects associated with water loading during the PGMT (Chappell et al., 1982; Lambeck and Nakada, 1990). However, the details of cross-shelf hydro-isostatic adjustments remain poorly understood due to the lack of sea-level data from the mid-shelf or outer-shelf GBR (Harris et al., 2015). Nevertheless, many fringing reefs established reef flats during the mid-Holocene when sea level was 1.0 – 1.5 m above present and many of these older (relict) reef flats are now exposed during contemporary low tidal stages due to subsequent relative sea-level fall (Smithers et al., 2006).

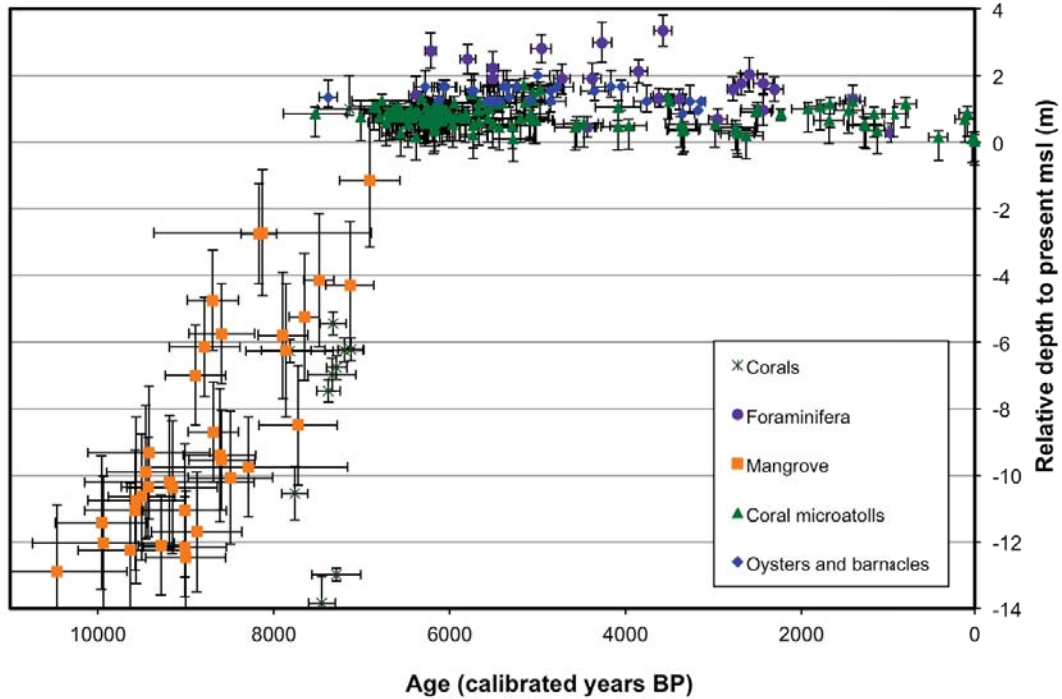


Figure 1.1 Summary of Holocene sea-level data relative to present mean sea level (msl) for the Queensland region modified after Lewis et al. (2013). Sea-level indicators include corals, coral microatolls, foraminifera, mangrove and oyster beds and these data are presented in Lewis et al. (2013) and references therein.

1.5 Tropical cyclones

Tropical cyclones are systems of low atmospheric pressure that develop over warm tropical waters (>26.5°C) with high speed, circular winds (120 – 300 km/hr) that generate high wave energy, storm surges (Scoffin, 1993; BOM, 2016a) and commonly high rainfall (Puotinen et al., 1997). Tropical cyclones differ in intensity across the five-category Saffir-Simpson Scale (Simpson and Reihl, 1981) according to wind speeds. On the GBR, tropical cyclones commonly occur during the austral summer (December to March) and the frequency, location and intensity of cyclones varies inter-annually. Between 1969 and 1997 a total of 80 cyclones moved through the GBR region, averaging 2.8 cyclones per year (Puotinen et al., 1997).

Tropical cyclones can cause a range of catastrophic impacts on coral reef ecosystems (see reviews by Scoffin [1993] and Harmelin-Vivien [1994] for details). On the GBR, the short-term effects of tropical cyclones on coral communities and reefs have been well documented over recent decades and include: mass coral breakage (Done, 1992; Fabricius et al., 2008); the deposition of new geomorphological features on reef flats, such as storm ridges comprised of reef-derived and re-worked coral rubble (Scoffin, 1993) and coral blocks (Yu et al., 2012; Liu et al., 2014); sediment movement (Gagan et al., 1987; Perry et al., 2014); and elevated turbidity and decreased salinity due to flood waters (van Woosik et al., 1995; DeVantier et al., 1997).

However, the impacts of cyclones on reefs over longer timescales (centennial-millennial) have rarely been reported (Hubbard et al., 1990) and are less well understood. This is partly due to the lack of long-term chronostratigraphic investigations of reefs that contain chronological information with adequate temporal resolution to detect cyclones (Blanchon et al., 1997; Braithwaite et al., 2000). Furthermore, instrumental records of cyclone data are generally short (<100 years) and few studies have accurately and confidently extended the temporal range of these instrumental records (Nott et al., 2007).

In the GBR region, long-term records of cyclone occurrence have been reconstructed using a range of techniques, including radiometrically dated beach ridges, terraces and shingle ridges (Chappell et al., 1983; Chivas et al., 1986; Nott and Hayne, 2001; Nott et al., 2009; Forsyth et al., 2010), radiometrically dated storm transported coral blocks (Yu et al., 2012; Liu et al., 2014), and oxygen isotope signatures of cyclonic rainfall preserved in speleothems (Nott et al., 2007; Haig et al., 2014). It has been inferred that the frequency of high-intensity tropical cyclones in eastern Australia over recent decades has been relatively low compared to average conditions during the past ~6,000 years (Nott and Hayne, 2001; Nott et al., 2009). Some records indicate Holocene cyclone frequency was relatively constant throughout the Holocene (Hayne and Chappell, 2001), with cyclones of extreme intensity occurring on average every 200 – 300 years (Nott and Hayne, 2001). Other researchers suggest there has been considerable variation in both cyclone frequency and intensity since the mid-Holocene (Nott et al., 2007; Forsyth et al., 2010), possibly driven by El Niño Southern Oscillation (ENSO) variability (Nott and Forsyth, 2012) or trade wind strength (Nott et al., 2007). There remains much to be learnt about the nature and frequency of tropical cyclones in the mid-Holocene and their influence on reef development.

1.6 Aims and objectives

The main aim of this research was to investigate in detail the Holocene development of fringing reefs located at a range of sites along a cross-shelf transect in the central GBR extending from the mainland to the mid-shelf. In taking this approach, this study also aimed to better understand the influence of environmental parameters that vary across the transect (i.e. sea-level history, sedimentation regime, exposure to cyclones) and may influence reef growth across the GBR shelf. This research contributes to the global baseline knowledge about past reef growth, condition and variability, providing new reef chronologies from the central GBR.

The key objectives of this research are:

- 1) To determine the timing and location of reef initiation over the cross-shelf transect;
- 2) To reconstruct the chronostratigraphy of the fringing reefs along this transect to establish past rates and styles of reef development and any variability over time, including detailed examinations of palaeo-ecological coral community compositions;
- 3) To understand the influence of natural stressors on past reef development;
- 4) To describe and quantify the contemporary ecological community composition and structure and determine whether this has changed since European settlement;
- 5) To investigate Holocene reef development and present reef condition across the shelf, to identify variability and similarities across this gradient, and to examine how such patterns reflect the influence of key environmental parameters.

1.7 Significance of research

This research presents five new reef growth histories reconstructed from reef cores using high-precision dating techniques, detailing pre-reefal substrates, reef initiation ages, the timing of reef flat development, modes of reef development, reef matrix sediments and palaeo-ecology. The high-precision U-Th ages (mean age error [$\pm 1\sigma$ standard deviation] of 19 ± 12 years) deliver a considerably higher temporal resolution of reef and coral age than is presented within most existing datasets of reef growth, which generally have larger error terms (around 50 – 200 years). Reef flat and microatoll elevation data were collected with extremely high precision (generally $\sim 0.01 - 0.005$ m) using a Real Time Kinematic Global Positioning System (RTK GPS), providing some of the most accurate information about reef flat ecological zonation and microatoll elevations collected on any reef globally to date. This study contributes new knowledge relevant to the GBR region by providing: a) a unique record of variations in fringing reef development across a transect on the GBR shelf from the mainland shore to the mid-shelf, allowing a gradient of anthropogenic influence and exposure to be investigated; b) the first reconstructions of reef development in Edgumbe Bay; c) the first example of the internal structure of a mainland-attached fringing reef located in a sheltered bay on the GBR (Bramston Reef); d) a new record of last interglacial reef from the mid-shelf central GBR; and e) new context to assess the significance of changes in reef condition that have been inferred using comparisons between historical and contemporary photographs and descriptions of reef flat condition at the same site. Furthermore, new information on the geomorphological effect of cyclones on long-term reef development is presented, which has implications for reef studies globally.

1.8 Study location

This research focused on four study sites located offshore from Bowen in the central GBR (Figure 1.2): Bramston Reef (148°15'E, 20°03'S); Stone Island (148°17'E, 20°02'S); Middle Island (148°22'E, 19°59'S); and Holbourne Island (148°21'E, 19°43'S). These four sites were chosen due to their position across a mainland shore to mid-shelf gradient along a 40 km transect, over which cross-shelf variations in reef development and exposure to natural and anthropogenic factors could be examined. Furthermore, historical descriptions exist for these four sites (Saville-Kent, 1893; Agassiz, 1898; Hedley, 1925; Rainford, 1925; Stanley, 1928; Richards, 1938; Stephenson et al., 1958) that describe reef flat condition at different points in time post European settlement in Bowen (which occurred around ~1861 AD, McIntyre-Tamwoy, 2004). Bramston Reef is a mainland-attached fringing reef located in the inner part of Edgumbe Bay where surrounding water is turbid and shallow (~6 m depth). Stone, Middle and Holbourne Islands are continental islands located ~3 km, ~10 km and ~40 km offshore from the mainland coast near Bowen, respectively. Stone Island lies within Edgumbe Bay on the shallow (6 – 7 m depth) inner-shelf just 3 km seaward of Bramston Reef. It is partly fringed by two reefs, one on the northern side (in Shoalwater Bay) and one on the southern side of the island. Middle Island is situated at the seaward margin of Edgumbe Bay, near the boundary between the inner-shelf and mid-shelf where water depths are ~16 m. At Middle Island, a fringing reef extends along part of the southern shoreline. Holbourne Island is located ~40 km from Bramston Reef on the mid-shelf, where surrounding water depths are ~45 m (Hopley, 1975). At Holbourne Island, a fringing reef extends from the southern shoreline. Detailed descriptions of each study site are provided in the relevant chapters (Chapter 2 for Bramston Reef; Chapter 3 for Stone Island; Chapter 4 for Middle Island; and Chapter 5 for Holbourne Island).

Rainfall, tropical cyclones and high river flows in the Queensland dry tropics are usually restricted to the austral summer months (December to March). As a result, freshwater and sediment discharge to the inner GBR lagoon is highly seasonal. Inter-annual variation can also be significant and is strongly influenced by ENSO conditions and the Pacific Decadal Oscillation (Rodriguez-Ramirez et al., 2014). Large flood plumes from the Burdekin River, Pioneer River and O'Connell River (~80 km to the north, ~160 km to the south and ~120 km to the south of Bowen, respectively) episodically influence Edgumbe Bay (Devlin et al., 2001, 2012; Lewis et al., 2006). Flood plumes from the Burdekin River (that delivers the highest sediment loads to the GBR lagoon [Kroon et al., 2012]) typically travel northward (Bainbridge et al., 2012) and infrequently influence Edgumbe Bay (4 – 6 times per decade) and rarely affect Holbourne Island further offshore (1 – 3 times per decade) (Devlin et al., 2012). Terrestrial sediment yields to Edgumbe Bay are largely from the Proserpine Basin (2,535

km²), a modified catchment where more than 50% of the land use is dedicated to grazing (Packett et al., 2014). The Gregory River, a major waterway of the Proserpine Basin, discharges into southern Edgumbe Bay (Figure 1.2). Gregory River flow gauge data for 33 years (1972 – 2005) were analysed by Lewis et al. (2006), who identified six major flow events (where daily discharge exceeded 10,000 ML) for this period. The largest event discharged 90,576 ML of water to the bay in December 1990. The mouth of the Don River is located ~10 km north of Edgumbe Bay (Figure 1.2) and during the 1990/1991 flood event, 1,096,447 ML of water was discharged from the Don River (The State of Queensland, 2015). Several minor creeks also enter Edgumbe Bay (Duck Creek, Eden Lassie Creek, Greta Creek and Billy Creek), but these sites are not gauged (Lewis et al., 2006).

Edgumbe Bay is relatively sheltered from higher-energy waves and currents generated by prevailing south-easterly trade winds by Cape Gloucester and Gloucester Island (Figure 1.2), while Holbourne Island is relatively exposed, with a fetch distance of ~60 – 70 km to the south-east. Tides in this part of the central GBR are semi-diurnal, with a maximum spring tidal range of 3.6 m. The reef flats are largely exposed during lower tidal stages. Hydrodynamic and ecological conditions within Edgumbe Bay are poorly known with few field data available. Brodie et al. (2014) inferred inshore waters within Edgumbe Bay were poorly flushed based on a hydrodynamic model developed by Andutta et al. (2013), although the model was not developed specifically for Edgumbe Bay and no field data exist to validate the model results.

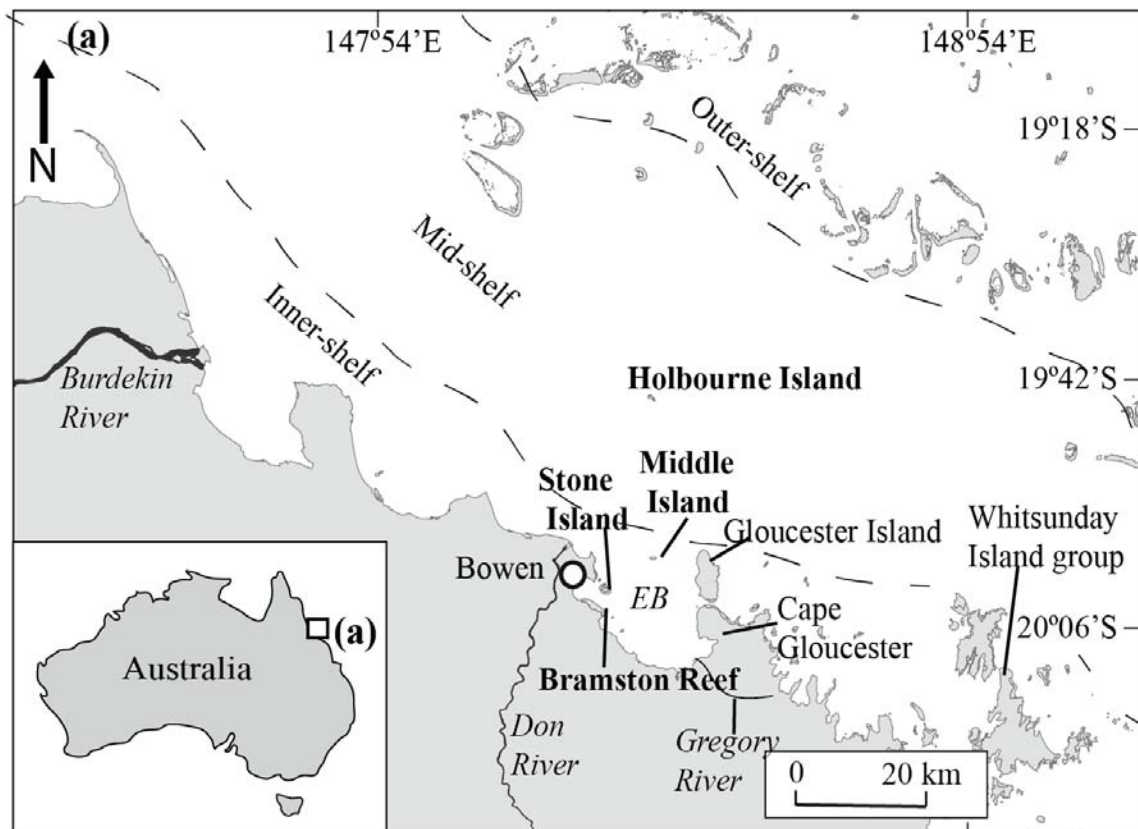


Figure 1.2 Location of study sites and Edgumbe Bay (EB) in Queensland, Australia. The approximate extent of the inner-, mid-, and outer-shelf regions are shown.

1.9 Methodology

The general methodologies used for this research are detailed in this section. Specific details for each reef (including sample numbers and locations) and any deviations from the methods described here are documented in the relevant chapters. Field studies were conducted between April 2013 and November 2014 during low spring tides (<0.5 m relative to lowest astronomical tide [LAT] during daylight hours), allowing access to the exposed reef flats. High turbidity conditions in Edgumbe Bay limit observations when the reefs are submerged so the best time to view inshore fringing reefs is during daytime low spring tide windows, which on the central GBR typically occur in the austral winter (June to September). Techniques were similar at each study site, allowing comparison between the four sites and different reefs.

1.9.1 Topography and contemporary ecology

All location and elevation data were collected using a Trimble RTK GPS with a vertical and horizontal precision of ~0.01 – 0.005 m (Figure 1.3). All high-precision elevation data were reduced to a common datum of LAT at the Abbot Point tide gauge (port number 59300, BOM [2016b]) relative to datum RTK GPS base station values obtained from AUSPOS 2.1 (an online

GPS processing service provided by the Commonwealth of Australia [Geoscience Australia], 2015), allowing accurate inter- and intra- site comparison.

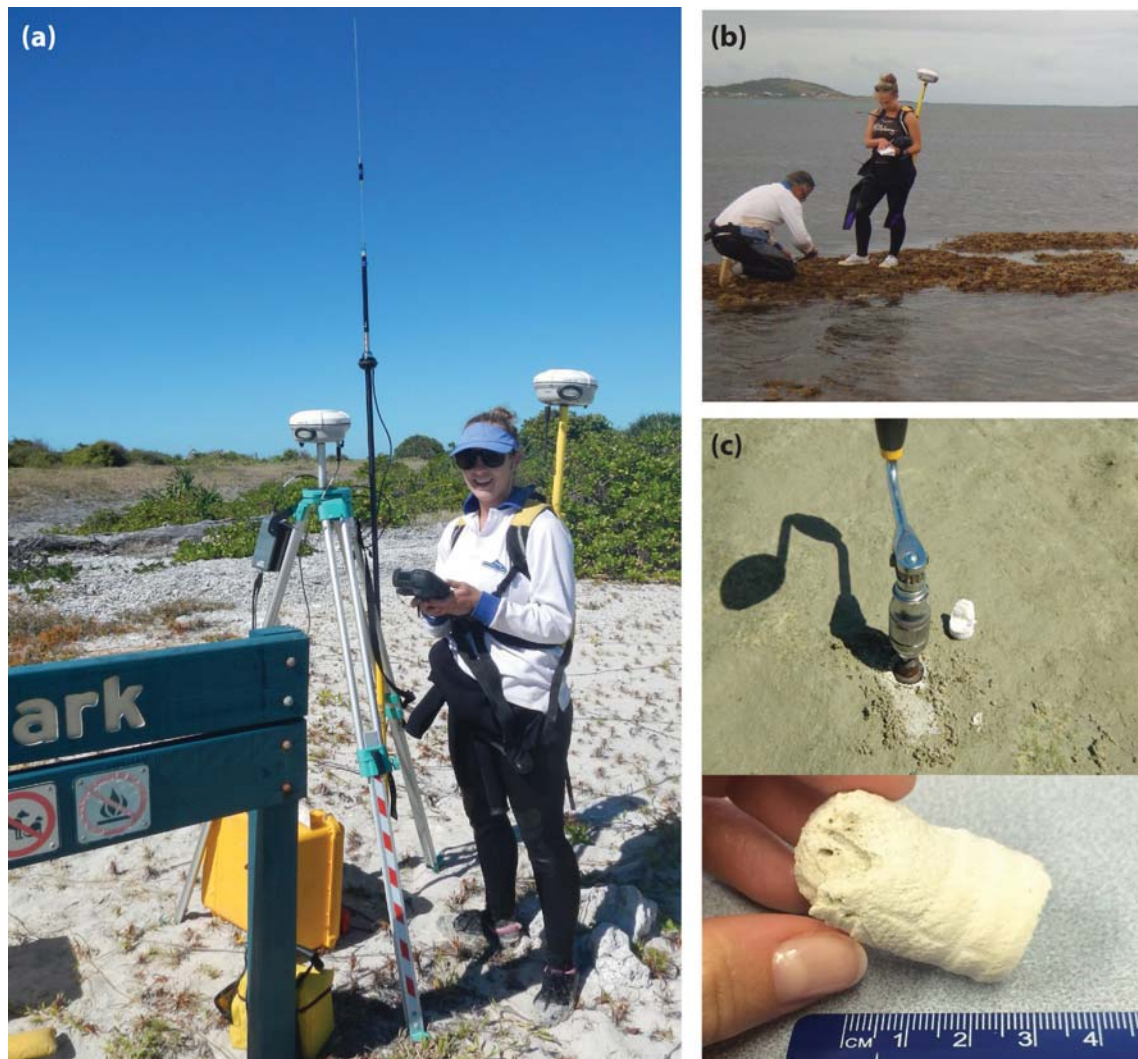


Figure 1.3 (a) Trimble RTK GPS set up, with base station set up on the tripod and rover attached to the backpack; (b) measuring co-ordinates and elevation of the fossil *Porites* microatoll (shown exposed above water level) and taking a coral sample using a hand drill shown in (c) along with retrieved coral core.

Ecological surveys of the contemporary reef flat and slope were conducted across one or more shore-perpendicular transects on each reef. The topography of the reef flat was surveyed with high accuracy using the RTK GPS (Figure 1.3). Reef flat eco-geomorphological zones were differentiated across each transect based on variations in reef flat elevation, coral cover, vegetation type and cover, sediment type and other morphological features. Provided the reef flat was exposed during LAT periods, the benthic cover of each reef flat eco-geomorphological zone was surveyed using digital photo quadrats, which are an effective way to quantify benthic composition on coral reefs (Carleton and Done, 1995; Done et al., 2007). In each zone, five 1

m² quadrats were randomly placed and photographed with a digital camera. In order to photograph the reef slope and outer parts of the reef flat that were not exposed during low tide, spatially-referenced video-photography was captured across seaward extensions of the reef flat transects extending to the base of the reef slope where possible. An underwater SeaViewer drop camera paired with a Trimble Juno GPS was used for capturing video-photography. Reef slope eco-geomorphological zones were differentiated from the video footage based on variations in coral cover and type, vegetation cover and type, and substrate. Benthic composition was determined from the reef flat quadrat photographs and still images extracted from the video footage using the stratified point count method in Coral Point Count with Excel Extensions (CPCe) software (Kohler and Gill, 2006), following Browne et al. (2010). The average percent ecological composition for each zone was calculated. Live corals and macroalgae were identified from photographs and video footage to genus level where possible. When poor image quality and/or turbid water conditions limited confident identification, which was commonly the case, the corals were classified based on their structural morphology (i.e. branching, massive, plate, foliaceous, columnar, encrusting, or free-living).

1.9.2 Holocene reef growth

Holocene reef growth, palaeo-ecology and sediment regimes were reconstructed using reef cores driven vertically into the reef flat structure using either percussion coring (total of 37 cores) or rotary drill coring (total of 5 cores). Percussion coring involves manually hammering aluminium pipes (9.5 cm diameter, 2 mm thick walls) into the reef structure (Figure 1.4), capturing both reef framework and sediment matrix (Perry and Smithers, 2006; Perry et al., 2008, 2009). The amount of compaction was measured and recorded. On extraction the cores were capped and labelled. Rotary drill cores allowed deeper penetration (up to 9 m) than could be achieved using percussion coring (maximum 6 m penetration). Drill cores were retrieved using a portable rotary drill rig system (Partain and Hopley, 1989) comprised of a core barrel (1.0 m long) with a diamond-toothed coring bit on the end for cutting through the substrate (Figure 1.4). The core tube is located within the core barrel and remains stationary despite the core barrel spinning during operation. A core catcher at the cutting end of the core barrel prevents captured core falling out of the core tube when the drill string is extracted from the reef. Extension rods (1.5 m long) were progressively attached to the core barrel allowing penetration to depths up to ~9 m. Notes were taken by the driller on the penetration and 'feel' as each core was collected, allowing cores to be corrected for compaction and for recovered material to be assigned a depth below substrate when recovery was <100% of the drive depth. After each core drive or 1.5 m extension, the captured material was carefully transferred to a

core tray, labelled and logged. After collection, all percussion and drill cores were transported to James Cook University where they were stored in a refrigerated room to prevent drying out.



Figure 1.4 (a) Percussion coring on the reef flat at Middle Island; (b) rotary drill rig set up on a fossil microatoll at Holbourne Island flat.

Following collection all percussion cores were split in half using a circular saw. Ensuring both halves were representative, one half was used for logging and analysis while the other was stored as an archive. Each core (including the drill cores) was logged and different reef facies were identified based on major changes in framework and sediment matrix composition downcore, including the presence/absence and type of coral and shell fragments, sediment matrix type, sorting and size, and whether the unit was matrix- or clast-supported, as in Perry and Smithers (2006).

To determine the sediment matrix grain size and carbonate percent characteristics (percussion cores only), standard techniques used for percussion cores were adopted (Perry et al., 2008, 2009, 2011), where around 20 g of sediment was sampled from 20 cm downcore (uncompacted) intervals throughout each core. Samples were rinsed, dried and split into two sub-samples: the carbonate content was analysed on one sub-sample and the grain size on the other. To determine carbonate content, the dry sub-sample was weighed before being digested in 2M hydrochloric acid until all carbonate material was dissolved (i.e. fizzing ceased). The remaining sample was dried and re-weighed to give the percent dry weight loss of the sample (carbonate material) after digestion. To determine the mud fraction of the sediment matrix (<63 micron

[μm] fraction), the dry sub-sample was weighed before being wet-sieved at 63 μm . The remaining sample $>63 \mu\text{m}$ was dried and weighed to calculate the percent dry weight loss of the original sample. The grain size distribution of the $>63 \mu\text{m}$ fraction was determined using a Rapid Sediment Analyser (RSA) settling tube with SedRep software (Gibbs et al., 1971; Kench and McLean, 1997). Carbonate content and grain size were not analysed for the drill core sediments because fine-grained material (muds and fine sands) was flushed out during the drilling process. Any sediment matrix that was retained was visually described according to Udden-Wentworth nomenclature.

1.9.3 Palaeo-ecology

Ecological composition throughout the percussion cores was analysed by removing all coral and shell material $>1 \text{ cm}$ from each 20 cm (uncompacted) downcore section. All material was washed, dried and weighed before coral clasts were identified and grouped according to genus using descriptions in Veron (1986), Coral Finder 2.0 (Kelley, 2009) and Budd et al. (2012). The weight of each taxonomic group relative to the total weight of the section was recorded and thus percent ecological composition was calculated, as per the methods in Perry and Smithers (2006) and Perry et al. (2008). In all cores, some clasts could not be accurately identified to genus level due to poor preservation and/or encrustation with coralline algae and these clasts were grouped together as 'un-identified' and classified as rubble. *In situ* coral clasts within the drill cores were identified to genus level where possible.

1.9.4 Fossil microatolls

Microatolls are discoid coral colonies with living polyps around their vertical edges and mostly dead flat upper surfaces, developed by the coral in response to prolonged sub-aerial exposure at low tide (Scoffin and Stoddart, 1978). The upper surfaces of open-water (freely connected with open-water tidal fluctuations) *Porites* microatolls are elevated within a narrow range ($\sim 10 \text{ cm}$) close to mean low water spring tide level (Chappell et al., 1983; Hopley and Isdale, 1977; Smithers and Woodroffe, 2000). Fossil microatolls that grew under higher mid-Holocene sea levels are preserved on many inshore reef flats, often more than a metre above their contemporary living counterparts (Hopley and Isdale, 1977; Scoffin and Stoddart, 1978; Chappell et al., 1983). A minimum age for the time a reef has been at sea level can be approximated from the ages of open-water fossil *Porites* microatolls. Thus, the elevations of fossil *Porites* microatolls of known age can be compared with the modern living equivalents to determine elevation changes in the confining water level over time. The location of and upper surface elevation of *Porites* microatolls at each reef flat were precisely measured using the RTK

GPS (Figure 1.3) and elevations were reduced to LAT. Small cores of coral skeleton (around 2.5 cm in diameter and 3.0 cm in length) were sampled from the surface outer edge of each fossil microatoll (Figure 1.3) to determine the age of the colony using either U-Th dating techniques (described in the following section) or radiocarbon dating (described in Chapter 5, section 5.4).

1.9.5 U-Th dating

Well-preserved corals that were considered to be in or very close to their growth position were selected from the cores for dating to determine the timing of reef initiation and key changes in reef development. Corals selected were regarded as *in situ* due to well-preserved delicate skeletal structures indicative of limited transport and the upward positioning and orientation of corallites. The core samples and fossil microatoll samples were vigorously cleaned and prepared for U-Th dating in the clean laboratory at James Cook University closely following procedures in Clark et al. (2014 a, b). Approximately 2 g of the cleanest section of each sample was collected and crushed to 1 mm grain size chips using an agate mortar and pestle, soaked in 10% AR grade hydrogen peroxide for 24 hours and then repeatedly rinsed with Milli-Q water in an ultrasonic bath until the water remained clear. This rigorous cleaning procedure ensures all detrital contaminants are removed from the coral skeleton. Each clean sample was then visually screened under a binocular microscope and approximately 500 – 1,500 mg of only the cleanest material (with no obvious cements or staining) was selected for U-Th dating. This rigorous visual inspection ensures the cleanest chips are selected for dating, which are the least likely to be affected by diagenesis and produce an incorrect U-Th age (Webb et al., 2016).

These samples were transported to the Radiogenic Isotope Facility at the University of Queensland for sample digestion, spiking, U-Th column chemistry and dating (using a Nu Plasma multi-collector inductively coupled plasma mass spectrometer [MC-ICP-MS]). Procedures closely followed those described in Zhou et al. (2011) and Clark et al. (2014a, b). Approximately 0.03 ml of a $^{229}\text{Th} - ^{233}\text{U}$ mixed spike was added to ultraclean beakers and the total weight was recorded. The spike was dried down on a hot plate and ~150 mg of pre-cleaned coral sample was added to the spiked beaker. The sample and spike were then dissolved in double distilled concentrated nitric acid and several drops of hydrogen peroxide were added to remove any organic contaminants. Each beaker was tightly capped and left on a hot plate overnight to completely dissolve. The beakers were then uncapped and the solution was dried down on a hot plate. Samples were then re-dissolved with 1 ml of 7M nitric acid before being passed through ion-exchange columns to separate the U from Th using standard column chemistry procedures, as in Clark et al. (2014 a, b). After collection, the separate U and Th

solutions were centrifuged at 4,000 rpm for 10 minutes and then screened to calculate amounts of each solution to be measured. All samples were subsequently measured for U-Th isotopes using the MC-ICP-MS using detailed procedures described in Clark et al. (2014a). Initial/detrital Th corrections were applied following procedures in Clark et al. (2014a) (see Appendix 2). Throughout this thesis, U-Th ages are presented as calendar years before present (yBP) \pm two standard deviations (σ), where present is defined as 1950 AD, to allow comparison with other published radiometric ages, the majority of which represent radiocarbon ages (calendar years before 1950 AD). U-Th ages of fossil microatoll samples from Holbourne Island are an exception, which are presented as calendar years AD (this is further explained in section 5.4, Chapter 5).

1.10 Thesis structure

Figure 1.5 presents a schematic overview of the thesis, identifying the major gaps in knowledge addressed in each chapter. Each data chapter (chapters 2 – 5) presents a new chronostratigraphic record of Holocene reef development and quantitative ecological data from each of the study sites, providing site-specific reef development histories and information about present reef benthic cover. Additionally, each data chapter presents unique and important insights into particular aspects of reef development (terrigenous sedimentation, cyclones and sea-level fall).

Chapter 2 is focused on the mainland-attached fringing reef at Bramston Reef. Very few reconstructions of reef development exist for mainland-attached fringing reefs, despite their close proximity to anthropogenic stressors and river mouths. This chapter presents the first record of internal reef growth structure from a mainland-attached fringing reef growing in a protected bay setting in the central GBR. A detailed sedimentological and palaeo-ecological record of the entire period of Holocene reef development was developed using percussion cores revealing that mainland-attached reefs can initiate and develop in muddy, sheltered locations upon unconsolidated substrates.

Chapter 3 highlights the importance of using long-term core records of reef development to understand present reef condition. Several studies have compared historical photographs of Stone Island reef flat from the late 1800s with recent photographs at the same site to reveal a change in coral cover and structural diversity. A decline in inshore reef condition has been inferred from these photographic comparisons without quantitative data on present reef condition or an understanding of the long-term reef development. This chapter aims to fill the gaps in knowledge about past and present reef condition at Stone Island and other inshore reefs in Edgumbe Bay. Two long-term records of fringing reef growth at Stone Island were

produced using percussion cores, which reveal important details about the timing and nature of reef development that are required to understand and contextualise the present reef condition. This chapter emphasises the value of combining datasets that cover multiple spatial and temporal scales when examining the effect of anthropogenic impacts on regional reef condition.

Chapter 4 addresses a knowledge gap surrounding the influence of cyclones on Holocene fringing reef development and is focused on Middle Island, located at the seaward margin of Edgecumbe Bay. The chronostratigraphy of the fringing reef at Middle Island was developed based on percussion and drill cores. Combined with descriptions and data on the present geomorphology at Middle Island reef and shoreline, the chronostratigraphy reveals new information about the potential morphological impacts of cyclones on reef development during the mid-Holocene. Evidence from Middle Island indicates that cyclones stripped the upper and outer reef structure in the mid-Holocene with the resultant excavated accommodation space being infilled by subsequent reef growth, possibly several times, but with the last phase occurring since 1,600 yBP.

Chapter 5 is focused on mid-shelf fringing reef development at Holbourne Island. The reef chronostratigraphy, based on percussion and drill cores, provides a rare record of fringing reef development on the mid-shelf in the central GBR with which inshore fringing reef records can be compared. Furthermore, this chapter reveals that last interglacial reef provides the basal foundation for the Holocene reef at Holbourne Island, revealing new insights about Pleistocene reef foundations in the central GBR. The influence of cyclones on mid-Holocene reef development and reef flat geomorphology over the past 600 years is investigated. The evidence from Holbourne Island conforms to the cyclone-stripping concept presented in Chapter 5.

Chapter 6 provides a general synthesis and discussion of the findings from the previous four chapters, presenting a detailed cross-shelf comparison of fringing reef development and present condition from the mainland to the mid-shelf in the central GBR. Details of fringing reef development (i.e. reef growth mode, initiation, vertical accretion rates, reef flat development, palaeo-ecological coral community composition) are compared between sites to identify any similarities and/or variations along the cross-shelf transect. The possible influences of accommodation space, sea-level change, and location with respect to exposure to cyclones and sedimentation on Holocene reef development are investigated.

Chapter 7 provides a brief overview of the thesis conclusions and suggestions for future research.

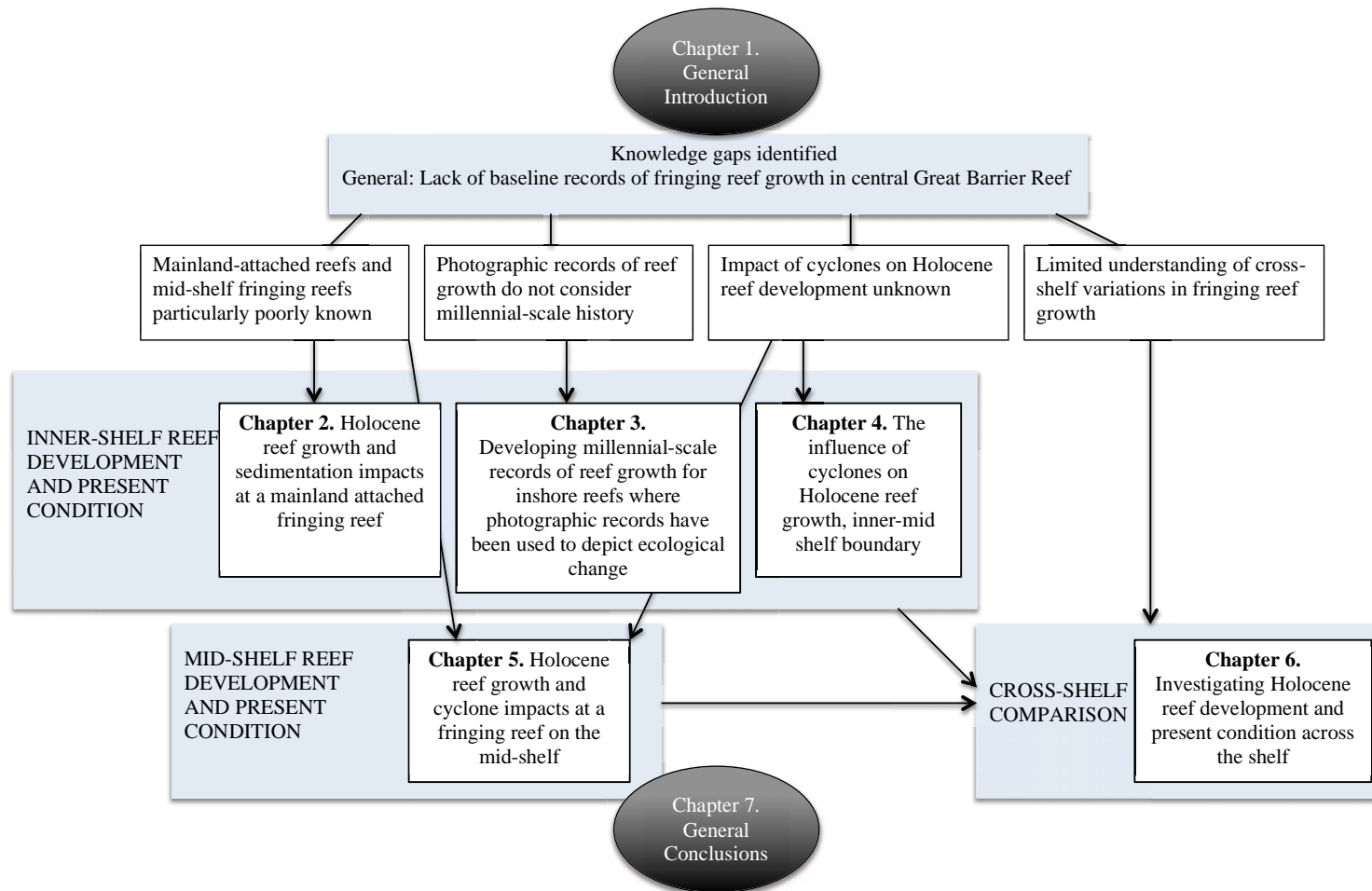


Figure 1.5 Schematic diagram of the overview of this thesis by chapter.

2 Chronostratigraphy of Bramston Reef reveals a long-term record of fringing reef growth under muddy conditions in the central Great Barrier Reef

Article published in 2016:

Ryan, E.J., Smithers, S.G., Lewis, S.E., Clark, T.R. and Zhao, J.X. 2016 Chronostratigraphy of Bramston Reef reveals a long-term record of fringing reef growth under muddy conditions in the central Great Barrier Reef. *Palaeogeography, Palaeoclimatology, Palaeoecology*, 441: 734-747.

In Chapter 1 I detailed the importance of long-term records from fringing reefs for understanding past and present reef condition. I identified several knowledge gaps, including the lack of long-term records from mainland-attached fringing reefs in the Great Barrier Reef, which are located closest to human impacts. In this chapter I present the first long-term record of reef growth from a mainland-attached reef in a sheltered bay setting in the central Great Barrier Reef.



Plate 2. Part of a percussion core from Bramston Reef, looking downcore and showing the excellent preservation of *in situ* coral material among a muddy sediment matrix.

2.1 Abstract

Inshore reefs on Australia's Great Barrier Reef (GBR) are widely argued to be in decline, although recent reports suggest that some may be more resilient than traditionally assumed. Resolution of this debate requires long-term insights into past reef development and variability to provide context for the assessment of present reef condition. Long-term reef growth histories can preserve extended records of reef growth and condition, however they are rare, especially for mainland-attached fringing reefs, which are themselves uncommon on the GBR. I examined the internal structure and ecology at Bramston Reef, a mainland-attached fringing reef located in a protected bay on the central GBR. Eight percussion cores were collected across the reef flat on a transect extending from the reef crest to the shore. Sedimentological and palaeo-ecological analyses coupled with uranium-thorium (U-Th) dating were used to develop the first reef growth history for a shore-attached fringing reef in this region. Twenty-five hard coral genera were identified in the palaeo-ecological analyses. The key reef-building genera (including *Acropora*, *Montipora*, *Euphyllia*, *Porites* and *Goniopora*) have contributed to reef growth since initiation and are represented in the extant coral community, despite a change in accretion 'mode' during the late Holocene. Sedimentological and stratigraphic investigations demonstrate that Bramston Reef has always grown in a mud-rich setting. U-Th ages indicate that reef initiation occurred at or before $5,396 \pm 51$ yBP in a palaeo-water depth of 2 – 3 m. Bramston Reef reached sea level by $4,256 \pm 14$ yBP when sea level was approximately 1 m higher than present, after which rapid seaward progradation occurred until around 3,000 yBP (~19 cm/yr on average). Between approximately 3,000 and 1,000 yBP seaward progradation of the reef flat slowed (to ~9.8 cm/yr on average). This deceleration of reef growth occurred long before European settlement of the Queensland coast and was driven by natural constraints, probably associated with limited accommodation space due to late-Holocene sea-level fall. The results of this chapter demonstrate that mainland-attached reefs can initiate and develop in muddy inshore environments over long timeframes (centuries to millennia).

2.2 Introduction

The capacity of coral reefs to withstand and/or recover from various natural and anthropogenic disturbances over longer timescales (centennial to millennial) remains poorly understood. Human activities can exacerbate the negative impacts of natural stressors on coral reefs (e.g. cyclone frequency and intensity [Done, 1992], changes in ocean temperature [Hoegh-Guldberg et al., 2007], terrestrial sedimentation [Risk, 2014], outbreaks of crowns-of-thorns starfish [Fabricius et al., 2010], and sea-level change [Woodroffe and Webster, 2014]) and are often implicated as drivers of changed reef condition (Wilkinson, 2008; De'ath et al., 2012; Roff et al., 2012). However, the impact of many natural and human-induced stressors on long-term

coral reef growth remains contentious. Arguably, inshore reefs on Australia's Great Barrier Reef (GBR) are threatened by a two- to ten-fold increase in sediment and nutrient loads since European settlement of the Queensland coast in the mid-1850s (van Woerik et al., 1999; Brodie et al., 2012; Kroon et al., 2012; Waters et al., 2014). Proximity to the coast potentially exposes inshore reefs to these pressures and elevates their vulnerability to degradation (Fabricius et al., 2005; Jupiter et al., 2008). However, many inshore coral reefs grow in naturally turbid settings, and have been shown to have high coral cover, diversity, and reef growth rates (Smithers and Larcombe, 2003; Perry et al., 2008; Roche et al., 2011; Roff et al., 2015), suggesting that inshore reefs may be more resilient than traditionally assumed. The debate as to whether anthropogenic-driven water quality decline is the main driver of recent changes in inshore reef condition thus continues, partly due to the paucity of historical baseline data on reef condition and poor understanding of reef-scale disturbance, resilience and recovery (with the exception of long-term coral community monitoring by Done et al. [2007]).

Many inshore reefs in the GBR initiated around 7,000 calendar years before present (yBP, where present is defined as 1950 AD), well before monitoring began (Hopley et al., 2007). Long-term sedimentological and palaeo-ecological records captured in the internal structures of these reefs can provide insights into reef condition over their accretion history, and critical context for the assessment of contemporary reef condition (Perry and Smithers, 2011; Roche et al., 2011; Roff et al., 2012). Although chronostratigraphic investigations of coral reefs are widely acknowledged as valuable archives of reef condition and growth (refer to Hopley [1982]; Kennedy and Woodroffe [2002]; Montaggioni [2005] and Hopley et al. [2007] for informative summaries), and improved methods have been applied to collect and date reef materials (Kennedy and Woodroffe, 2002; Smithers et al., 2006; Clark et al., 2012), detailed investigations of inshore reefs are rare, both globally and on the GBR. Of all inshore reefs in the GBR, it is the mainland-attached fringing reefs that are particularly poorly known, despite their proximity to anthropogenic pressures. To date, all studies of mainland-attached fringing reefs on the GBR have focused on reefs in relatively exposed coastal settings (Bird, 1971; Partain and Hopley, 1989; Roche et al., 2011).

Sea level is an important control on reef growth as it largely influences accommodation space and the timing of reef initiation and reef flat development (Kennedy and Woodroffe, 2002), and must be considered in interpretations of reef development and condition. Many inshore reefs on the GBR reached the sea surface at a time of higher relative sea level compared to today (Partain and Hopley, 1989; Kleypas, 1996; Smithers et al., 2006). As a result emergent backreef flats, which formed at elevations above the contemporary elevation of reef flat development,

characterise many of these reefs. On the GBR, by 7,000 yBP the post-glacial marine transgression (PGMT) had flooded most of the continental shelf, terminating at the mid-Holocene sea-level highstand and allowing inshore reefs to begin to grow (Hopley et al., 2007). The details of the timing, elevation and duration of this sea-level highstand remain contentious, but it is generally agreed that by around 6,000 or 7,000 yBP mean sea level was ~1 m higher than present (Perry and Smithers, 2011; Lewis et al., 2013).

This study presents the first ecological and sedimentary record of a mainland-attached fringing reef growing in an enclosed bay setting in the central GBR, where restricted water circulation might be expected to enhance the negative impacts of modified catchment land-use on coral reefs compared to open coast settings. This record, based on eight percussion cores pushed deep into the Holocene reef structure along a landward to seaward transect, spans the entire period of Holocene reef growth to reveal the age of reef initiation, how the reef developed (growth 'mode'), and rates of lateral and vertical growth (along with variability through time). I examine past and present coral community assemblages and sedimentary regimes to improve our understanding of changes in reef development over the Holocene.

2.3 Study site and environment

Bramston Reef (148°15'E, 20°03'S) is a mainland-attached fringing reef located in Edgecumbe Bay, ~4 km south of the Bowen township (Figure 2.1). A detailed description of the climatic and hydrodynamic setting of Edgecumbe Bay is presented in section 1.8. The modern reef flat at Bramston Reef is ~900 m wide. The muddy backreef zone is sparsely covered with seagrass and extends ~100 m from the shoreline where it transitions into a reef flat surface dominated by coarse carbonate sands (mainly shell and coral fragments with minor foraminifera, *Halimeda*, coralline algae and terrigenous components), coral gravels and fossil corals at ~0.6 m above the lowest astronomical tide (LAT) level. This surface extends approximately 400 m seaward before sloping toward the reef edge at approximately -0.1 mLAT a further 400 m offshore. Terrigenous sands and muds that dominate the seafloor of Edgecumbe Bay are regularly re-worked and re-suspended by waves and currents, creating persistently turbid water conditions.

Historical photographs and descriptions of Bramston Reef made circa. 1890 (Saville-Kent, 1893, photographs presented in Appendix 1) provide a valuable snapshot of reef condition at the time of Saville-Kent's visit. Saville-Kent (1893 pp.15) described a mainland reef "in the immediate neighbourhood of Adelaide Point", which is at the south-eastern end of Bramston Reef. Saville-Kent (1893) detailed "a grand mass of *Porites*... its exposed, horizontal surface is for the most part dead and eroded... the eroded upper surface has been adopted as a fulcrum of

attachment by various coral types that flourish on a higher vertical plane including *Goniastrea* and *Madrepora*” (p.15). Saville- Kent (1893) is clearly describing a *Porites* microatoll, fine specimens of which can be observed near the contemporary reef crest (Figure 2.2). He also noted “abundant development thereon of a luxuriant crop of seaweeds...an extensive crop of these algae, mixed with coral growths, is conspicuous” (Saville-Kent, 1893 p.15).

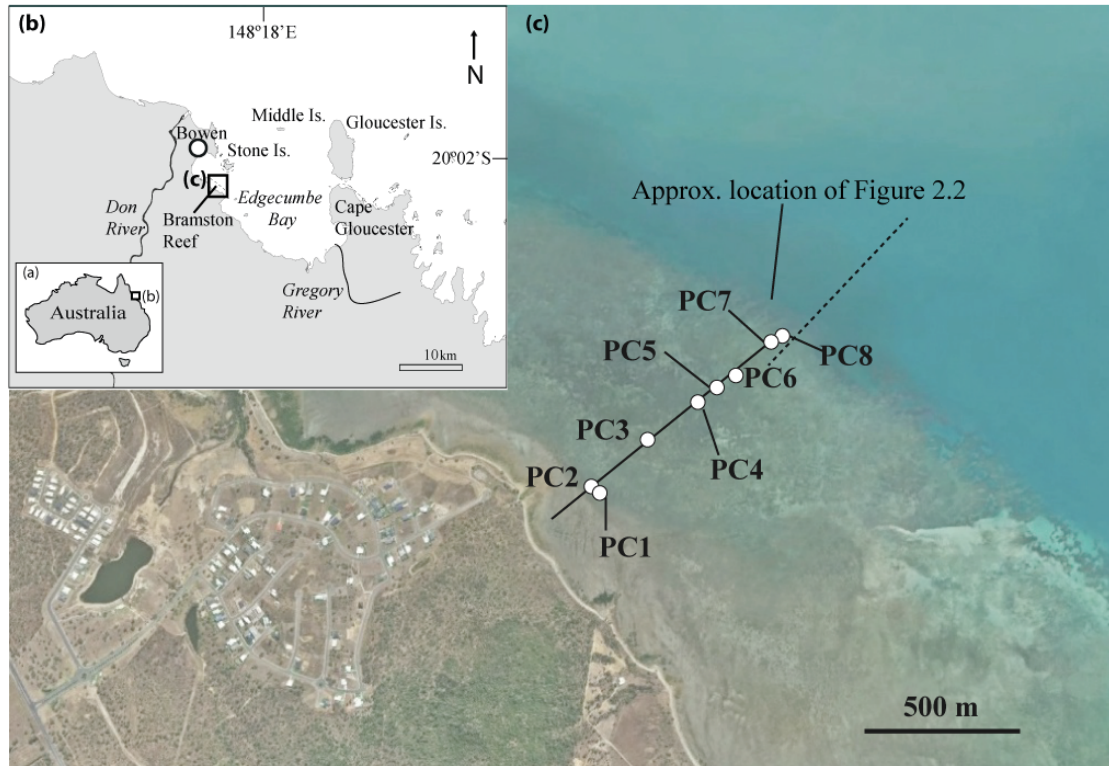


Figure 2.1 Location of a) Edgcumbe Bay in Australia, b) Bramston Reef in Edgcumbe Bay and c) Bramston Reef flat transect (solid line) indicating percussion core locations (white circles) and drop camera transect (dashed line).



Figure 2.2 Photograph of *Porites* colonies at Bramston Reef, showing upper surfaces colonised with macroalgae, hard corals and soft corals, with Stone Island (SI), Gloucester Island (GI) and Cape Gloucester (CG) in the background. The approximate location of this photograph is shown in Figure 2.1 and the elevation is given in Appendix 10.

2.4 Materials and methods

A detailed description of the research methods is provided in Chapter 1, section 1.9. Reef flat morphology and topography was surveyed along a transect running perpendicular to the shore (Figure 2.1) using a Real Time Kinematic (RTK) Global Positioning System (GPS). Elevation data were reduced to LAT at the Abbot Point tide gauge (BOM, 2016b). The contemporary benthic composition was quantified from reef flat and slope photographs from each eco-geomorphological zone that were captured using photo quadrat or video surveys. Benthic cover was quantified using Coral Point Count with Excel extensions software (Kohler and Gill, 2006) based on the proportional cover of living coral, reef framework, algae, seagrass, sand, lithic rubble and coral rubble.

The elevations of the tops of fossil *Porites* microatolls across Bramston Reef flat were measured using the RTK GPS and compared with modern living equivalents to determine the relative elevation difference (and thus the difference in the limiting water level elevation at the time each colony grew). Twelve fossil microatoll ages were determined from coral cores sampled from the colony rim on each fossil microatoll. Samples were thoroughly cleaned and dated using high precision uranium-thorium (U-Th) techniques described in section 1.9.5.

Eight percussion cores extending down to 4.6 m below the present surface (Table 2.1) were collected across the reef flat transect (Figure 2.1). The percussion coring technique is detailed in section 1.9.2. Total compaction within the eight cores varied from 5.0% to 30.1% (Table 2.1). Following collection, cores were split in half and seven different sediment facies were identified throughout the cores (five reefal facies and two terrigenous facies) based on logs of downcore changes in framework and matrix characteristics, including the presence or absence of coral and shell fragments, sediment type, sorting and size, and whether the unit was matrix- or clast-supported. Matrix sediments were sampled at 20 cm (uncompacted) intervals throughout each core, ensuring all facies were sufficiently sampled. Samples were split into two sub-samples: the carbonate content was determined using one sub-sample and particle size distribution on the other, as described in section 1.9.2. Acid digestions indicate that the mud fraction of the sediment matrix (<63 microns [μm]) at Bramston Reef is predominantly composed of non-carbonate terrigenous sediments. Ecological composition of carbonate producers throughout the cores was analysed by measuring the proportional dry weight of different groups of coral genera and shell material >1 cm from each 20 cm (uncompacted) downcore section, as described in section 1.9.3. Thirteen *in situ* coral clasts were selected from the cores for dating, using U-Th techniques described in section 1.9.5. The ages of corals within

the cores and microatolls can be used to reconstruct histories of reef growth and reef flat formation.

Table 2.1 Details of percussion cores (total length, penetration and compaction rates) collected from the Bramston Reef flat.

Core	Date recovered	Core length (m)	Penetration (m)	Compaction (%)
PC1	24/05/13	1.6	1.8	9.5
PC2	24/05/13	2.0	2.2	8.3
PC3	18/08/13	3.4	4.0	15.1
PC4	06/05/13	1.9	2.3	18.1
PC5	06/05/13	1.7	2.0	12.7
PC6	18/08/13	3.4	4.5	25.1
PC7	18/08/13	3.2	4.6	30.1
PC8	24/05/13	3.2	3.8	16.4

2.5 Results

2.5.1 Present morphology and ecology

Ten eco-geomorphological zones were identified across the transect at Bramston Reef, five on the reef flat and five on the reef slope (Figure 2.3), the details of which are summarised in Table 2.2. Zone 1 extends 14 m from the shoreline and is characterised by terrigenous rubble among muddy sands. Zone 2 extends a further 100 m offshore and consists of a muddy backreef zone with sparse seagrass cover. Zone 2 gradually transitions to zone 3, which is 200 m wide and dominated by biogenic reefal carbonate sediments with some terrigenous sands but no mud. The shoreward 100 m or so of zone 3 was dominated by seagrass ($54.1 \pm 17.8\%$ [mean $\pm 1\sigma$ standard deviation]) and macroalgae ($33.2 \pm 19.0\%$). Zone 4 lies between 314 – 774 m along the transect and was also dominated by seagrass ($54.1 \pm 22.2\%$) and macroalgae ($43.0 \pm 22.9\%$) cover. Although no live corals were encountered in zone 4 on the transect due to the random sampling strategy, live coral was found on the reef flat adjacent to the transect location at similar elevations to that of zone 4 ($\sim 0.4 - 0.1$ mLAT). The presence of fossil microatolls on the reef flat surface differentiates zone 4 from zone 3. Fossil microatolls (mainly *Porites*) distributed across zone 4 varied between 1.7 – 5.7 m in diameter with their upper surfaces elevated between 20 – 50 cm above the reef flat surface, corresponding to 0.8 – 0.4 mLAT. Zone 5 includes 130 m of reef flat extending seaward from zone 4 (marked by the most seaward fossil microatoll) towards the reef edge. Zone 5 was also characterised by mixed carbonate and terrigenous sands with sparse coral rubble, but in contrast to zones 3 and 4, had a lower cover of seagrass ($25.9 \pm 49.4\%$) and macroalgae ($20.4 \pm 40.7\%$). Here, live corals also contributed to benthic cover ($13.9 \pm 19.2\%$). Groups of living *Porites* colonies (Figure 2.2) were present in

zone 5 but were not included in the benthic composition because they were not captured by the random sampling strategy. The living *Porites* colonies had upper surfaces elevated ~0.7 m above the reef flat surface with the colonies' living rims being on average 0.3 m LAT. 'Fields' of coalesced microatolls (Figure 2.2) measured up to 28 m wide. The dead upper surfaces of these living microatolls were colonised by a variety of live soft and hard corals (commonly *Lobophyllia*, branching *Acropora* and massive *Goniastrea* and *Platygyra*), macroalgae, and *Tridacna*.

Although there was no abrupt reef crest, the reef slope began approximately 900 m offshore at an elevation of -0.5 m LAT and was divided into 5 zones (beginning at zone 6) with spatially variable benthic cover according to the substrate and the dominance of macroalgae (including *Amphiora*, *Padina* and *Sargassum*) or hard corals. Thirteen coral genera were recorded living on the reef slope: *Acropora*, *Calaustrea*, *Dipsastraea*, *Euphyllia*, *Fungia*, *Galaxea*, *Goniastrea*, *Goniopora*, *Montipora*, *Porites*, *Seriatopora*, *Stylophora* and *Turbinaria*. Zone 6 extended ~180 m offshore from the reef edge and was characterised by a sandy substrate with high macroalgae cover ($92.6 \pm 8.5\%$). At approximately -2.0 m LAT, zone 6 abruptly transitioned to a live coral framework zone (zone 7), with reduced macroalgae cover ($21.7 \pm 29.7\%$). Live corals covered over half ($51.3 \pm 19.4\%$) of the sandy substrate in this zone, which extended for ~130 m. An abrupt end to the coral framework zone occurred -3.5 m LAT, where high macroalgae cover ($89.6 \pm 16.2\%$) dominated zone 8 and extended for ~80 m until the substrate transitioned to silty-sand at a depth of -4.5 m LAT (start of zone 9). Live coral cover ($35.2 \pm 30.8\%$) increased in zone 9 which was ~200 m wide and gradually sloped down to -5.5 m LAT where the reef slope ended and terrigenous muds and sands dominated thereafter (zone 10).

2.5.2 Palaeo-ecology

The excellent preservation of coral skeletal material throughout the cores allowed identification to genus level. Palaeo-ecological abundance data are presented in Figure 2.4 and variation throughout and between cores was examined. Skeletal material from 25 hard coral genera was identified throughout the eight cores (*Acropora*, *Astreopora*, *Calaustrea*, *Coelerosis*, *Cyphastrea*, *Dipsastraea*, *Echinopora*, *Euphyllia*, *Favites*, *Fungia*, *Galaxea*, *Goniastrea*, *Goniopora*, *Hydnophora*, *Isopora*, *Lobophyllia*, *Montipora*, *Oxypora*, *Pavona*, *Pectinia*, *Porites*, *Seriatopora*, *Stylophora*, *Trachyphyllia* and *Turbinaria*). The most abundant genera were *Acropora*, *Montipora*, *Calaustrea* and *Euphyllia* and the least abundant were *Astreopora*, *Coelerosis*, *Isopora*, *Seriatopora* and *Trachyphyllia*. Each of the least abundant genera were recovered in only one core and comprised <25% of one 20 cm downcore section. The genera *Acropora*, *Montipora* and *Euphyllia* were each recovered in seven of the eight cores. *Montipora*

was only found in the upper 1.8 m of the cores, while *Acropora* and *Euphyllia* were recovered at all depths throughout the cores (up to 3.4 m and 4.4 m downcore, respectively). The upper 2 m of most cores contained material from as many as 10 different genera comprising relatively small percent abundances, in contrast to sections below this depth, which tended to be dominated by material from a single coral genus (e.g. *Goniopora*, *Calaustrea* or *Echinopora*). Molluscan shell and spiculite clusters derived from soft corals were dominant contributors to the community assemblage in only a few sections (e.g. shell comprised 77% of the total weight in the 40 – 60 cm downcore section of PC1, while soft coral spiculite represented 54% of the total weight in the 160 – 180 cm downcore section of PC1; Figure 2.4). In all cores, the abundance of shell fragments was greatest in the uppermost metre, with the exception of PC3, in which shell was more abundant in the bottom metre directly above the pre-reefal surface (between 2.5 – 3.5 m below the surface).

Table 2.2 Eco-geomorphological zones on the transect at Bramston Reef. Oldest known surficial ages are based on uranium-thorium ages obtained from (Figure 2.3) and Appendix 2. Elevations are relative to lowest astronomical tide (LAT).

Zone number	Description	Width (m)	Approximate elevation relative to LAT (m)	Live coral cover (mean $\pm 1\sigma$ %)	Oldest known surficial age
1	Terrigenous rubble	14	0.6	0	~3,000 yBP
2	Silt-covered backreef	100	0.6	0	~3,000 yBP
3	Sandy backreef with algae and seagrass	200	0.6	0	3,526 yBP
4	Reef flat fossil microatoll zone with algae and seagrass	460	0.6 to -0.1	0	4,256 yBP
5	Reef flat live coral zone	130	-0.1 to -0.5	13.9 \pm 19.2	~1,000 yBP to modern
6	Beginning of sandy reef slope with macroalgae dominant	180	-0.5 to -2.0	0	Modern
7	Live coral zone on slope	130	-1.5 to -3.5	51.3 \pm 19.4	Modern
8	Macroalgae dominant slope	80	-3.5 to -4.5	3.0 \pm 6.6	Modern
9	Reef front with living coral and macroalgae	200	-4.5 to -5.5	35.2 \pm 30.8	Modern
10	Terrigenous muds and sands	-	> -5.5	0	Modern

2.5.3 Reef growth and variability

The chronostratigraphy of Bramston Reef was inferred from the cores collected along the transect (Figure 2.4). The entire Holocene reef sequence was penetrated in PC2 and PC3 (located at the backreef), which both terminated in pre-reefal Pleistocene clays. A sand and gravel layer deposit on which the reef initiated lies above these clays (Figure 2.4). The main Holocene reef unit is ~4 m thick and includes five distinct sediment facies (A – E; see Table 2.3

for descriptions). The five reefal sediment facies overlie two pre-reefal facies; facies F includes transgressive sands and gravels and facies G consists of weathered Pleistocene clays. In general, the cores coarsen upwards, as the $<63 \mu\text{m}$ mud fraction decreases towards the surface where medium-coarse sands dominate. The $>63 \mu\text{m}$ fraction of the matrix for all facies is generally poorly sorted (Table 2.3) and mostly dominated by medium-coarse sand between 2,000 – 250 μm in size (Figure 2.4).

Facies containing $>30\%$ mud dominate (facies C – E), making up all but the uppermost metre of the reef units in most cores (Figure 2.4). Terrigenous mud-rich units varying from 25 – 75 cm thick that lack coral clasts (facies E) occur in four cores (PC3, 5, 6 and 7). Facies E contains $41.1 \pm 19.1\%$ mud and a relatively low carbonate content ($47.3 \pm 10.8\%$) compared to other facies (Table 2.3). The terrigenous mud layers are relatively horizontally uniform and occur throughout the Holocene period of reef growth: prior to $4,175 \pm 12$ yBP (PC3), just after $3,786 \pm 14$ yBP (PC6) and between $2,265 \pm 9$ – $1,969 \pm 13$ yBP (PC7).

The U-Th ages throughout the cores allow a reef growth chronology to be developed (Figure 2.3). Bramston Reef began to grow $\sim 5,396 \pm 51$ yBP 150 – 250 m offshore from the beach, approximately 2 m below the present reef flat surface. The reef rapidly accreted to reach sea level and form a reef flat, indicated by a microatoll age of $4,256 \pm 14$ yBP located on the reef flat very close to the top of PC3 (Figure 2.3). Vertical accretion averaged between 2.5 – 3.6 mm/yr between $\sim 5,396$ – 3,000 yBP. For a thousand or so years after reef flat development began, seaward reef flat progradation averaged 19 cm/yr (Figure 2.3). Reef flat progradation slowed after 3,000 yBP, averaging 9.8 cm/yr. However, over this same period, episodes of rapid vertical reef accretion (up to 9.8 mm/yr) can be identified in cores collected from the seaward section of the reef flat.

2.6 Discussion

A growing number of studies have linked changes in inshore coral reef ecology on the GBR with water quality declines associated with European modification of catchments (van Woesik et al., 1999; Fabricius et al., 2005; Cooper et al., 2007) together with global climate change impacts (Hoegh-Guldberg et al., 2007; De'ath et al., 2012). However, the ecological condition of inshore coral reefs on the GBR is particularly variable in time and space and few long-term data are available, making it difficult to directly determine the extent and causes of declines in reef condition. My data provide insights into how a mainland-attached fringing reef in a protected bay setting has developed over the mid-late Holocene, and thus provides useful context for assessments of changes in reef condition since European settlement. The sheltered

and supposedly poorly flushed (Brodie et al., 2014) setting of Bramston Reef may lead to expectations that this site would be more vulnerable to the negative impacts of human land use changes than similar reefs in open coast settings.

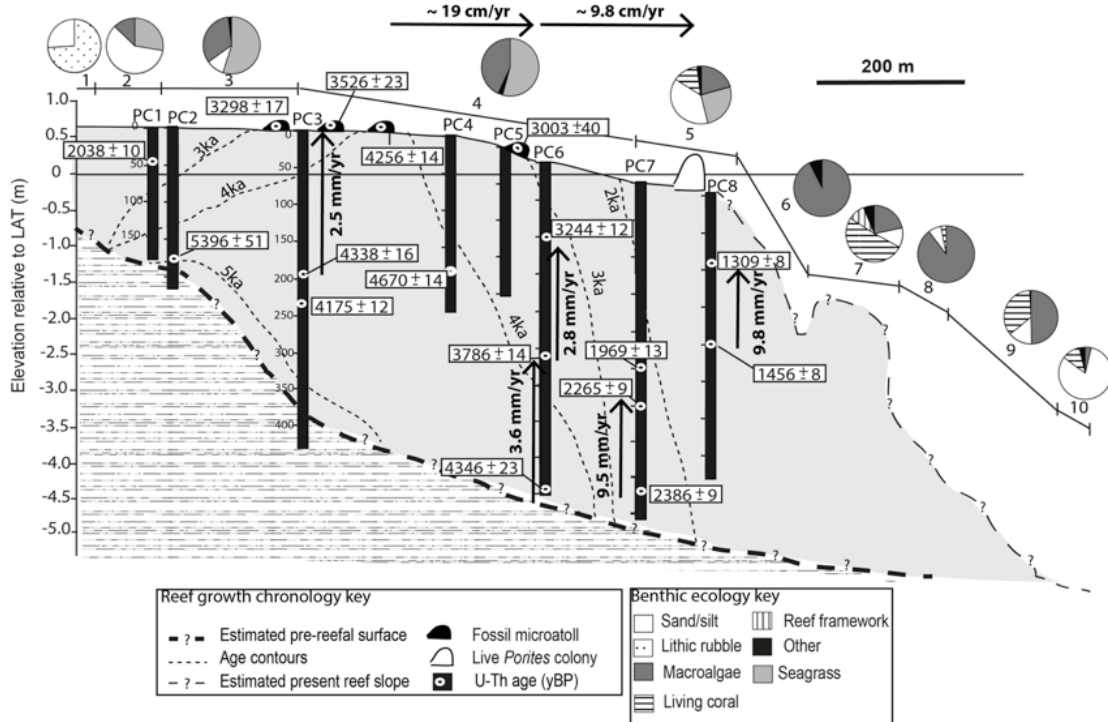


Figure 2.3 Bramston Reef flat profile extending seaward, with reef age indicated by the uranium-thorium (U-Th) ages (yBP $\pm 2\sigma$) from percussion cores (core locations shown by black rectangles) and microatolls. Vertical and horizontal arrows show average reef growth rates. Benthic composition of each eco-geomorphological zone on the present reef flat (numbered 1 – 10) is indicated by the shaded pie charts. Elevation is relative to lowest astronomical tide (LAT).

2.6.1 Comparing past and present ecology

The palaeo-ecological record preserved in the reef cores indicates high coral diversity with at least 25 coral genera having persisted through time at Bramston Reef (Figure 2.4), similar to inshore reefs elsewhere in the GBR (Smithers and Larcombe, 2003; Perry et al., 2008; Browne et al., 2010). The most common and abundant genera were *Acropora*, *Montipora* and *Euphyllia*, which were each recovered throughout seven of the eight cores. Less abundant coral genera that were found sporadically throughout the palaeo-ecological record included *Astreopora*, *Coelerosis*, *Isopora* and *Seriatopora*, which were each recovered in only one core; *Dipsastraea* in two cores; and *Galaxea* and *Stylophora* each in three cores. The upper 2 m of the percussion cores contained a more diverse coral assemblage, but in lower percent abundance than downcore segments below this depth (Figure 2.4 and Figure 2.5). This shift was visible in most cores across the transect (thus at different times over the mid- to late-Holocene), suggesting the

Table 2.3 Core facies descriptions and matrix components including percent (mean \pm 1 σ) sand vs. mud, percent (mean \pm 1 σ) carbonate content, and mean grain size (mgs) of the sand fraction.

Facies		A	B	C	D	E	F	G
Facies name		Contemporary intertidal sands	Reef framework, sandy matrix	Reef framework, sandy-mud matrix	Reef framework, mud matrix	Terrigenous mud-silt unit	Transgressive sands and gravels	Pleistocene clay
Description		Sandy matrix with matrix-supported encrusted coral rubble, shell hash and organic material	Sandy matrix (generally clast-supported) with coral clasts, shell hash, bivalves	Sandy-mud matrix with coral clasts (clast-supported) bivalve, shell hash	Mud matrix dominated by coral clasts, generally clast-supported with some matrix supported units	Muddy silt matrix (terrigenous dominant) with a little shell hash or small coral rubble (matrix-supported), but no coral clasts	Small unit (~10 cm thick) of lithic gravels and sand	Weathered clay (pre-transgression)
Matrix component	% sand	85.8 \pm 5.2	82.9 \pm 4.6	67.6 \pm 12.5	46.2 \pm 17.4	58.9 \pm 19.1	53.0 \pm 2.6	-
	% mud	14.2 \pm 5.2	17.1 \pm 4.6	32.4 \pm 12.5	53.8 \pm 17.4	41.1 \pm 19.1	47.0 \pm 2.6	-
	% carbonate	56.0 \pm 24.1	73.1 \pm 12.0	63.6 \pm 13.7	55.6 \pm 7.1	47.3 \pm 10.8	-	-
	mgs (μ m)	392	503	624	543	323	506	-

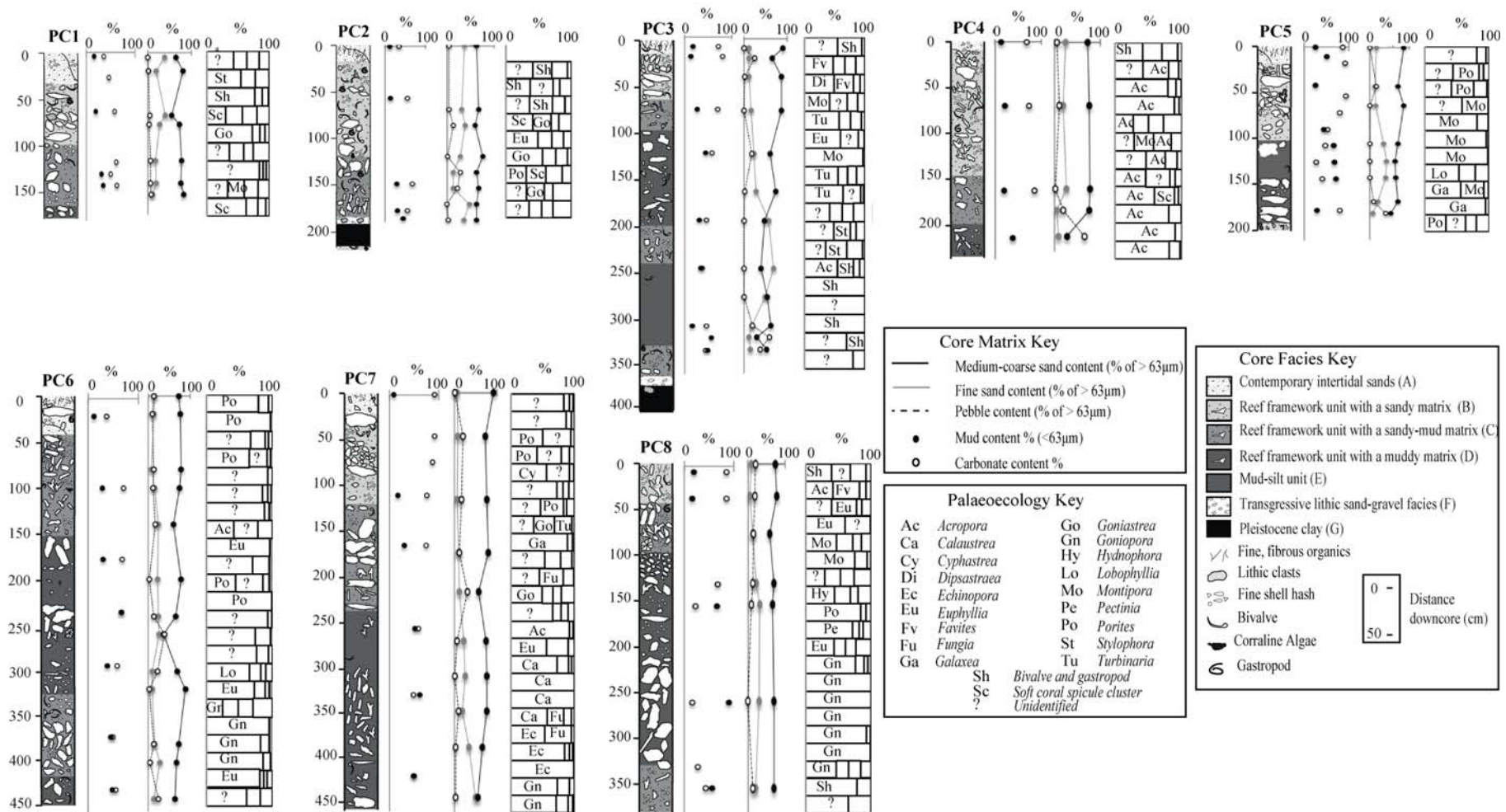


Figure 2.4 Composite core logs showing (left to right) sedimentary facies, carbonate and terrigenous mud content of the matrix, grain size content and palaeoecology data. Palaeo-ecology data are shown as percent abundance of the total carbonate content >1 cm in size. Dominant coral genera (comprising >25% of each segment) are labelled for each 20 cm downcore segment.

upcore shift to a higher diversity suite of corals is independent of time and reliant on depth. It is likely a function of the reef shallowing to sea level and experiencing altered hydrodynamic and water quality conditions (Perry et al., 2008, 2009), rather than a temporal shift in coral ecology.

Depth downcore is not indicative of time (Figure 2.5) as the cores were collected from different parts of the reef flat that developed at different times in the mid- to late-Holocene (Figure 2.3). Skeletal material from the major contributors to the palaeo-ecological record (*Acropora*, *Montipora*, *Euphyllia*, *Porites*, *Goniopora*, *Goniastrea*, *Favites*, *Turbinaria*, *Galaxea*, *Fungia*, *Dipsastraea*, *Stylophora*, *Lobophyllia* and *Pectinia*) was recovered throughout the cores, independent of time (Figure 2.5). Although there were changes within and between cores, these changes appear to be driven not by time, but by changes in palaeo-depth associated with upwards reef growth towards a confining sea level. The persistence of most key reef-building corals through time is consistent with the results reported from other inshore reefs on the GBR (Browne et al., 2013). Many of the persistent genera are turbidity and sedimentation tolerant corals (including *Porites*, *Turbinaria*, *Montipora*, *Goniopora* and *Galaxea*) and they were present in the video transect survey of the modern reef slope. The video survey revealed that present coral growth was patchy on the contemporary reef slope and there were zones of abundant macroalgae growth (covering up to $92.6 \pm 8.5\%$). However, all 13 living coral genera (listed in section 2.5.1) identified along the drop camera video transect of the reef slope were present in the palaeo-ecological record established from the percussion cores and contributed to reef-building throughout the Holocene (Figure 2.4). Both the extant corals and those in the palaeo-ecological record display a variety of growth morphologies, including branching, foliaceous, massive, plate, encrusting and free-living colonies (Figure 2.6).

2.6.2 Holocene reef evolution

The chronostratigraphy established from the cores along with U-Th ages (Figure 2.3) indicates that Bramston Reef was constructed in two temporally distinct phases. Only one age reversal (163-year reversal in PC3 separated by a 40 cm interval) occurred across all the cores, increasing confidence that corals selected for dating were *in situ* corals or subject to limited post-mortem transport or re-working. Johnson and Risk (1987) suggested that reversals in closely-spaced age data from reef cores reflect the dynamic nature of storm-associated re-working and erosion of coral debris. Absence of such reversals may reflect limited storm re-working of coral material at Bramston Reef, as might be expected given its sheltered shore-attached location. During the first growth phase (extending from or before 5,396 yBP to ~3,000 yBP) most of the presently exposed reef flat was emplaced. The second phase extended from

~3,000 yBP to the present, under falling sea-level (Lewis et al., 2013), during which seaward progradation dominated and the reef flat surface became progressively lower in elevation. Similar sedimentary facies characterised the two phases of growth (Figure 2.4) indicating that the entire accretion history occurred in a predominantly muddy environment. This accretion pattern and timing is similar to that established for other fringing reefs in the central GBR, where sea-level constraints on accommodation space have been inferred to be likely drivers (Perry et al., 2011). A detailed model of Holocene reef development at Bramston Reef is presented in Figure 2.7 and discussed below.

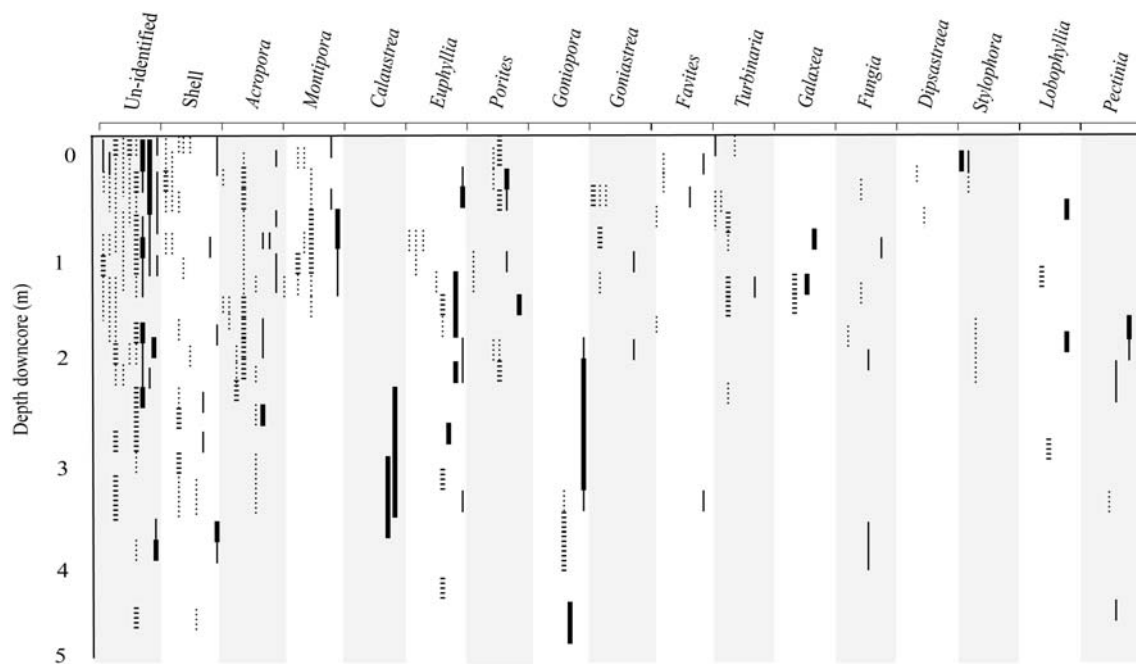


Figure 2.5 Downcore abundance of major coral genera (comprising >10% of total composition in more than one percussion core). Each core is represented individually within each group; PC1 at the start of the group through to PC8 at the end of the group. Time is indicated by dashed lines (older than 3,000 yBP) and solid lines (younger than 3,000 yBP). A thick line represents coral genera contributing to $\geq 50\%$ of the total coral composition, while a thin line represents a contribution $< 50\%$.

Growth phase 1 – initiation, rapid vertical growth and progradation

Coral colonies at Bramston Reef established $\sim 5,396 \pm 51$ yBP during the mid-Holocene sea-level highstand (Chappell et al., 1983; Lewis et al., 2013), probably within a shallow, subtidal setting (in a palaeo-water depth 2 – 3 m below LAT at the time). Bramston Reef initiated upon a layer of terrigenous sands and gravels overlaying weathered Pleistocene clay. The sands may

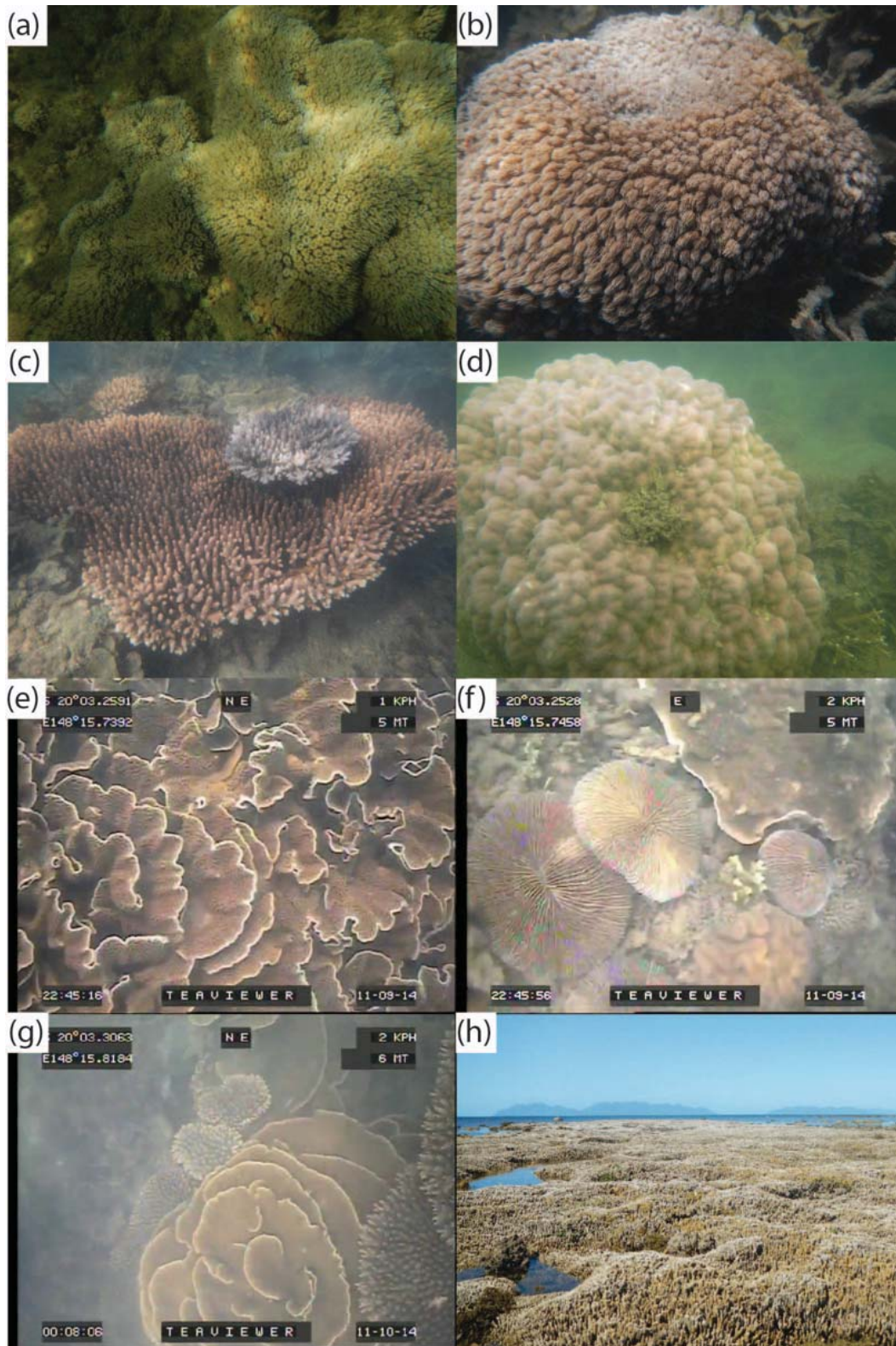


Figure 2.6 Photographs of the various live coral morphologies at Bramston Reef. Massive colonies of *Galaxea* (a) and *Goniopora* (b), plate colony of *Acropora* (c), massive *Porites* colony (d), foliaceous *Turbinaria* (e), free-living *Fungia* and encrusting coral (f), plate *Acropora* and *Turbinaria* (g) and branching *Montipora* on the reef flat (h). See Appendix 10 for elevation of (h).

have been worked onshore during the PGMT (Hopley et al., 1983), however the gravels were angular (similar to those in zone 1 of the eco-geomorphological transect) indicating that they were probably lag deposits left behind as fine sediments were mobilised and exported as the substrate was transgressed. These are common pre-reefal substrates in the inshore GBR (Hopley et al., 1983; Smithers and Larcombe, 2003; Perry et al., 2009; Lewis et al., 2012). The timing of initiation is similar to that at King Reef (initiation 5,600 – 5,900 yBP; Roche et al., 2011); a mainland-attached reef located approximately 350 km north of Bramston Reef. However, reef initiation occurred around two thousand years earlier on other fringing reefs as the inshore GBR was transgressed near the end of the PGMT (Perry and Smithers, 2011). The lag between the sea-level transgression and reef growth that occurred at Bramston Reef may reflect past water quality or substrate limitations making reef initiation difficult (Hopley et al., 1983). Indeed, the 75 cm-thick mud unit (facies E) near the base of PC3 (Figure 2.4) indicates terrigenous sedimentation was high in the early stages of Bramston Reef development.

After initiation in a subtidal environment, Bramston Reef rapidly vertically accreted in ‘catch up’ mode (Neumann and MacIntyre, 1985) to reach sea level. Current literature indicates sea level was approximately 1 m higher than present for the central GBR region ~7,000 – 5,000 yBP (Lewis et al., 2013). Based on the elevation difference between modern microatolls at Bramston Reef and a U-Th age of $4,256 \pm 14$ yBP obtained from a fossil microatoll, sea level at Bramston Reef ~4,000 yBP was at least 0.3 m higher than present and must have begun falling from the highstand (Lewis et al., 2013). During this catch-up phase around 3 – 4 m of reef framework was deposited in less than 1,000 years over what is now the backreef section of Bramston Reef as accommodation space was ample (Figure 2.7). Once the reef initially reached sea level $\sim 4,256 \pm 14$ yBP, reef flat development began as the reef accreted seaward because vertical accommodation space was limited by the defining sea level (Figure 2.7). The ‘up and out’ growth mode displayed at Bramston Reef conforms to Kennedy and Woodroffe’s (2002) fringing reef growth model Type A. Similar growth modes have been observed on other fringing reefs in the GBR (Hopley et al., 1983; Lewis et al., 2012) and Hawaii (Easton and Olsen, 1976).

Average rates of vertical accretion (determined from U-Th dated cores) between ~4,500 and 3,000 yBP were rapid (between 2.5 – 3.6 mm/yr) for fringing reefs. These rates exceed those for fringing reefs (average of ~1.6 mm/yr; Hopley et al., 2007) over this time period and are comparable to average rates of vertical accretion on outer platform reefs (average of ~3.3 mm/yr; Hopley et al., 2007) and other inshore fringing reefs in the central GBR (average of 3.0 – 6.5 mm/yr; Perry and Smithers, 2011). High rates of vertical accretion at Bramston Reef can be attributed to rapid accumulation of carbonate and terrigenous material (including terrigenous

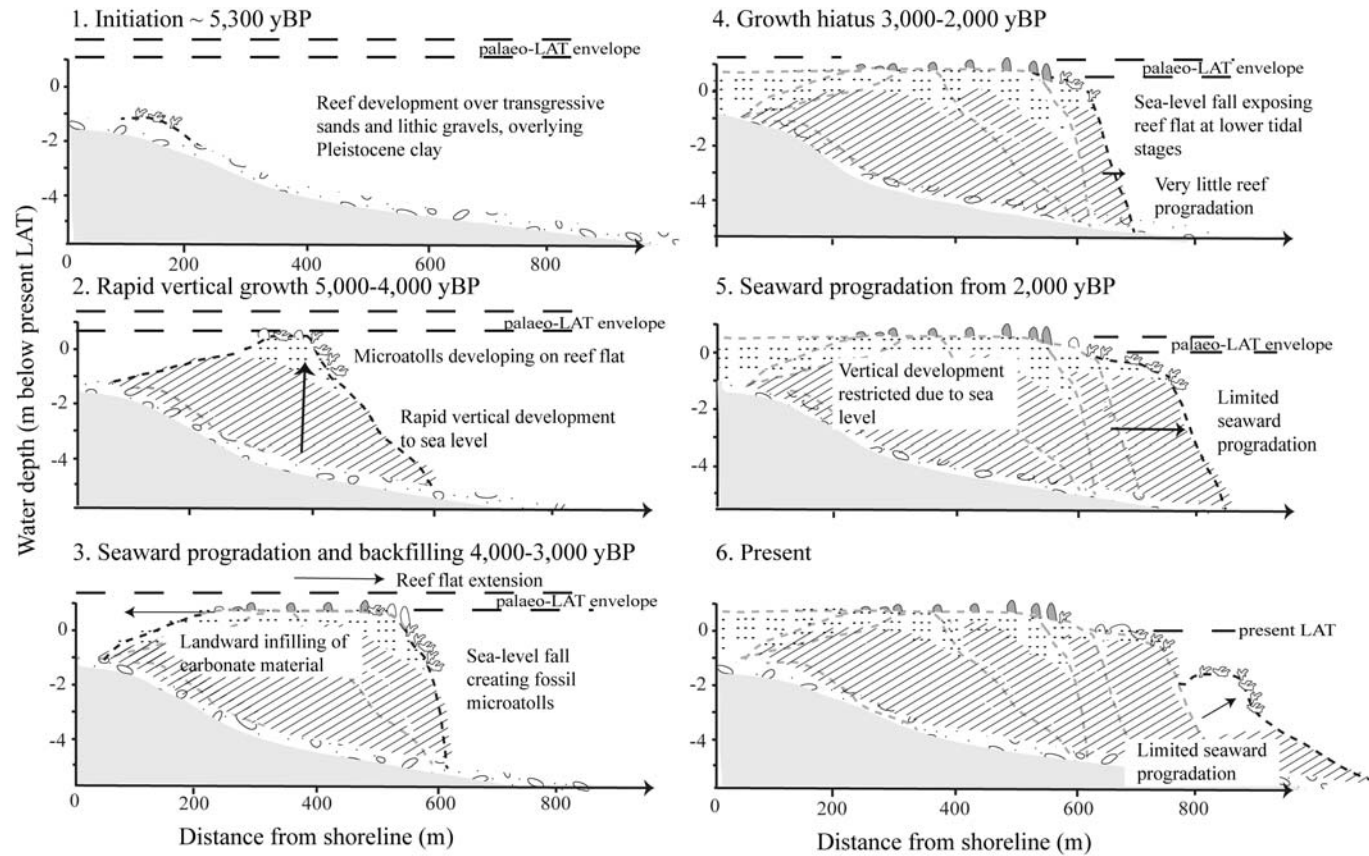


Figure 2.7 Conceptual model of reef development at Bramston Reef in two morphological phases (growth phase 1: 1 – 3, growth phase 2: 4 – 6). Late Holocene sea-level fall is represented by a palaeo-lowest astronomical tide (LAT) envelope at each time period. Reef matrix composition is indicated by the shading (diagonal lines: muddy matrix, dots: sand matrix) and was approximated based on the core facies in Figure 2.4.

mud) infilling around reef framework. High sedimentation is indicative of limited export and thus high net to gross production ratios compatible with rapid reef growth rates, and is unsurprising given the sheltered setting in which Bramston Reef has grown. Perry et al. (2012) also suggest that high sedimentation rates may limit post-depositional coral skeletal destruction, thus further enhancing high vertical accretion rates.

Analyses of matrix sediments within the reef cores show that mud-rich facies occur throughout the reef structure, but a general trend of decreased mud content in the upper 1.0 – 1.5 m of the cores was observed. This trend is indicative of the reef shallowing towards sea level, as increased winnowing of fine particles occurred as the reef grew towards the (palaeo) intertidal zone, due to increased hydrodynamic energy in shallower environments (Wolanski et al., 2005; Perry et al., 2011, 2012). Furthermore, sediment sorting by bioturbation ejects fine particles into the water column where they are available for transportation (Suchanek et al., 1986). Thus, the very fine sediments (<63 µm) in lower facies in the cores ($41.1 \pm 19.1 - 53.8 \pm 17.4\%$ mud, Table 2.3) were most likely deposited when the reef was subtidal. Drop camera footage and sediments collected from the reef slope deeper than -5 mLAT show mud deposits. These mud deposits are below the depth of wave re-suspension. Wolanski et al. (2005) determined that sediments at a depth of 5 m on the leeward side of High Island, an inshore island located ~380 km north of Bramston Reef, are re-suspended by ambient waves. Although no field data are available to quantitatively verify, hydrodynamic conditions at the leeward reef flat on High Island are comparable to (or possibly more energetic than) those at Bramston Reef, and thus the inference that mud deposition mainly occurs below the wave base appears sensible.

Growth phase 2 – hiatus followed by recovery

After a phase of rapid reef development between 5,396 – 3,000 yBP, the chronostratigraphy established from the dated cores at Bramston Reef shows a decline in reef growth, with relatively little net reef development between 3,000 – 2,000 yBP (Figure 2.7). Potential causal factors for reef ‘turn-off’ (*sensu* Buddemeier and Hopley, 1988) include intrinsic shifts in reef state associated with shallowing to sea level (i.e. a loss of accommodation space) (Smithers et al., 2006; Browne et al., 2012) and extrinsic forces such as exposure to terrigenous sediment influx (Palmer et al., 2010) and/or El Niño Southern Oscillation intensity (Toth et al., 2012). Periods of major terrigenous mud deposition are documented in the Bramston Reef cores by sediment facies E, indicating a phase of mud deposition upon the reef. It is pertinent to note that the thickness of the deposits preserved in the cores (varying between 25 – 75 cm) may only be a

fraction of the original deposit, as the excellent preservation and orientation of *in situ* coral framework below the terrigenous mud layers indicates that the space around the framework was infilled. Although the slowing of reef accretion at Bramston Reef (~3,000 – 1,000 yBP) can be attributed to processes and impacts of local origin (such as framework burial $\sim 2,265 \pm 9$ yBP by mud deposition), it is coincident with a regional hiatus in reef growth between ~4,000 – 2,000 yBP detected in many reefs of the inshore GBR (Smithers et al., 2006; Perry et al., 2011) which ceased active accretion between ~4,000 – 2,000 yBP, probably due to accommodation space constraints associated with late-Holocene sea-level fall. Notably, this ‘turn-off’ period of reef growth at Bramston Reef occurred long before European settlement of the Queensland coast in the mid-19th Century.

Bramston Reef began to prograde seaward again after 2,000 yBP when sea-level stabilised near the present level (Figure 2.7). Recovery of reef growth at Bramston Reef coincided with the regionally recognised ‘turn-on’ phase of inshore reefs in the GBR around 2,200 yBP (Perry and Smithers, 2011; Perry et al., 2011) when many new inshore reefs initiated and several older inshore reefs re-commenced active accretion. Contrary to the initial rapid ‘up and out’ growth mode during the first reef development phase, slow seaward progradation occurred between 2,000 yBP to present as reef growth was vertically constrained by sea level (vertical accommodation space full) and horizontally constrained by the depth at which coral growth (and thus reef accretion) can occur. Coral growth is generally restricted to above -4 to -6 mLAT on inshore, turbid-zone reefs in the GBR (Larcombe and Wolfe, 1999b; Perry and Smithers, 2011; Browne et al., 2012). Drop camera footage of the reef slope at Bramston Reef supports this, revealing that beyond approximately 5.5 m depth, the reef front transforms into a terrigenous mud dominated substrate (Figure 2.3). In this most recent phase of ‘turned on’ reef growth, rates of growth were slower than during initial stages of development (average lateral accretion rate ~ 9.8 cm/yr between ~3,000 – 2,000 yBP compared with ~ 19 cm/yr between ~4,000 – 3,000 yBP; Figure 2.3). Slow progradation may reflect the filling of the deeper slope area, given the switch from ‘up and out’ growth to seaward progradation. Approximate lateral accretion rates from Bramston Reef are comparable with other reefs in the GBR that also indicate reduced lateral accretion in the late Holocene (Smithers et al., 2006). Lateral accretion rates at Nelly Bay reef, Magnetic Island, vary from ~ 5.7 – 12.0 cm/yr (Lewis et al., 2012) and rates at Fantome Island reef vary from ~ 6.0 – 17.0 cm/yr (Johnson and Risk, 1987).

2.6.3 Considerations for future research

The data presented here indicate that coral cover and diversity at Bramston Reef today are comparable with those described and displayed by Saville-Kent (1893) in the late 1800s (see

Chapter 3 for a more detailed discussion of changes in reef condition since European settlement). Although very brief, Saville-Kent's (1893) reef description in the vicinity of Adelaide Point, shortly after European settlement on the Queensland coast at Bowen is not dissimilar to Bramston Reef flat today; large *Porites* colonies covered in living corals, growing alongside clusters of macroalgae (Figure 2.2, Appendix 1). My long-term palaeo-ecological record highlights that the major reef-building coral genera (which are present on the reef flat and slope today) have persisted through time at Bramston Reef under a comparable sediment regime. The work of Saville-Kent (1893) is often used to depict reef flat demise in Edgacumbe Bay since the late 1800s (Wachenfeld, 1997; GBRMPA, 2014). It cannot be contested that the condition of many reefs has declined over the past century due to human impacts. However, the data from Bramston Reef suggest that this may not be the case for all reefs in Edgacumbe Bay. Persistence of coral genera through time is one measure of reef resilience, however, knowledge of other reef dynamics such as coral cover and rates of recovery are also important in making robust conclusions on the overall health of the reef. Nevertheless, detailed analyses of reef chronostratigraphic records provide valuable archives of reef growth and dynamics prior to European settlement critical to understanding natural and anthropogenically impacted reef states and trajectories.

2.7 Conclusions

The framework and matrix captured in reef flat percussion cores, together with U-Th ages, allowed for the reconstruction of the growth history of Bramston Reef. Reef initiation occurred at or before $5,396 \pm 51$ yBP and most of the reef and reef flat was rapidly constructed within approximately 2,000 years in a terrigenous mud-rich setting. The now relict Holocene reef flat developed under conditions of higher mid-Holocene sea level and is today now algae and seagrass dominated, with live corals restricted to grow at elevations close to or below present LAT level near the reef flat edge and on the reef slope. The ecological composition of the reef has remained similar throughout the history of growth, independent of time and despite reef progradation slowing around 3,000 yBP associated with late-Holocene relative sea-level fall. The turbidity and sedimentation tolerant corals found in the palaeo-ecological record have always grown in a naturally muddy environment and have always been exposed to episodic drapes of terrigenous mud that buried reef framework. Based on the Bramston Reef chronology, changes in reef growth and exposure to episodic sedimentation events occurred well prior to European settlement of adjacent coastal catchments. Altered land use practices since European settlement in coastal catchments have no doubt elevated the delivery of sediments and other contaminants to many inshore reefs of the GBR (Brodie et al., 2012; Kroon et al., 2012). However, this and other chronostratigraphic investigations of inshore reef growth since the mid-

Holocene demonstrate that many inshore reefs have been able to initiate, grow, decline and recover in muddy environments that are typically considered antithetic to rapid reef growth. Inshore reefs are clearly different in many ways from their better-studied clear water counterparts. More research to better understand the long-term growth and dynamics of these historically resilient inshore ecosystems, and the relative influence of local and regional impacts on them, is required.

3 Multi-scale records of reef development and condition provide context for contemporary changes on inshore reefs

Submitted to *Global and Planetary Change*, 10 February 2016

Authors: E.J. Ryan, S.E. Lewis, S.G. Smithers, T.R. Clark and J.X. Zhao

Photographic comparisons of the reef flat at Stone Island in Edgcumbe Bay have been used to depict declines in reef condition without consideration of the long-term reef development history or the condition of other reefs in Edgcumbe Bay. In this chapter I address this knowledge gap by presenting the first records of Holocene reef growth based on reef cores for two Stone Island fringing reefs. The present reef condition is assessed using data that span multiple temporal and spatial scales.



Plate 3. Live faviid and *Porites* corals growing among macroalgae at Stone Island outer reef flat. See Appendix 10 for elevation of these corals.

3.1 Abstract

Comparisons between historical and contemporary photographs from a coral reef flat have been used by various authors and agencies to document changes in condition since European settlement on the inshore Great Barrier Reef (GBR), and have been presented as evidence for widespread reef decline. The declining condition is inferred from reduced live coral cover and structural diversity in the contemporary photographs. Anthropogenic causes for this deterioration are most often proposed, usually because it is argued to have coincided with European modifications to coastal catchments. However, changes in reef condition inferred from photographic comparisons have rarely been verified against quantitative assessments of past or current reef status. Photographs of the reef flat at Stone Island, located in Edgumbe Bay in the inshore central GBR, taken in the late 1800s have been compared with more recent images and suggest a major decline in reef condition over the past 120 or so years. Here, I examine the internal structure and ecology of fringing reefs at two locations on Stone Island by collecting 14 percussion cores across the reef flats. Sedimentological and palaeo-ecological analyses coupled with uranium-thorium dating allowed for the reconstruction of reef development over the past ~7,000 years. Both reefs at Stone Island initiated prior to 7,000 calendar years before present (yBP, where present is 1950 AD) and the reef flats were almost entirely emplaced by 4,000 yBP. Benthic ecological surveys of the contemporary reef condition at Stone Island and another fringing reef in Edgumbe Bay (Middle Island) indicate that coral cover and diversity across reef flats and slopes was patchy and varied spatially within each location and throughout the region. Live coral cover on the Middle Island reef flat reached an average ($\pm 1\sigma$ standard deviation) of $63.1 \pm 20.2\%$. This was much higher than the live coral cover at Stone Island, where only a few small living coral colonies were recorded. I evaluate the use of photographic records from Stone Island to depict regional changes in reef condition by comparing the trends in reef condition determined from photographic records with those reconstructed from reef cores. I conclude that inferred changes in reef condition at Stone Island are localised and should not be used as evidence of widespread regional decline.

3.2 Introduction

Major declines in live coral cover have been documented on coral reefs globally over the past four decades (Gardner et al., 2003; Bruno and Selig, 2007; Wilkinson, 2008; De'ath et al., 2012). Anthropogenic stressors such as over-fishing (Hughes et al., 2007), and contaminants and elevated sediment loads exported from modified catchments (Fabricius, 2005) have been linked to ecological phase-shifts on coral reefs, whereby a coral-dominated ecosystem is transformed into a macroalgae-dominated ecosystem with relatively few corals (Hughes, 1994; Bellwood et al., 2004). However, the global magnitude and regional extent of such phase-shifts

is not well documented or understood (Bruno et al., 2009) and some coral reefs have experienced long periods of recovery while being exposed to human influences (Maragos et al., 1985; Kittinger et al., 2011; Gilmour et al., 2013). Furthermore, how shifts in reef condition forced by human activities interplay with those produced by natural disturbances is also poorly understood. On the Great Barrier Reef (GBR) of Australia, inshore reefs (usually defined as those situated within the 20 m isobath and the mainland coast [Hopley et al., 2007]) are considered most susceptible to ecological phase-shifts due to their proximity to modified coastal catchments and river discharge (Fabricius et al., 2005; Browne et al., 2012; Waterhouse et al., 2012). Since European settlement of the Queensland coast in the early-mid 19th Century, sediment, nutrient and pollutant loads exported to the GBR lagoon have increased two- to ten-fold (McCulloch et al., 2003; Kroon et al., 2012; Waters et al., 2014) and more frequent large floods have been recorded (Lough et al., 2015). However, direct evidence of the impact these changes have on inshore reefs is lacking and whether they are localised or system-wide is contested (see Hughes et al., 2011; Sweatman and Syms, 2011; Sweatman et al., 2011).

Evidence for coral loss on inshore reefs of the GBR is largely derived from reef monitoring studies undertaken across a wide range of reefs on the GBR since the 1980s (e.g. Done et al., 2007; Thompson and Dolman, 2010; De'ath et al., 2012). These ecological data collected over decades are enormously valuable for informing management, but nonetheless provide very restricted temporal records of reef condition compared to those preserved in historical sources (Thurstan et al., 2015) and the fossil record (Pandolfi and Kiessling, 2014), which for most inshore reefs on the GBR may encompass several millennia (Smithers et al., 2006). Historical and contemporary photographs of reef flats have been compared to determine changes in coral cover and structure on inshore reefs over a 'longer-term' centennial-scale period (Wachenfeld, 1997). In 1994, Wachenfeld (1997) attempted to replicate the historical photographs of Stone Island reef flat taken by Saville-Kent (1893) at low tide (shown in Figure 3.1), taking photographs that depict a conspicuous change from a coral-dominated reef flat in the late 1800s/early 1900s to a macroalgae- and sediment-dominated reef flat (Wachenfeld, 1997). More recent photographs taken in 2012 by Clark et al. (2016) and those in Figure 3.1 show this condition persists. The sequence of photographs from Stone Island have been broadly used as evidence of widespread reef degradation in the inshore GBR (Hughes et al., 2010; GBRMPA 2013, 2014; Bell et al., 2014; Hoegh-Guldberg, 2014), despite Wachenfeld (1997, pp. 147) concluding that the results from the historical photograph project "...throws doubt on the proposition that the GBR is subject to broad scale decline". Concerns with the validity of the photographic comparison were emphasised by Wachenfeld (1997) and remain unresolved today, including: 1) a single photograph from one location on a reef flat may not be representative of the entire reef flat; and 2) each photograph captures just one point in time and

does not provide sufficient temporal resolution, given the dynamic nature of coral cover across reefs, and especially across reef flats. Furthermore, it is likely that the original photographs taken by Saville-Kent were deliberately taken in areas of high benthic cover. Indeed, Saville-Kent (1893) stated intentions for the photographs to be used to monitor future coral growth. In addition, the elevation of the reef flat at the location where the historical and contemporary photographs were taken is not properly referenced to a tidal datum (with the exception of recent work by Clark et al. [2016]) and thus the possible influence of the elevation of these commonly emergent reef flats cannot be determined. Accordingly, firm conclusions about regional-scale inshore reef condition should not be drawn from historical photograph evidence alone and quantitative baseline data on contemporary and past (centennial-millennial scale) reef condition (which do not currently exist at Stone Island) are required. When used together with quantitative data about past and present reef condition, historical and contemporary photographs may provide additional supplementary evidence of changes in reef condition.

Long-term reef growth records provide valuable baseline knowledge about past reef development, condition and variability throughout the Holocene (Smithers et al., 2006). On the GBR, records of long-term reef growth have revealed that many inshore reefs began to develop in the early- to mid-Holocene some 7,000 years ago and reef flats were established within 1,000 - 3,000 years of initiation (Smithers et al., 2006) under a relative mean sea level that was around 1 m higher than present (Lewis et al., 2013). Late-Holocene sea-level fall, the precise timing and nature of which remains debated (Perry and Smithers, 2011; Lewis et al., 2015), has exposed the older, back areas of these reef flats which are now elevated above the level of modern reef flat formation (Kleypas, 1996; Smithers et al., 2006). Not only are long-term reef growth studies rare, they are seldom considered in assessments of contemporary reef condition despite their ability to provide valuable baseline knowledge.

In this study I present data over multiple timeframes (millennial-centennial-present) to assess the use of historical and contemporary photographic comparisons from Stone Island as indicators of regional inshore reef decline. Evidence is incorporated from descriptions and photographs of reef flat condition collected over the past century or so that exist for the fringing reefs in Edgumbe Bay (Stone Island and Middle Island, Figure 3.2), with a focus on Stone Island. The Holocene development of fringing reefs at Stone Island is determined using uranium-thorium (U-Th) dated percussion cores and fossil microatolls. Chronostratigraphic records detail the timing and mode of reef growth and reef flat development, as well as changes through time in reef sediment matrix and palaeo-ecology. The contemporary geomorphology, benthic cover and distribution are also quantified, with high-precision elevation control, at two fringing reefs at Stone Island and the fringing reef at Middle Island.

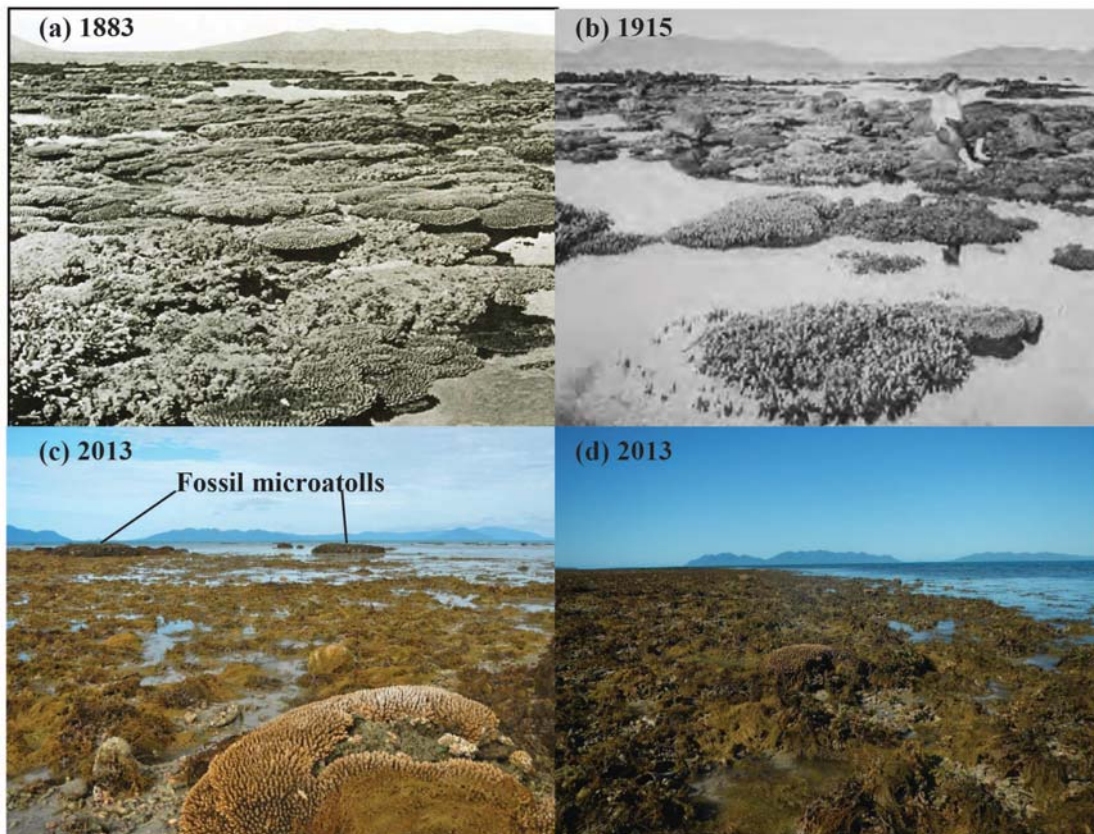


Figure 3.1 Photographs of the Stone Island reef flat: (a) taken by Saville-Kent (1893) in 1883, (b) taken in 1915 by unknown photographer, (c) and (d) taken by E. Ryan during spring low tides (0.13 and 0.23 m above lowest astronomical tide on 22 [c] and 21 July [d] 2013, respectively). Note the high standing fossil microatolls at the waters edge in (c). For elevations of (c) and (d) see Appendix 10 and for additional photographs see Appendix 3.

3.3 Regional setting

Stone Island (20°02'S, 148°17'E) and Middle Island (19°59'S, 148°22'E) are located 3 km and 10 km offshore from Bowen in Edgumbe Bay, respectively (Figure 3.2a). Stone Island is located in the inshore turbid zone where surrounding waters are <6 m deep, while Middle Island is situated on the inner-mid shelf margin in waters ~16 m deep. Stone Island is fringed by two reefs: one located on the windward, south-eastern side of the island (Stone Island South [SI-S]) with a ~450 m wide reef flat, and one located in Shoalwater Bay on the northern side of the island (Stone Island North [SI-N]) with a ~400 m wide reef flat (Figure 3.2c). SI-S is the larger of the reefs on Stone Island, extending around 1.5 km alongshore. On the southern side of Middle Island a reef flat as much as 330 m wide extends along ~600 m of shoreline (Figure 3.2b). The reefs at Stone Island and Middle Island experience a semi-diurnal tidal regime with a spring tidal range around 3.6 m where reef flats at both islands are largely exposed at lower tidal stages. A ~400 m long spit has developed at the western extent of the SI-S reef flat (Figure

3.2c), indicating that waves and currents generated by prevailing south-easterly trade winds predominantly transport sediment to the north-west. This occurs even though both Middle and Stone Islands are relatively protected from swells generated by the dominant south-east trade winds by Gloucester Island and Cape Gloucester (Figure 3.2). For details of regional climate, setting and terrestrial discharge to Edgumbe Bay, the reader is referred to section 1.8.

Europeans settled in Bowen ~1861 AD (McIntyre-Tamwoy, 2004) and began to modify the landscape on Stone Island soon after. In contrast, Middle Island has been largely untouched by Europeans. At Stone Island, sheep and goats were introduced in the late 19th and early 20th Centuries (Bowen Independent, 1916, 1934), a tourist resort was developed on the island during the mid-20th Century, and a 23-acre lake was dammed in the centre of the island to create a freshwater supply in 1972 (Bartram, 1972). Although the tourist resort has closed, infrastructure and roads remain. Dredging in Edgumbe Bay began in 1886 to develop the Bowen shipping channel and jetty (Steen, 1972) but no data are available to assess the impacts of dredging on the hydrodynamics and sediment movement within the bay. Brodie et al. (2014) suggested nearshore areas of Edgumbe Bay were poorly flushed based on hydrodynamic modelling (Andutta et al., 2013), however the model used was not specifically developed for Edgumbe Bay and no field data exist to validate the model results.

Excellent historical descriptions and photographs exist for Stone Island (Saville-Kent, 1893) and Middle Island (Agassiz, 1898), which establish that the reef flats at both islands were in good condition in the late 1800s. Saville-Kent's detailed descriptions include several photographs of the reef flat at SI-S taken during spring low tide (location revealed by Hedley [1925]) that show high coral cover, including *Madrepora (Acropora)*, *Montipora*, *Goniastrea grayi (Goniastrea pectinata)*, *Turbinaria cinerascens* and *Losphoseris (Pavona) cristata* (Saville-Kent, 1893). In 1896 the outer face of Middle Island's reef flat was "coated with fine heads of corals... becoming less prominent as they tend towards the shallower edge of the flat" (Agassiz, 1898 p.107). However, by the 1920s no trace of living coral was documented at either Stone or Middle Island (Hedley, 1925; Rainford, 1925). Two cyclones in 1918 caused high rainfall and a large freshwater plume, which in concert with low spring tides and northerly winds are argued to have caused total mortality of the reef flats (Hedley, 1925; Rainford, 1925). Stanley (1928) reported that in June 1925 live coral cover at Stone Island was recovering and small colonies of *Goniastrea*, *Merulina*, *Turbinaria*, *Fungia* and soft corals were flourishing. Stanley (1928) refers to both the 'extensive fringing reef to the south' (presumably the SI-S reef) and the reef in Shoalwater Bay but does not specify which reef was recovering in the mid-1920s. In 1936 the reef flats at Stone Island and Middle Island were "dead on their upper surfaces" (Steers, 1937) and negligible recolonisation of coral had occurred by 1953

(Stephenson et al., 1958). According to anecdotal evidence in Wachenfeld (1997), the reef flat at SI-S was apparently in good condition in the 1970s. In contrast, Hopley (1975), who conducted the first comprehensive geomorphological investigation at Middle Island, described the reef flat there during the same period as ‘largely dead’. Although these sites in Edgcumbe Bay have detailed historical records that provide snapshots of reef condition over the past century or so, a longer-term perspective on reef development and disturbance/recovery regimes has to date not been established and used as context for interpreting recent changes.

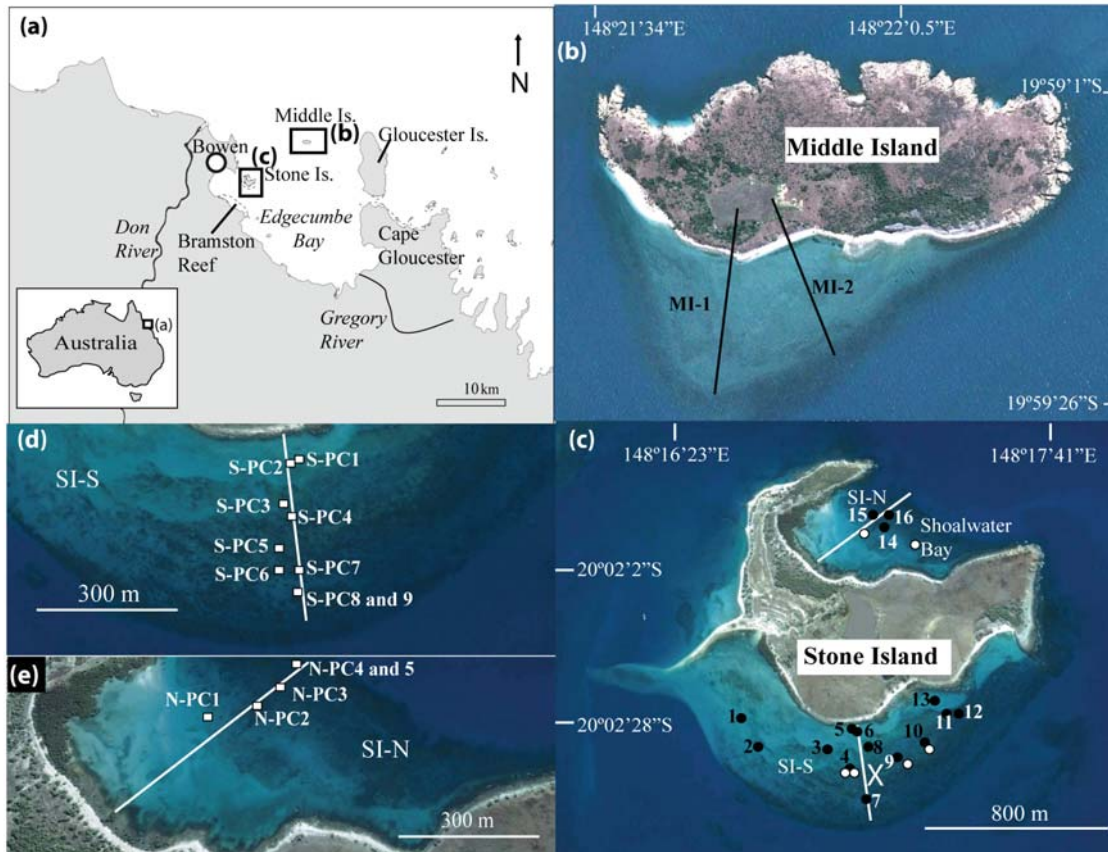


Figure 3.2 (a) Location of Stone Island, Middle Island and Bramston Reef in Edgcumbe Bay, Australia; (b) the reef flat and transects one (MI-1) and two (MI-2) at Middle Island; (c) the reef flats at Stone Island South (SI-S) and Stone Island North (SI-N). Fossil microatolls (numbered 1 – 16) are shown by black dots and living open-water microatolls are shown by white dots. The approximate location of the photographs taken by Saville-Kent (1893) and Wachenfeld (1997) is shown by the white X; (d) the location of percussion cores (white squares) on the transect at SI-S; and (e) the location of percussion cores (white squares) on the transect at SI-N.

3.4 Materials and methods

Field studies were conducted in the austral winters of 2013 and 2014 during low spring tides (<0.5 m above lowest astronomical tide [LAT] during the day). All location and elevation data were collected using a Trimble Real Time Kinematic (RTK) Global Positioning System (GPS) with the vertical and horizontal precision being ~0.01 – 0.005 m. The high-precision elevation

data were reduced to LAT as described in section 1.9.1 (Chapter 1), allowing accurate inter- and intra-site comparisons.

3.4.1 Past reef development

To examine Holocene reef development at Stone Island, nine reef cores were collected from SI-S and five from SI-N using the percussion coring technique described in section 1.9.2. The cores were collected along shore-perpendicular transects on the reef flat (Figure 3.2d, e) and the number of cores collected was a function of the width of the reef flat and the time available in the field. Cores between 1.2 and 5.1 m long extended from the reef flat surface vertically into the reef structure (Figure 3.3) and captured reef framework, detrital material and reef matrix sediments. Total compaction rates across the cores from both reef flats varied between 19 and 45%. The compaction rate in core S-PC3 below 2.0 m downcore was 59% due to a coral clast that was wedged in the core at 2.0 m depth.

In the laboratory, each core was first halved lengthways and visually logged to differentiate facies that had similar reef framework material and matrix composition (see section 1.9.2). Sediment samples (~20 g) were taken from the cores at 20 cm (uncompacted) downcore intervals and analysed for grain size, carbonate content and mud content using sieving, Rapid Sediment Analyser and acid digestion techniques described in section 1.9.2. Palaeo-ecological analyses were also conducted on each core using the method in section 1.9.2 where corals were grouped and weighed according to the genus. Note that sediment and palaeo-ecological analyses were not performed on S-PC3 below 2.0 m downcore due to the high compaction rate. In total, 25 well-preserved *in situ* corals were selected from throughout the cores for dating using U-Th techniques (described in section 1.9.5) to reconstruct detailed chronostratigraphies for the reefs examined.

The locations and surface elevations of fossil microatolls (mainly *Porites*) were surveyed using the RTK GPS. A coral core sample was extracted from the surface rim of 16 fossil microatolls, as described in section 1.9.2. Each fossil microatoll sample was dated using U-Th techniques to determine the colony age. Ten fossil microatoll samples from Middle Island reef flat were also collected and dated (see Chapter 4, section 4.3.3 for details).

3.4.2 Present geomorphology and benthic cover

RTK GPS surveys of reef flat topography were undertaken across shore-perpendicular transects (Figure 3.2b, c). Eco-geomorphological zones were differentiated along transects based on variations in reef flat elevation, coral cover, sediment type, morphological features and

algae/seagrass cover. To determine the substrate composition within each eco-geomorphological zone, reef flat photographs and still images extracted from reef slope video footage were analysed in Coral Point Count with Excel extensions software (Kohler and Gill, 2006) as described in section 1.9.1. At Stone Island, reef slope depth was estimated using a depth sounder and calibrated against predicted tides to reduce depths to LAT. Where possible live corals were identified to genus. However, if poor image quality and/or turbid water conditions limited confident identification, which was often the case, corals were classified according to their structural morphology (i.e. branching, massive, plate, foliaceous, columnar, encrusting or free-living).

3.5 Results

3.5.1 Holocene reef development at Stone Island

The chronostratigraphy was inferred for each Stone Island reef from the percussion cores, fossil microatoll samples and U-Th ages (Figure 3.3). All U-Th ages from core and fossil microatoll samples are presented in Appendix 2. The chronostratigraphies reveal details about the timing and mode of reef development, the reef palaeo-ecology and the reef matrix sediments. The cores from the two reefs captured up to 5 m of reef framework and matrix and did not reach the pre-reefal surface, indicating that the entire Holocene thickness of each reef is >5 m. Given the water depth immediately seaward of the reef slope is ~6 – 7 m, the pre-reefal surface is probably ~6 – 6.5 m below the present surface, and thus the percussion cores likely captured the majority of the reef structure.

Four reefal facies were differentiated in the cores collected at SI-S and SI-N (facies A, B, C and D) (Table 3.1, Figure 3.4). For both Stone Island reefs, the matrix sediments generally coarsen upwards, as the mud fraction (<63 μm) in the cores decreased towards the surface to a minor component ($4.2 \pm 2.0\%$ [mean $\pm 1\sigma$ standard deviation] or $9.6 \pm 5.2\%$) and medium-coarse carbonate sands (grain size 2000 – 250 μm) dominated ($96.9 \pm 2.3\%$ carbonate in facies A) (Table 3.1). Mud-containing facies dominated the cores from SI-S (mud content up to $47.8 \pm 13.9\%$ in facies D), comprising all but the uppermost metre or so of the cores. A lower mud content characterised the facies in SI-N cores; the muddiest facies C contained $20.7 \pm 5.3\%$ mud. Throughout the cores, carbonate sediments dominated (>70%), with terrigenous fractions that were higher in SI-S cores (24.6 ± 7.9 and $29.5 \pm 9.5\%$ in facies C and D, respectively) than SI-N cores ($18.3 \pm 9.7\%$ in facies C). Coral clasts (framework and detrital material), shell hash and disarticulated bivalves were recovered amongst the sediment matrix throughout all cores.

Coral clasts were generally rubble, derived from branching corals; some were heavily encrusted with coralline algae and others were well-preserved. In addition, echinoderm spines (some remarkably well-preserved) were recovered in S-PC6.

Well-preserved coral material from 28 different coral genera was recovered in the cores collected across SI-S and SI-N, however most material was so encrusted and/or abraded that accurate identification was not possible (such clasts were classified as 'un-identified rubble'). Identified coral genera were: *Acropora*, *Anacropora*, *Astreopora*, *Australogyra*, *Calaustrea*, *Cyphastrea*, *Dipsastraea*, *Echinophyllia*, *Echinopora*, *Euphyllia*, *Favites*, *Fungia*, *Galaxea*, *Goniastrea*, *Hydnophora*, *Isopora*, *Lobophyllia*, *Montipora*, *Oxypora*, *Pachyseris*, *Pavona*, *Platygyra*, *Porites*, *Psammocora*, *Seriatopora*, *Stylophora*, *Tubastrea* and *Turbinaria*. The dominant framework contributors (e.g. *Acropora*, *Porites*, *Montipora*, *Goniastrea*, *Galaxea*) were found in the cores from both sites, however five genera were unique to cores from SI-S (*Anacropora*, *Echinophyllia*, *Favites*, *Psammocora* and *Tubastrea*) and eight genera were unique to cores from SI-N (*Australogyra*, *Calaustrea*, *Dipsastraea*, *Echinopora*, *Isopora*, *Lobophyllia*, *Oxypora* and *Platygyra*). Spiculite clusters produced by soft corals were only recovered in cores from SI-N.

Reef development at SI-S

U-Th ages obtained from coral clasts in the percussion cores collected across the reef flat at SI-S were between $7,247 \pm 23$ and $4,324 \pm 22$ yBP, indicating that most of the reef was constructed during this period (Figure 3.3a). Reef initiation occurred prior to $7,247 \pm 23$ yBP, as indicated by the U-Th age at the base of S-PC6 4.6 m below the present reef flat surface. Basal ages of $\sim 7,000$ yBP were established for S-PC1, S-PC5 and S-PC6. Initial reef development was detached ~ 330 m seaward of the contemporary shoreline (Figure 3.3a), and vertical reef accretion occurred in two parallel, detached parts of the reef. Average vertical reef growth rates during initial stages of reef development were 3.0 mm/yr, which increased to 4.4 – 4.8 mm/yr between 7,000 and 6,000 yBP (Figure 3.3a). The fossil microatoll age of $6,716 \pm 23$ yBP on the SI-S transect confirms that reef flat development at sea level had begun by this time ~ 200 m offshore from the modern beach. Emplacement of the entire reef flat took $\sim 1,000$ years, as indicated by mid-Holocene aged fossil microatolls that occur across the breadth of the reef flat: $6,683 \pm 23$ yBP close to the shoreline and $5,894 \pm 22$ yBP at the contemporary reef edge (Figure 3.3a). Negligible reef progradation has occurred since this time.

Table 3.1 Core facies descriptions and matrix components including percent sand, mud and carbonate (CaCO₃) content (mean and 1σ standard deviation [SD]).

Facies		A	B	C	D
Facies name		Contemporary intertidal sands	Reef framework, sandy matrix	Reef framework, muddy-sand matrix	Reef framework, mud matrix
Description		Sandy matrix with encrusted coral rubble and shell hash. Coral clasts are matrix-supported.	Sandy matrix with coral clasts (mainly detrital and matrix-supported), shell hash and bivalves.	Muddy-sand matrix with coral clasts (mainly clast-supported), bivalves and shell hash.	Muddy matrix dominated by coral clasts (mainly clast-supported) with some shell hash.
Environmental interpretation		Contemporary intertidal reef flat.	Lower intertidal reef flat environment where most fine material remains in suspension.	Shallow subtidal reef environment where fine sediments can settle.	Subtidal reef slope where fine sediments can settle.

Location		SI-S	SI-N	SI-S	SI-N	SI-S	SI-N	SI-S*
Matrix component	% sand	Mean	95.8	90.4	91.4	86.5	64.1	52.2
		SD	2.0	5.2	4.4	7.0	12.7	13.9
	% mud	Mean	4.2	9.6	8.6	13.5	35.9	47.8
		SD	2.0	5.2	4.4	7.0	12.7	13.9
	% CaCO ₃	Mean	96.9	92.7	91.7	87.4	75.4	81.7
		SD	2.3	2.8	8.8	6.0	7.9	9.7

*Facies D only recovered in cores from SI-S.

Reef development at SI-N

Reef development in Shoalwater Bay (SI-N) began prior to $7,064 \pm 17$ yBP, as indicated by the U-Th age in N-PC5 4.6 m below the present reef flat surface and ~30 cm above the base of the core (Figure 3.3b). After initiation, the reef accreted vertically towards sea level and the oldest fossil microatoll age on the reef flat surface shows that reef flat formation had begun by $4,475 \pm 45$ yBP (Figure 3.3b). Vertical reef growth rates were generally slower between 7,000 – 4,300 yBP compared to SI-S, ranging from 0.9 – 1.7 mm/yr, however there were periods when average rates of reef growth were higher (5.0 mm/yr between $6,812 \pm 16$ – $6,718 \pm 26$ yBP documented in N-PC2, Figure 3.3b). The majority of the reef flat was emplaced by around 4,000 yBP. Fossil microatoll ages at the outer reef flat of $2,091 \pm 9$ and $2,018 \pm 19$ yBP indicate that limited reef flat accretion has occurred over the past two millennia (Figure 3.3b).

3.5.2 Contemporary eco-geomorphology

Eco-geomorphological zones were differentiated across the reef transects based on the benthic surveys (Figure 3.5, Table 3.2). The number of zones differentiated varied between sites. Eight zones were identified across the transect at SI-S, seven zones across the transect at SI-N, six zones across transect MI-1, and eight zones across transect MI-2 at Middle Island. Generally, the backreef flat environment at all reefs extended from the shoreline at an elevation ~1.0 mLAT (Figure 3.3, Figure 3.6). Each reef flat gently sloped seaward from the backreef flat

towards the reef crest, which was elevated close to LAT level at Middle Island (Figure 3.6), and below LAT at Stone Island (~0.8 and 0.2 m below LAT at SI-S and SI-N, respectively, Figure 3.3). Transitions between zones were subtle in most cases, however a distinctive benthic composition and surface elevation depicted each zone. At all sites the backreef flat was comprised of sand, coral rubble and macroalgae, however live coral cover on the outer reef flat was highly variable between sites, as outlined below.

The fringing reef at SI-S

The elevated backreef flat extended ~130 m from the shoreline and comprises zones 1 and 2 (Figure 3.3a), which were characterised by rippled sands (63.0 ± 19.9 and $48.1 \pm 13.4\%$ cover, respectively) with sparse, patchy macroalgae cover (9.6 ± 15.8 and $39.3 \pm 20.3\%$, respectively). At the end of zone 2, the reef flat abruptly transitioned to zone 3, where the cemented reef pavement was largely covered with turf algae, along with patchy sand cover ($20.0 \pm 19.7\%$) and coral rubble ($18.5 \pm 7.7\%$). The outer ~160 m of the reef flat comprises zones 4 and 5, which were both characterised by a sand and coral rubble substrate, dominated by macroalgae (53.3 ± 22.6 and $67.1 \pm 22.3\%$ macroalgae cover in zones 4 and 5, respectively). Three key macroalgae genera were identified at SI-S (*Padina*, *Sargassum* and *Halimeda*), however several other unidentified genera were encountered.

Fossil microatolls, mostly *Porites*, were common in all zones across the reef flat. The fossil microatolls across the backreef flat (zones 1 and 2) were generally smaller (1.0 – 2.8 m in diameter) with upper surfaces at higher elevations (1.0 – 1.2 mLAT) than those on the outer reef flat (zones 3 – 5), which tended to be larger (1.5 – 4.7 m in diameter) with upper surfaces elevated 0.1 – 0.6 mLAT. Fossil microatolls across the SI-S reef flat varied in age from $7,103 \pm 40$ to $3,787 \pm 12$ yBP (Appendix 2).

The narrow reef slope at SI-S began at the end of zone 5 ~400 m offshore at an elevation ~0.8 m below LAT (Figure 3.3a). The reef slope was characterised by a sand and coral rubble substrate, dominated by macroalgae (largely *Sargassum*, Figure 3.5). Macroalgae cover on the upper reef slope (zone 6) averaged $51.1 \pm 28.6\%$ (Table 3.2). A narrow 20 m wide live coral zone (zone 7) extended across the reef slope at a depth ~1.9 – 2.5 m below LAT (Figure 3.3a, Figure 3.5). Here, the substrate was sandy ($38.5 \pm 41.8\%$ cover) with sparse macroalgae cover ($17.0 \pm 21.2\%$). Live coral cover was $33.3 \pm 21.1\%$. Mature branching and plate *Acropora* dominated (accounting for 67% of the live corals), but massive corals (genus un-identified) also occurred (see Appendix 3 for reef slope photographs). Macroalgae cover on the lower reef slope

(zone 8) averaged $24.7 \pm 28.3\%$, with no live corals on the slope below -2.5 mLAT depth. Beyond the end of the reef slope at -3.4 mLAT, a muddy-sand substrate was encountered.

The fringing reef at SI-N

The elevated backreef flat environment, extending ~220 m from the shore, was partly covered by two discrete patches of sand that were almost entirely rippled sand and/or muddy-sand (zones 2 and 4, Figure 3.3b). These sand areas were generally elevated ~1.0 – 1.3 mLAT. The reef flat surface that was buried by the sand deposits was exposed at zone 3 at ~0.8 mLAT and was largely sandy ($66.3 \pm 30.8\%$ cover) with sparse coral rubble and macroalgae (Figure 3.3b). The outer ~240 m of the reef flat (zone 5) was dominated by macroalgae (*Padina* and *Sargassum*) which averaged $60.9 \pm 26.4\%$ of the benthic cover (Figure 3.3b) and was found to be at a lower elevation (ranging from 0.7 m above LAT to 0.2 m below LAT). Live corals were sparsely distributed across the outer half of zone 5 (though these were not included in the benthic survey as they were not captured by the random sampling strategy). Two open-water live *Porites* microatolls were surveyed with upper living rims elevated at 0.4 and 0.5 mLAT. Fossil *Porites* microatolls were also surveyed across the reef and varied from 1.0 – 5.5 m in diameter with upper surfaces elevated 0.6 – 0.8 mLAT. The age of these fossil microatolls at SI-N varied from $4,475 \pm 45$ to $2,018 \pm 19$ yBP (Appendix 2).

Zone 5 terminated ~400 m offshore and ~0.2 m below LAT, beyond which a subtle transition from the reef flat to the narrow reef slope occurred. The reef slope at SI-N was characterised by living corals, coral rubble and sand (Figure 3.3b, Figure 3.5, see also Appendix 4). The upper reef slope (zone 6) extended to a depth ~1.8 m below LAT, and live coral cover was high ($46.0 \pm 36.2\%$ and maximum 96.3% live coral cover). The lower reef slope (zone 7) extended from 1.8 – 3.2 m below LAT and here, the substrate was dominated by coral rubble ($75.7 \pm 23.4\%$ cover); live coral cover averaged $18.5 \pm 23.7\%$. Across the reef slope, the dominant coral morphologies were branching (accounting for 32% and 63% of live corals in zone 6 and 7, respectively) and encrusting corals such as *Acropora* and *Montipora* (33% of live corals in zone 6), followed by plate corals of *Acropora* (24% of live corals in zone 6). Columnar, foliaceous, free-living and massive corals were also encountered on the surveys but were uncommon (<5% of the live corals in zone 6). The reef slope ended ~3.2 m below LAT, beyond which the seafloor comprised rippled muddy sands.

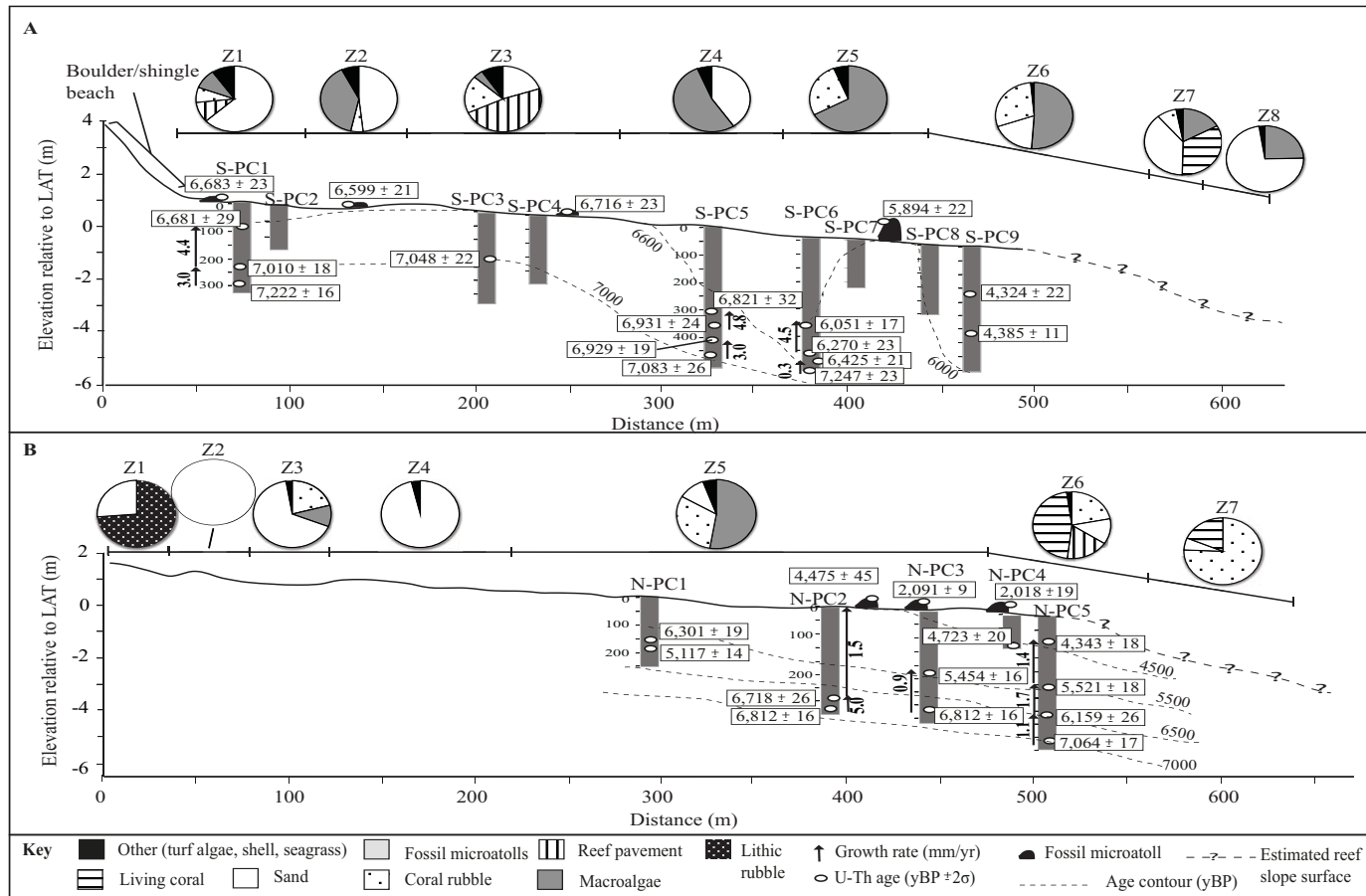


Figure 3.3 Profiles of the reef at (a) Stone Island South and (b) Stone Island North extending seaward, with reef age indicated by the uranium-thorium (U-Th) ages on the fossil microatolls and in the percussion cores (labelled grey rectangles). The arrows indicate average vertical accretion rates (mm/yr). Elevation is relative to lowest astronomical tide (LAT). Benthic composition of each contemporary eco-geomorphological zone (numbered Z1 – Z8) is indicated by the shaded pie charts.

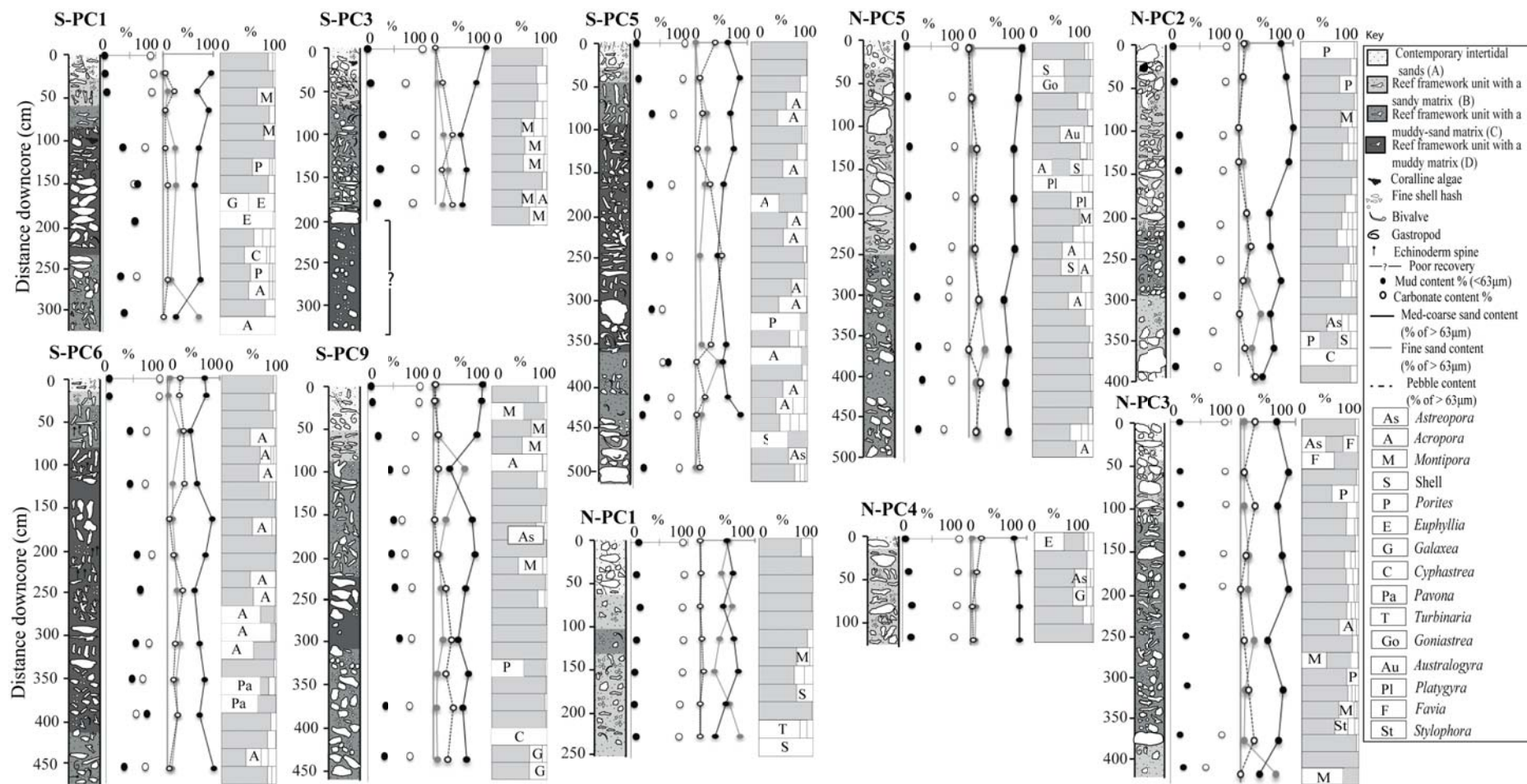


Figure 3.4 Composite core logs of the uranium-thorium dated percussion cores (PC) from Stone Island South (S) and Stone Island North (N) showing (left to right) sedimentary facies, carbonate and mud content of the matrix, grain size of the matrix, and palaeo-ecology data (shown as % relative abundance of the total carbonate content >1 cm in size). Dominant coral genera (comprising >25% of each segment) are labelled for each 20 cm downcore segment. Unlabelled white bars represent coral genera <25%. Grey bars represent the % contribution of the remaining un-identified carbonate fraction.

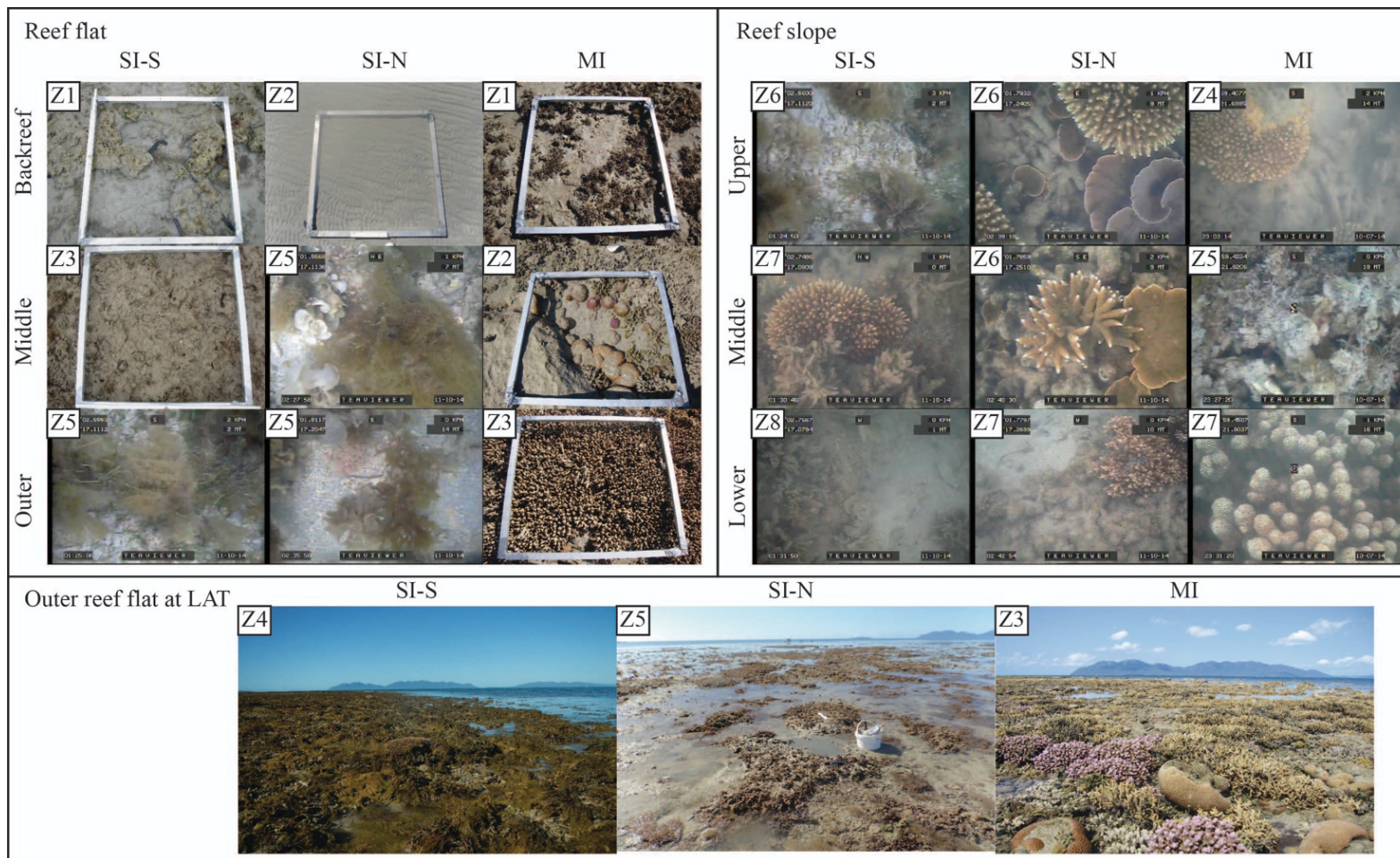


Figure 3.5 Upper photographs are from the quadrat and drop camera surveys, illustrating the differences in benthic cover across the reef at Stone Island South (SI-S), Stone Island North (SI-N) and Middle Island (MI). Eco-geomorphological zone numbers indicated in top left corner of each photograph. Lower photographs are of the outer reef flat at lowest astronomical tide (LAT). See Appendix 10 for elevations of the reef flat photographs.

Table 3.2 Contemporary eco-geomorphological zones at Stone Island and Middle Island. Elevation is relative to lowest astronomical tide (LAT).

Site	Zone	Description	Width (m)	Approximate elevation relative to LAT (m)	Average live coral cover (mean \pm 1 σ %)	Notes	Coral genera present (order of dominance)
Stone Island South	1	Sandy backreef flat	70	1.0 – 0.7	0	Fossil <i>Porites</i> microatolls	
	2	Sandy backreef flat with high macroalgae cover	57	0.9 – 0.7	0	Fossil <i>Porites</i> microatolls	
	3	Cemented reef pavement, sand and rubble	112	0.9 – 0.3	0	Fossil <i>Porites</i> microatolls	
	4	Sandy intertidal outer reef flat largely covered in macroalgae	85	0.3 to -0.2	0	Fossil <i>Porites</i> microatolls	
	5	Subtidal outer reef flat dominated by macroalgae	76	-0.2 to -0.8	0	Fossil <i>Porites</i> microatolls	
	6	Upper reef slope with sand, macroalgae and rubble	114	-0.8 to -1.9	0		
	7	Living coral zone on reef slope with macroalgae	20	-1.9 to -2.5	33.3 \pm 21.1	Branching and massive corals dominant	<i>Acropora</i> , <i>Pocillopora</i> , un-identified massive corals with meandering corallites
	8	Lower reef slope with sand and sparse macroalgae	26	-2.5 to -3.4	0		
Stone Island North	1	Terrigenous rocks and sand	24	1.6 – 1.0	0		
	2	Muddy-sand flat covering backreef flat	56	1.3 – 0.9	0		
	3	Backreef flat dominated by sand and rubble with sparse macroalgae	52	0.8	0		
	4	Sand flat covering old reef flat	112	1.0 – 0.6	0		
	5	Sandy outer reef flat dominated by macroalgae	240	0.7 to -0.2	0	Fossil and live <i>Porites</i> microatolls	<i>Porites</i>
	6	Upper reef slope live coral zone	50	-0.2 to -1.8	46.0 \pm 36.2	Encrusting and branching corals dominant	<i>Acropora</i> , <i>Montipora</i> , <i>Turbinaria</i> , <i>Favites</i> , <i>Fungia</i> , Soft corals
	7	Lower reef slope live coral and rubble zone	85	-1.8 to -3.2	18.5 \pm 23.7	Branching corals dominant	<i>Acropora</i> , <i>Montipora</i> , <i>Pocillopora</i> , <i>Platygyra</i> , <i>Fungia</i>
Middle Island Transect 1	1	Sandy backreef flat with macroalgae and rubble	90	1.0 – 0.8	0		
	2	Reef flat zone with live corals and fossil microatolls	90	0.8 – 0.7	21.0 \pm 28.7	Branching corals dominant	<i>Montipora</i> , <i>Goniastrea</i> , <i>Porites</i>
	3	Reef flat live coral zone	75	0.7 – 0.6	47.5 \pm 28.2	Fossil <i>Porites</i> microatolls, branching corals dominant	<i>Montipora</i> , Soft corals, <i>Goniastrea</i> , <i>Acropora</i> , <i>Porites</i> , <i>Pocillopora</i>
	4	Reef flat edge live coral zone with rubble	75	0.5 – 0	27.0 \pm 32.3	Branching and massive corals dominant	<i>Acropora</i> , <i>Dipsastraea</i> , <i>Goniastrea</i> , Soft corals, <i>Porites</i> , <i>Pocillopora</i>
	5	Upper reef slope, macroalgae dominated	64	?	2.0 \pm 5.6	Macroalgae covering branching coral rubble	<i>Acropora</i>
	6	Sandy lower reef slope, live coral zone	47	?	13.3 \pm 24.1	Encrusting and foliaceous corals dominant	<i>Leptoseris</i> , <i>Galaxea</i>

Middle Island Transect 2	1	Sandy backreef flat dominated by rubble	150	1.0	0.2 ± 0.6	Fossil and live <i>Porites</i> microatolls (moated)	<i>Porites</i> (moated), <i>Montipora</i> (moated)
	2	Sand and rubble zone on reef flat	70	1.0 – 0.6	5.3 ± 7.7	Branching corals dominant	<i>Montipora</i> , <i>Goniastrea</i>
	3	Live coral zone on reef flat	100	0.6 – 0	63.1 ± 20.2	Branching corals dominant	<i>Montipora</i> , <i>Acropora</i> , <i>Goniastrea</i>
	4	Reef crest/upper slope	38	~0	22.9 ± 31.3	Branching corals dominant	<i>Acropora</i> , <i>Platygyra</i> , Soft corals
	5	Upper/mid-reef slope macroalgae zone	74	?	4.1 ± 9.7	Macroalgae covering branching coral rubble	Un-identified encrusting corals
	6	Mid-reef slope live coral zone	14	?	43.7 ± 42.0	Branching corals dominant	<i>Acropora</i> , Soft corals, un-identified massive coral, <i>Galaxea</i>
	7	Lower slope live coral zone	23	?	100.0 ± 0.0	Widespread massive coral colonies	<i>Goniopora</i> , <i>Galaxea</i>
	8	Sandy lower slope	19	?	17.3 ± 18.6		<i>Galaxea</i> , un-identified foliaceous coral

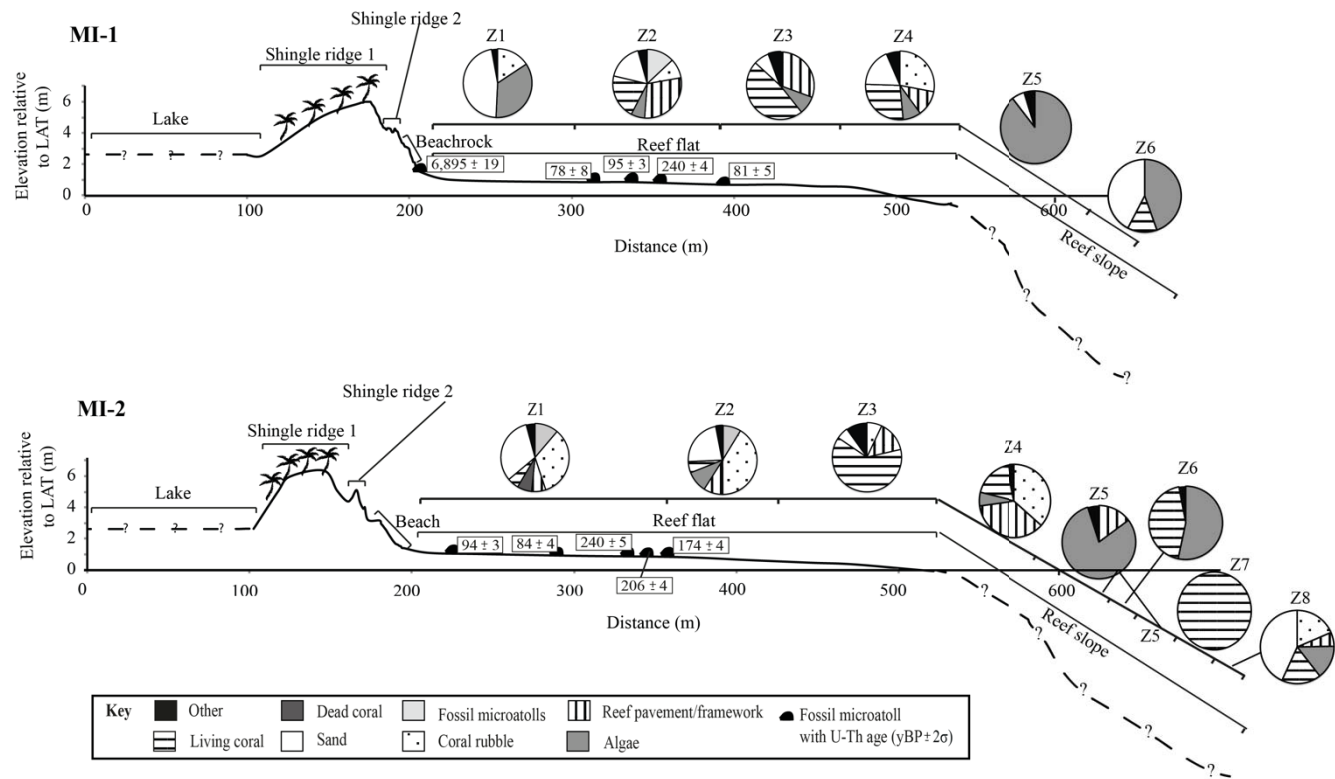


Figure 3.6 Profiles of transects MI-1 and MI-2 at Middle Island extending seaward where elevation is relative to lowest astronomical tide (LAT). Benthic composition of each eco-geomorphological zone (numbered Z1 – Z8) is indicated by the shaded pie charts. Note that the depth of slope is roughly estimated. The fossil microatoll ages are derived from Chapter 4 and are presented in Appendix 2.

The fringing reef at Middle Island

The higher elevation backreef flat at Middle Island (zones 1 and 2) extended 180 – 220 m offshore (Figure 3.6), and mainly comprised sand, rubble and macroalgae ($34.5 \pm 15.4\%$ macroalgae cover on MI-1, including *Padina*, *Sargassum* and *Halimeda*). Fossil microatolls (mainly *Porites*) varying between 1.0 – 5.3 m in diameter and with upper surfaces elevated between 0.9 – 1.4 mLAT were scattered throughout zones 1 and 2. Most of the fossil microatolls sampled at Middle Island were much younger than at Stone Island (Figure 3.6, and see Chapter 4), ranging from 240 ± 5 to 78 ± 8 yBP. A single mid-Holocene aged fossil microatoll at the backreef dating to $6,895 \pm 19$ yBP was the only exception. Open-water live corals occurred on the backreef flat at elevations below 0.8 mLAT, but they were more abundant on the lower elevation MI-1 ($21.0 \pm 28.7\%$ cover in zone 2) than MI-2 ($5.3 \pm 7.7\%$ cover in zone 2) (Table 3.2). Live coral cover was highest (27.0 ± 32.3 to $63.1 \pm 20.2\%$) on the outer parts of the reef flat <0.6 mLAT (zones 3 and 4 on MI-1, and zone 3 on MI-2) (Figure 3.6, Appendix 5). Live hard corals from six genera were recorded across the reef flat: branching *Acropora*, *Montipora* and *Pocillopora*, and massive *Goniastrea*, *Porites*, and *Dipsastraea*. Soft corals were also surveyed, including *Lobophytum*, *Sinularia* and *Sarcophyton*. Branching corals of *Montipora* and *Acropora* were dominant (71% and 92% of live corals in zone 3 on MI-1 and MI-2, respectively).

Different ecological zones were identified across the reef slope (Figure 3.5, Figure 3.6). The upper reef slope was dominated by macroalgae ($89.6 \pm 15.8\%$ in zone 5 at MI-1), including *Sargassum*, *Turbinaria ornata*, *Padina*, *Chnoospora* and several un-identified genera. Macroalgae mostly grew upon/amongst branching coral rubble. Live coral cover was highest on the lower slopes, particularly on MI-2 in zone 7, which was completely covered by monospecific stands of *Goniopora* and *Galaxea* ($100 \pm 0.0\%$ coral cover). Other areas of the lower slope contained 13.3 ± 24.1 to $17.3 \pm 18.6\%$ live coral cover, where encrusting and foliaceous corals were dominant on MI-1 in zone 6 (including *Leptoseris* and *Galaxea*). A featureless muddy-sand substrate extended beyond the end of the reef slope.

3.6 Discussion

Comparisons of historical and contemporary photographs of the Stone Island reef flat (Wachenfeld, 1997) have shown a decline in coral cover and structural diversity between 1883 and 1994. These changes have been interpreted as an ecological phase-shift from a coral-dominated to macroalgae-dominated reef flat and have been used to demonstrate widespread inshore reef decline on the GBR (Hughes et al., 2010; GBRMPA, 2014). This conclusion was

reached without consideration of a) documented changes in reef condition between the two photographed periods; b) the longer (millennial-scale) record of coral growth and diversity preserved in the reef structure; and c) the condition of other coral reefs within Edgumbe Bay. My data from Stone Island provide information and context over multiple timescales to allow for a more comprehensive interpretation of the photographic records of reef condition. The Holocene reef chronostratigraphies established from Stone Island provide baseline long-term data, which combined with other historically documented changes, are valuable for interpreting recently observed variations and changes in reef condition. Coupled with photographic and other evidence, the benthic survey data show that the reef at SI-S had less hard coral cover and more macroalgae than the reef at SI-N and there is nowhere on either reef flat at Stone Island that is comparable to the reef flat condition shown in photographs presented by Saville-Kent (1893). To better understand the drivers of this change, I first discuss my findings from Stone Island in the context of different temporal scales and consider the timing and extent of ecological change. Second, I investigate the extent of the present reef condition at SI-S across local and regional scales by comparing my findings from Stone Island with other fringing reef flats in Edgumbe Bay. Collectively, the comprehensive temporal and spatial datasets on the variability in reef condition across Edgumbe Bay allow for the examination of reef recovery timeframes and to evaluate the prospects of recovery at Stone Island.

3.6.1 Stone Island reef condition – temporal variability

Early- to mid-Holocene (millennial scale)

Coral colonies established at both Stone Island reefs prior to 7,000 yBP (Figure 3.3). Although the percussion cores collected at Stone Island did not penetrate to pre-reefal substrates, it is likely that coral colonies established in a subtidal setting, upon similar substrates to those elsewhere in Edgumbe Bay. Middle Island reef initiated about the same time as the Stone Island reefs (~7,800 yBP) directly upon weathered regolith (see Chapter 4) and Bramston Reef, located ~2 km south-west of Stone Island, developed upon terrigenous transgressionary sands and lag gravels overlaying Pleistocene clay (see Chapter 2). However, the substrate at Bramston Reef was first colonised ~2,000 years after reef initiation at Stone Island (Chapter 2).

After initiation, each reef at Stone Island developed in a different way, resulting in distinct modes/styles of growth: episodic reef progradation (Kennedy and Woodroffe, 2002) at SI-S and ‘up and out’ at SI-N. This resulted in reef flat formation ~2,000 years earlier at SI-S, despite similar timing of reef initiation at both locations. At SI-S, between ~7,200 – 6,000 yBP the

landward part of the reef rapidly accreted vertically towards sea level (up to 4.8 mm/yr on average) at a similar time and pace as a seaward detached, parallel reef (Figure 3.3a). The reef first reached sea level at ~6,700 yBP. Subsequently, reef flat formation occurred by landward and seaward progradation of the detached reef sections. The spaces intervening the initially detached reef sections were infilled by a combination of *in situ* reef growth and detrital reef-derived coral rubble material. The majority of the reef flat was emplaced within 1,000 years (by 5,800 yBP). The age structure of the SI-S reef presented here showing episodic reef progradation (Figure 3.3a) is largely dependent on the age of a fossil microatoll at the seaward edge of the reef flat ($5,894 \pm 22$ yBP). Potential issues with this fossil microatoll age could interfere with the interpreted growth mode, including diagenesis of the coral sample rendering a too-old age. Alternatively, the isochrons may represent a local topographic irregularity in the reef structure (Webb et al., 2016). However, these possibilities are considered unlikely because additional fossil microatolls at the seaward edge alongshore from the transect location at SI-S were also comparatively old, dated at $6,777 \pm 20$ and $7,103 \pm 40$ yBP (Figure 3.2 and Appendix 2). Furthermore, the growth mode inferred in the present study conforms to an early reef growth model proposed by Chappell et al. (1983), in which the majority of reef establishment occurred by 6,000 yBP, followed by secondary infilling. Chappell et al. (1983) based this model on the pattern of radiocarbon ages of fossil microatolls (dating to 6,800 – 6,000 calibrated yBP) across the width of the reef flat at Stone Island, which are similar to the ages obtained in this study: $6,683 \pm 23$ yBP at the backreef flat, and $5,894 \pm 22$ yBP at the reef flat edge (Figure 3.3a). Other fringing reefs where detached reef coalescence has been documented (Kennedy and Woodroffe, 2002) include at Hayman Island (Hopley et al., 1983; Kan et al., 1997), located ~60 km east of Stone Island, and Yam Island (Woodroffe et al., 2000) in the Torres Strait.

At SI-N, after initiation the reef accreted vertically towards sea level and the majority of the reef structure was developed between ~7,000 – 4,500 yBP. Once vertical accommodation space was restricted by the defining sea level, reef flat seaward progradation occurred, about 2,000 years after reef flat formation at SI-S. Vertical reef accretion rates were slower at SI-N (0.9 – 1.7 mm/yr) compared to SI-S (3.0 – 4.8 mm/yr, Figure 3.3), which may be partly attributed to the lower terrigenous mud content in the cores (less than half that compared to SI-S in the lower mud-dominated sediment facies, Table 3.1). Mud deposition is indicative of low export rates and may enhance reef accretion rates by preserving reef framework material (Perry et al., 2012). Furthermore, the relatively exposed location of SI-N may mean this reef is more subjected to higher frequency disturbances and higher export rates, which would result in lower net reef accretion rates. The ‘up and out’ mode of reef growth displayed in the reef chronostratigraphy at SI-N is typical of inshore fringing reefs in island embayment settings, such as Pioneer Bay at Orpheus Island, central GBR (Hopley et al., 1983).

Late-Holocene (millennial scale)

The majority of both reef structures at SI-N and SI-S have been in place for at least ~4,000 years, when reef accretion slowed or ‘turned off’ (*sensu* Buddemeier and Hopley, 1988), despite the reefs developing under different modes of growth. At SI-S, the reef developed and achieved high accretion rates under constantly muddy conditions during the mid-Holocene. While the reef crest has not prograded significantly since ~4,000 yBP, it is possible that the subtidal reef slope may have continued to prograde, although at a reduced pace, and has not reached sea level to form a reef flat as in the mid-Holocene (Figure 3.3a). After 4,000 yBP reef growth was probably limited to a veneer of living coral at the outer edge of the reef, which is common for mid-Holocene aged fringing reefs in the inshore GBR (Smithers et al., 2006). No reef material younger than $4,324 \pm 22$ yBP at SI-S was dated, likely due to the targeted sampling strategy and/or because material has been moved away by storms/cyclones. The effects of storms and cyclones on reef growth are evident at Middle Island, where considerable quantities of reef material were removed from the reef structure during cyclones in the mid-Holocene and deposited onshore as shingle ridges (Figure 3.6 and see Chapter 4 for further details). The potential for such storm activity at Stone Island is indicated by storm-deposited beach ridges on the shoreline in Shoalwater Bay and along the south-eastern side of the island, first documented by Hopley (1975).

Although reef accretion slowed or ceased around 4,000 yBP at SI-N, reef accretion may have ‘turned on’ (*sensu* Buddemeier and Hopley, 1988) again around 2,000 yBP, as indicated by the fossil microatoll ages of $2,091 \pm 9$ and $2,018 \pm 19$ yBP at the outer reef flat. A similar turn-off and/or hiatus in active reef accretion between ~4,000 – 2,000 yBP to that observed at Stone Island has been detected in many reefs of the inshore GBR (Smithers et al., 2006; Perry et al., 2011), including Bramston Reef in Edgecumbe Bay (detailed in Chapter 2). The causes of this regional hiatus are not completely clear but likely include one or a combination of the following factors: accommodation space constraints caused by late-Holocene sea-level fall (Smithers et al., 2006; Perry et al., 2011); shifts in mid-Holocene sea-surface temperature or climate (Gagan et al., 1998); and/or terrigenous mud deposition events (see Chapter 2). Notably, the deceleration in active reef accretion at Stone Island occurred well before European settlement of the coast and was thus driven by natural factors. Indeed, the most productive time for active reef accretion at Stone Island fringing reefs was ~7,000 – 4,000 yBP. After this, negligible reef accretion occurred at Stone Island, despite regional conditions being

suitable for reef accretion between 4,000 – 1,000 yBP, as Bramston Reef continued to prograde during this time (with the exception of a hiatus ~3,000 – 2,000 yBP) (Chapter 2).

Contemporary (centennial-scale to present)

Both reef flats at Stone Island were dominated by sand, coral rubble and macroalgae, with very little live coral cover, in accord with benthic surveys conducted by Clark et al. (2016) where live coral cover at the SI-S reef flat was $0.09 \pm 0.12\%$. At SI-S macroalgae was more abundant, comprising >50% cover in three zones at SI-S and just one zone at SI-N (Figure 3.3). Live coral cover on the reef slope was high at SI-N comprising $46.0 \pm 36.2\%$ cover (Table 3.2, Appendix 4). Here, live coral occurred across the upper to lower slope, while on the SI-S reef slope, live coral was restricted to a narrow 20 m wide zone that also contained macroalgae (Table 3.2, Figure 3.3, see also Appendix 3). In addition, live coral diversity was higher at SI-N with eight hard coral genera identified (*Acropora*, *Montipora*, *Turbinaria*, *Favites*, *Fungia*, *Pocillopora*, *Porites* and *Platygyra*) compared with three identified genera (*Acropora*, *Porites* and *Pocillopora*) at SI-S (Table 3.2). Ideally, a comparison of the palaeo-ecological diversity in the long-term percussion core records with the present reef slope diversity would be valuable. However, differentiating coral genera in the video footage was often impossible due to turbidity and thus the eight coral genera identified at SI-N are probably an underestimate of the true generic diversity at this site. Furthermore, the palaeo-ecological data are largely derived from subtidal reef slope environments, which cannot be directly compared to the intertidal reef flat data (benthic surveys, reef flat photographs) due to differences in environmental conditions resulting in naturally different coral assemblages (Chappell, 1980). Videography was a suitable technique in this study for simply quantifying benthic cover, but a more detailed study on reef slope coral cover and diversity at these inshore reefs is needed.

Surveys of contemporary ecological benthic cover confirm that neither reef flat at Stone Island currently supports coral cover comparable with that depicted in Saville-Kent's (1893) photographs, which show a variety of live corals exposed at low water on the reef flat. Rather, the reef flats were dominated by sand, rubble and macroalgae, as shown in the more recent photographs of the reef flat in Wachenfeld (1997) and Clark et al. (2016) taken in 1994 and 2012, respectively (see also Figure 3.1 and Appendices 3 and 4). My study has provided insight to address some of the issues with using the photographic comparisons alone to make conclusions about regional reef condition. The critical issues are: 1) the exact location of the Stone Island photographs from the late 1800s; 2) the elevation of the reef flat shown in historical and contemporary photographs; and 3) the significance of any documented changes in the context of a longer-term Holocene reef growth history. The location of Saville-Kent's

(1893) photographs was indicated by Hedley (1925), which conforms to the landforms in the horizon of several photographs. However, the exact location of Saville-Kent's photographs is unknown, and thus so too is the elevation of the reef flat and corals shown in the photographs. Knowing the accurate elevation of the reef flat surface where historical and recent photographs were taken is crucial to ensure the possible influence of emergence of the mid-Holocene aged reef flat can be determined. However, elevation is unknown for all existing photographs from Stone Island, except very recent photographs presented in Clark et al. (2016) and this thesis (Appendix 10). The tops of the corals in the historical photographs that were taken during spring low tide by Saville-Kent (1893) must have been elevated approximately 0.5 – 0.3 m above LAT based on my surveys of uppermost open-water coral growth elevation within Edgcombe Bay (Table 3.2). If these photographs were of the outer reef flat (which is now ~0.2 – 0.8 m below LAT) it is implied that a significant amount of reef material from the outer reef flat has been eroded or scoured away since the photo was taken, as suggested by Clark et al. (2016). Dated fossil microatolls aged between $6,716 \pm 23$ and $5,894 \pm 22$ yBP indicate that the entire part of the reef flat at SI-S that is presently exposed at low water developed during the early- to mid-Holocene (Figure 3.3a) when sea level was 1.0 – 1.5 m higher than present (Chappell et al., 1983; Lewis et al., 2013). Thus, much of the backreef flat surface is elevated ~1.0 mLAT, too high for modern open-water reef flat live coral growth, which at Middle Island was restricted to below 0.8 mLAT (Table 3.2) and at Bramston Reef to below ~0.4 – 0.3 mLAT (Chapter 2). This finding casts doubt that the location/elevation of some of the recent photographs of Stone Island reef flat are true replicates of Saville-Kent's images, and raises the possibility that they are in fact images of the older, elevated section of the reef flat. For example, the photograph presented in Bell et al. (2014) taken in 1994 reportedly showing the 'nearshore region' (Bell and Elmetri, 1995), is probably of the higher and senescent mid-Holocene backreef because of the distance it is located from the water's edge. It is easy to misinterpret these photographs without an understanding of the Holocene reef growth history, subtle changes in elevation, and the control this has on intertidal coral growth and survival. Regardless of water quality, coral cover and diversity will naturally never be high if the reef flat elevation is too high and emergence is prolonged. Nevertheless, contemporary photographs of the outer reef flat at Stone Island (Figure 3.1, Clark et al., 2016) still show very little or no live coral cover. Ultimately, conclusions should not be drawn about changes in reef condition based on the historical photographs that are not spatially (and elevationally with respect to the tidal frame) referenced with great precision and accuracy. However, when combined with quantitative data and long-term knowledge of reef development and palaeo-ecology, photographs can provide additional useful evidence of reef condition.

3.6.2 Local versus regional effect

Sediment and nutrient loads delivered to the GBR from the Queensland coast have undoubtedly increased since European settlement (McCulloch et al., 2003; Kroon et al., 2012; Waters et al., 2014). Concern that these water quality changes have limited the recovery potential of inshore reefs and caused persistent shifts in ecosystem states (from coral to macroalgae dominated) is widespread. However, direct evidence is lacking and difficult to measure. Contemporary reef benthic composition varied between SI-N and SI-S (Figure 3.3, see section 3.6.1), and also varied between other sites in Edgumbe Bay. While the SI-S and SI-N reef flats contained very little live coral, other reef flats in the region displayed high coral cover ($63.1 \pm 20.2\%$ at Middle Island).

All the fringing reefs in Edgumbe Bay for which reef growth histories are known began to develop in the early- or mid-Holocene and have not prograded much since $\sim 2,000$ yBP (Table 3.3). Nevertheless, live coral cover blankets parts of these old reef structures as a thin veneer of growth, including at Middle Island (Figure 3.5) and Bramston Reef (see Chapter 2). The amount of live coral cover and the elevations at which corals survive varies between reefs and these variations are particularly pronounced on the outer reef flat zones. While living coral cover was scarce on the outer reef flats at Stone Island, despite the reef flat surfaces being elevated 0.3 mLAT to -0.8 mLAT, live coral cover on the outer reef flat at Middle Island (0.6 – 0.0 mLAT) was $63.1 \pm 20.2\%$ (Figure 3.5, Figure 3.6, Table 3.2). Middle Island is clearly an example of an inshore fringing reef flat with exceptionally high coral cover, exceeding the average cover quantified for nearshore patch reef flats ($\sim 35\%$: Perry et al., 2009; $\sim 7\%$: Browne et al., 2010) and inshore fringing reef flats (5 – 33%: Bull, 1982; 14%: Ryan et al., 2016) and slopes (30 – 40%: Thompson et al., 2013). Furthermore, average coral cover between 1985 and 2012 on the central GBR (largely mid-shelf reef slopes) was only around 15 – 30% (De'ath et al., 2012); well below that established for the reef flat at Middle Island even though reef flat environments typically have lower coral cover and are more vulnerable to disturbances than reef slopes.

Open-water living coral has been documented on areas of the reef flat elevated < 0.8 mLAT at Middle Island (Table 3.2) and < 0.4 mLAT at Bramston Reef (see Chapter 2). Based on these other locations in Edgumbe Bay (including one closer to the mainland than Stone Island) it would be expected that live corals could grow at similar elevations (below at least 0.4 mLAT) at the Stone Island reef flats, providing all other requisites for coral growth were met. Yet this was not the case and live coral cover was very poor on the Stone Island reef flats. Coral growth is possible up to 0.5 mLAT at Stone Island as the upper living rims of *Porites* microatolls were elevated 0.5 – 0.3 mLAT at SI-N and SI-S (Figure 3.2). However, some of the living

microatolls were partly smothered by macroalgae, which can impede coral settlement and growth (Fabricius, 2005; Foster et al., 2008; Diaz-Pulido et al., 2010).

Presently, coral cover varies between reefs in Edgcumbe Bay as it has done over the past ~150 years (Table 3.4). However, whether shorter-term fluctuations in reef condition occurred in the longer-term records provided by reef cores is uncertain, as most long-term records do not provide age data at adequate resolution to answer such ecological questions (Pandolfi and Kiessling, 2014). Nevertheless, the longer-term records do suggest that reef accretion has stopped and started on millennial scales, independently of anthropogenic impacts (Figure 3.3b, Chapter 2). If recent anthropogenic impacts such as increased sediment and nutrient loads to the inshore GBR have contributed to low coral cover at Stone Island, similar effects are not regionally evident within Edgcumbe Bay. Indeed, parts of Bramston Reef today appear similar to the condition photographed and described by Saville-Kent (1893), while the coral growth at Middle Island matches the descriptions by Agassiz (1898) (Table 3.4). Thus, the condition of the reefs at Stone Island appears to be a local effect. When using high coral cover at Middle Island as an example, it could be argued that the greater distance offshore is advantageous to reef health due to the location away from major river influences. However, the high coral cover at SI-N upper reef slope ($46.0 \pm 36.2\%$) clearly demonstrates that healthy reef growth is possible at this inshore site. A long-term understanding of disturbance and recovery regimes is required to investigate the effects of local factors that may have influenced the recovery potential at Stone Island.

The rate at which a reef recovers after a disturbance is influenced by a myriad of factors (Connell et al., 1997; Graham et al., 2011; Kittinger et al., 2011) and inshore reefs likely recover at different rates to their offshore, clear water counterparts (Done et al., 2007). Observed rates of recovery on inshore reefs are variable and poorly understood due to a lack of long-term studies. Observed inshore reef recovery rates were >14 years in Jamaica after a hurricane (Hughes and Connell, 1999), while longer recovery periods (over decades to centuries) have been reported in Hawaii, revealing that over long timeframes reefs may maintain resilience to recover from human impacts (Kittinger et al., 2011). Estimated rates of inshore reef recovery vary from 7 years (Johns et al., 2014) to 15 years (Jones and Berkelmans, 2014) after various disturbance types. Clark et al. (2016) estimated the recovery time at Stone Island reef flat (SI-S) to be 40 to 50 years.

The available qualitative and quantitative data for reef condition in Edgcumbe Bay (Table 3.3, Table 3.4) allow for an appreciation of ecological trends despite being punctuated in time. At Middle Island, the appearance of the reef flat today is remarkably similar to the description of

its state in the late 1800s provided by Agassiz (1898), and strong coral community recovery must have occurred over the past 40 years since Hopley's (1975) description. The results of Middle Island reef slope benthic cover showing high coral cover on the lower slope (Table 3.2, Figure 3.6) are compatible with DeVantier et al.'s (1998) description of the ecological condition of Middle Island reef slope in 1994 – 1995 as top quality on the lower slope, with above average hard coral cover, richness and diversity, but poor quality on the upper slope, with below average hard coral cover and above average turf algae cover. At Stone Island however, no recovery is apparent over the past 40 years. Anecdotal evidence and ages from dead *in situ* coral colonies on Stone Island reef (Clark et al., 2016) suggests that coral communities may have been on the way to recovery during the 1970s (Table 3.4), fifty years after the 1918 cyclone. The potential of the reef to recover may still exist, but requires further and regular ecological monitoring.

Table 3.3 Reef condition in Edgcumbe Bay over millennia based on reef cores. Time is thousands of years before present (k yBP).

	8-7 k yBP	7-6 k yBP	6-5 k yBP	5-4 k yBP	4-3 k yBP	3-2 k yBP	2 k yBP to present	Reference
Bramston Reef			Initiation, vertical accretion	Rapid vertical accretion (rates up to 3.6 mm/yr), reached sea level	Reef flat prograded seaward	Little accretion	Negligible seaward progradation	Chapter 2
Stone Island South	Initiation, vertical accretion	Rapid vertical accretion (rates up to 4.5 mm/yr), reached sea level	Reef flat prograded, lateral accretion	Negligible seaward progradation	No accretion	No accretion	Negligible seaward progradation	This chapter
Stone Island North	Initiation, vertical accretion	Rapid vertical accretion (rates up to 5.0 mm/yr)	Vertical and lateral accretion (vertical rates up to 1.7 mm/yr)	Vertical and lateral accretion, reached sea level	No accretion	No accretion	Negligible seaward progradation	This chapter
Middle Island	Initiation, vertical accretion	Rapid vertical accretion (rates up to 7.6 mm/yr), reached sea level and reef flat prograded	Reef lateral accretion and cyclone stripping	Reef lateral accretion and cyclone stripping	No accretion	No accretion	Veneer of vertical (<1.2 m) and lateral growth	Chapter 4

Recovery on inshore reefs may be hindered by shorter intervals between disturbances and/or the reduced supply of coral larvae for recolonisation (Done et al., 2007). The high coral cover on sections of the reef at SI-N and other reefs in Edgcumbe Bay implies that no major regional

Table 3.4 Statements of reef condition in Edgcumbe Bay over the past ~150 years derived from various sources.

Reef site in Edgcumbe Bay	Time (year AD)	Statement of reef condition	Source type	Reference
Bramston Reef	c. 1890	Exposed at low tide was “a grand mass of <i>Porites</i> ... it’s exposed, horizontal surface is for the most part dead and eroded...the eroded upper surface has been adopted as a fulcrum of attachment by various coral types that flourish on a higher vertical plane”, including <i>Goniastrea</i> and <i>Acropora</i> . “abundant development...of a luxuriant crop of seaweeds”.	Historical photographs and associated descriptions	Saville-Kent (1893, pp. 15)
Bramston Reef	1994	“Large numbers of faviid colonies...the vast majority are dead and those that are alive are comparatively small (<15 cm)...typically covered in algae and/or mud”. Living large <i>Porites</i> colonies and microatolls with mud and algae on top of the microatolls.	Photographs and descriptions	Wachenfeld (1997, pp. 138)
Bramston Reef	2012	Live coral cover on outer reef flat on average $7.0 \pm 4.7\%$, including <i>Acropora</i> , <i>Goniastrea</i> , <i>Montipora</i> , <i>Goniopora</i> , <i>Lobophyllia</i> , <i>Favites</i> , <i>Turbinaria</i> , <i>Pocillopora</i> , <i>Favia</i> (<i>Dipsastraea</i>).	Ecological survey	Clark et al. (2016)
Bramston Reef	2014	Live coral cover on outer reef flat on average $13.9 \pm 19.22\%$, including large <i>Porites</i> colonies with dead upper surfaces, colonised by a variety of live soft and hard corals and algae. Reef slope contains zones of high coral cover (up to $51.3 \pm 19.4\%$) and zones dominated by macroalgae.	Ecological survey	Chapter 2
Stone Island	c. 1890	Extensive hard coral cover on the reef flat exposed at spring low tide, including <i>Acropora</i> , <i>Montipora</i> , <i>Goniastrea</i> , <i>Turbinaria</i> , <i>Pavona</i> .	Historical photographs and associated descriptions	Saville-Kent (1893)
Stone Island	c. 1920	No trace of living coral. “This famous, wonderful and immense structure has now completely vanished. Not only has the coral all died, but every vestige of it, except the foundation, has been swept away”	Descriptions	Hedley (1925); Rainford (1925)
Stone Island	1925	Live coral cover recovering, small colonies of <i>Goniastrea</i> , <i>Merulina</i> , <i>Turbinaria</i> and <i>Fungia</i> observed. Soft corals flourishing.	Descriptions	Stanley (1928)
Stone Island	1936	Reef flats “dead on their upper surfaces”. Recovery negligible.	Descriptions	Steers (1937); Richards (1938)
Stone Island	1953	Negligible recolonisation.	Anecdotal evidence from personal communications	Stephenson et al. (1958)
Stone Island	c. 1970s	Healthy reef flat.	Anecdotal evidence from local residents	Wachenfeld (1997)
Stone Island	1990	Reef flat surface dominated by coral rubble and macroalgae. No colonies of <i>Acropora</i> exposed on the reef flat at spring low tide. Few massive colonies.	Photographs and descriptions	Wachenfeld (1997)
Stone Island	2012	Reef flat dominated by sand and macroalgae. Extremely low coral cover on the reef flat ($0.09 \pm 0.12\%$). Live <i>Acropora</i> , <i>Cyphastrea</i> , <i>Pocillopora</i> , <i>Goniastrea</i> , <i>Platygyra</i> , <i>Favia</i> (<i>Dipsastraea</i>) observed.	Photographs and ecological survey	GBRMPA (2014); Clark et al. (2016)
Stone Island	2013-2014	Reef flats dominated by sand, coral rubble and macroalgae with very sparse, small live corals. Reef slope at Shoalwater Bay averaged 46.0 ± 36.2 and $18.5 \pm 23.7\%$ live coral cover (branching, encrusting, plate, columnar, foliaceous, free-living and massive). Reef slope on southern side of island dominated by macroalgae with narrow zone containing $33.3 \pm 21.11\%$ live coral (branching and massive).	Ecological survey	This chapter
Middle Island	1896	The outer face of Middle Island’s reef flat was “coated with fine heads of corals...becoming less prominent as they tend towards the shallower edge of the flat”.	Historical descriptions	Agassiz (1898, pp. 107)
Middle Island	1970s	Reef flat largely dead.	Geomorphological description	Hopley (1975)
Middle Island	1994-1995	Below average hard coral cover and above average turf algae cover on upper slope. Above average hard coral cover, hard coral richness and diversity on the lower slope.	Ecological survey	DeVantier et al. (1998)
Middle Island	2014	High coral cover on outer parts of the reef flat ($63.1 \pm 20.2\%$) and lower parts of the reef slope (17 ± 18.6 to $100 \pm 0.0\%$).	Ecological survey	This chapter

disturbance has affected these sites in the last decade or so. Small coral recruits were present, although rare at Stone Island, indicating that recruitment can still occur at this site (van Woesik et al., 1999; Done et al., 2007). Whether or not the supply/abundance of recruits has changed over time is unknown. However, the low abundance of coral recruits on Stone Island reef flats compared with Bramston Reef (Chapter 2) and Middle Island suggests that either settlement or prolonged survival of recruits is impeded. This warrants further investigation, however hydrodynamic processes such as current velocities and direction may influence recruit settlement (van Woesik et al., 1999). The high abundance of macroalgae at SI-S compared with other locations (Figure 3.5) may be contributing to the survival and recovery of coral communities (McCook et al., 2001; Fabricius, 2005; Diaz-Pulido et al., 2010). Furthermore, rippled sand areas at SI-N are probably quite mobile and coral recruitment would be difficult on these soft substrates. Soft rippled sand substrates were also observed (though not surveyed) on the western side of SI-S reef flat near the sand spit. Indeed the ~400 m long sand spit (Figure 3.2) indicates a large supply of sediment to this part of the island. The sand spit would be mobile under normal and storm conditions and spit migration may influence the survival of coral recruits in this area of the reef flat (Hopley et al., 1983).

3.7 Conclusion

Holocene reef development was reconstructed at two fringing reefs at Stone Island to provide baseline, Holocene data on past reef condition as context for assessing contemporary reef state. The high-precision U-Th ages from the reef cores show that both reefs began to develop in the early-Holocene, prior to ~7,000 yBP. Despite each reef at Stone Island developing according to different modes/styles of growth and under different sediment regimes, the majority of reef growth occurred by 4,000 yBP at both sites. The reef flats developed under a higher mid-Holocene sea level, with the backreef flat environment elevated up to a metre above the level of present reef flat formation. The elevation of the reef flat surface influences the contemporary variability in benthic cover across each reef, with the higher elevation backreef zones at all reefs dominated by sand, coral rubble and macroalgae. Open-water live coral cover was restricted to the lower elevation outer reef flats. At Stone Island, live coral cover on the outer reef flats was very scarce, while the outer reef flat at Middle Island was characterised by high coral cover reaching as much as $63.1 \pm 20.2\%$.

The reef at SI-S was in a comparatively poor condition relative to other reefs in Edgumbe Bay and there was nowhere on either reef flat at Stone Island that was comparable to photographs taken in the late 1800s. Thus, localised factors are probably inhibiting reef flat

recovery at Stone Island (particularly SI-S). These results highlight why photographs of reef flats over time that are not spatially referenced should not be solely used to document changes in reef condition, particularly on a regional scale. Interpretations of photographic records should take into account the long-term development of the reef, the elevation of the reef flat where the photos are taken, and the decadal scale ecological trends and recovery rates, if possible. There is no doubt that phase-shifts have occurred on some inshore reefs on the GBR, but further studies on the reefs where it appears phase-shifts have occurred through photographic evidence (Wachenfeld, 1997) or the lack of accretionary corals (e.g. van Woesik et al., 1999) would be beneficial to gain a more comprehensive understanding. Such studies will provide further insights on the ability of inshore reefs to recover from natural and anthropogenic disturbances.

4 The influence of sea level and cyclones on Holocene reef flat development: Middle Island, central Great Barrier Reef

Article published in 2016:

Ryan, E.J., Smithers, S.G., Lewis, S.E., Clark, T.R. and Zhao, J.X. 2016 The influence of sea level and cyclones on Holocene reef flat development: Middle Island, central Great Barrier Reef, *Coral Reefs*, DOI 10.1007/s00338-016-1453-9.

Chapter 1 revealed a key knowledge gap relating to the influence of cyclones of reef growth on millennial scales. The results of Chapter 3 revealed that the reef flat at Middle Island is an excellent example of an inshore reef with high coral cover. In this chapter I present the first record of Holocene reef growth at Middle Island, located near the boundary between the inner- and mid-shelf. New insights into the effects of cyclones on Holocene reef development are presented.



Plate 4. View across Middle Island looking to the west showing from left to right: part of the exposed reef flat at low tide, beach, shingle ridges, large vegetated shingle ridge (centre) extending to the enclosed ephemeral lake (far right).

4.1 Abstract

Geomorphological and chronostratigraphic investigations of the reef flat (including microatoll ages and elevations) were conducted to better understand the long-term development of the reef at Middle Island, inshore central Great Barrier Reef. Eleven cores across the fringing reef captured reef initiation, framework accretion and matrix sediments, allowing a comprehensive appreciation of reef development. Precise uranium-thorium ages obtained from coral skeletons revealed the reef initiated $\sim 7,873 \pm 17$ yBP, and most of the reef was emplaced in the following 1,000 years. Average rates of vertical reef accretion ranged between 3.5 – 7.6 mm/yr. Reef framework was dominated by branching corals (*Acropora* and *Montipora*). An age hiatus of $\sim 5,000$ years between $6,439 \pm 19$ to $1,617 \pm 10$ yBP was observed in the core data and attributed to stripping of the reef structure by intense cyclones during the mid- to late-Holocene. Large shingle ridges deposited onshore and basset edges preserved on the reef flat document the influence of cyclones at Middle Island, and represent potential sinks for much of the stripped material. Stripping of the upper reef structure around the outer margin of the reef flat by cyclones created accommodation space for a thin (<1.2 m) veneer of reef growth after $1,617 \pm 10$ yBP, which grew over the eroded mid-Holocene reef structure. Although limited fetch and open water exposure might suggest the reef flat at Middle Island is quite protected, the results presented here show that high-energy waves presumably generated by cyclones have significantly influenced both Holocene reef growth and contemporary reef flat geomorphology.

4.2 Introduction

Coral reefs globally have been exposed to a range of natural stressors throughout their development in the Holocene. These include: cyclones (Done, 1992); sea-level change (Woodroffe and Webster, 2014); and exposure to terrestrial sediments washed from coastal catchments (Risk, 2014). The degree and frequency of exposure to such stressors influences a coral reef's rate and style/mode of reef geomorphological development. For example, changes in sea level influence the accommodation space available for coral growth (Kennedy and Woodroffe, 2002), while terrestrial sediment accumulation can enhance reef accretion rates by reducing bioerosion and physical erosion (Perry et al., 2012). Widespread decline in reef condition has occurred in recent decades (Bruno and Selig, 2007; Wilkinson, 2008), raising concerns that stressors associated with anthropogenic activities amplify the effects of natural stressors on reefs, reducing coral cover and lengthening post-disturbance reef recovery intervals (Wilkinson, 2008). Recent declines in reef condition on Australia's Great Barrier Reef (GBR) have been attributed to cyclones, crowns-of-thorns starfish outbreaks and coral bleaching (De'ath et al., 2012). Many inshore reefs of the GBR (defined as those between the 20 m isobath and the coast) are located close to the coast and have been exposed to elevated riverine

sediment and nutrient loads since European settlement of Queensland coastal catchments from the early 19th Century (Fabricius et al., 2005; Kroon et al., 2012; Waters et al., 2014). Increased sediment and nutrient loads can negatively impact coral reefs by reducing water quality through increased turbidity and sedimentation (see Fabricius, 2005). The exposure of inshore reefs to these conditions means that they are commonly considered vulnerable to ecological phase-shifts from coral-dominated to sediment- and macroalgae-dominated environments, with limited capacity to recover (Hughes et al., 2010). However, the cumulative effects of multiple stressors on reef ecological and geomorphological condition remain poorly understood, partly because of limited long-term baseline information on reef condition and natural variability prior to European settlement.

The impacts of cyclones on coral reef ecology and geomorphology have been well documented over recent decades (Done, 1992; Scoffin, 1993; Harmelin-Vivien, 1994; van Woerik et al., 1995; Perry et al., 2014). However, the impacts of cyclones on reef development over longer timescales (centennial-millennial) are less well known. This is largely because few long-term chronostratigraphic investigations of reefs exist on the GBR or elsewhere (Blanchon and Jones, 1997; Blanchon et al., 1997; Braithwaite et al., 2000) that have been undertaken with sufficiently high temporal resolution needed to detect such events. Furthermore, few storm histories that extend the temporal range of generally short (<100 years) instrumental records have been developed. Long-term cyclone data have been reconstructed for the GBR region based on radiometric ages from beach ridges, gravel beach terraces, shingle ridges (Chappell et al., 1983; Chivas et al., 1986; Nott and Hayne, 2001; Nott et al., 2009; Forsyth et al., 2010), storm-transported coral blocks (Yu et al., 2012; Liu et al., 2014), and oxygen isotope signatures of cyclonic rainfall preserved in speleothems (Nott et al., 2007; Haig et al., 2014). However, the influence of cyclones on long-term (millennial-scale) reef development has received little attention, despite observations of extensive ecological and geomorphological changes during recent cyclones (Scoffin, 1993).

Long-term reef growth chronologies developed from reef cores provide insights into reef initiation, accretion rates, coral palaeo-ecology and sediment influence throughout the development of a reef (Hopley, 1982; Kennedy and Woodroffe, 2002; Montaggioni, 2005; Hopley et al., 2007). Such records demonstrate that many GBR inshore reefs initiated ~8,000 – 7,000 yBP and rapidly developed reef flats within 2,000 years of initiation (Partain and Hopley, 1989; Kleypas, 1996; Smithers et al., 2006). Reef flat development at many inshore reefs occurred in the mid-Holocene when relative sea level was at least 1 m higher than present (Perry and Smithers, 2011; Lewis et al., 2013). Although the precise details of timing and elevation continue to be debated, relative sea level along the inner GBR fell to its present level

by around 2,000 – 1,000 yBP (Lewis et al., 2013; Lewis et al., 2015). As a result, reef flats formed during higher mid-Holocene sea levels are now emergent at low tides (Smithers et al., 2006).

This study presents a long-term reef chronology from a fringing reef flat on Middle Island in the central inshore GBR established using a combination of percussion and rotary drill cores paired with high-precision uranium-thorium (U-Th) ages. The precise dating technique used here allows better interpretation of reef growth signatures (including hiatuses) than other common dating techniques available. Middle Island is an ideal location to examine long-term reef growth because: a) historical records (~100 years) descriptions exist of the reef flat (Agassiz, 1898; Rainford, 1925; Hopley, 1975) that have not been considered in the context of Holocene reef development; and b) Middle Island is located in a semi-protected setting on the outskirts of Edgumbe Bay and includes a range of elevated coral shingle ridges deposited by past storms. The sedimentary and ecological record from 11 cores recovered along a transect on the Middle Island reef flat spans the complete period of Holocene growth to reveal the reef initiation age and basal substrate. The chronostratigraphic development of the reef is presented, including rates of vertical growth. The influences of sea level and cyclones on past reef growth and present geomorphology are discussed.

4.3 Materials and methods

4.3.1 Study site

Middle Island (19°59'S, 148°22'E) is a 1.1 km long and 0.5 km wide vegetated continental island located ~10 km offshore from Bowen in the central inshore GBR, Australia (Figure 4.1a, b). Gloucester Island and Cape Gloucester shelter Middle Island from swells generated by prevailing south-easterly trade winds. A fringing reef flat has developed on the southern side of Middle Island (Figure 4.1b, c). This reef flat is ~330 m wide and slopes from ~1.0 m above lowest astronomical tide (LAT) at the shoreline to close to LAT at the reef crest. The backreef flat is emergent at lower tidal stages. Tides are semi-diurnal and the tidal range is 3.6 m. Water depths immediately around Middle Island reach ~16 m depth. An ephemeral lake (the surface of which is elevated ~2.6 mLAT) occurs on the interior of the island, impounded on the reef flat side by a 50 – 75 m wide vegetated shingle ridge, with a crest elevated at 6.3 mLAT (Figure 4.1b, d). Two smaller unvegetated shingle ridges (varying alongshore between 2.6 – 10 m wide and at 4.3 – 5.1 mLAT) are located at the top of the contemporary beach, seaward of the larger vegetated ridge (Figure 4.1d).

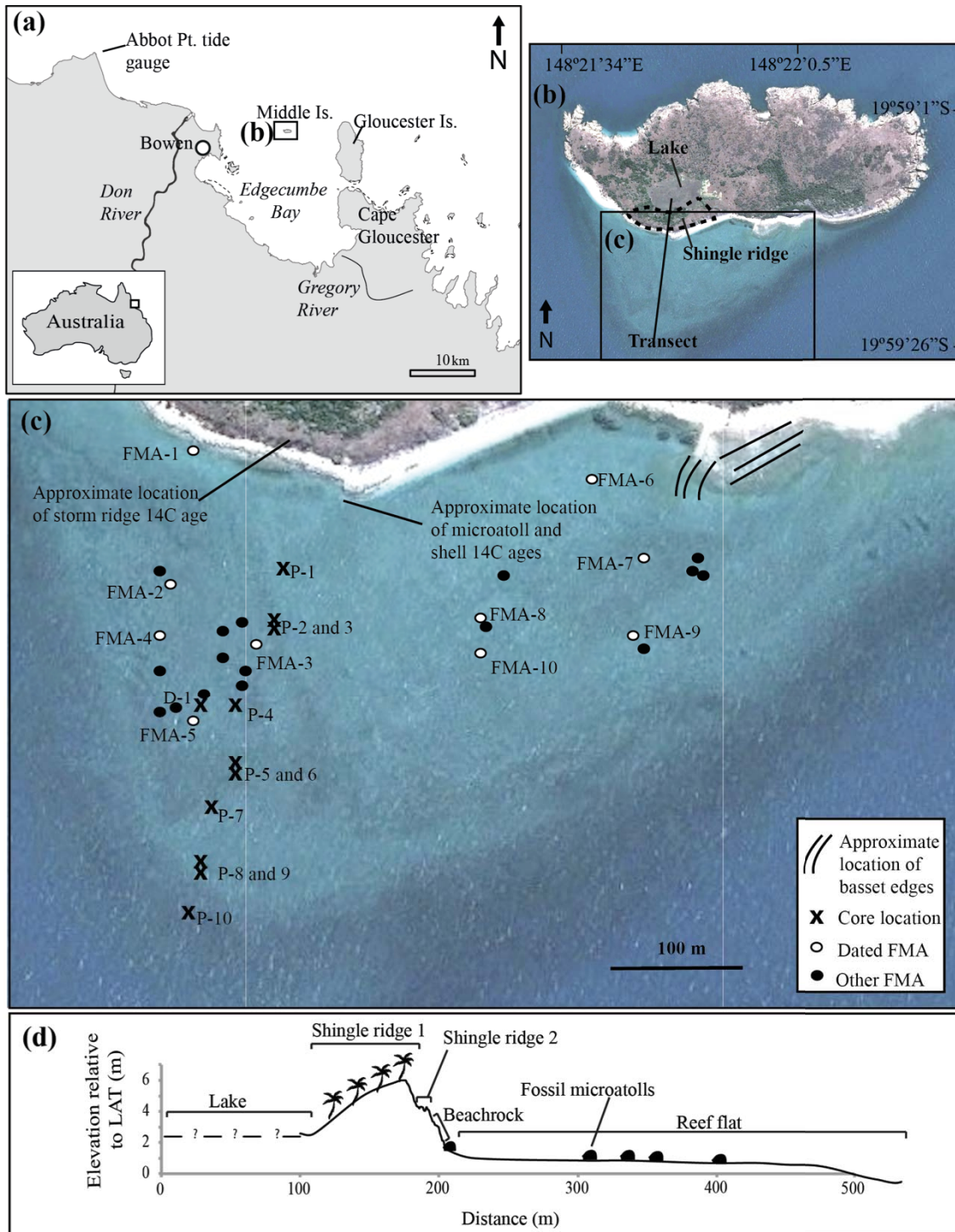


Figure 4.1 Location of (a) Middle Island in the central Great Barrier Reef, Australia; (b) core transect at Middle Island; (c) percussion cores (P), drill core (D), fossil microatolls (FMA) on the reef flat. The approximate locations of previously reported radiocarbon (^{14}C) ages (Hopley, 1975) from Middle Island are shown; (d) reef flat profile extending seaward with major morphological zones labelled. Elevation is relative to lowest astronomical tide (LAT) at the Abbot Point tide gauge.



Figure 4.2 Photograph of basset edges at the backreef flat, Middle Island.

Freshwater and sediment discharge to the inner central GBR lagoon is highly seasonal. Middle Island is located >10 km from minor river mouths and >70 km from major river systems and is less frequently affected by turbid water conditions caused by flood plumes than many GBR inshore reefs. The Burdekin River delivers the highest sediment loads to the GBR lagoon (Kroon et al. 2012) and is located ~80 km north of Middle Island. However, Burdekin flood plumes typically travel northward (Bainbridge et al. 2012) and influence Middle Island just 4 – 6 times per decade, according to Devlin et al. 2012).

Coral cover on the reef flat at Middle Island has been described several times over the past 120 years, which when viewed together reveal phases of reduced and higher cover over more than a century of observation (see section 3.3 in Chapter 3). Agassiz (1898) described high coral cover across the outer reef flat at Middle Island in 1896, which Rainford (1925) later argued was completely destroyed during freshwater plumes associated with two cyclones in 1918. The coral cover on Middle Island reef flat has since recovered (see section 3.5.2 in Chapter 3). Records over the past 150 years document the episodic influence of cyclones within the Bowen region (Appendix 6), with many passing over or close to Middle Island. A photograph taken in 1896 by Agassiz shows a coral shingle ridge composed of material stripped from the living reef (of the type normally emplaced by storms [Scoffin, 1993]) on the reef flat at Middle Island that is

no longer there. However, basset edges (cemented remnants of the basal parts of storm deposits, Figure 4.2) are preserved on the reef flat and can document the former positions of now destroyed ridges (Scoffin, 1993). Such features indicate a long history of cyclone occurrence and ecological and geomorphological impacts at Middle Island and many reef flats across the GBR (Hopley, 1975; Chappell et al., 1983).

4.3.2 Core recovery, logging and analysis

Rotary drilling (Hopley et al., 1978; Hopley et al., 1983; Johnson and Risk, 1987; Kleypas, 1996) or percussion coring (Perry and Smithers, 2010; Roche et al., 2011; Lewis et al., 2012; Roff et al., 2012, 2015) are common techniques used for coring fringing reefs on the GBR to examine long-term reef development. Rotary drilling does not capture unconsolidated reef matrix material but allows deep penetration (up to ~20 m) of consolidated reef substrates (Partain and Hopley, 1989). Percussion coring on the other hand captures both reef framework and matrix material and preserves stratigraphic arrangement, but penetration depth is restricted with this technique (maximum ~6 m depth) (Perry and Smithers, 2006). Rarely, however, have the methods been applied together to achieve a more complete understanding of reef development. At Middle Island, Holocene reef ecology, growth and variation were reconstructed from 11 cores driven vertically into the reef flat, extending up to 7.2 m below the present surface (Figure 4.1c, d). Ten cores were collected using percussion coring, detailed in section 1.9.2, with cores penetrating up to 4.5 m below the reef flat surface and capturing both reef framework and matrix sediment. One long core (7.2 m penetration) that terminated in the pre-Holocene substrate was retrieved using a portable rotary drill rig system, similar to the device described in Partain and Hopley (1989). The compaction rate was recorded to calculate total compaction for each core, which varied from 11 – 64% in the percussion cores. The rotary drill coring technique is detailed in section 1.9.2. Total recovery of the drill core was 18% (1.3 m recovery of 7.2 m penetration). Low drill core recovery was due to the open framework/detrital nature of the reef's structure, and poor recovery of finer unconsolidated reef matrix sediments, as is typical when using the rotary drilling method. Nevertheless, the rotary drilling recovery rate is comparable with those of Kleypas (1996) who investigated fringing reef structures on high islands in the southern GBR.

Following collection, cores were logged and major sediment facies were differentiated based on the ratio of coral framework to matrix material, whether the unit was matrix- or clast-supported, sediment texture (according to Udden-Wentworth nomenclature) and a visual assessment of sediment composition. To determine variations in matrix characteristics downcore, two sediment samples (~10 g each) were collected at 20 cm intervals (uncompacted), ensuring all

facies were sufficiently sampled. The dry weight of all samples was recorded and one set of samples was used for carbonate content analysis and the other for mud content (<63 microns) analysis using acid digestion and sieving techniques detailed in section 1.9.2 in Chapter 1. The palaeo coral community composition captured in the percussion cores was determined following the techniques in section 1.9.3. Coral clasts in the cores were commonly encrusted with coralline algae or bio-eroded, making identification to genus level impossible. These clasts were classed as 'rubble'. Coral rubble that was clearly derived from branching corals was allocated to the subclass of 'branching rubble' with most derived from the genus *Acropora*. The difficulty in coral identification did not detract from the main objectives of this study, although where possible, coral genera were documented to capture some palaeo-ecological information for Middle Island reef.

Fifteen well-preserved *in situ* corals were selected from the percussion and drill cores for dating. Sampling preference was given to well-preserved coral clasts near facies boundaries that were considered *in situ* based on the preservation of delicate skeletal structures (indicating limited post-mortem transport) and the accordance of the position and orientation of corallites with living colonies. All sample preparation and U-Th dating techniques are described in detail in section 1.9.5. All age data are presented in Appendix 2. Core ages herein are presented as calendar years before present (yBP $\pm 2\sigma$), where present is defined as 1950 AD, to allow comparison with published reef growth chronologies, which mainly present radiocarbon ages (^{14}C , calendar years before 1950 AD).

4.3.3 Fossil microatolls

The location and elevation of the upper surfaces of fossil *Porites* microatolls on Middle Island reef flat were precisely (~0.01 – 0.005 m horizontal and vertical accuracy) measured using a Trimble Real Time Kinematic Global Positioning System (RTK GPS). Elevations were reduced to a common datum (LAT) using a base station value as detailed in section 1.9.1. Small plugs (2.5 cm in diameter and 3.0 cm in length) of coral skeleton were collected from the surface rims of ten RTK GPS surveyed fossil microatolls to determine their age using the U-Th dating techniques previously described for the core samples in section 1.9.5.

4.4 Results

4.4.1 Holocene reef growth

The chronostratigraphy of the fringing reef at Middle Island was reconstructed from 11 cores collected along a shore-perpendicular transect (Figure 4.3, Figure 4.4). The entire Holocene reef sequence (which is ~2.5 – 4.0 m thick at the backreef and ~6.0 m thick in central and outer parts of the reef flat) was penetrated in core P-1 and D-1, while cores P-3, 5 and 8 captured the upper 4.5 m of the reef sequence. Core D-1 terminated ~7.0 m below the present reef flat surface in a compacted regolith clay substrate, while core P-1 terminated in mixed carbonate and terrigenous sediments ~2.5 m beneath the reef flat. Four distinct reefal sediment facies were determined from core logs (facies A – D; Table 4.1) that overlie two different pre-reefal facies (facies E and F; Table 4.1). In general, matrix sediments coarsen upcore as mud content decreases toward the surface where carbonate sands ($96.0 \pm 0.5\%$ carbonate [mean $\pm 1\sigma$ standard deviation]) dominate contemporary reef flat sediments. Facies containing $>20\%$ mud (facies C and D) comprised the lower two thirds of most cores (Table 4.1). Facies A (intertidal sands) and B (sandy reef framework) near the tops of the cores are dominated by a sand matrix and contain $<10\%$ mud. Carbonate sediments ($>67.9 \pm 10.2\%$ carbonate) with only minor terrigenous fractions (up to $32.1 \pm 10.2\%$) dominate all reefal facies within the cores, especially the upper sandy facies ($4.0 \pm 0.5\%$ terrigenous).

U-Th ages of coral clasts selected from within the cores (Figure 4.3) reveal that the reef at Middle Island began to grow at or before ~7,900 yBP as indicated by the oldest U-Th age in core D-1 of $7,873 \pm 17$ yBP (Figure 4.3). Age data suggest that the reef initiated 100 – 200 m seaward of the present shoreline, approximately 7.0 m below the contemporary reef flat surface. The reef rapidly accreted vertically to reach sea level and prograded seaward to form a reef flat, indicated by an *in situ* coral clast age close to the surface in core P-2 of $6,887 \pm 27$ yBP (Figure 4.3) and a fossil microatoll age of $6,895 \pm 19$ yBP from FMA-1 located at the landward extent of the reef flat (Figure 4.1c). Average rates of vertical accretion were 3.5 – 7.6 mm/yr between ~7,900 – 6,900 yBP. The spread of ages $7,873 \pm 17$ – $6,439 \pm 19$ yBP throughout all cores across the transect reveals most of the reef was constructed during this period. No ages between $6,439 \pm 19$ – $1,617 \pm 10$ yBP were recovered from the cores (Figure 4.3). All ages younger than $1,617 \pm 10$ yBP occurred within the upper 1.2 m of cores within (or very close to) the sandy reefal facies B or on the reef flat surface.

Coral clasts of varying size (1 – 40 cm) and growth form (branching, massive, plate, foliaceous, free-living) occurred throughout the cores, although branching rubble dominated (56 – 82%). Branch and branch tip morphology identifies *Acropora* colonies as the primary source of these clasts. Well-preserved coral skeletal material was also recovered from the cores, allowing

Table 4.1 Core facies descriptions and matrix components including percent sand, mud and carbonate (CaCO₃) content (mean and 1σ standard deviation [SD]).

Facies		A	B	C	D	E	F	
Facies name		Contemporary intertidal sands	Reef framework, sandy matrix	Reef framework, muddy-sand matrix	Reef framework, mud matrix	Carbonate and terrigenous sands	Regolith clay	
Description		Sandy matrix with encrusted coral rubble, largely matrix-supported, and shell hash	Sandy matrix with coral clasts (matrix-supported) shell hash, bivalves	Muddy-sand matrix with coral clasts (mostly clast-supported) shell hash	Muddy matrix dominated by coral clasts (mostly clast-supported) with some shell hash	Encrusted carbonate sands and gravels and lithic sands in a mud matrix	Compacted orange-coloured clay	
Environmental interpretation		Contemporary intertidal reef flat. Most fine material in suspension	Lower intertidal reef environment where fine material cannot settle	Shallow subtidal reef environment where terrigenous sediments can settle and accumulate	Subtidal reef slope ~3 m below palaeo-low tide, where fine terrigenous sediments can settle	Quaternary beach	Pre-reefal regolith clays	
Matrix component	% sand	Mean	96.7	90.2	78.0	53.5	90.7	-
		SD	1.0	4.4	10.2	15.6	-	-
	% mud	Mean	3.3	9.8	22.0	46.5	9.3	-
		SD	1.0	4.4	10.2	15.6	-	-
	% CaCO ₃	Mean	96.0	92.9	84.2	67.9	82.9	-
		SD	0.5	1.9	5.4	10.2	-	-

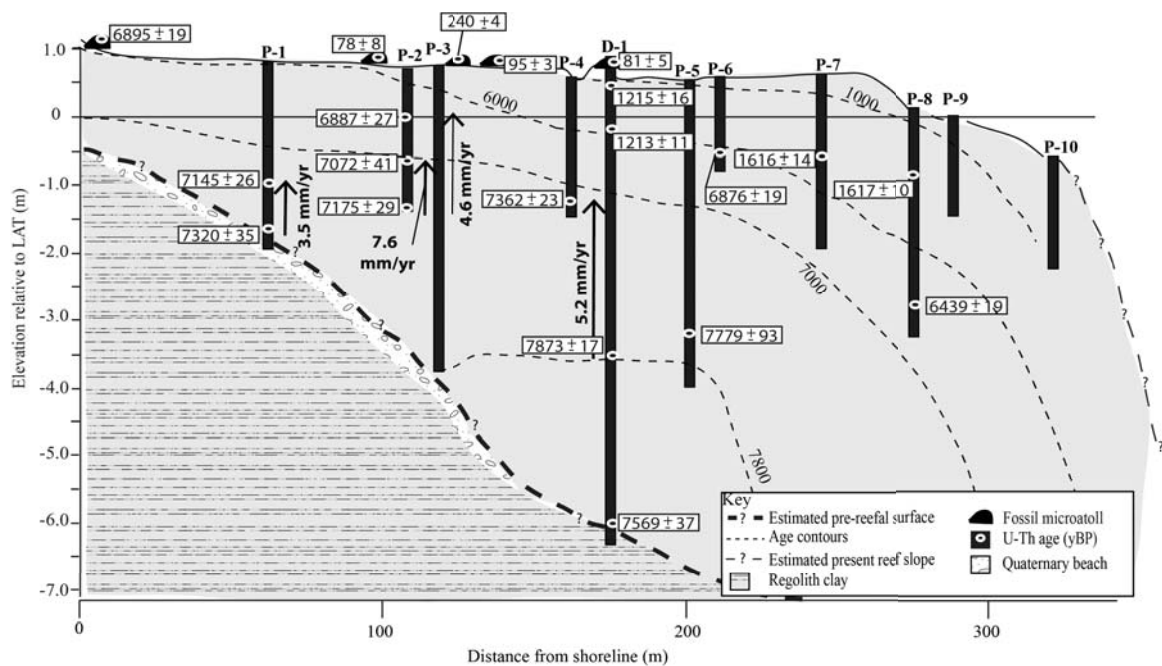


Figure 4.3 Middle Island reef flat profile extending seaward, with reef age indicated by the coral uranium-thorium (U-Th) ages (yBP ± 2σ) from within the percussion cores (core locations shown by thick black lines) and fossil microatolls on the reef flat. Vertical arrows show the average reef growth rates. Elevation is relative to lowest astronomical tide (LAT).

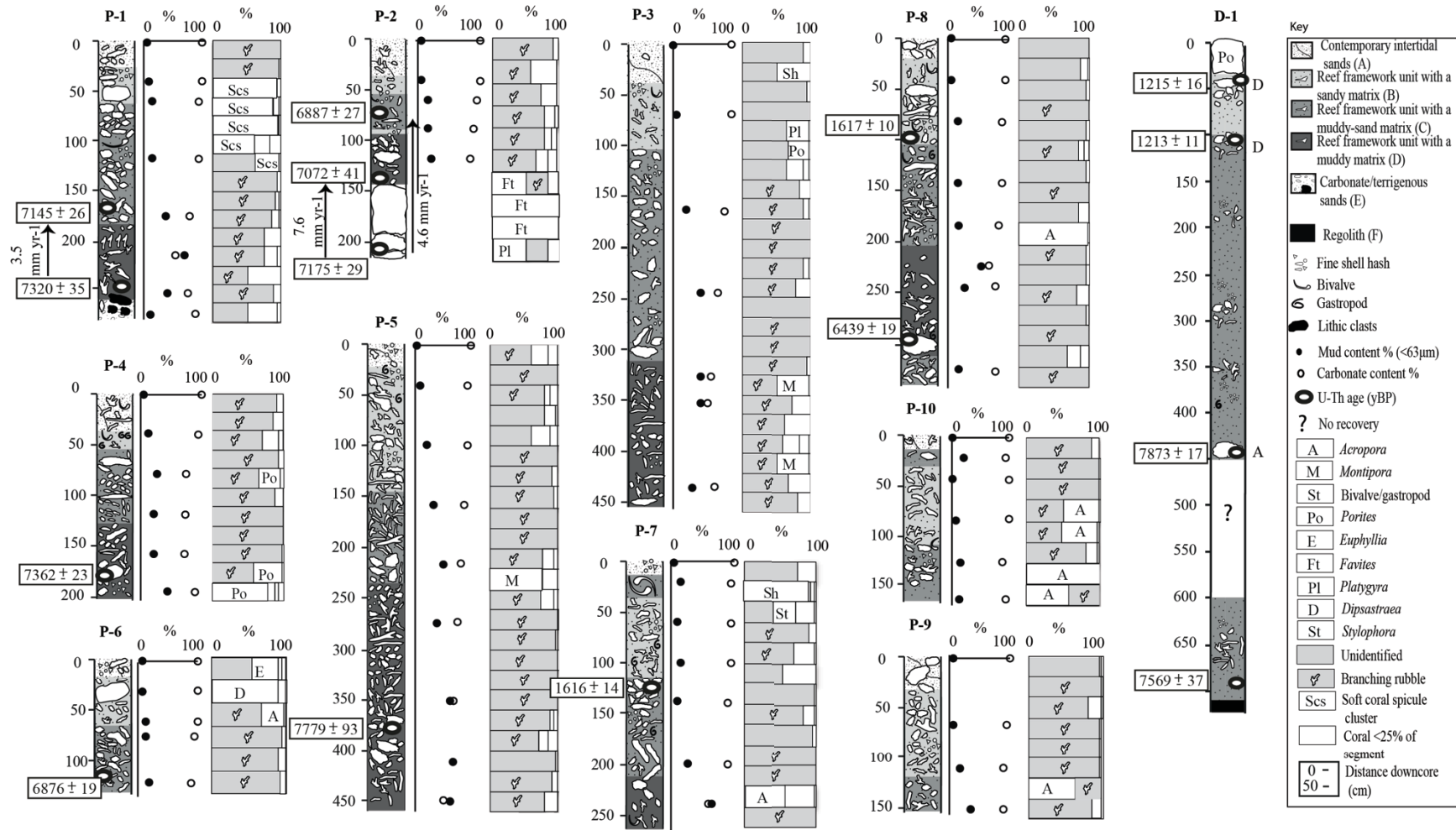


Figure 4.4 Composite core logs showing (left to right) sedimentary facies and uranium-thorium (U-Th) ages (yBP ± 2σ), carbonate and mud content of the matrix and palaeo-ecology data. Palaeo-ecology data are shown as % abundance of the total carbonate content >1 cm in size. Dominant coral genera (>25% of each segment) are labelled for each 20 cm downcore segment in the percussion cores. Arrows indicate average vertical reef accretion rates.

identification to genus level for palaeo-ecological analyses. Skeletal material from 15 hard coral genera was identified from the 11 cores (*Acropora*, *Dipsastraea*, *Euphyllia*, *Favites*, *Fungia*, *Galaxea*, *Goniastrea*, *Montipora*, *Pavona*, *Platygyra*, *Porites*, *Seriatopora*, *Stylophora*, *Tubastrea* and *Turbinaria*). Well-preserved *Acropora* (accurately identifiable to genus) was common in the four most seaward percussion cores (P-7 to P-10), which penetrated the younger section of the reef flat (Figure 4.3). Molluscan shell and clusters of spicules derived from soft corals ('spiculite') were dominant contributors to the community assemblage in some sections (e.g. shell comprised 92% of the total weight in the 20 – 40 cm downcore section of P-7, while spiculite represented 97% of the total weight in the 80 – 100 cm downcore section in P-1; Figure 4.4).

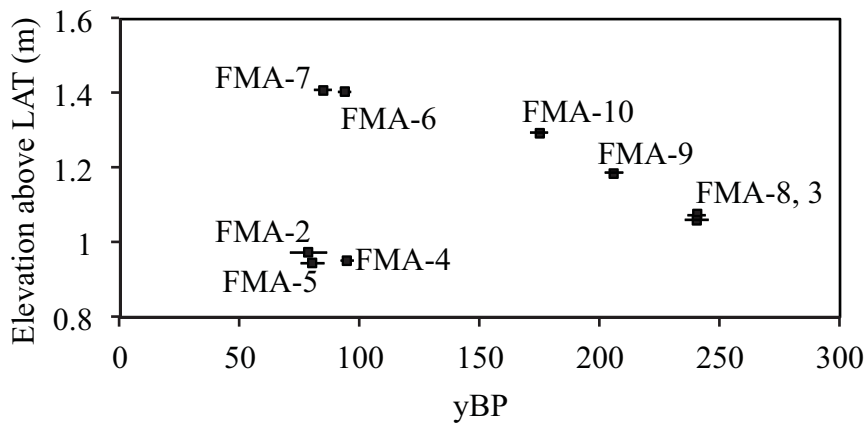


Figure 4.5 Middle Island fossil microatoll (FMA) ages (yBP with 2σ error bars) and elevations above lowest astronomical tide (LAT), excluding FMA-1 due to the comparatively old age ($6,895 \pm 19$ yBP; Appendix 2).

4.4.2 Fossil microatolls

Fossil microatolls (mainly *Porites*) were located across the back- and mid-reef flat (Figure 4.1c). The fossil microatolls varied between 1.0 – 5.3 m in diameter and had upper surfaces elevated between 0.9 and 1.4 mLAT (Figure 4.5). Fossil *Porites* microatoll samples yielded ages between 240 ± 5 and 78 ± 8 yBP, with the exception of FMA-1, which was aged at $6,895 \pm 19$ yBP and had a surface elevation of 1.2 mLAT. Of the younger fossil microatolls, two groups died around 78 ± 8 to 95 ± 3 yBP (i.e. 1860 – 1870 AD): 1) a higher elevation group (microatoll surfaces ~1.4 mLAT) on the eastern part of the reef flat; and 2) a lower elevation group (microatoll surfaces ~0.95 mLAT) further seaward, on the western part of the reef flat (Figure 4.1c and Figure 4.5). The other four dated fossil microatolls died between $\sim 240 \pm 5$ and 174 ± 4 yBP, and had surface elevations between 1.1 and 1.3 mLAT (Figure 4.5).

4.5 Discussion

Long-term palaeo-ecological and sedimentary records from coral reefs can provide important insights into past reef development and the influence of natural stressors on reef growth. Chronostratigraphic records obtained from 11 reef cores, together with high-precision U-Th dating reveal a history of reef growth at Middle Island spanning the past 8,000 years. Reef initiation began ~7,900 yBP and rapid reef accretion occurred until ~6,500 yBP, after which a gap of 5,000 years occurred in the age of reef framework beneath the reef flat. This and other geomorphic evidence (shingle ridges and basset edges) suggests multiple cyclones struck Middle Island during the mid-Holocene and caused considerable geomorphic change. In this section I discuss the influence of cyclones and sea-level changes on reef development at Middle Island and the implications for present reef flat geomorphology.

4.5.1 Early-Holocene – and the role of sea level

U-Th dating of reef cores from Middle Island reef flat reveals how the reef structure developed over time (Figure 4.6). Despite many cores being dominated by rubble, only one age reversal occurred across all the cores examined. This reversal occurred in core D-1, where a clast ~300 years older ($7,873 \pm 17$ yBP) was established ~2.8 m higher in the core than the basal age ($7,569 \pm 37$ yBP). Irregularities in the relief of the living reef structure may account for the reversed age structure (Easton and Olson, 1976), although it is possible that post-mortem diagenesis of the lower coral produced a younger age despite careful selection of the cleanest section of coral for U-Th dating from the best preserved material near the base on the core. Regardless, the ~300 year age reversal does not significantly alter or impact the general age structure of reef development.

Corals established at Middle Island at or before ~7,900 yBP at the start of the Holocene sea-level highstand (Lewis et al., 2013), probably within a subtidal setting of palaeo-water depths of 4 – 6 m below LAT based on the depths of basal U-Th ages relative to the Holocene sea-level curve for the central GBR (Lewis et al., 2013) (Figure 4.6). The reef initiated upon compacted regolith clays flooded during the post-glacial transgression (Hopley et al., 1983), or over a sand and gravel (mixed carbonate and terrigenous but carbonate dominated [82.9%], Table 4.1) unit similar to that interpreted elsewhere as a Quaternary beach deposit and/or transgressive sediment unit (Smithers and Larcombe, 2003).

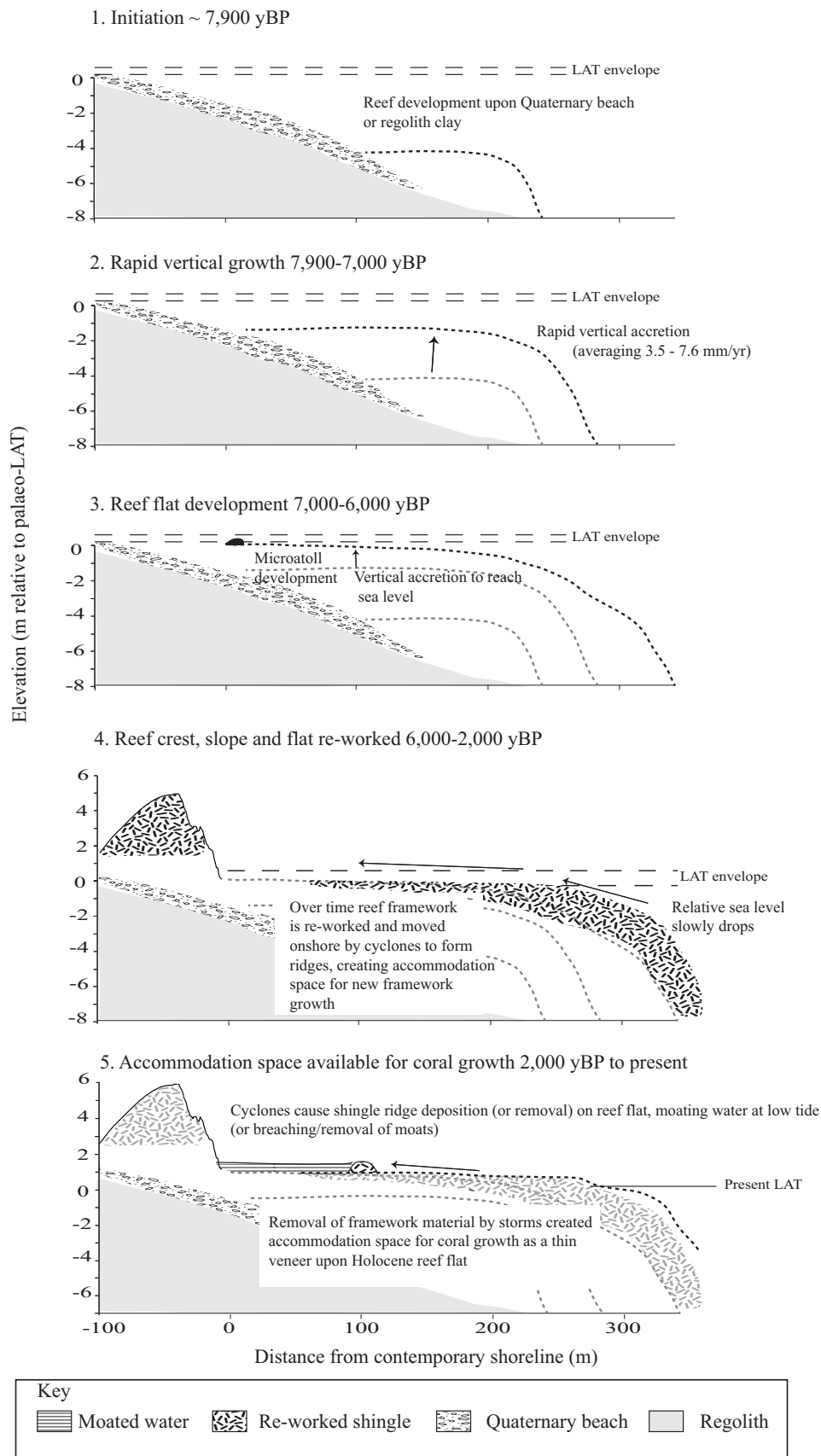


Figure 4.6 Conceptual model of reef development at Middle Island. Late Holocene sea-level fall is represented by a lowest astronomical tide (LAT) envelope at each time period, based on the sea-level curve presented in Lewis et al. (2013).

The reef at Middle Island initiated in shallow water compared to other inshore fringing reefs developed over similar substrates at around the same time; for example, Pioneer Bay, Orpheus Island initiated in ~12 m depth (Hopley et al., 1983) and the fringing reef at Hayman Island in the Whitsundays Group initiated in ~15 m palaeo-depth (Hopley et al., 1983). The shallow initiation depth at Middle Island is probably a function of the topography of the pre-transgressive surface, which steeply rises from the surrounding seafloor. Despite the shallow depth of the underlying substrate, the timing of reef initiation was not delayed, occurring at a similar time to many other fringing reefs (including those with shallow substrates) across the GBR (Hopley et al., 2007).

After initiation, the reef at Middle Island grew upwards to reach sea level within 1,000 years (i.e. by ~6,800 yBP). During this time, the reef was dominated by a branching coral assemblage based on the relative weight (approximately 56 – 82% branching material) of coral skeletal material of different forms present in the cores. Whether or not this is a true estimate of the palaeo-abundance of living branching coral is questionable due to the dominance of storm-derived material in the cores and the susceptibility of branching corals to breakage during storms (Done, 1992). At the time Middle Island reef flat reached sea level, sea level is argued to have been ~1 m above the present level (Lewis et al., 2013). Fossil microatoll evidence from Middle Island supports this interpretation, with FMA-1 dated at $6,895 \pm 19$ yBP and elevated at 1.2 mLAT, or 0.86 m above the average elevation of open-water living microatolls growing on the contemporary reef flat. Hopley (1975) inferred that the reef flat extends landward beneath the onshore shingle ridges and under the now-impounded lake. Fossil microatolls that are older and higher than those on the reef flat may be located beneath the lake sediments, but could not be investigated in the present study. Average rates of vertical reef accretion at Middle Island during this rapid growth phase 7,900 – 6,900 yBP (3.5 – 7.6 mm/yr; Figure 4.3) exceeded the 2.5 mm/yr average for GBR fringing reefs over this 1,000-year interval (Hopley et al., 2007) but were comparable with average growth rates for outer reefs at that time (6.4 mm/yr; Hopley et al., 2007). Rapid initial vertical accretion rates at Middle Island are attributed to high preservation of reef framework due to burial by muddy sediments (e.g. Perry et al., 2012), which dominated the lower reefal facies in the cores, together with the dominance of branching detrital material (predominantly fast-growing *Acropora*) produced by storms (Davies and Montaggioni, 1985). The age structure of the reef suggests that seaward reef flat progradation occurred once the reef had reached sea level and all vertical accommodation space was filled (Figure 4.6). Vertical accommodation space was ample between 7,000 and 6,500 yBP, due to sea level being at least 1 m higher than present, and this was a key influence on reef accretion during this period.

4.5.2 Mid- to late-Holocene – the role of cyclones

No coral framework material aged $6,439 \pm 19 - 1,617 \pm 10$ yBP was recovered in the internal reef structure, as indicated by the age gap in the core dates (Figure 4.3). The 15 U-Th ages recovered from the cores were spread downcore and across the reef flat, encompassing all sediment facies. It is unlikely that corals of this age were simply not selected for dating, however the possibility that the length of the 5,000-year age gap may be attributed to sampling resolution cannot be completely ruled out. Reef slope coral growth probably continued from $\sim 6,000$ yBP onwards at Middle Island, because regional environmental conditions were capable of sustaining coral communities at this time, as indicated by reef growth at other nearby locations (Hopley et al., 1978; Kleypas, 1996; see also Chapters 2 and 3). An explanation for the lack of reef structure across this time period may be that intense cyclones (that occur on average every 200 – 300 years on the central GBR; Nott and Hayne, 2001) have stripped material from the upper outer reef flat and slope at Middle Island and deposited material on the inner reef flat (where it was later moved onshore or lost) or directly onshore as shingle beaches and ridges (Figure 4.6). A large 6.3 m-high (above LAT), vegetated shingle ridge is a conspicuous landform on Middle Island, as well as several lower elevation shingle ridges (Figure 4.1d).

The above interpretation is based on the following evidence: 1) a coral clast from the 6.3 m high ridge has a calibrated ^{14}C age of $4,555 \pm 140$ yBP which coincides with the age hiatus in the reef structure, indicating that coral growth must have occurred during this time and that this material was transported onshore (radiocarbon age presented in Hopley [1975] and calibrated in Calib 7.02 [Stuiver and Reimer, 1993]); 2) the ridge crest is currently vegetated (including mature trees), suggesting no re-working has occurred on this ridge for an extended period. Hence, the ridge was either deposited under conditions of higher mid-Holocene sea level or under similar sea-level conditions but on top of an elevated mid-Holocene age reef flat; 3) the dominance of branching coral rubble material within the internal structure of Middle Island reef indicates a significant amount of rubble was generated. Cyclones may have contributed to reef-building by providing detrital sedimentation at the backreef since reef initiation (e.g. Blanchon and Jones, 1997; Blanchon et al., 1997; Braithwaite et al., 2000), however cyclones have continued to have a destructive effect once vertical accommodation space was filled and the reef flat was originally emplaced by $\sim 6,500$ yBP; 4) ridge deposition in the mid-Holocene also occurred at Curacoa Island in the central GBR ($\sim 4,000$ yBP: Hayne and Chappell, 2001). This finding confirms that intense cyclones were capable of stripping and transporting coral rubble onshore to form ridges during this period of the mid-Holocene, even within relatively protected

settings. Indeed, the crest elevation of the Curacao shingle ridge is similar (~6.8 mLAT) to that at Middle Island (6.3 mLAT), and the ridge has been interpreted as a deposit emplaced during an extreme cyclone (Nott and Hayne, 2001). Higher mid-Holocene sea levels (Lewis et al., 2013) would have allowed larger storm waves to travel closer inshore and deposit material at higher elevations. Subsequent relative sea-level fall and reef flat development would have constrained strong wave energy to the front of the emergent reef flat, allowing for previously deposited storm ridges to be preserved. Refraction of waves generated by cyclones around both sides of Middle Island would focus wave energy at the reef flat. This, in conjunction with the nature of the typically sheltered reef structure (open-fabric, dominated by branching corals), means Middle Island reef is vulnerable to being stripped of reefal material during cyclones.

The 5,000-year age hiatus in the reef structure may also reflect the influence of mid-Holocene sea-level variability. On the inner central GBR, relative sea-level fall began around 5,000 yBP (Lewis et al., 2013) and has been suggested as a possible driver for regional reef 'turn-off' between 5,500 and 2,300 yBP on reefs that developed reef flats during the highstand (Perry and Smithers, 2011). Post-highstand relative sea-level fall would have reduced accommodation space at Middle Island reef, restricting vertical reef flat accretion. However, coral material derived from the 6.3 m high ridge was dated at $4,555 \pm 140$ yBP by Hopley (1975), indicating that continued coral growth occurred during the mid-Holocene at Middle Island but was removed and deposited onshore sometime after $4,555 \pm 140$ yBP. Therefore, the cyclone-stripping theory provides the most likely explanation for the 5,000-year age gap in the chronostratigraphy.

Despite the ~5,000-year age gap in the core data from $6,439 \pm 19$ – $1,617 \pm 10$ yBP, four ages obtained from within the cores were younger than 1,700 yBP (Figure 4.3), all occurring within the upper 1.2 m of the cores in sandy intertidal reef flat facies. Vertical accommodation space must have been available after ~1,700 yBP for corals (including microatolls) to colonise and grow as a shallow (<1.2 m) veneer overlying the mid-Holocene age reef flat (or the stripped reef surface) that formed ~5,000 years earlier. Indeed, re-working and removal of reef framework material on the reef slope and flat during cyclones may have created the necessary vertical accommodation space for renewed growth. Importantly, this process (stripping and renewed growth) may have been a common occurrence throughout the mid- to late-Holocene as three separate shingle ridges exist onshore and basset edges present evidence for former reef flat ridges, although only the final episode of reef stripping/regeneration has been preserved in the core record.

Interestingly, renewed growth at Middle Island began $\sim 1,617 \pm 10$ yBP, the same time that new inshore coral communities initiated in other parts of the central GBR $\sim 2,000 - 1,500$ yBP (Perry and Smithers, 2011). At Middle Island, repeated stripping of the upper outer reef flat structure by intense cyclones provided accommodation space for renewed growth over the older mid-Holocene reef structure. This scenario demonstrates that age gaps in reef chronostratigraphies are not always records of past hiatuses in reef growth or collapsed palaeo-ecological performance and cautions against such interpretations even in relatively sheltered locations where the potential impacts of cyclones may not be conspicuous.

Shingle ridges have been deposited on the Middle Island reef flat in the late-Holocene and have since been eroded, which has influenced both past and present reef flat ecology and geomorphology. Historical photographs taken in 1896 (Agassiz, 1898) and basset edges on the reef flat show that shingle ridges once existed on the reef flat (Figure 4.2). Furthermore, the fossil microatoll ages and elevations (Figure 4.5) indicate that water was ponded up to 1.4 mLAT (10 cm above mean low water neap tide) on the reef flat behind shingle ridges for a period of at least 120 years and was able to support coral growth at elevations above the current maximum elevation for open-water corals. One mid-Holocene age fossil microatoll dated at Middle Island ($6,895 \pm 19$ yBP, FMA-1) and two previously published calibrated ^{14}C ages obtained from a fossil *Platygyra* microatoll and an *in situ* *Tridacna* shell (in an adjacent coral head) located close to FMA-1 (Figure 4.1) are also mid-Holocene in age (5570 ± 270 and 5645 ± 260 yBP, respectively; radiocarbon ages presented in Hopley [1975] and calibrated in Calib 7.02 [Stuiver and Reimer, 1993]). The other fossil microatolls were much younger than mid-Holocene corals, ranging between 240 ± 5 and 78 ± 8 yBP (Figure 4.5). These results, together with field and historical photographic evidence, suggest that moating must have been active across the reef flat at the time that these microatolls were alive (due to shingle ridges), when it is possible that more luxuriant coral growth may have occurred in the water moated above the low tide level. Removal or re-working of shingle ridges on the reef flat that resulted in lowering of the moated water depth may have caused mortality of the fossil microatolls and associated ponded coral growth (Hopley, 1975; Hopley and Isdale, 1977). The range of the nine young fossil microatoll ages between 240 ± 5 and 78 ± 8 yBP (Figure 4.5) suggests that ridge removal or re-working occurred approximately every 40 – 70 years. Importantly, the age data indicate that fossil microatolls of similar ages can have elevations that differ by ~ 0.5 m (Figure 4.5). Such elevation differences reflect the effects of ponding on different parts of the reef flat and is an important factor to consider when fossil microatolls are used for reconstructing past sea level (e.g. Lewis et al., 2013). Despite cyclones causing ridge deposition and subsequent removal on the reef flat over the past $\sim 1,600$ years since reef growth re-commenced, a ridge comparable to the 6.3 m high mid-Holocene age ridge has not been deposited and/or preserved onshore. This

suggests that either a cyclone of similar magnitude has not occurred and produced a comparable sized ridge during the past ~1,600 years or that supply of coral material for ridge formation is now limited.

4.6 Conclusions

Cyclones have clearly played an important role in the Holocene development (and present geomorphology) of Middle Island reef flat, despite its position in a semi-protected inshore location. The results presented here emphasise the importance of recognising that during the mid- to late-Holocene, reefal material could be stripped from the reef structure and deposited onshore at relatively frequent timescales (Nott and Hayne, 2001); perhaps more frequently than the present (Haig et al., 2014). Though cyclones can initially cause reef-scale destruction (Done, 1992), the renewed coral growth over the past 1,600 years at Middle Island shows that over longer time-scales, cyclones have the ability to create accommodation space for reef regeneration (should all other requisites for coral growth be met). The results presented here have important implications for palaeo-ecological and chronostratigraphic reef studies as well as contemporary reef ecology; age gaps in reef cores do not necessarily suggest that reef growth did not occur over that period. Healthy, active reef growth may have occurred but the reef constructed may have been eroded by storms. Such a scenario must be considered, particularly in locations where shingle ridges and basset edges indicate past high-energy storm activity, but also in other settings where such evidence may not be so well preserved. This study provides a good example of the value of an integrated investigation of reef geomorphology and biochronostratigraphy to provide insights into reef development processes and environmental conditions.

5 Fringing reef growth over a shallow last interglacial reef foundation at a mid-shelf high island: Holbourne Island, central Great Barrier Reef

To be submitted to *Geomorphology* in July 2016

Authors: Ryan E.R., Smithers S.G., Lewis, S.E., Hua, Q., Clark, T., Zhao, J.X.

Chapters 2, 3 and 4 presented new chronostratigraphic records of long-term (millennial-scale) reef development at four inshore fringing reefs. However, few chronostratigraphic records of mid-shelf reef development exist with which inshore reef records can be compared. In this chapter I present a new record of fringing reef development from the mid-shelf.

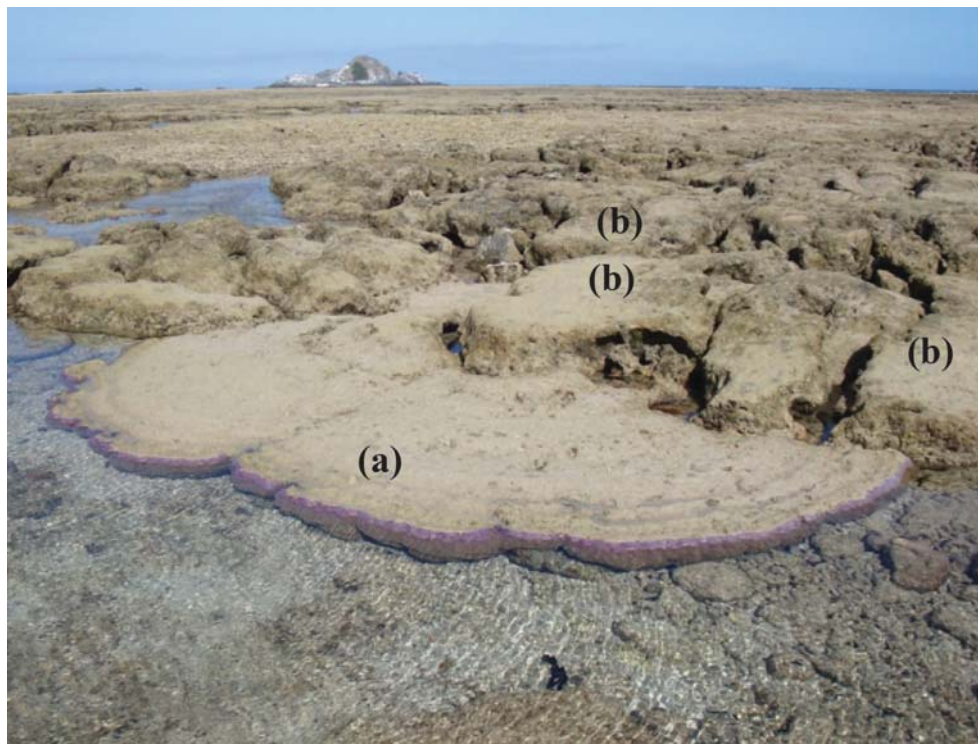


Plate 5. Photograph of (a) a *Porites* microatoll (living edges and dead upper surface) growing in ponded water on the Holbourne Island reef flat and (b) fossil microatolls previously moated at a higher level.

5.1 Abstract

Fringing reefs are rare on the mid-shelf of the central Great Barrier Reef, with Holocene development histories established for a few examples. The paucity of longer-term reef growth records from mid-shelf fringing reefs has constrained opportunities for comparisons with inshore reef growth records to better understand the influence of changes in environmental conditions with distance offshore. The long-term development of the fringing reef at Holbourne Island was reconstructed using percussion and drill cores that captured the entire Holocene period of reef growth. The cores were chronologically constrained by 16 high-precision uranium-thorium (U-Th) ages. A weathered, Pleistocene reef substrate was U-Th dated as last interglacial ($137,778 \pm 608$ yBP) and this provides the underlying foundation upon which the Holocene reef initiated prior to $\sim 7,520 \pm 20$ yBP. The last interglacial reef was encountered 5.9 m below the present reef surface and is the shallowest confirmed Pleistocene reef in the central GBR region. Most of the Holocene reef structure was emplaced within 1,000 years of initiation. Evidence for significant re-working and stripping of the reef structure by cyclones is prevalent in both the reef chronostratigraphy and the contemporary geomorphology. This evidence includes: 1) an age hiatus in core data of $\sim 3,500$ years ($6,238 \pm 18 - 2,683 \pm 10$ yBP); 2) the abundance of detrital branching coral rubble material within the core facies; 3) fossil microatoll ages and elevations, which reveal that ponding of water during low tidal stages up to 55 cm deep has been active (but intermittent) across the reef flat for at least 600 years and is still active today; and 4) long-standing shingle ridges onshore and modern shingle ridges on the reef flat. Storm and cyclone events have strongly influenced the Holocene growth and the present geomorphology of the fringing reef at Holbourne Island.

5.2 Introduction

Fringing reefs in the Great Barrier Reef (GBR) have developed directly attached to the mainland coast or attached to the shorelines of continental islands on the inner-shelf (within the 20 m isobath) or mid-shelf (between the 20 – 50 m isobaths) (Hopley et al., 2007). Like all reefs they develop where suitable substrates for colonisation are available and environmental conditions are conducive for reef growth. Fringing reefs have developed in a variety of environmental settings including attached to headlands or rocky shores, within embayments, attached to sandy coastlines, and in the nearshore where they may initially develop as shoals not directly attached to the shoreline (Smithers, 2011). Understanding how and when fringing reefs developed over millennia provides important baseline information to interpret present reef condition and predict future reef trajectories. Long-term reef records can be constructed by coring deep into the reef structure, examining and characterising the internal reef framework and matrix, and obtaining ages of *in situ* coral material in the cores to establish patterns and

rates of reef growth (Kennedy and Woodroffe, 2002; Montaggioni, 2005). A comprehensive reef growth dataset for the GBR has been developed over the past few decades, comprising reef core records from ~29 nearshore and fringing reefs and is summarised in Smithers et al. (2006), Hopley et al. (2007), and Perry and Smithers (2011). Additional studies published since 2011 extend this dataset, including: Lewis et al. (2012); Perry et al. (2012, 2013); Roff et al. (2012, 2015); and this thesis. Although the fringing reefs from the GBR are among the best studied in the world (Hopley et al., 2007), there remain many reefs for which growth records do not exist.

Ideally, reef cores should attempt to capture the entire Holocene reef sequence, terminating in the underlying, pre-Holocene foundation to reveal the details of reef initiation. Most fringing reefs on the GBR initiated during the early- or mid-Holocene ~7,000 years before present (yBP) once the continental shelf had been flooded at the end of the post-glacial marine transgression (PGMT) (Hopley et al., 2007). Unlike the outer-shelf reefs of the GBR, which developed exclusively upon Pleistocene reef limestone foundations (Marshall and Davies, 1984), fringing reefs have developed upon a wide variety of consolidated and unconsolidated substrates. These substrates include unconsolidated transgressive sands and gravels (Hopley et al., 1983; Perry et al., 2011; Lewis et al., 2012; Ryan et al., 2016), mangrove muds, coffee rock (Roche et al., 2011), consolidated terrigenous clay (Hopley et al., 1983; Johnson and Risk, 1987), a terrigenous boulder beach (Hopley and Barnes, 1985); and last interglacial (Pleistocene) reef (Hopley et al., 1978).

Fringing reefs on the GBR are considered vulnerable to degradation caused by human activities due to their relatively high exposure to human populations and proximity to river discharge (Roff et al., 2012). This perceived vulnerability has largely motivated increased effort to recover more reef growth records from the inner-shelf (Smithers and Larcombe, 2003; Perry et al., 2008, 2009, 2011, 2012, 2013; Palmer et al., 2010; Perry and Smithers, 2010; Lewis et al., 2012; Roff et al., 2015; Ryan et al., 2016). In comparison, few detailed chronostratigraphic records from mid-shelf fringing reefs exist (Kleypas, 1996), as mid-shelf fringing reefs are themselves rare (particularly in the central GBR region north of the Whitsunday Islands) and they are more difficult to access than reefs close to the mainland. Mid-shelf fringing reefs are generally attached to the shorelines of high continental or volcanic islands and are located further offshore from most anthropogenic impacts than inner-shelf fringing reefs (Hopley et al., 2007). Detailed chronostratigraphic records from mid-shelf fringing reefs would be valuable to compare with inshore reef records to further understand the influence of cross-shore variations in environmental conditions on reef development. Of the mid-shelf reefs for which reef growth records are known, most are platform reefs which developed upon last interglacial reef antecedent substrates (Marshall and Davies, 1984; Davies et al., 1985; Dechnik et al., 2015).

Geographic variations in relative sea-level history across the continental shelf have been shown to exert a strong control on reef growth and morphology (Davies et al., 1985; Chappell et al., 1982, 1983). The continental shelf of the GBR was flooded during the PGMT by ~8,000 yBP. At the end of the PGMT, a highstand was reached ~7,000 – 6,000 yBP, where sea level was about 1.0 – 1.5 m higher than present (Chappell et al., 1983; Lewis et al., 2013). The highstand lasted a few thousand years, after which sea-level fell towards the present level. However, the nature and precise timing of this post-highstand sea-level fall remains unresolved (Perry and Smithers, 2011; Lewis et al., 2015; Leonard et al., 2016). The effects of late-Holocene sea-level fall are likely to be more pronounced on the inner GBR, due to spatial variations in hydro-isostatic shelf deformation effects associated with water loading during the PGMT (Chappell et al., 1982; Lambeck and Nakada, 1990). However, precise sea-level data from the mid-shelf are lacking (Harris et al., 2015) and thus the importance of cross-shelf variations in Holocene sea level for reef development remains poorly understood. Many fringing reef flats in the GBR were formed during the sea-level highstand, at elevations ~1.0 m above the level for modern reef flat formation. Late Holocene sea-level fall has resulted in the emergence of large parts of these reef flats during low tidal stages today (Smithers et al., 2006).

Here I present a detailed chronostratigraphic record of fringing reef development at Holbourne Island, an exposed mid-shelf fringing reef located on the central GBR. The record was developed using a combination of percussion and drill cores that extend deep through the reef structure, combined with high-precision uranium-thorium (U-Th) dating of *in situ* coral framework from the cores. The cores capture a new record of last interglacial reef at 5.9 m below the present surface at Holbourne Island. The Holocene reef at Holbourne Island initiated upon this Pleistocene reef prior to ~7,500 yBP and the majority of the reef structure was developed within 1,000 years of initiation. The mode of reef development, average reef accretion rates and timing of reef flat formation are reported. Results of precise topographic surveys combined with ecological assessments of contemporary reef flat benthic cover reveal complex zonation on the contemporary reef flat.

5.3 Regional setting

Holbourne Island (148°21'E, 19°43'S) is a continental high island situated ~40 km north-east of the mainland coast near Bowen, on the mid-shelf of the central GBR (Figure 5.1) and is one of very few high islands in this region. Marshall et al. (1925) first described the geomorphology of Holbourne Island, but Hopley (1975) and Hopley and Isdale (1977) provided more detailed

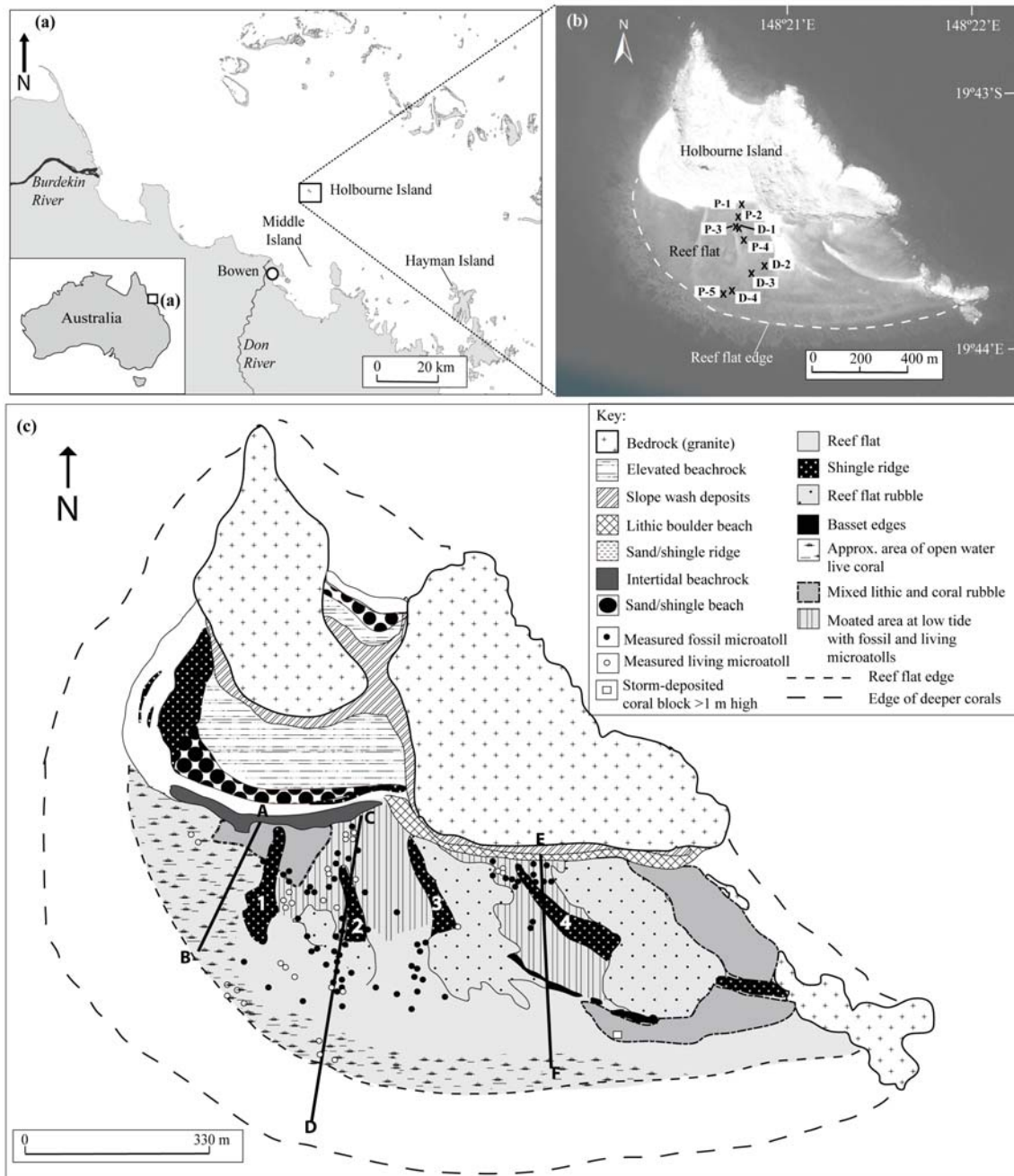


Figure 5.1 (a) Location of Holbourne Island, central Great Barrier Reef, Australia; (b) aerial image of Holbourne Island showing reef core sites on the reef flat; (c) geomorphological map of Holbourne Island and reef flat, using survey data augmented with a previous map presented by Hopley (1975), showing important zones across the reef flat, transect locations (A – B: Transect 1; C – D: Transect 2; E – F: Transect 3), and surveyed fossil microatolls and storm deposits (reef flat shingle ridges numbered 1 – 4).

descriptions including accounts of the reef flat. The island is 1.1 km long by 0.6 km wide and comprises two major granitic outcrops fringed by Quaternary sedimentary deposits. These deposits include a series of shingle ridges, sand/shingle beach ridges, and a series of elevated Holocene beachrock terraces (Hopley, 1975; Figure 5.1c). Shell and coral within two of these

beachrock terraces were dated at $6,420 \pm 280$ and $3,180 \pm 260$ yBP, respectively (conventional radiocarbon ages presented in Hopley [1975] and calibrated in Calib 7.02 [Stuiver and Reimer, 1993]).

A fringing reef flat reaching 440 m wide has developed on the southern side of Holbourne Island, bounded by several granitic outcrops at the south-eastern extent. A boulder beach borders the landward extent of the eastern half of the reef flat, while the western half is bordered by a 20 – 25 m wide beachrock exposure that lies seaward of a sand and coral rubble beach (Figure 5.1c). Hopley (1975) and Hopley and Isdale (1977) noted the complex geomorphology of the reef flat, which is sub-aerially exposed during lower tidal stages. Fields of fossil coral microatolls form part of this complex geomorphology. Microatolls are discoid corals that have flat upper surfaces, constrained by sub-aerial exposure during low tide (Scoffin and Stoddart, 1978) and mid-Holocene age fossil microatolls are commonly preserved on reef flats in the GBR (Hopley and Isdale, 1977; Chappell et al., 1983). Conspicuous groups of elevated, well-preserved fossil microatolls are widespread on the reef flat at Holbourne Island (Figure 5.2b), and were initially incorrectly interpreted as a raised reef by Marshall et al. (1925). Rainford (1925) suggested that the reef flat corals on Holbourne Island (presumably including the microatolls) were killed by freshwater exposure associated with a large cyclone in 1918. Alternatively, Hopley (1975) suggested that the microatolls died when a shingle rampart that moated water over the reef flat above the open-water low tide level was destroyed during this cyclone. This breach drained the moat, which, based on the size of many of the microatolls killed, must have been stable for ~200 years prior to the cyclone. Hopley (1975) argued that a radiocarbon age (uncalibrated) of 60 ± 90 yBP from one of these emerged fossil microatolls on Holbourne Island supported the view that the 1918 cyclone event killed these microatolls. However, the error-term of the age is too large to link the mortality to a specific cyclone, and once re-calibrated the age is ‘modern’ (i.e. equal to or younger than 1950 AD).

Holbourne Island is relatively exposed to prevailing south-easterly waves and currents generated by trade winds, with a fetch distance of ~60 – 70 km to the south-east. The reef flat is partially protected from easterly swells by the granitic outcrops located at the south-eastern margin of the reef flat, but is exposed to northerly and north-westerly swells. Tides are semi-diurnal with a spring tidal range of ~3.6 m in this part of the GBR. Around the island and reef the water depth reaches ~45 m (Hopley, 1975). Holbourne Island is located ~80 km east of the Burdekin River mouth (the largest river in the region) and is far enough offshore that it is rarely (1 – 3 times per decade) affected by riverine flood plumes containing sediments, nutrients and pollutants flushed from coastal catchments (Devlin et al., 2012). Holbourne Island’s mid-shelf location means the reef is less influenced by turbid water associated with flood plumes or the

re-suspension of the inshore terrigenous sediment wedge (Larcombe and Woolfe, 1999b) compared to most other fringing reefs on the GBR, which are generally located further inshore.

5.4 Materials and methods

Nine cores were collected from Holbourne Island reef flat (Figure 5.1b) using a combination of percussion coring and rotary diamond drilling (techniques are described in section 1.9.2, Chapter 1). Percussion cores penetrated up to 2.0 m below the present surface and captured both reef framework and matrix. Compaction throughout the percussion cores varied between 13 – 20%. The solid nature of the cemented reef framework and the time available for field work (days on the island were limited, and the reef flat could only be worked safely during lower tidal stages) meant that retrieving percussion cores >2.0 m depth was not logistically possible. Four cores drilled using a rotary drill rig were undertaken to achieve deeper penetration into the reef structure, reaching a maximum depth of 8.0 m below the present surface. Recovery rates of the drill cores varied between 18 – 75%. Low recovery rates were due to the open framework nature of the reef structure; Kleypas (1996) reported similar results when drilling fringing reef flats in the Northumberland Island Group, around 140 - 240 km south of Holbourne Island. Cores were visually logged to differentiate reef facies and 16 *in situ* coral clasts were selected from the cores for U-Th dating at the Radiogenic Isotope Facility at the University of Queensland. See section 1.9 for detailed descriptions of core logging and U-Th dating techniques. Sediment analyses (carbonate and mud content) were conducted on matrix sediment samples from the percussion cores taken at 20 cm (uncompacted) downcore intervals, following the acid digestion and wet sieving procedures described in section 1.9.2.

A Real Time Kinematic (RTK) Global Positioning System (GPS) was used to map geomorphological zones across the reef flat and shoreline (Figure 5.1c) and to obtain high precision elevation data (horizontal and vertical precision typically 0.01 – 0.005 m) for the reef flat surface and geomorphological features. All elevation data were reduced to lowest astronomical tide (LAT) (see section 1.9.1). Three shore-perpendicular transect lines were mapped across the reef flat (Figure 5.1c), along with the location and elevation of shingle ridges, basset edges, the tops of fossil and living microatolls, and other important features or zones on the reef flat or shoreline. Eco-geomorphological zones were differentiated across each transect based on variations in the elevation of the reef flat surface, substrate, live coral cover, vegetation cover and other geomorphological features. Within each zone, ten 1 m² photo quadrats were photographed and analysed in Coral Point Count with Excel Extensions (Kohler and Gill, 2006) to determine average percent benthic composition for each zone, as described in section 1.9.1. The benthic composition of the upper reef slope was also surveyed using video-

photography (section 1.9). The video survey extended from the reef crest at transect two and terminated approximately half way down the reef slope (Figure 5.1c).

Seventeen fossil microatolls were sampled (see section 1.9.4 for sampling technique) for dating using either U-Th techniques described in section 1.9.5 (five samples) or radiocarbon dating using accelerator mass spectrometry (AMS) (12 samples). The samples for AMS radiocarbon dating were analysed using the method described by Fink et al. (2004) at the Australian Nuclear Science and Technology Organisation. Age calibration for AMS radiocarbon ages was performed using the Marine13 radiocarbon “global” marine calibration dataset (Reimer et al., 2013) within the OxCal program version 4.2.3 (Bronk Ramsey, 2009) using a ΔR (regional variation from the average global marine reservoir age) of 4 ± 40 years (Druffel and Griffin, 2014) for samples older than 1950 AD. For samples younger than 1950 AD, calibration was performed using radiocarbon data (1951 – 2010 AD) from Heron Island, Abraham Reef and Holmes Reef (see Dawson et al., 2014). For AMS radiocarbon ages, the median age is reported with $\pm 2\sigma$ errors. All age data are presented in Appendix 2 (U-Th ages) and Appendix 7 (AMS radiocarbon ages).

5.5 Results

5.5.1 Holocene reef development

Two cores (D-1 and D-2) penetrated the entire Holocene reef sequence, which is 6 – 8 m thick, terminating in the basal pre-reefal surface, which differed in each of the two cores (Figure 5.3). A cemented, weathered reefal facies (facies E, Figure 5.4) was encountered at the base of D-2, comprising the lower ~30 cm of core, which terminated ~6.2 m below the present surface. The U-Th age of $137,778 \pm 608$ yBP obtained from facies E (Figure 5.3) indicates that this material is Pleistocene reef that would have been growing during the last interglacial period. In contrast, granite (facies F) was encountered at the base of D-1, ~8.2 m below the present surface. The earliest Holocene age obtained in the cores is $7,520 \pm 20$ yBP, from an *in situ* faviid coral ~6 m downcore in D-1 and ~2 m above the underlying foundation (Figure 5.3). This coral is located above ~2 m of reefal material that was classified as rubble (not *in situ*) and thus the reef must have initiated some time prior to $7,520 \pm 20$ yBP.

The chronostratigraphy of the reef, based on U-Th ages in the cores, reveals that after initiation upon last interglacial reef or granitic foundations, the reef rapidly accreted vertically towards palaeo-sea level over a period of ~1,000 years. The reef approached within 1 m of palaeo-LAT by $6,406 \pm 19$ yBP as indicated by the U-Th age in P-3 from a coral clast ~50 cm downcore.

Reef flat formation probably began shortly after this time once the reef reached sea level and further vertical accretion was restricted (Figure 5.3). The spread of U-Th ages between $7,520 \pm 20 - 6,238 \pm 18$ yBP throughout the majority of the cores from the back and central reef flat indicate that most of the reef was constructed during this time period. Average vertical reef accretion rates between $\sim 7,500 - 6,500$ yBP varied from $1.7 - 3.2$ mm/yr (Figure 5.3). The palaeo-ecology of the core facies indicate the reef slope during this time was comprised of a hard coral assemblage that included branching *Acropora* and massive faviid corals, such as *Favites* and *Platygyra* (Figure 5.3) growing in palaeo-water depths of $3 - 5$ m. No ages between $6,238 \pm 18$ and $2,683 \pm 10$ yBP were recovered from the cores. However, two U-Th ages of $2,683 \pm 10$ and $1,326 \pm 15$ yBP were obtained in the two most seaward cores within 1.2 m of the present reef flat surface (Figure 5.3). This suggests that over the past $\sim 2,500$ years, seaward progradation of the outer ~ 100 m of reef flat (at least the upper 1.5 m) occurred.

Four Holocene reef facies were differentiated in the cores (facies A – D: Table 5.1). The percussion cores captured the upper ~ 2 m of reef matrix sediments, which were differentiated into facies A, B and C (Table 5.1). Although the percussion cores did not penetrate beyond 2 m depth into the reef structure, the cores are spread across the width of the reef flat and contain coral material aged between $7,178 \pm 20 - 517 \pm 48$ yBP (Figure 5.3), covering the majority of the Holocene period of reef development. Therefore, it is likely the cores have captured reef matrix sediments that are representative of the entire period of reef growth. Facies A, the contemporary intertidal sands (Table 5.1), comprises the upper $\sim 10 - 15$ cm of the percussion cores (Figure 5.3). Below this, facies B and C comprise the remainder of the percussion cores, including coral material (framework and detrital) that varies in age from $7,178 \pm 20$ yBP in P-3 to $1,326 \pm 15$ yBP in P-5 (Figure 5.3). Facies D (*Acropora* rubble assemblage) characterised sections of the drill cores up to 4.5 m long, and was dominated by re-worked branching *Acropora* clasts largely encrusted with coralline algae. It is likely that a similar sediment matrix to that observed in facies B and C also comprised facies D, however, the matrix sediments were not recovered as they were flushed out during the drill coring process. In general, the reef matrix sediments coarsened upwards, with mud content (the $<63 \mu\text{m}$ fraction) being greatest in the lower muddy facies C ($18.0 \pm 8.3\%$ [mean $\pm 1\sigma$ standard deviation]), compared with $6.5 \pm 2.0\%$ in facies B (Table 5.1). Terrigenous components in the reef sediment matrix were very limited ($<7.2\%$) and throughout the cores the matrix sediments were composed of primarily carbonate (reef-derived) material, averaging between $92.8 \pm 3.9 - 97.3 \pm 0.7\%$ (Table 5.1).

Table 5.1 Reef core facies descriptions with average percent mud and carbonate (CaCO₃) values of the sediment matrix. Standard deviations (SD) are 1σ.

Facies			A	B	C	D	E	F
Facies name			Contemporary intertidal sands	Reef framework, sandy matrix	Reef framework, muddy-sand matrix	<i>Acropora</i> rubble	Last interglacial reef	Granite
Description			Sandy matrix with encrusted coral rubble (matrix-supported) and shell hash	Sandy matrix with coral clasts, shell hash, bivalves. Coral clasts mostly clast-supported, some units matrix-supported.	Muddy sand matrix with coral clasts (clast-supported), bivalves, shell hash	Recovered in drill cores, coral rubble dominated by branching <i>Acropora</i>	Cemented and altered reef framework	Granite
Environmental interpretation			Contemporary intertidal reef flat	Lower intertidal reef environment where most fine material remains in suspension	Subtidal reef environment where fine sediments can settle	Subtidal reef environment where fine sediments can settle (but were largely washed out during drill coring)	Reef that was growing during the last interglacial	Underlying boulder beach or bedrock that the present reef grew upon
Matrix component	%	Mean	2.1	6.5	18.0	-	-	-
		SD	0.8	2.0	8.3	-	-	-
	CaCO ₃	Mean	97.3	97.4	92.8	-	-	-
		SD	0.7	1.3	3.9	-	-	-

5.5.2 Contemporary geomorphology

Geomorphological features were surveyed across the width and breadth of the reef flat, along with three shore-perpendicular transect lines, revealing complex zonation across the reef flat (Figure 5.1c). The high-precision RTK GPS surveying used in this study allowed for the most accurate geomorphological survey and mapping to date, extending previous work by Hopley (1975) and Hopley and Isdale (1977). The zones differentiated across the transect lines were largely related to the elevation of the reef flat surface relative to the tide and the location of storm-deposited shingle ridges on the reef flat (Figure 5.5, Table 5.2). Generally, the backreef flat extended from the shoreline at an elevation ~1.0 – 1.3 mLAT and sloped seaward towards the reef crest which was elevated close to LAT at transects 1 and 2 (Figure 5.5). Below, I describe the major reef flat geomorphological zones and features shown in Figure 5.1c and Figure 5.5 and detailed in Table 5.2, focusing on the features that were derived from or shaped by storm events.

Storm-derived geomorphological features and zones

Geomorphological features on the reef flat and shoreline at Holbourne Island indicate a long history of cyclone occurrence and associated impacts. These features include: basset edges (the cemented remnants of storm-deposited shingle ridges) on the reef flat (Figure 5.1, Figure 5.2d); storm-deposited shingle ridges (Figure 5.1, Figure 5.2c) and coral blocks (~1.5 m high) emplaced on the reef flat; living and fossil moated microatolls (Figure 5.2a, b); and storm-deposited shingle ridges on and above the modern shoreline (Figure 5.1). The crest of the highest ridge on the shoreline reached 7.0 mLAT. Four shingle ridges, numbered 1 – 4 (Figure 5.1), comprised of storm-deposited coral clasts stripped from the living reef and re-worked detrital coral rubble, were surveyed on the reef flat (Figure 5.2c). Similar sized and shaped ridges have been observed elsewhere in the Pacific and termed ‘gravel tongues’ (Etienne and Terry, 2012). The reef flat shingle ridges were all elongated in a roughly similar direction perpendicular to the reef crest (north-south) and were of similar shape and size; generally 19 – 21 m in width and 140 – 200 m long (Figure 5.1). The ridge deposits were broader (width) and thinner (i.e. lower elevation) near the seaward edge, where the coral rubble that comprised the ridges splayed out, covering the surrounding reef flat. The landward edges were abrupt and thicker, with curved ends (Figure 5.2c). The elevation of the shingle ridge crest varied between ridges, from 1.0 mLAT on ridge 1 to 2.3 mLAT on ridge 3. The crest elevations of ridge 2 and 4 were 1.4 mLAT and 2.1 mLAT, respectively. Cemented remnants of an old shingle ridge (basset edges, Figure 5.2d) were located on the south-eastern part of the reef flat, oriented in the same direction as the modern shingle ridge 4 (Figure 5.1). The upper surface of the basset edges reached an elevation of 1.6 mLAT.

Two moated areas on the backreef flat were surveyed, where during low tidal stages, water was trapped and remained moated (~10 – 40 cm deep) on the reef flat due to the presence of elevated shingle ridges and/or higher sections of reef flat. The eastern moat corresponds to zones 1 and 2 on transect 3 and the western moat corresponds to zone 1 on transect 2 (Figure 5.1, Figure 5.5). Coral rubble ($46.2 \pm 24.1\%$) and sand ($20.0 \pm 13.8\%$) dominated the substrate of the western moat, while coral rubble ($53.4 \pm 30.9\%$ in zone 1) and turf algae upon the reef pavement ($47.7 \pm 27.4\%$ in zone 2) dominated the substrate of the eastern moat. The presence of ponded water allows living microatolls to grow over these backreef zones (Figure 5.2a) at elevations 50 – 100 cm above open-water coral growth. The moated microatolls varied between 0.6 – 3.0 m in diameter and were mostly of the genus *Porites*, with fewer *Goniastrea* microatolls also present. The living upper rims of the *Porites* microatolls in the western ponded area were elevated between 0.94 – 1.0 mLAT and those in the eastern area were ponded at a slightly higher level, between 1.21 – 1.31 mLAT. Fossil microatolls were perhaps the most conspicuous features in the moated areas (Figure 5.2b), interspersed between the living microatolls. The fossil microatolls were generally tall and large, reaching up to 3.6 m in

diameter and elevated around 8 – 40 cm (or more) above their modern live moated counterparts. The fossil microatolls in the western moat were up to 40 cm taller than those in the eastern moat.

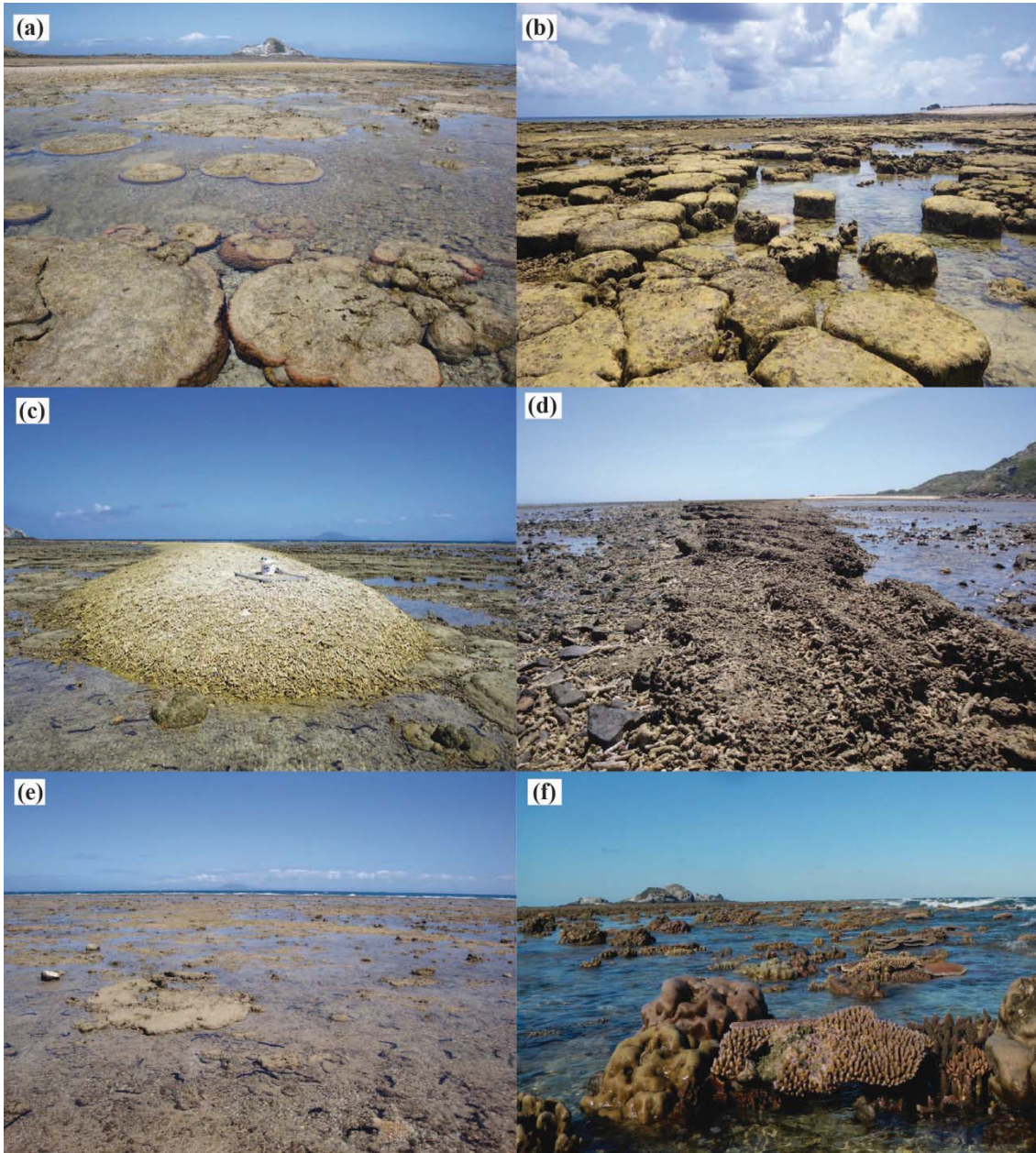


Figure 5.2 Photographs of some of the geomorphological features or zones on the reef flat at Holbourne Island. a) moated backreef zone with living *Porites* microatolls; b) moated backreef zone with high fossil microatolls; c) landward edge of a coral shingle ridge on the reef flat; d) basset edges (photo looking towards the north-west); e) outer reef flat algal turf zone; f) outer reef flat living coral zone showing live branching, massive and plate coral morphologies. See Appendix 10 for the elevations of the reef flat and features shown.

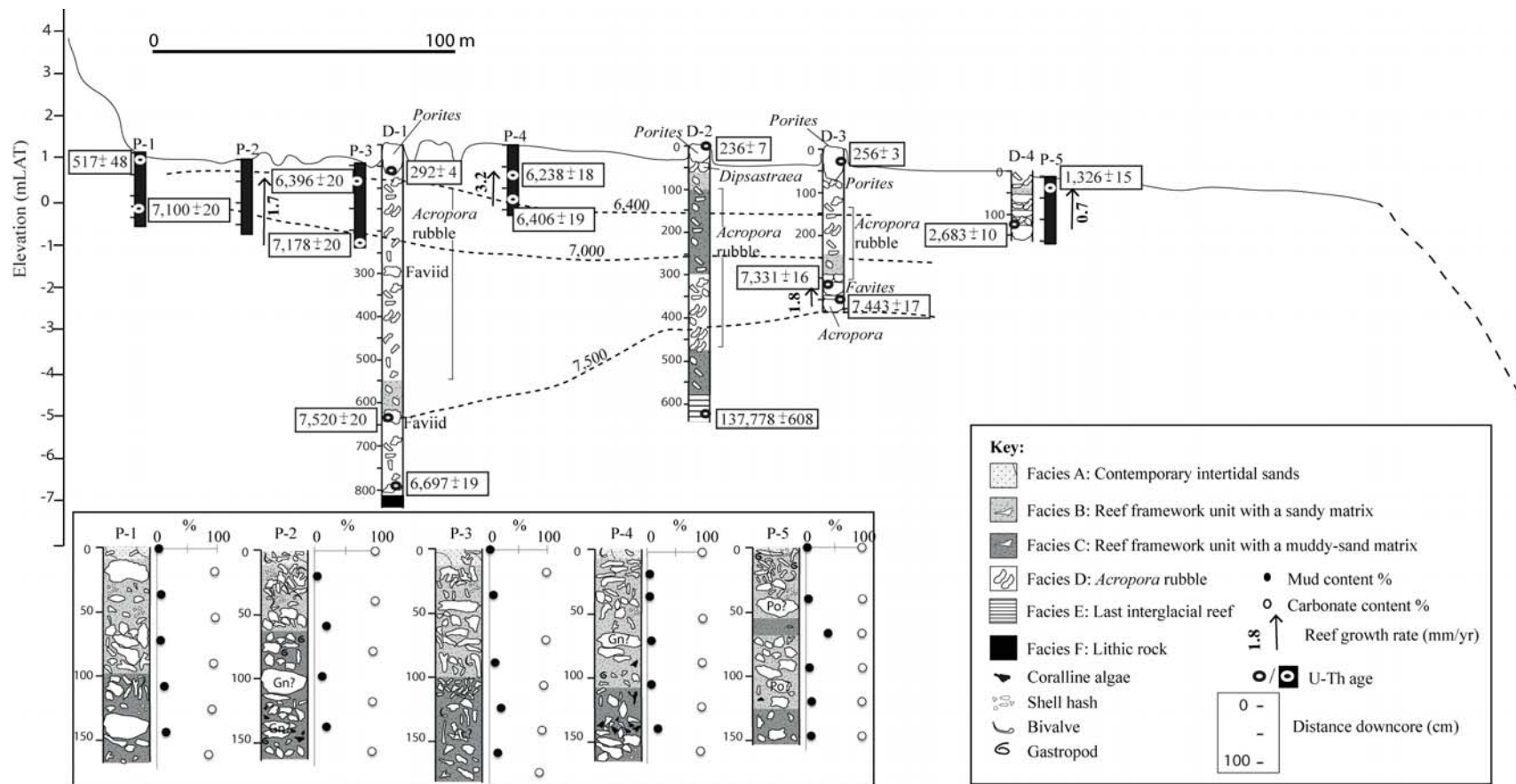


Figure 5.3 Profile of transect 2 at Holbourne Island reef flat extending seaward, with reef age indicated by the uranium-thorium (U-Th) ages (yBP $\pm 2\sigma$) from the percussion cores (P1 – P5; core locations shown by black rectangles) and drill cores (D1 – D4). Percussion core logs are shown in the inset below the profile, indicating the reef facies and the carbonate and mud content of the sediment matrix. Vertical arrows indicate average reef growth rates. Elevation is relative to lowest astronomical tide (LAT).

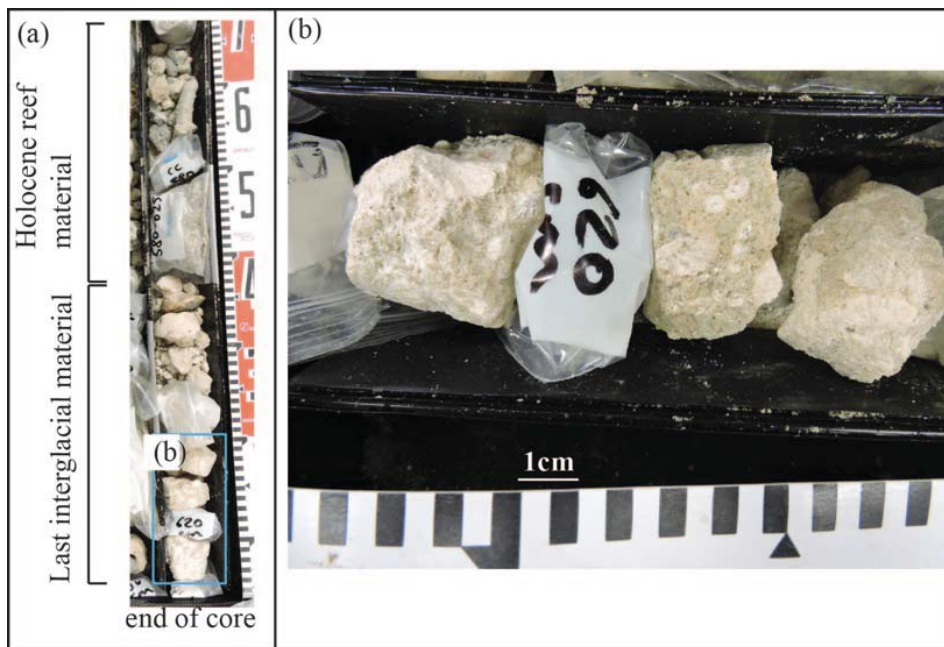


Figure 5.4 a) photograph of the lower section of core D-2 showing the last interglacial reef material and the Holocene reef branching rubble material above it, and b) photograph of the last interglacial reef material.

Fossil microatolls were not restricted to just the conspicuously moated areas; they were common across the entire backreef flat (Figure 5.1). The 17 fossil microatoll samples that were dated using a combination of U-Th and AMS radiocarbon techniques yielded median ages (calendar years AD) between 1361 and 1984 AD (Appendix 2, Appendix 7). The relatively young ages indicate the fossil microatolls were all likely moated at the time they were alive; thus groups of fossil microatolls with similar ages and elevations may reflect the timing of shingle ridge removal during cyclones and associated moat draining. The large, overlapping age errors (up to 166 years) on many of the young samples that were radiocarbon dated make interpretation somewhat problematic. The five high-precision U-Th ages with extremely low error margins (4 – 10 years) provide confidence to group the fossil microatolls into six age/elevation groups (Table 5.3, Figure 5.6). Groups 1, 3 and 5 contain fossil microatolls with similar upper surface elevations (1.17 – 1.39 mLAT) and similar diameters (1.92 – 3.6 m). Furthermore, the fossil microatoll ages varied between these three groups from 1361 AD in group 1, ~1734 AD in group 3, and 1897 to 1909 AD (with overlapping age errors) in group 5. Groups 2 and 4 contain smaller fossil microatolls (diameters between 1.0 – 2.0 m) with similar elevations (~0.79 – 1.0 mLAT): group 2 were aged 1591 to 1631 AD and group 4 were aged 1845 to 1852 AD (with overlapping age errors). Group 6 contained fossil microatolls between 0.7 – 2.7 m in diameter, with upper surfaces elevated 0.84 – 1.37 mLAT. Fossil microatolls in group 6 were ‘modern’, aged 1964 to 1984 AD.

Other reef flat zones

An algal turf zone (zone 3 on transects 2 and 3) covered much of the outer reef flat (Figure 5.2e), which began ~190 m offshore and extended ~120 – 150 m seaward (Table 5.2). Here, the reef flat was relatively featureless and turf algae growing upon consolidated reef pavement dominated the substrate ($41.3 \pm 12.7\%$ on transect 2 and $50.8 \pm 27.7\%$ on transect 3), along with scattered coral rubble and sparse living corals (coral cover $2.0 \pm 1.9\%$ and $7.1 \pm 15.9\%$ on transects 2 and 3, respectively). The surface of zone 3 was elevated ~0.5 – 0.8 mLAT on transect 2 and was slightly higher on transect 3 (~0.7 – 1.0 mLAT). An algal turf zone was absent on transect 1.

Live coral from six genera (*Acropora*, *Porites*, *Goniastrea*, *Favites*, *Montipora* and *Platygyra*) were surveyed in open-water (not moated) environments on the outer reef flat (Figure 5.2f), at elevations below ~0.64 mLAT. Living open-water microatolls (*Porites*) were located on the outer reef flat, with upper living rims elevated 0.37 mLAT on average. Live coral cover averaged $27.7 \pm 7.4\%$ in zone 2 on transect 1, $38.1 \pm 32.0\%$ in zone 4 on transect 2, and $7.1 \pm 15.9\%$ in zone 3 on transect 3 (Table 5.2). Open-water live coral cover was highest on the lower elevation western side of the outer reef flat (transects 1 and 2, ~0.4 – 0.0 mLAT) than the higher elevation eastern part (transect 3, ~0.7 mLAT).

Reef slope

The benthic cover of the reef slope was quantified according to the video survey of the upper half of the reef slope at transect 2. Depths were not measured and thus the zones that were differentiated must be considered as generalisations. Nevertheless, six genera of live hard coral were confidently identified (*Acropora*, *Montipora*, *Fungia*, *Porites*, *Stylophora* and *Turbinaria*) (Appendix 8). Corals from up to eight other genera were surveyed but identification was not possible due to poor image quality due to turbidity. Living corals were most abundant and diverse (in terms of their structural morphology) in zone 6 between approximately 2 – 4 m below the reef crest. In zone 6, live coral cover averaged $74.0 \pm 22.4\%$ and branching, massive, plate, foliaceous, columnar and free-living coral growth forms existed, including *Acropora*, *Fungia* and *Montipora* and up to eight other un-identified genera. In contrast, the shallower zone 5 (within ~2 m of the reef crest) contained only robust branching and plate corals (including *Acropora*, *Porites* and *Montipora*) covering $47.6 \pm 38.1\%$ of the substrate in this survey. The deeper zone 7 (which was still on the upper half of the reef slope) was comprised of

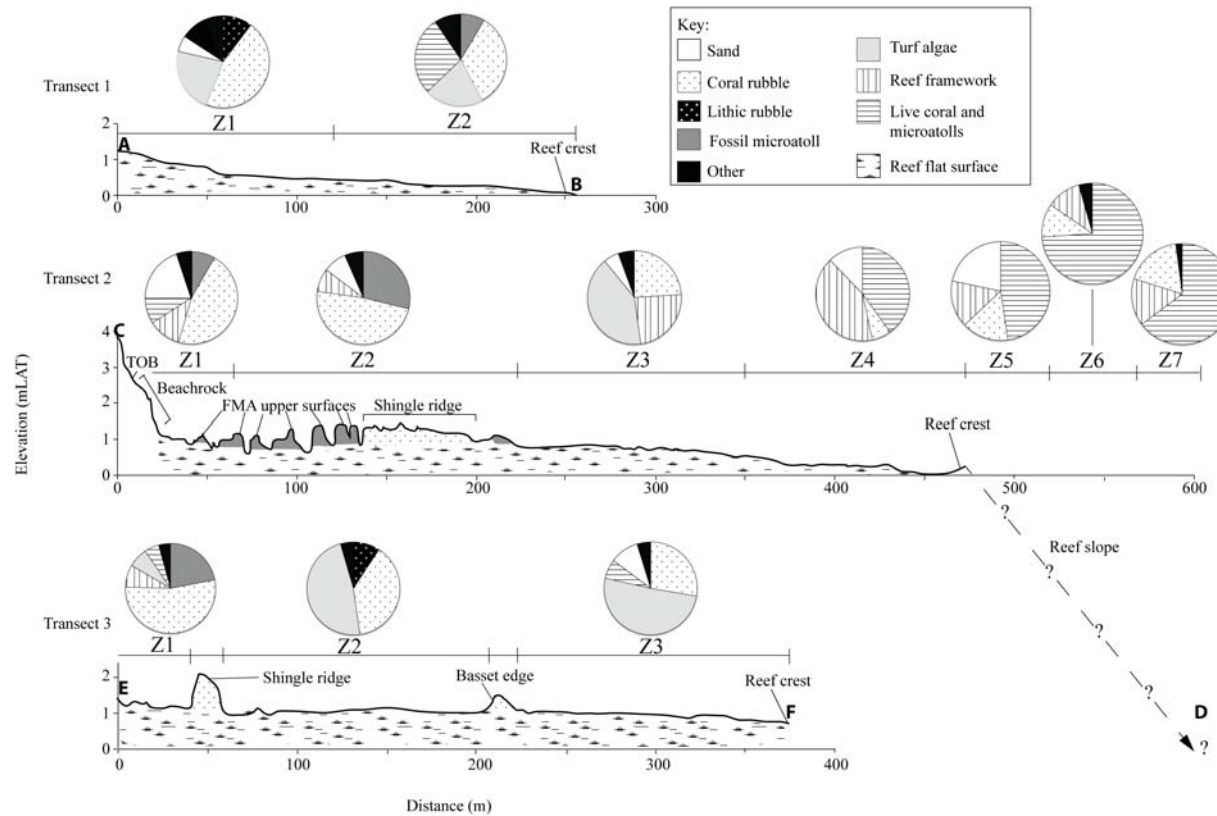


Figure 5.5 Profiles of transects 1, 2 and 3 at Holbourne Island extending seaward showing elevation of the reef flat surface relative to lowest astronomical tide (LAT) and the benthic composition for each eco-geomorphological zone (numbered) in pie charts. TOB: Toe of beach. The upper surfaces of high, moated fossil microatolls (FMA) are shown. Letters A – F represent the transect locations shown in Figure 5.1 for reference. Examples of the high FMA, reef flat shingle ridges and basset edges are shown in Figure 5.2b, c, d, respectively. Note that the depth of the reef slope on transect 2 is estimated.

branching, foliaceous and plate corals (including *Acropora*, *Stylophora* and *Turbinaria*, along with soft corals) covering on average $64.7 \pm 41.6\%$.

Table 5.2 Details of the eco-geomorphological zones on the reef flat at Holbourne Island, across transect 1 (T1), transect 2 (T2) and transect 3 (T3). Elevations are relative to lowest astronomical tide (LAT).

Zone	Description	Width (m)	Approximate elevation relative to LAT (m)	Average \pm 1 σ live coral cover (%)	Notes	Coral genera present (order of dominance)
T1	1 Backreef flat with coral and lithic rubble	120	-0.4 – 1.2	2.8 \pm 3.4	Living microatolls present (open-water)	<i>Porites</i> , <i>Goniastrea</i> , <i>Favites</i>
	2 Outer reef flat live coral zone	135	-0.0 – 0.4	27.7 \pm 7.4	Living microatolls common, branching and massive corals present (open-water)	<i>Porites</i> , <i>Goniastrea</i> , <i>Acropora</i> , <i>Platygyra</i> , <i>Favites</i>
T2	1 Moated backreef flat	40	-0.7 – 1.0	10.3 \pm 8.8	Moated corals	<i>Porites</i> , <i>Goniastrea</i>
	2 High fossil microatoll zone with coral rubble	150	-0.7 – 1.4	0.6 \pm 0.7	Shingle ridge crosses this zone. Living microatolls (moated)	<i>Porites</i>
	3 Outer reef flat algal turf zone	120	-0.5 – 0.8	2.0 \pm 1.9	Small open-water coral recruits	<i>Goniastrea</i> , <i>Acropora</i> , <i>Porites</i>
	4 Outer reef flat live coral zone	130	-0.0 – 0.5	38.1 \pm 32.0	Branching and massive corals dominant (open-water)	<i>Acropora</i> , <i>Montipora</i> , <i>Goniastrea</i> , <i>Porites</i> , Soft coral, <i>Favites</i>
T3	1 Moated backreef flat with microatolls	40	-1.1 – 1.3	5.6 \pm 5.9	Living microatolls (moated)	<i>Porites</i> , <i>Goniastrea</i>
	2 Moated reef flat with turf algae and rubble	150	-1.0 – 1.1	0.2 \pm 0.6	Moated corals	<i>Goniastrea</i> , <i>Porites</i>
	3 Outer reef flat algal turf and living microatolls	150	-0.7 – 1.0	7.1 \pm 15.9	Small open-water coral recruits	<i>Porites</i> , <i>Goniastrea</i>

Table 5.3 Fossil microatoll groups on the Holbourne Island reef flat differentiated according to the age of the sample (note that ages are presented as calendar years AD) the elevation of the fossil microatoll upper surface (relative to lowest astronomical tide [LAT]), and the diameter of the fossil microatoll.

Group	Median age of samples (years AD) (age range in parentheses)	Elevation range (mLAT)	Diameter range (m)	Notes
Group 1	1361 (1370 – 1351)	1.34	1.92	Only one sample in this group, ~0.55 m high
Group 2	1591 (1599 – 1584) to 1631 (1504 – 1796)	0.87 – 0.95	1.0 – 1.1	Surface elevated close to reef flat surface
Group 3	1734 (1730 – 1739) to 1819 (1688 – 1933)	1.2 – 1.39	2.1 – 3.5	Generally ~0.35 m high
Group 4	1845 (1737 – 1975) to 1852 (1848 – 1856)	0.79 – 1.0	1.4 – 2.0	Generally ~0.2 m high, eroded
Group 5	1897 (1835 – 2016) to 1909 (1859 – 1996)	1.17 – 1.38	1.0 – 3.6	0.2 – 0.5 m high
Group 6	1964 (1963 – 1965) to 1984 (1978 – 1997)	0.84 – 1.37	0.7 – 2.7	Generally ~0.2 m high

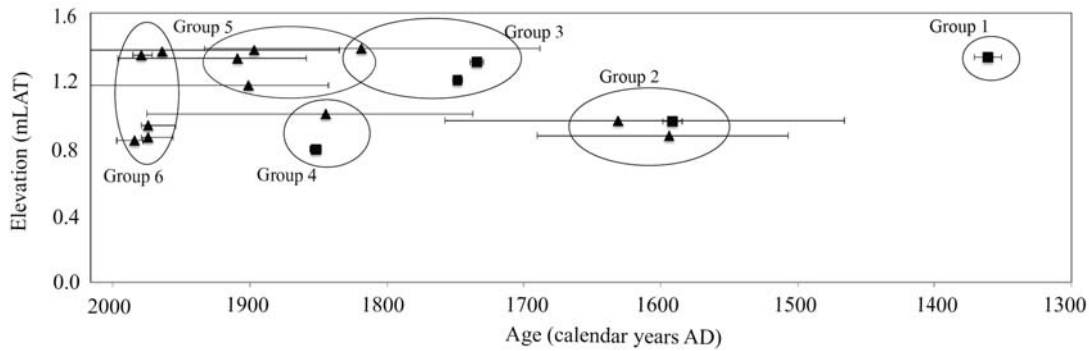


Figure 5.6 Microatoll ages (note that ages are presented as calendar years AD) and elevations (relative to lowest astronomical tide [LAT]). Triangles represent radiocarbon ages and squares represent uranium-thorium ages. 2σ age errors shown by bars.

5.6 Discussion

Numerous long-term records of fringing reef growth have been developed for reefs on the inner-shelf of the GBR (see Smithers et al., 2006; Hopley et al., 2007). However, detailed records of mid-shelf fringing reef growth are rare (Kleypas, 1996; Hopley et al., 1978) but provide important comparisons with inshore reef records. The precisely and densely dated record of mid-shelf fringing reef development presented here reveals a new record of last interglacial reef from the mid-shelf GBR. Four key stages in reef development at Holbourne Island are identified (Figure 5.3): initiation over last interglacial reef foundations $\sim 7,500$ yBP; vertical accretion towards sea level by $\sim 6,500$ yBP; mid-Holocene reef flat progradation around 6,000 yBP; and late-Holocene reef flat progradation from $2,683 \pm 10$ yBP continuing to the present. Here, I discuss the last interglacial reef foundation in the context of other records of last interglacial reef from the GBR and the influence of cyclones on Holocene reef development and contemporary reef flat geomorphology and ecology.

5.6.1 Last interglacial reef foundation

The recovery of last interglacial reef with a U-Th age of $137,778 \pm 608$ yBP at 5.9 m below the present surface (~ 5.0 m below present LAT) is an important discovery, as accounts of last interglacial coral are rare along eastern Australia (Murray-Wallace and Belperio, 1991). The timing and duration of the last interglacial period are debated (see review by Muhs et al. [2002]). However, a broad pattern of global last interglacial sea level is presented in Murray-Wallace and Woodroffe (2014), indicating that sea level reached a maximum of ~ 6 m above present between 120,000 – 116,000 yBP, but was close to the present level ($+1.0$ – 2.0 m) $\sim 138,000$ yBP. Evidence for the precise age of the Pleistocene-Holocene reef boundary in the GBR is lacking. Radiocarbon ages $>30,000$ yBP are most often reported from coral material

that is interpreted as last interglacial (Kleypas, 1996; Hopley et al., 1978), but these ages are highly inaccurate as eustatic sea level was too low for coral growth on the GBR at this time (Murray-Wallace and Woodroffe, 2014). Although U-Th dating provides more accurate and precise ages, U-Th ages are rare for the GBR and a wide range of ages have been reported. For example, U-Th ages of last interglacial reef from the GBR include $125,700 \pm 600$ yBP (Braithwaite et al., 2004) and $172,000 \pm 12,000 - 107,000 \pm 8,000$ yBP (Marshall, 1983; Marshall and Davies, 1984; Kleypas, 1996). The variability in U-Th ages reported from last interglacial corals on the GBR may be due to varying degrees of sub-aerial erosion of last interglacial reef surfaces during the glacial sea-level lowstand prior to the most recent sea-level transgression (Marshall and Davies, 1984). Alternatively, varying degrees of diagenesis of the corals used for dating would also produce variable ages (Johnson et al., 1984).

To date, last interglacial reef foundations have been recovered beneath few fringing reefs in the GBR (Hopley et al., 1978; Kleypas, 1996) and the Torres Strait (Woodroffe et al., 2000). However, last interglacial reef provides the foundation for all Holocene reef growth so far investigated on the outer shelf of the GBR (Marshall and Davies, 1984) as well as mid-shelf platform reefs (Thom et al., 1978; Marshall and Davies, 1984). On the central GBR, last interglacial reef is the known foundation for just one other fringing reef, at Hayman Island (Hopley et al., 1978; Kan et al., 1997), located on the inner-mid shelf margin ~65 km south-east of Holbourne Island (Figure 5.1). At Hayman Island the depth to the last interglacial reef surface was greater (~20 – 15 m below the surface: Harvey et al., 1979; Kan et al., 1997), than at Holbourne Island, where last interglacial reef was encountered just 5.9 m below the surface.

At ~5.0 m below present LAT, the last interglacial reef recovered at Holbourne Island is the shallowest confirmed last interglacial reef recovered beneath fringing reefs in the GBR. Indeed, the depth to the Pleistocene-Holocene reef boundary at Holbourne Island is by far the shallowest known of all reefs in the central GBR region, where this boundary was considered to be much deeper than in the northern and southern GBR regions by Hopley et al. (2007). In a study by Kleypas (1996) last interglacial reef was recovered on the southern GBR beneath two mid-shelf fringing reefs at various depths: Cockermouth Island (~40 km offshore) at a minimum depth of 8.4 m below LAT; and Penrith Island (~70 km offshore) at a minimum depth of 6.4 below LAT. Weathered reef material assumed to be last interglacial reef was exposed at the surface at Digby Island (also in the southern GBR ~45 km offshore) (Kleypas, 1996), however this assessment of age was based on the appearance of the material and is yet to be confirmed as last interglacial age by dating. In comparison, the Pleistocene-Holocene reef boundary at Britomart Reef, a mid-shelf platform reef in the central GBR, was recovered ~20 – 25 m below LAT (Johnson et al., 1984).

Granite was encountered at the base of core D-1 beneath the Holocene reef (Figure 5.3). The granite may represent a Pleistocene boulder beach similar to that exposed at the surface today at the base of the eastern granite island outcrop (Figure 5.1). Hopley and Barnes (1985) established that a terrigenous boulder beach formed the foundation upon which a Holocene fringing reef developed at Iris Point, Orpheus Island on the inshore GBR. This boulder beach was also exposed at the surface landward of the reef flat at Iris Point and was estimated to be of last interglacial age (Hopley and Barnes, 1985). Indeed, Hopley (1975) discovered a boulder beach beneath Holbourne Island ~1.5 m below the surface of the sand ridge located on the island behind transect 2. This finding supports the inference that the terrigenous rock captured in core D-1 forms part of a boulder beach that extends from the island beneath the back part of the reef flat. However, this material could alternatively be a granitic rubble deposit, and this possibility cannot be ruled out, as there are areas of the modern reef flat that contain lithic rubble that has been re-distributed alongshore from the rock outcrops and boulder beach that adjoin the eastern side of the reef flat (Figure 5.1). The lack of last interglacial reef material in D-1 may be a result of either burial of last interglacial reef by the Pleistocene boulder beach, erosion, or simply because a reef did not grow in this position during the last interglacial period.

Although last interglacial reef provides the foundation for all mid-shelf fringing reefs in the GBR studied so far (Hopley et al., 1978; Kleypas, 1996), last interglacial reef foundations have not yet been recovered beneath reefs within ~20 km of the mainland. Whether this reflects a paucity of data is unknown, but will be revealed in future studies. However, the possibility that inshore fringing reefs similar to those that have developed in the mid- and late-Holocene (Smithers et al., 2006) grew during the last interglacial period cannot be ruled out. It is possible that their remnants have been eroded, particularly given the detrital and ephemeral nature of some Holocene inshore reefs (Smithers and Larcombe, 2003) compared with their offshore counterparts which develop solid, cemented limestone structures.

5.6.2 The Holocene reef chronostratigraphy

Initiation of the Holocene reef occurred at or prior to $7,520 \pm 20$ yBP in a subtidal environment, ~6.2 – 9.0 m below palaeo-LAT; either directly upon a weathered last interglacial reef or granitic substrate (Figure 5.3). In the 1,000-year period after Holocene reef initiation, the reef accreted vertically towards sea level and reef flat formation began once the reef reached (palaeo) sea level and all vertical accommodation space was occupied. The majority of reef development occurred between 7,500 – 6,000 yBP. Reef initiation occurred later at Holbourne Island ($\sim 7,520 \pm 20$ yBP) than at the mid-shelf fringing reef at Hayman Island ($\sim 9,320 \pm 730$

yBP, Hopley et al., 1978) according to the earliest known ages from each reef. This probably occurred due to earlier flooding of the deeper substrate at Hayman Island during the PGM. Hayman Island reef is situated in a more protected environment than Holbourne Island, largely sheltered from prevailing south-easterly swells (Figure 5.1), and these conditions may have been favourable for earlier reef start up. A radiocarbon age from Hayman Island reef of $5,360 \pm 240$ was presented in cores collected by Hopley et al. (1978) at an approximately equivalent depth to the earliest age from Holbourne Island ($7,520 \pm 20$ yBP ~5.0 m below present LAT). The shallower substrate beneath Holbourne Island reef (6.0 m depth compared with 15 – 20 m depth at Hayman Island) means that this reef had less accommodation space to vertically accrete into until it reached sea level, while Hayman Island reef accreted over a greater depth in ‘catch-up’ mode (Neumann and MacIntyre, 1985) for a longer time. Hopley et al. (1978) established average rates of reef accretion at Hayman Island were faster (4 – 5 mm/yr) compared to those at Holbourne Island (1.7 – 3.2 mm/yr). Reefs growing from deeper foundations often have rapid vertical accretion rates (Davies et al., 1985).

Only one age reversal was encountered in the chronostratigraphy of Holbourne Island reef in D-1 (Figure 5.3), where an age ~820 years older ($7,520 \pm 20$ yBP) was encountered ~1.7 m above the basal age ($6,697 \pm 19$ yBP). Easton and Olsen (1976) suggest age gaps in reef cores can be due to irregularities in the shape of the growing reef. The younger, lower age could alternatively be due to storm re-working (Johnson and Risk, 1987). Although this possibility is unlikely given the 1.7 m distance between the clasts, it cannot be completely ruled out given the prevalence of re-worked branching rubble material throughout the cores (e.g. facies D) and the presence of large storm-deposited shingle ridges onshore and on the contemporary reef flat. The lower coral clast was selected for dating because it was the most appropriate clast (most likely to be *in situ*) within the lower 1.5 m of the core and it was anticipated that this clast would provide a minimum age for reef initiation. However, it is also possible that either clast has undergone post-mortem diagenesis, rendering altered ages (Webb et al., 2016). Nevertheless, the age reversal does not significantly alter the general age structure of reef development.

It must be acknowledged that the lack of dates across long lengths (up to 6.0 m) of some cores (e.g. D-1, D-2, D-3) is problematic for confident reconstruction of reef growth isochrons, and thus the isochrons presented in Figure 5.3 should be considered approximate, but are highly plausible given the available data. The lack of dates reflects the scarcity of well-preserved *in situ* coral material in the cores of a quality that would yield accurate *in situ* reef growth ages. This in itself is an interesting feature of the chronostratigraphy of Holbourne Island reef. The cores were dominated by *Acropora* rubble material encrusted with coralline algae (facies D), indicating the clasts have undergone substantial re-working. Given the considerable amount of

storm-deposited, encrusted rubble characterising the modern reef flat (Figure 5.1), the branching rubble material comprising facies D is likely to be imported detrital material (transported by storms/cyclones).

The large age gap in coral framework material recovered in the internal reef structure, as indicated by the gap in U-Th ages from $6,238 \pm 18 - 2,683 \pm 10$ yBP may be the result of either cyclone stripping or sea-level variability during the mid-Holocene. Indeed, a similar age gap between $6,439 \pm 19 - 1,617 \pm 10$ yBP was observed in the internal structure of the fringing reef at Middle Island, located 28 km south of Holbourne Island (Figure 5.1) (see Chapter 4). The age gap at Middle Island reef was attributed to cyclone stripping of the upper and outer reef structure during the mid-Holocene based on the abundance of re-worked rubble material in the chronostratigraphy and the nature, size and age of shingle ridge deposits located onshore. The stripped reefal material at Middle Island was moved onshore during intense cyclones and deposited in the form of shingle ridges (see Chapter 4). The similarities in the chronostratigraphy of the reefs at Holbourne and Middle Islands (open-fabric reefs largely dominated by branching rubble with a considerable age gap during the mid-Holocene) and the presence of large shingle ridges (up to 7.0 mLAT) composed of mainly branching rubble material above the shoreline at both islands provides sufficient reason to infer that the cyclone-stripping concept may also apply at Holbourne Island. The presence of shingle ridges onshore is clear evidence that material has been stripped from the reef structure and deposited onshore where it has been preserved. The maximum shingle ridge crest elevation at Holbourne Island was very similar (7.0 mLAT) to that at Middle Island (6.3 mLAT). These shingle ridges at Middle and Holbourne Island may have been deposited during the same cyclone(s), due to the similar height and nature of both ridges (heavily vegetated at the time of this study) and the similar timing of the age gap in reef cores. However, additional ages from material within these ridges are required to refute or support this possibility. The shingle ridge at Middle Island was dated to $4,555 \pm 140$ yBP (radiocarbon age presented in Hopley [1975] and re-calibrated in Calib 7.02 [Stuiver and Reimer, 1993]). This age lies within the age gaps in the chronostratigraphies of both Middle Island and Holbourne Island reefs, supporting the hypothesis that coral material was transported from the reef onshore around this time. The age from a coral fragment ($3,180 \pm 260$ yBP) within a beachrock terrace deposit on Holbourne Island reported by Hopley (1975) also suggests that coral growth on the reef must have persisted during this age gap in the core record. Indeed, a shingle ridge at Curacoa Island in the central GBR has a similar crest elevation (~6.8 mLAT) to that at Holbourne and Middle Islands and is interpreted to have been deposited during intense cyclones ~4,000 yBP (Hayne and Chappell, 2001; Nott and Hayne, 2011). This reveals that intense cyclones occurred in the GBR

during this time, which were capable of depositing shingle ridges onshore that remain well-preserved today in more sheltered locations than Holbourne Island.

Interestingly, although the age gap in the reef chronostratigraphy at Holbourne Island may be attributed (at least in part) to cyclone stripping, a smaller hiatus in reef accretion has been detected in many other reefs on the GBR, where active accretion ceased between ~4,000 – 2,000 yBP (Smithers et al., 2006; Perry and Smithers, 2011). Accommodation space constraints associated with late-Holocene relative sea-level fall (Perry and Smithers, 2011) or relative sea-level oscillations (Leonard et al., 2016) have been suggested as potential causal factors for this cessation in reef accretion. Relative sea-level fall in the late-Holocene (Lewis et al., 2013) would have reduced vertical accommodation space at Holbourne Island reef, contributing to reduced vertical reef accretion. The age gap ($6,238 \pm 18 - 2,683 \pm 10$ yBP) in the reef chronostratigraphy at Holbourne Island probably resulted from a combination of both late-Holocene sea-level fall and cyclone stripping.

5.6.3 The role of cyclones over centennial scales

Cyclones have clearly influenced the ecology and geomorphology at Holbourne Island reef over millennia, including reef development. The nature and age of geomorphological features surveyed on the modern reef flat (fossil microatolls and reef flat shingle ridges) provide insights into the effects of cyclones over centennial scales. The fossil microatolls on the Holbourne Island reef flat reached 0.55 m tall and 3.6 m in diameter, indicating that ponded water up to 55 cm deep must have existed on the reef flat for a period of up to ~180 years, based on average growth rates of *Porites* corals in this region of ~1 cm/yr (Lough and Barnes, 2000). The range of fossil microatoll ages (note the samples taken for analysis were taken from the outer rims of the microatoll and hence provide the time of mortality that likely coincided with a cyclone/disturbance event) from 1361 to 1984 AD indicates that moating of water above the low tide level has been active (but intermittent) on this reef flat for at least 600 years and still occurs today (allowing microatolls to grow above elevations of open-water coral growth by ~0.6 – 1.0 m today, and up to 1.0 m higher in the past). Rainford (1925) initially proposed that a cyclone event in 1918 was responsible for the mortality of all the corals on the Holbourne Island reef flat, which Hopley (1975) confirmed based on just one radiocarbon age from a fossil microatoll that corresponded with this 1918 event. In fact, the fossil microatoll data presented here (including precise U-Th ages) show that the 1918 cyclone was not solely responsible for microatoll mortality, even though groups of fossil microatolls display similarities in height and diameter. The ages indicate that it is possible that the 1918 cyclone killed some of the fossil microatolls (those in groups 4 and 5), but others died earlier, such as those in groups 1 and 2

(Table 5.3, Figure 5.6). In that regard, my data suggest that at least four separate major cyclones impacted Holbourne Island over the past 600 years, and caused considerable geomorphological and ecological change over the reef flat. The ponded microatoll data from Holbourne Island have important implications for studies where past sea level is reconstructed from fossil microatoll data (e.g. Lewis et al., 2013; Leonard et al., 2016). The potential effects of ponding on a reef flat must be considered when interpreting fossil microatoll data for reconstructing past sea level, including the possibility that differences in ponded water level across the same reef flat at the same time period may occur. Group 6 at Holbourne Island demonstrates this, where fossil microatolls within the same age range (1963 – 1997 AD) have two different upper surface elevations that vary by around 50 cm (~0.84 mLAT and ~1.37 mLAT) (Figure 5.6).

5.7 Conclusions

The percussion and drill cores coupled with U-Th ages allowed the chronostratigraphy of the fringing reef at Holbourne Island to be developed. Last interglacial reef was encountered 5.9 m below the reef surface (~5.0 m below present LAT) at Holbourne Island. This is the shallowest confirmed record of Pleistocene reef beneath a mid-shelf fringing reef in the GBR and the shallowest confirmed Pleistocene-Holocene reef boundary of all reefs in the central GBR to date. Holocene coral colonies at Holbourne Island developed upon this last interglacial reef (or directly upon a granitic foundation) at or prior to ~7,500 yBP. The fringing reef at Holbourne Island accreted vertically towards sea level and began to form a reef flat by around 6,400 yBP. Reef flat formation occurred when sea level was ~1.0 – 1.5 m higher than present, and following late-Holocene sea-level fall, the majority of the Holbourne Island reef flat is now exposed at low tide today. An age gap of ~3,500 years exists in the chronostratigraphy of the reef, which is attributed to cyclones. The case for cyclone stripping of the upper/outer reef structure in the mid-Holocene and deposition as shingle ridges onshore identified in Chapter 4 is strengthened by the chronostratigraphy and geomorphology of Holbourne Island reef. Cyclones have long had catastrophic and abrupt impacts on reef flat ecology and geomorphology at Holbourne Island, through the deposition, movement, or removal of shingle ridges. Ponding of water above the low tide level occurs today (due to shingle ridges) and has occurred at various times over the last 600 years, creating complex fields of fossil microatolls of different ages. Holbourne Island is a unique fringing reef due to its relatively exposed and isolated location on the mid-shelf of the central GBR. The exposure of the reef to cyclone events is evident in the present geomorphology and cyclones have clearly played an important role in the Holocene development of the reef. However, a further detailed investigation of the ages of the shingle ridges at Holbourne Island would complement this chronostratigraphic record of mid-shelf fringing reef development.

6 General discussion: Fringing reef development along a cross-shelf transect

To be submitted to *Geology* in 2016

Chapters 2, 3, 4 and 5 each present a novel long-term record of fringing reef development, beginning at a shore-attached location at one end of a four site transect and ending with an investigation of a mid-shelf fringing reef, 40 km offshore from the Queensland coast near Bowen. The importance of sea level in shaping reef development is highlighted in all four chapters, however each chapter additionally provides insights into the effects of other factors that have influenced reef growth. The ability of a diverse reef to develop and persist in a protected bay setting under a constantly muddy sediment regime was shown in Chapter 2. Reef condition over multiple spatial and temporal scales was explored in Chapter 3, showing that not all reefs in Edgecumbe Bay are degraded. The impacts of cyclones on long-term reef development were highlighted in Chapters 4 and 5. In this chapter I compare the variability of Holocene reef development and present reef condition across the shelf, addressing key research objective number five, detailed in Chapter 1.

6.1 Introduction

Coral cover and diversity on inshore reefs of Australia's Great Barrier Reef (GBR) are argued by many researchers to have declined over the past few decades (Cheal et al., 2010; Hughes et al., 2010; Thompson and Dolman, 2010), but others contend that some inshore reefs are more resilient than widely assumed (Perry and Smithers, 2011; Browne et al., 2012). Where recent declines are inferred, anthropogenic impacts associated with European settlement of coastal catchments are commonly proposed as the cause (Hughes et al., 2010; Roff et al., 2012). However, the degree to which human impacts are responsible is contested (Hughes et al., 2011; Sweatman and Syms, 2011; Sweatman et al., 2011). A major factor impeding resolution of this debate is that modern ecological data span a very short time period (usually 20 to 40 years) relative to the time period over which anthropogenic pressures might have been exerted (~150 years) and the timeframe preserved in reef structures and captured in reef cores, which can include several millennia (Figure 6.1). Furthermore, differentiating natural and anthropogenic stressors is difficult due to the paucity of data on both baseline reef condition and temporal and spatial variability of natural stressors to coral reefs. Long-term insights into past reef development and natural variability are required to provide baseline (pre-European settlement) context (Smithers et al., 2006). Long-term knowledge can help assess whether recent documented changes in reef condition are unprecedented (Pandolfi and Jackson, 2006) and, to isolate the relative importance of various reported stressors to coral reefs (Bruno et al., 2014).

Since European settlement of the Queensland coast in the early- to mid-1800s, sediment and nutrient loads exported to the inshore GBR have increased two- to ten-fold (McCulloch et al., 2003; Kroon et al., 2012; Waters et al., 2014). This has generated concern for the health of inshore fringing reefs that are located close to the coast and are most exposed to elevated nutrient and suspended sediment loads (Fabricius et al., 2005; Cooper et al., 2007). Coral cover and diversity on the GBR have been shown to decline along a gradient of increasing suspended sediment and nutrients in the water column (van Woerik et al., 1999; Fabricius et al., 2005; DeVantier et al., 2006). However, proximity to human stressors is not always an indicator of poor reef condition, as indicated by Lirman and Fong (2007) who found higher coral cover on reefs closer to the mainland in the Florida Keys. Indeed, many inshore reefs on the GBR have developed close to the coast in naturally turbid settings (Larcombe and Woolfe, 1999b) and have been shown to have high coral cover, diversity and accretion rates (Browne et al., 2010; Palmer et al., 2010; Perry et al., 2012; Roff et al., 2015), highlighting their ability to flourish in conditions typically considered unfavourable for reef health (Browne et al., 2012).

In this thesis I developed detailed millennial-scale records of fringing reef development in the central GBR based on a total of 42 reef cores and 112 high-precision uranium-thorium (U-Th)

ages of coral material from within the cores and on the reef flats (refer to section 1.9 in Chapter 1 for detailed descriptions of the methodologies). Temporal and spatial variations in reef growth were explored to differentiate drivers of past changes in reef evolution. The four study sites (see Figure 1.2 in Chapter 1) include fringing reefs located in diverse environmental settings including: mainland-attached (Bramston Reef); within an island embayment (Stone Island North [SI-N]); and attached to headlands/shorelines of offshore islands located between 3 and 40 km from the mainland (Stone Island South [SI-S], Middle Island and Holbourne Island). A detailed description of the regional setting is provided in section 1.8 in Chapter 1. The study sites are located along a cross-shelf transect extending from the mainland coast across the inner-shelf to the mid-shelf. This transect captures a gradient of terrestrial and direct anthropogenic influences that diminish with distance from the mainland. Variations in exposure to natural disturbances may also occur with distance across the GBR shelf, including greater re-suspension of the terrigenous sediment wedge in inshore areas (Larcombe et al., 2001) and greater exposure to the physical effects of tropical cyclones further offshore (Wolff et al., 2016). Furthermore, hydro-isostatic adjustment of the continental shelf associated with water loading during the post-glacial marine transgression (PGMT) may have resulted in uplift of the inner-shelf during the late-Holocene, so that reefs across the shelf developed under different relative sea-level histories (Hopley et al., 2007). Geophysical models suggest that the inner-shelf experienced greater uplift and thus more pronounced relative sea-level fall than the outer-shelf over the late-Holocene (Chappell et al., 1982; Lambeck and Nakada, 1990). However, the degree to which these natural variations, such as sea-level histories and exposure to sedimentation and cyclones, influenced fringing reef development over millennia is poorly understood.

This chapter examines cross-shore variations in Holocene reef growth characteristics (i.e. antecedent substrates, timing and depth of reef initiation, reef accretion rates and timing, and palaeo-ecology) by synthesising and discussing the results of Chapters 2, 3, 4 and 5. The relative influences of various natural environmental parameters (sea-level change, cyclones and sedimentation) on reef development are considered. Descriptions and photographs of reef flat condition from the studied reefs capturing periods in time over the past 120 years also exist in this region and reveal considerable variability in coral cover and diversity over this period. Here I apply this historical information coupled with quantitative data on contemporary reef geomorphology and ecological condition along the cross-shelf transect to better understand the influence of variations in environmental parameters that may influence reef growth. This study presents a new detailed comparison of Holocene fringing reef growth across a transect that extends from the mainland to the mid-shelf in the central GBR, allowing a gradient of anthropogenic influence and exposure to be investigated.

6.2 Variations in reef growth across the shelf

6.2.1 Timing of reef initiation upon antecedent foundations

For a coral reef to form, a suitable substrate is required on which coral colonies can initiate (Hopley et al., 1983; Cabioch et al., 1995). Fringing reefs commonly develop upon a range of unconsolidated and consolidated substrates unlike their outer-shelf counterparts, which more typically develop upon consolidated substrates (Kennedy and Woodroffe, 2002; Smithers et al., 2006). Along the cross-shelf transect presented in this study, variability in the nature of and depth to the pre-Holocene antecedent surface was observed (Table 6.1). Unconsolidated transgressive sands and lag gravels overlaying Pleistocene clay were recovered at a depth of 1.9 – 3.7 m below the present reef flat surface at Bramston Reef. Compacted regolith clay (interpreted as the pre-Holocene surface) was recovered 7.0 m below the present surface of the fringing reef flat at Middle Island, while a weathered last interglacial reef deposit and granite were each recovered 5.9 and 8.1 m below the surface of the fringing reef flat at Holbourne Island, respectively (Table 6.1). The pre-Holocene surface was not identified at Stone Island (Chapter 3) because the cores did not penetrate to sufficient depth (maximum 5.1 m penetration). Nevertheless, it is probable that the pre-Holocene surface at Stone Island would be comparable to the transgressive sands encountered at Bramston Reef less than 3 km away (Chapter 2) or to the regolith clay recovered from Middle Island approximately 8 km away (Chapter 4). The pre-Holocene substrates identified in this study are analogous to other published studies of fringing reef growth on the inner GBR, which reveal most form on weathered terrigenous foundations (unconsolidated or consolidated) (Hopley et al., 1983; Hopley and Barnes, 1985; Johnson and Risk, 1987; Perry et al., 2011; Roche et al., 2011; Lewis et al., 2012). Mid-shelf fringing reefs likely have consolidated last interglacial reef foundations (Hopley et al., 1978; Kleypas, 1996), similar to the platform reefs of the mid- and outer-shelf (Thom et al., 1978; Marshall and Davies, 1984; Webster and Davies, 2003).

Last interglacial reef foundations were only recovered at Holbourne Island, with various terrestrial foundations underlying the Holocene reefs at other sites. This section explores the possibility that a fringing reef existed at Middle Island, Stone Island and Bramston Reef during the last interglacial period. This possibility could be reasonably expected, particularly at Middle Island, given its proximity to Holbourne Island and Hayman Island (located 28 km north and 58 km south-east of Middle Island, respectively), where fringing reefs at both islands developed upon last interglacial reef foundations (Hopley et al., 1978; Chapter 5). Furthermore, the depth of Holocene reef initiation was comparable between Middle Island (7.0 m) and Holbourne

Table 6.1 Summary of Holocene reef growth attributes at the study reefs. uranium-thorium (U-Th) ages are presented as years before present (1950 AD).

Site	Distance offshore from mainland coast near Bowen	Reef flat width (m)	Number of cores collected	Maximum core depth (m)	Number of U-Th ages in cores	Earliest known age of initiation (yBP)	Antecedent substrate	Shallowest depth [^] to antecedent surface (m)	Maximum depth [^] to antecedent surface (m)	Earliest known age for reef flat development (yBP)	Time when ~80% of reef had been developed (yBP)	Range of average net vertical accretion rates (mm/yr)	Number of coral genera recorded in cores
Bramston Reef	0 km	900	8	4.6	13	5,396 ± 51	Transgressive sands and lag gravels overlying Pleistocene clay	1.9	3.7	4,256 ± 14	2,000	2.5 – 9.8	25
Stone Island South	3 km	450	9	5.1	14	7,247 ± 23	Not recovered	n/a	>5.1	6,716 ± 23	5,000	0.3 – 4.8	20
Stone Island North	3 km	400	5	5.0	11	7,064 ± 17	Not recovered	n/a	>5.0	4,475 ± 45	4,000	0.9 – 5.0	23
Middle Island	10 km	330	10	7.2	14	7,873 ± 17	Regolith clay or unconsolidated carbonate sediments	2.6	7.0	6,895 ± 19	6,000	3.5 – 7.6	15
Holbourne Island	40 km	440	9	8.3	16	7,520 ± 20	Last interglacial reef or granite	6.0	8.1	~6,400	6,000	0.7 – 3.2	At least 10

[^] Depth reported as depth downcore from present reef flat surface

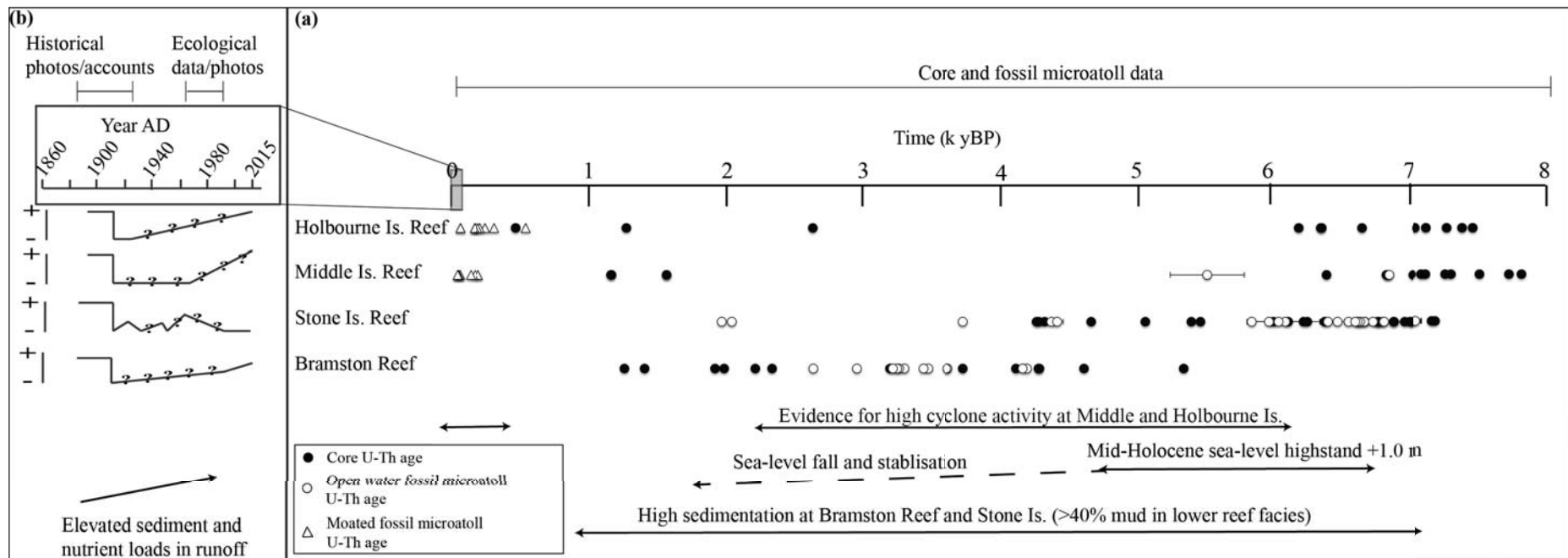


Figure 6.1 (a) Millennial-scale timeline showing the main period of Holocene reef development for the four study sites. Uranium-thorium (U-Th) ages are those obtained in this thesis from cores and fossil microatolls. Re-calibrated radiocarbon ages from other sources are also presented with 2σ age errors (ages initially presented in Chappell et al. [1983]; Hopley, [1975] and re-calibrated using Calib 7.0 [Stuiver and Reimer, 1993]). Note age errors are too small to warrant inclusion for the U-Th ages. The period since European settlement of the Queensland coast is highlighted in the grey box and blown up in (b), showing estimated reef ‘condition’ (+ equals good condition [high coral cover and structural diversity] and – equals poor condition [low coral cover and limited structural diversity]) over time based on historical photographs (Saville-Kent, 1893; Clark et al., 2016), accounts (Hedley, 1925; Marshall et al., 1925; Rainford, 1925; Stanley, 1928; Steers, 1937; Richards, 1938; Stephenson et al., 1953; Hopley, 1975) contemporary photographs (Wachenfeld, 1997; Ryan et al., 2016; Clark et al., 2016) and available modern ecological data from this thesis and Ryan et al. (2016); Clark et al. (2016).

Island (8.1 m) (Table 6.1) and Holocene reef development has flourished at all sites. Generally, the recovery of non-reefal antecedent surfaces in reef cores (i.e. terrigenous foundations) is commonly interpreted as indicating the absence of last interglacial reef development at that location. The possibility that reef growth did occur but has not been preserved due to weathering/erosion (Purdy, 1974) is rarely considered (Partain and Hopley, 1989). Examples of inshore reefs comprised of mixed terrigenous and carbonate material have been preserved in the Pleistocene record on the GBR (Webster and Davies, 2003) and in the longer geological record elsewhere, including in Spain (Martin et al., 1989), England (Insalaco, 1999), and Indonesia (Wilson and Lokier, 2002; Santodomingo et al., 2015), revealing the potential of inshore reefs to have existed prior to the Holocene. In any case, detrital-dominated reefs that are comprised of both carbonate and terrigenous material, such as the Holocene reefs at Bramston Reef, Stone Island and Middle Island, might be more prone to physical disintegration (Smithers and Larcombe, 2003) than those dominated by cemented framework, typical of reefs further offshore (Davies et al., 1985) such as Holbourne Island (~35 km offshore) and Hayman Island (~20 km offshore). Of all reef flats on the GBR, inshore reef flats would be exposed for the longest period of time during glacial episodes due to their location on the shallower inner-shelf, further enhancing the potential for such fossil last interglacial reefs to be weathered and eroded (providing the reefs existed). The records of last interglacial reef from Holbourne Island, presented in Chapter 5, and Hayman Island (Hopley et al., 1978) are two of the most inshore records of last interglacial foundations for the central GBR. New chronostratigraphic investigations of inshore reefs on the GBR in the future will determine whether reefs flourished on the inner-shelf during the last interglacial and if such reefs remain preserved in the geological record.

In general, the depth to the pre-Holocene surface increased and Holocene reef initiation occurred earlier with distance from the coast (Table 6.1). Of all sites, the earliest age of Holocene reef initiation was determined for Middle Island ($7,873 \pm 17$ yBP), closely followed by Holbourne Island ($7,520 \pm 20$ yBP), Stone Island ($7,247 \pm 23$ yBP at SI-S; $7,064 \pm 17$ yBP at SI-N) and later Bramston Reef ($5,396 \pm 51$ yBP). Initiation at all sites, with the exception of Bramston Reef, occurred ~500 – 1,000 years after the PGMT flooded the shelf foundations and these initiation ages are comparable to many fringing reefs of the GBR (average initiation age of 7,100 yBP; Smithers et al., 2006). However, Perry and Smithers (2011) identified a period of reef-building ‘hiatus’ on the inshore GBR, between ~5,500 – 2,300 yBP, for which no known reef initiation occurred. Interestingly, the initiation age from Bramston Reef ($5,396 \pm 51$ yBP) is the first record of reef initiation in the inner GBR during this hiatus period. Although it could be argued that reef initiation may have occurred prior to $5,396 \pm 51$ yBP but was not captured in

my chronostratigraphic record (i.e. preceding the hiatus period identified by Perry and Smithers [2011]), the major period of reef-building at Bramston Reef occurred within the hiatus window (see section 6.2.2 and Figure 6.1). Initiation at Bramston Reef occurred around 2,000 years after the other three sites, notably around 600 years after the reef flats at Middle Island and Holbourne Island had been almost entirely emplaced (Figure 6.1 and Figure 6.2). Thus, the entire period of reef development at Bramston Reef occurred after the majority of reef development occurred at the other sites. The relatively mobile unconsolidated sands and gravels that underlie Bramston Reef, which present a challenging substrate for the coral colonisation and survival necessary for reef growth (Hopley et al., 1983), could plausibly explain the differences in the timing of reef initiation. Indeed, the nature of the underlying foundation has been suggested to control variations in reef initiation timing elsewhere (Cabiocch et al., 1995). The more solid nature of the antecedent surfaces at Middle Island and Holbourne Island would be preferential for coral colonisation by providing a stable substrate for larval recruitment compared with the terrigenous, unconsolidated sediments that underlie Bramston Reef. This also corresponds with the findings of Kleypas and Hopley (1992), who undertook a cross-shelf study of reef development in the southern GBR and found all reefs developed upon solid foundations, with little variation in the timing of reef initiation despite deeper pre-Holocene substrates further offshore.

Alternatively, the lag in reef initiation at Bramston Reef may be related to changing environmental or water quality conditions associated with the 1.0 – 1.5 m relative sea-level fall that occurred after the mid-Holocene highstand, which was reached around 7,000 – 6,000 yBP (Lewis et al., 2013). Sea level in Edgum Bay had commenced falling by around 5,000 yBP at the latest, as indicated by the ages and elevations of open-water fossil microatolls relative to modern counterparts as a sea-level proxy (Appendix 9). This relative sea-level fall may have improved the availability of favourable photosynthetically available radiation (PAR) and thus the potential for coral reef development around this time at Bramston Reef; limited PAR can constrain coral growth in turbid environments (Anthony and Fabricius, 2000). Earlier reef initiation (>7,500 yBP) further offshore at Holbourne and Middle Islands could be a result of earlier flooding of the deeper underlying foundations during the PGMT. However, an exception to the initiation-distance correlation was Middle Island, which exhibited the earliest signs of initiation despite not being the furthest offshore site. The fringing reefs at Stone Island also initiated relatively early (prior to 7,000 yBP) in shallow water depths that are similar to Bramston Reef (~6 m). Thus, I consider that the nature of the foundations and the potential interplay with sea-level fall and turbidity is the most plausible explanation for the ~2,000-year lag in reef initiation at Bramston Reef.

6.2.2 Holocene reef development

Variations were observed along the cross-shelf transect in reef growth mode, reef flat width and geomorphology (Figure 6.2), rates of accretion (Figure 6.3), the timing of reef flat development, palaeo-ecology (Table 6.1), and reef matrix sediment composition (Table 6.2). This section outlines these variations and discusses the relative influences of environmental parameters, including accommodation space, the degree of exposure to high-energy storms/cyclones and the sedimentation regime (Figure 6.2). Sea level has long been recognised as a crucial factor affecting reef growth as it influences accommodation space, timing and location of reef initiation, and reef flat development (Davies et al., 1985; Buddemeier and Smith, 1988; Kennedy and Woodroffe, 2002). While the effects of cyclones on reef development are less well known, reef evolution can be influenced by the degree of exposure of a reef to cyclones and high wave energy (Blanchon and Jones, 1997). Proximity to the mainland coast and more turbid conditions has been related to past reef-building potential (van Woosik and Done, 1997), where the effects of anthropogenic stressors were argued to have reduced coral cover and diversity to a level that would inhibit future reef-building potential.

Reef growth mode and reef flat development

The mode or style of reef development varied between sites along the transect, with growth modes represented by the isochrons in the reef chronostratigraphies (Figure 6.2), which were inferred based on the U-Th ages in the reef cores recovered from each reef and the microatoll ages across the reef flat surfaces. The fringing reefs at Holbourne Island and Middle Island developed under an ‘up and out’ growth style, similar to the classic Darwinian growth mode (Darwin, 1842) or model A in Kennedy and Woodroffe’s (2002) classification of fringing reef development. These reefs accreted vertically to sea level in ‘catch-up’ mode (*sensu* Neumann and MacIntyre, 1985) during the early- to mid-Holocene (~7,800 – 6,500 yBP) with subsequent reef flat progradation occurring within 1,000 – 2,000 years of initiation (Figure 6.2). At SI-N and Bramston Reef, similar reef growth modes were apparent, whereby ‘up and out’ reef development occurred between ~7,000 – 4,500 yBP at SI-N and 5,500 – 4,000 yBP at Bramston Reef, comparable to a fringing reef in Hawaii (Easton and Olson, 1976) and other fringing reefs in the GBR (Hopley et al., 1983; Lewis et al., 2012). At Bramston Reef, once the reef had ‘caught up’ to sea level, seaward reef front progradation occurred from ~3,000 yBP onwards, however this switch in growth mode was not observed at SI-N. At SI-S, however, the reef developed by episodic landward/seaward reef progradation and infilling between ~7,000 – 5,500 yBP, similar to the detached reef coalescence documented at the reef fringing at Yam Island in the Torres Strait (Woodroffe et al., 2000), and comparable with model D in Kennedy and Woodroffe (2002). At SI-S, dated fossil microatolls indicate that reef flat development was

underway by $6,716 \pm 23$ yBP (Table 6.1) and the reef flat was completely emplaced within 1,000 years.

The reefs at Bramston Reef and Stone Island continued to laterally prograde throughout the mid- to late-Holocene (until $\sim 4,000$ yBP at Stone Island and $\sim 1,000$ yBP at Bramston Reef) (Figure 6.2). Although no material aged $< 4,000$ yBP was recovered in cores from Stone Island (Figure 6.1) the inferred reef slope isochrons suggest that ~ 150 m of reef slope progradation occurred during the past 4,000 years; however, this part of the reef did not reach sea level and form a reef flat (Figure 6.2, see Chapter 3). Indeed, rapid late-Holocene reef progradation (over the past 2,000 years) is documented in the cores from Bramston Reef (~ 9.8 mm/yr on average, Figure 6.2, see also Figure 2.3 in Chapter 2) and also at a fringing reef in the Palm Island group, located on the inshore central GBR, where Roff et al. (2015) documented continuous and rapid (8.8 mm/yr on average) reef slope accretion during the past 1,000 years. There are also many examples of nearshore reefs on the inner GBR that initiated and rapidly vertically accreted during the late-Holocene (see Perry and Smithers, 2011). Provided accommodation space (vertical or lateral) was available, reef growth could evidently continue well into the mid- to late-Holocene on the inshore GBR, even though water quality indicators in inshore areas are traditionally but not universally considered marginal for reef growth (Pastorak and Bilyard, 1985; Larcombe and Woolfe, 1999a). In contrast, a deceleration in net reef accretion was observed at sites further offshore (Holbourne Island and Middle Island), where negligible reef accretion occurred over the past $\sim 6,000$ years. Possible reasons for these observed cross-shelf differences in late-Holocene accretion potential are discussed below.

The timing of reef flat development was approximated based on fossil microatoll ages on the reef flat or ages within the upper metre of cores, and these ages indicate that the earliest known time of reef flat development varied according to the reef initiation age and reef accretion rates (Table 6.1). Reef flat development first occurred at Middle Island (by $6,895 \pm 19$ yBP), where the earliest age of initiation was also recovered ($7,873 \pm 17$ yBP). The onset of reef flat development at Bramston Reef and SI-N, however, occurred at least 2,000 years later than at the other locations. Despite differences in the timing of reef flat development, at most sites reef flat development occurred rapidly within around 1,000 – 2,000 years of initiation (Table 6.1). Initial rapid reef accretion towards sea level within a 2,000-year period is common in the GBR (Davies et al., 1985; Smithers et al., 2006). Conditions would have been optimal for vertical reef accretion during rising sea levels (Smithers et al., 2006) between $\sim 8,000$ and 6,500 yBP (Lewis et al., 2013); however, reefs that initiated following sea-level stabilisation at the highstand ($\sim 6,000$ yBP), such as Bramston Reef, also had ample accommodation space to accrete towards sea level within a similar 2,000-year time period. Although reef flat

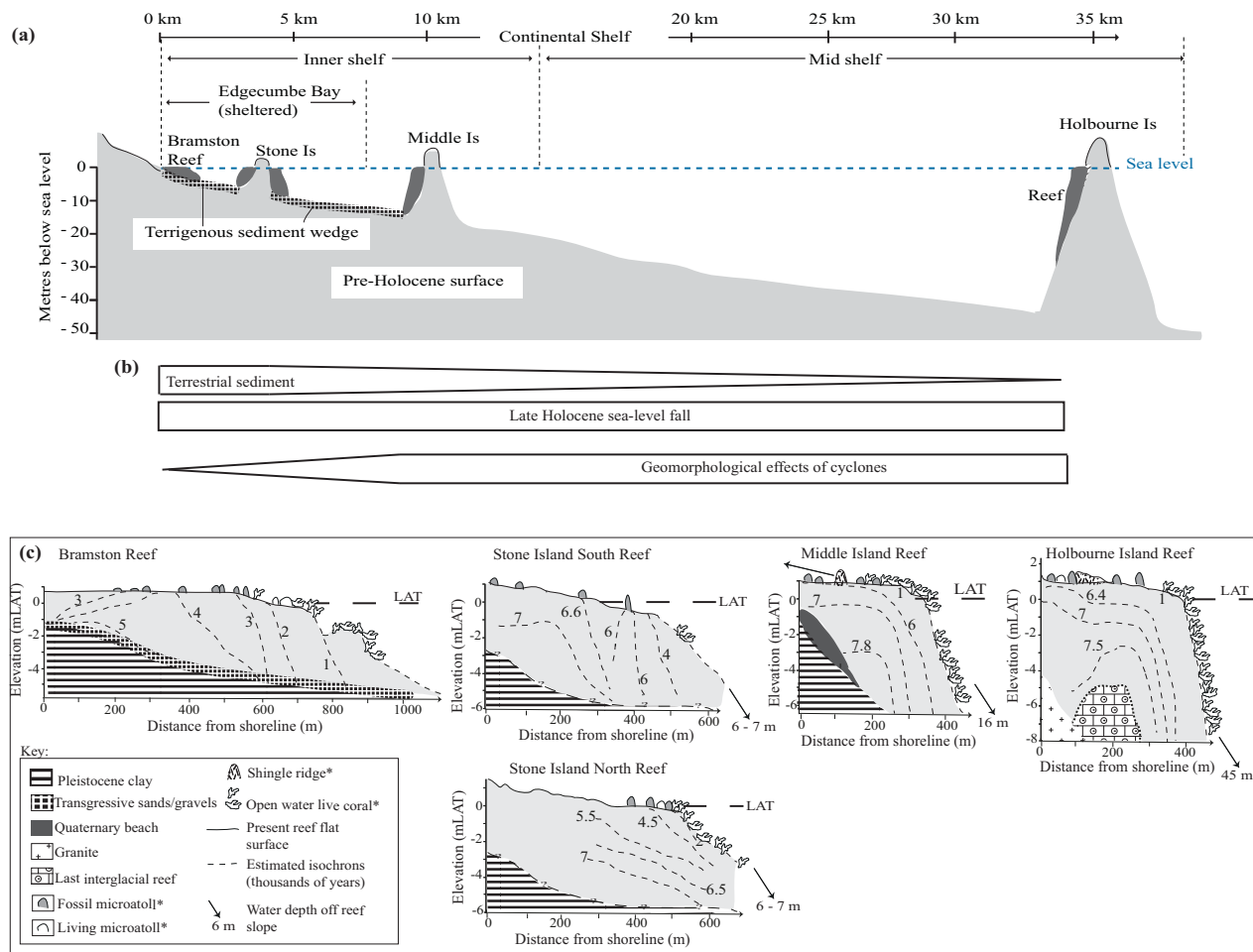


Figure 6.2 Schematic diagrams showing (a) cross-section through the inner- and mid-shelf Great Barrier Reef extending seaward from the coast at Edgecumbe Bay; (b) the cross-shelf relative influence of environmental parameters; and (c) scaled conceptual reef growth models for each site based on the chronostratigraphies present in Chapter 2 (Bramston Reef), Chapter 3 (Stone Island South and North), Chapter 4 (Middle Island) and Chapter 5 (Holbourne Island). Elevations are relative to lowest astronomical tide (LAT). In the key, * denotes where features are not to scale.

Table 6.2 A comparison of average ($\pm 1\sigma$) mud content (<63 microns) and carbonate content (CaCO_3) of the sediment matrix within upper facies (A – B) and lower facies (C – E) in the percussion cores from each study site.

Site	Facies A		Facies B		Facies C		Facies D		Facies E	
	% mud	% CaCO_3	% mud	% CaCO_3	% mud	% CaCO_3	% mud	% CaCO_3	% mud	% CaCO_3
Bramston Reef	14.2 \pm 5.2	56.0 \pm 24.1	17.1 \pm 4.6	73.1 \pm 12.0	32.4 \pm 12.5	63.6 \pm 13.7	53.8 \pm 17.4	55.6 \pm 7.1	41.1 \pm 19.1	47.0 \pm 2.6
Stone Island South	4.2 \pm 2.0	96.9 \pm 2.3	8.6 \pm 4.4	91.7 \pm 8.8	35.9 \pm 12.7	75.4 \pm 7.9	47.8 \pm 13.9	70.5 \pm 9.5	n/a	n/a
Stone Island North	9.6 \pm 5.2	92.7 \pm 2.8	13.5 \pm 7.0	87.4 \pm 6.0	20.7 \pm 5.3	81.7 \pm 9.7	n/a	n/a	n/a	n/a
Middle Island	3.3 \pm 1.0	96.0 \pm 0.5	9.8 \pm 4.4	92.9 \pm 1.9	22.0 \pm 10.2	84.2 \pm 5.4	46.5 \pm 15.6	67.9 \pm 10.2	n/a	n/a
Holbourne Island	2.1 \pm 0.8	97.3 \pm 0.7	6.5 \pm 2.0	97.4 \pm 1.3	18.0 \pm 8.3	92.8 \pm 3.9	n/a	n/a	n/a	n/a

Table 6.3 Descriptions of reef flat ecological/geomorphological condition at each study site. Elevations are relative to lowest astronomical tide (LAT).

Site	Backreef flat general description	Backreef flat typical elevation (mLAT)	Mid reef flat general description	Mid reef flat typical elevation (mLAT)	Outer reef flat general description	Outer reef flat typical elevation (mLAT)	Maximum recorded elevation of open-water coral (mLAT)	Average ($\pm 1\sigma$) elevation (mLAT) of the living rim of open-water <i>Porites</i> microatolls	Average ($\pm 1\sigma$) reef flat coral cover (%) in living coral zone	Coral genera recorded living on the reef flat	Range of average ($\pm 1\sigma$) coral cover values (%) in zones that contain live corals on the reef slope	Coral genera recorded living on the reef slope
Bramston Reef	Sandy substrate colonised by macroalgae and seagrass	0.6	Sandy substrate with macroalgae, seagrass and fossil microatolls	0.5 – 0.2	Sandy substrate with sparse live coral cover	0.2 to -0.5	0.5	0.31 \pm 0.08 (n=8)	13.9 \pm 19.2	<i>Porites</i> , <i>Montipora</i> , <i>Goniastrea</i> , <i>Turbinaria</i> , <i>Acropora</i> , soft corals	3.0 \pm 6.6 to 51.3 \pm 19.4	<i>Acropora</i> , <i>Calaustrea</i> , <i>Dipsastraea</i> , <i>Euphyllia</i> , <i>Fungia</i> , <i>Galaxea</i> , <i>Goniastrea</i> , <i>Goniopora</i> , <i>Montipora</i> , <i>Porites</i> , <i>Seriatopora</i> , <i>Stylophora</i> , <i>Turbinaria</i>

Stone Island South	Sandy substrate colonised by macroalgae, with fossil microatolls	1.0 – 0.7	Sand and rubble substrate with macroalgae and fossil microatolls	0.7 – 0.3	Sandy substrate dominated by macroalgae, with fossil microatolls	0.3 to -0.8	0.5	0.29 ± 0.18 (n=5)	0%*	<i>Porites</i> , <i>Acropora</i>	33.3 ± 21.1	<i>Acropora</i> , <i>Pocillopora</i> , un-identified massive coral
Stone Island North	Sandy substrate with sparse macroalgae	1.3 – 0.8	Sandy substrate	0.8 – 0.6	Sandy substrate dominated by macroalgae, with fossil microatolls	0.6 to -0.2	0.5	0.46 ± 0.1 (n=2)	0%*	<i>Porites</i>	18.5 ± 23.7 to 46.0 ± 36.2	<i>Acropora</i> , <i>Montipora</i> , <i>Turbinaria</i> , <i>Fungia</i> , <i>Favites</i> , <i>Pocillopora</i> , <i>Platygyra</i> , soft corals
Middle Island	Sand and rubble substrate with fossil microatolls (most were moated in the past) and macroalgae. Basset edges present.	1.0	Sandy substrate with rubble	1.0 – 0.6	Live coral dominant	0.6 – 0.0	0.8	0.34 ± 0.06 (n=8)	47.5 ± 28.2 (transect MI-1) 63.1 ± 20.2 (transect MI-2)	<i>Porites</i> , <i>Montipora</i> , <i>Goniastrea</i> , <i>Acropora</i> , <i>Pocillopora</i> , <i>Dipsastraea</i> , soft corals	2.0 ± 5.6 to 100.0 ± 0.0	<i>Acropora</i> , <i>Platygyra</i> , <i>Galaxea</i> , <i>Goniopora</i> , <i>Leptoseris</i> , soft corals, un-identified encrusting and foliaceous corals
Holbourne Island	Moated area with fossil and living microatolls, sand and rubble substrate. Coral shingle ridges present.	1.0	Sandy algal turf, with small live corals. Basset edges present.	0.8 – 0.5	Live coral zone with sand and rubble substrate	0.5 – 0.0	0.64	0.37 ± 0.04 (n=10)	27.7 ± 7.4 (transect 1) 38.1 ± 32.0 (transect 2) 7.1 ± 15.9 (transect 3)	<i>Porites</i> , <i>Montipora</i> , <i>Goniastrea</i> , <i>Acropora</i> , <i>Favites</i> , <i>Platygyra</i> , soft corals	47.6 ± 38.1 to 74.0 ± 22.4	<i>Acropora</i> , <i>Montipora</i> , <i>Fungia</i> , <i>Porites</i> , <i>Stylophora</i> , <i>Turbinaria</i>

* Denotes that no live corals were recorded in the benthic surveys of the transect(s), however small living corals and microatolls were occasionally encountered elsewhere on the reef flat.

development began last at Bramston Reef ($4,256 \pm 14$ yBP), the widest reef flat has developed at this most inshore location (900 m wide) (Table 6.1). The reef flats further offshore are generally narrower (440 and 330 m wide at Holbourne Island and Middle Island, respectively), but prograde into deeper water (16 – 45 m) than those inshore ($\sim 6 - 7$ m) (Table 6.1).

The differences in reef growth styles and resulting reef flat width and morphology over the cross-shelf transect may be influenced by two main factors: the underlying substrate and the energy setting. The depth and shape of the underlying substrate is a key factor influencing available accommodation space for reef development (Smithers et al., 2006). The underlying pre-reefal substrates in inner Edgecumbe Bay are shallow (6 – 7 m) and gently sloping, providing extended lateral accommodation space for wider reef flat development (up to 900 m at Bramston Reef) compared to the steep foundations surrounding Holbourne (~ 45 m [Hopley, 1975]) and Middle Islands (16 m) (Figure 6.2). The deeper, steep foundations underlying Holbourne and Middle Island reefs may present difficulties for seaward reef progradation. However, vertical accommodation space on the inner-shelf would be comparatively limited because of the shallow depths and the lower effective PAR depth (i.e. higher turbidity) for coral growth (Partain and Hopley, 1989).

The second factor that may influence reef growth style and reef flat width is the degree of exposure to high-energy events, which varies across the transect. Generally, the GBR inner-shelf is dominated by low-energy wind-generated waves (<7 s period) (Larcombe et al., 1995b; Hopley et al., 2007). Significant wave height at Abbot Point and Bowen (see Figure 4.1a in Chapter 4 for location of Abbot Point) is typically <1.0 m (Queensland Government, 1997; Orpin et al., 1999). However, during cyclones higher swell waves (>7 s wave period) may occur at Abbot Point, with a maximum recorded wave height of 5.96 m between 1977 and 1996 (Queensland Government, 1997). According to Orpin et al. (1999), swell waves (7 – 9 s period) that are >1.5 m only occur ~ 1 day/year in the inshore Bowen region. The physical effects of high wave energy during cyclones on coral reefs are well documented (Hubbard et al., 1991; Scoffin, 1993). The export of carbonate material from reefs, which can occur during cyclones, can be important for net reef accretion (Kleypas et al., 2001), as can the accumulation of detrital storm debris within a reef structure (Blanchon and Jones, 1997; Blanchon et al., 1997; Braithwaite et al., 2000). Higher export rates may characterise the further offshore sites, where large age gaps in the chronostratigraphies of Middle Island reef (5,000-year age gap) and Holbourne Island reef (3,500-year age gap) are attributed to stripping of reef framework during intense cyclones. Similar age gaps were not observed in the chronostratigraphies of the reefs at Stone Island or Bramston Reef (Figure 6.2). The age gaps reaching 5,000 years were attributed to cyclones stripping the upper and outer reef flats and slopes during the mid-Holocene (see

Chapters 4 and 5 for detailed discussions). It was argued that a considerable amount of coral framework material was stripped and re-distributed on the reef flat, transported offshore or downslope, or deposited onshore in the form of shingle ridges. This process of cyclone stripping occurred several times between 5,000 and 1,000 yBP, as indicated by several shingle ridge deposits on the same shoreline (Chapter 4). This has important implications for chronostratigraphic and palaeo-ecological studies of fringing reefs, whereby gaps in the palaeo-ecological or chronostratigraphic record do not necessarily mean that no coral growth or reef accretion occurred during this time. Researchers must consider the possibility that material could be stripped from the reef structure many times over the Holocene, even in settings that may appear relatively sheltered (i.e. Middle Island fringing reef is semi-sheltered from prevailing south-easterly swells by Gloucester Island; Figure 4.1, Chapter 4).

Combined with the influence of steep underlying foundations, the greater influence of cyclones inferred for the development of the fringing reefs at Middle and Holbourne Islands may have contributed to the formation of narrower reef flats (<440 m wide) at these sites by removing framework, and ultimately reducing net reef accretion, as observed for an export-dominated reef at the island of St Croix (Hubbard et al., 1990). While cyclones cause physical damage in the short-term (Done, 1992; Scoffin, 1993), my long-term core data from Middle Island show that cyclone stripping may create accommodation space for renewed coral growth on longer timeframes (see Chapter 4 for details). Any fringing reef accretion during the late-Holocene located at and beyond the inner/mid-shelf margin has been restricted to a thin (<1.5 m) veneer of growth upon the mid-Holocene reef structure (Figure 6.2) and has not been sufficient to create net reef accretion comparable to the early stages of reef development. Lower export rates are inferred for the inshore sites (Bramston Reef and Stone Island) due to their locations in more sheltered environments and the higher amounts of fine muddy sediments incorporated in the reef matrix (up to $53.8 \pm 17.4\%$ [mean $\pm 1\sigma$]), which is further discussed below (see '*Reef matrix sediments and reef accretion rates*').

Reef matrix sediments and reef accretion rates

The cross-shelf energy and export gradients are also reflected in the composition of the internal reef structure and matrix. The reef matrix sediments within cores from the offshore sites contained much less mud content (highest amounts of the <63 micron [μm] fraction averaged $18.0 \pm 8.3\%$ in facies C at Holbourne Island) compared to the inshore sites (<63 μm fraction $47.8 \pm 13.9\%$ and $53.8 \pm 17.4\%$ in facies D at SI-S and Bramston Reef, respectively) (Table 6.2). The reef sediment matrix throughout the cores from Middle and Holbourne Islands was

dominated by carbonate sediments, with terrigenous fractions of $4.0 \pm 0.5 - 32.1 \pm 10.2\%$ at Middle Island and $2.6 \pm 1.3 - 7.2 \pm 3.9\%$ at Holbourne Island (Table 6.2). In comparison, cores from the inshore reefs contained higher terrigenous sediment fractions (up to 53.0 ± 2.6 and $29.5 \pm 9.5\%$ at Bramston Reef and SI-S, respectively). Acid digestions revealed that terrigenous sediments were the dominant component of the $<63 \mu\text{m}$ (mud) fraction within cores from inner Edgcumbe Bay (see Chapter 2). The accumulation of sediment containing high proportions of terrigenous mud within the reef structure at Stone Island reefs and Bramston Reef indicates that these inshore sites are characterised by low export, as fine terrigenous sediment is able to settle and remain within the reef structure (Perry et al., 2012). The deposition of fine sediments may reduce the destructive effects of biological and physical erosion (Hayward, 1982; Perry and Smithers, 2006), enhancing preservation of reef framework and potentially enhancing vertical accretion rates (Tudhope and Scoffin, 1994). However, at all sites the reef matrix sediments generally coarsened upward, which indicates that export of fine sediments (due to hydrodynamics [Wolanski et al., 2005]) can occur as the reef shallows towards sea level (Perry et al., 2011). Thus, only the subtidal reef slopes below the wave base (below 5 m depth, according to Wolanski et al. [2005]) are characterised by low export and high mud deposition.

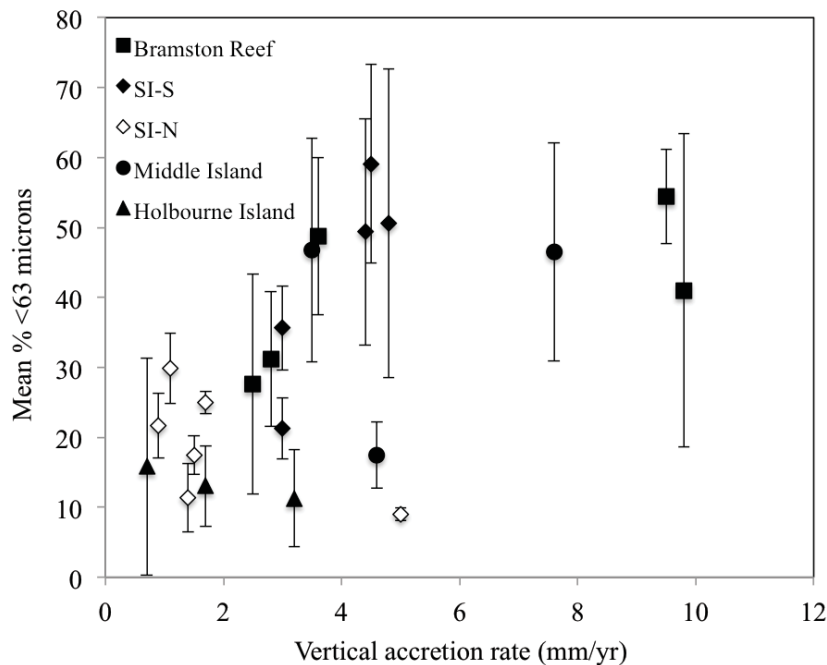


Figure 6.3 Estimated vertical reef accretion rates (based on uranium-thorium ages of coral material within reef cores) and the mean mud content ($<63 \mu\text{m}$) of the sediment that contributed to the reef matrix during the time period for which each growth rate was estimated. Vertical error bars show one standard deviation for the mud content. SI-S is Stone Island South reef and SI-N is Stone Island North reef.

Average vertical reef accretion rates across all sites varied between 0.3 – 9.8 mm/yr, which are considered relatively normal for fringing reefs, where vertical accretion rates between 2 – 7 mm/yr are commonly reported (Kennedy and Woodroffe, 2002). Vertical accretion rates were highest (up to 9.8 mm/yr) at Bramston Reef and were comparatively low at SI-N (generally 0.9 – 1.7 mm/yr) and Holbourne Island (0.7 – 3.2 mm/yr) (Table 6.1). In general, higher vertical accretion rates were associated with higher mud content of the reef matrix sediments (Figure 6.3). Accretion rates >4 mm/yr typically coincided with muddy sediment facies, where mud content of the reef matrix sediments was >40% (Figure 6.3), and is largely comprised of terrigenous sediment. At sites where the reef matrix sediments contained lower proportions of mud (<30 – 20% at SI-N and Holbourne Island), accretion rates were typically <4 mm/yr and terrigenous sediment input also was lower (<7 – 18%) (Table 6.2). This finding accords with the results of Cabioch et al. (1995) who reported that the reefs located in more protected settings in New Caledonia had the highest vertical reef accretion rates. Cabioch et al. (1995) also found that rapid vertical accretion rates generally coincided with early stages of reef development in the early-Holocene, typical of ‘catch-up’ reefs (Neumann and MacIntyre, 1985). A similar pattern was observed in my data from SI-S, Middle Island and Holbourne Island, where the highest vertical accretion rates corresponded to the early stages of reef development (Figure 6.4). This pattern is common for fringing reefs of the GBR (Smithers et al., 2006). However, the data from Bramston Reef did not conform to this trend; rather the highest vertical accretion rates (~10 mm/yr) occurred between 3,000 and 1,000 yBP, even though the majority of Bramston Reef flat was emplaced by this time (Figure 6.2, Table 6.1). Notably, these rates from Bramston Reef were also the highest rates recorded along the entire cross-shelf transect, but during the late-Holocene Bramston Reef was prograding seaward over shallow foundations and this must be considered when comparing accretion rates of further offshore fringing reefs, which were forced to prograde into much deeper water. Nevertheless, this finding highlights the ability of a shore-attached inshore reef slope in a sheltered bay setting to grow rapidly during the late-Holocene, despite most of the reef flat structure being emplaced by 3,000 yBP. Rapid net accretion rates at Bramston Reef in the later stages of reef development may be partly a result of high terrigenous sedimentation between 3,000 and 1,000 yBP, indicated by average mud content >50% in reef facies, including a terrigenous mud-rich unit ~60 cm thick in PC7, which lacks coral clasts (see section 2.5.3 in Chapter 2).

Palaeo-ecology

In this section, I explore the relationship between distance across the shelf and the results of palaeo-ecological analyses of coral material in the cores. Pandolfi and Minchin (1996) found that coral death assemblages at low-energy sites (compared with high-energy sites) more

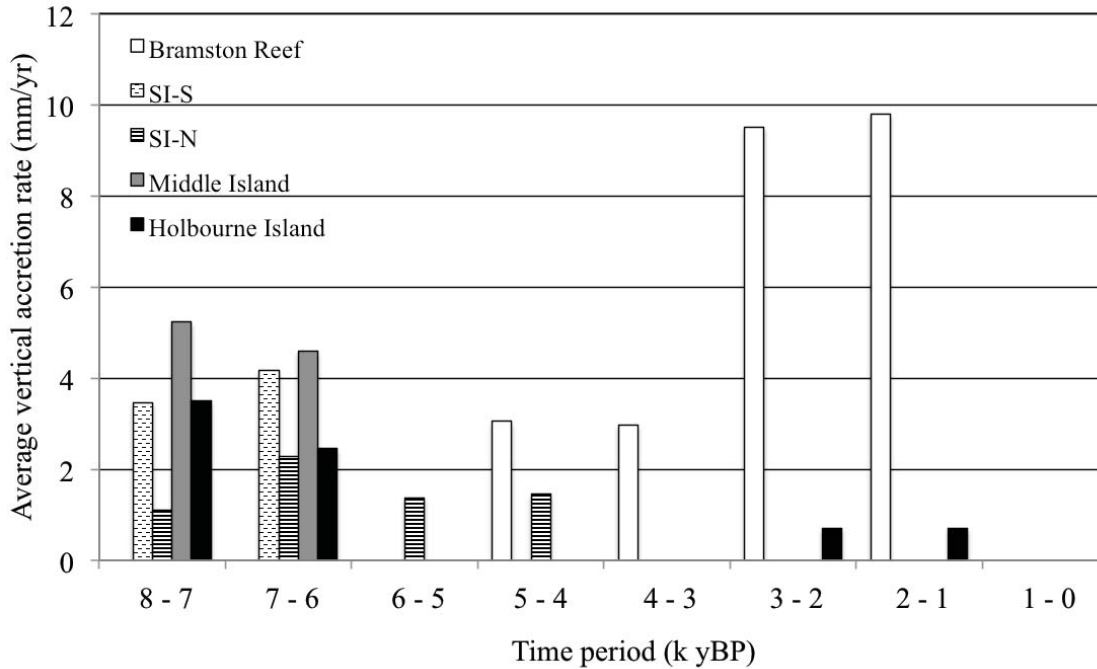


Figure 6.4 Average vertical accretion rates (estimated based on uranium-thorium ages of coral material within reef cores) for each reef over time. Time is grouped into thousands of years before present (k yBP) where present is 1950 AD. SI-S is Stone Island South and SI-N is Stone Island North.

accurately represented the taxonomic composition of living coral communities. Comparing palaeo-ecological results from Chapters 2 – 5 reveals that inshore reefs contained the highest coral palaeo-community diversity (e.g. 25 different genera identified at Bramston Reef compared with 15 at Middle Island; Table 6.1). However, cores from Middle and Holbourne Islands contained high amounts of coral rubble (e.g. 56 – 82% branching rubble at Middle Island, see Chapter 4), consistent with descriptions of storm-deposited detrital material (Blanchon et al., 1997; Perry, 2001). This rubble material was heavily encrusted with coralline algae and this, along with bioerosion traces, indicates that the rubble was at or near the surface for some time and was transported rather than *in situ* material. The higher palaeo-ecological coral diversity found in cores collected from inshore sites is likely a reflection of the superior preservation of the coral material at low-energy, sheltered inshore locations rather than actual differences in coral palaeo-diversity. Indeed, coral clasts were better preserved in cores from Bramston Reef and SI-S, where excellent preservation of corallites and fine skeletal structure allowed for much easier post-mortem identification of coral clasts compared with the cores from Middle and Holbourne Islands. Fine sediments that are deposited on the reef can bury reef framework, and if rapidly deposited (indicated by excellent corallite preservation [Perry and Smithers, 2006]), can reduce the effects of coral skeletal destruction due to physical and biological erosion (Hayward, 1982; Perry et al., 2012). The high mud content (averages up to

47.8 ± 13.9 – 53.8 ± 17.4%) contained in reef matrix sediments at Bramston Reef and SI-S seems to contribute to excellent preservation of coral skeletal material. This finding suggests that palaeo-ecological records from inshore reefs in relatively low-energy, protected settings (where sedimentation is relatively high) may provide more accurate information on past coral diversity than comparable records from reefs further offshore, which lack high amounts (>40%) of muddy terrigenous sediment and are more prone to export/re-working of coral material.

6.3 Contemporary reef ecology and geomorphology – cross-shelf variations

An understanding of how coral reefs in Edgcumbe Bay developed and were influenced by natural stressors over the Holocene is required to evaluate the significance of reported declines in reef condition since European settlement (Wachenfeld, 1997; Hughes et al., 2010; Clark et al., 2016). However, there is a temporal mismatch between long-term reef core records (millennial-scale), historical records (centennial-scale) and quantitative ecological data (decadal-scale) (Kittinger et al., 2011; Thurstan et al., 2015), highlighted in Figure 6.1. This mismatch means that it becomes difficult to assess the influence of natural variability in coral cover and reef recovery rates (Pandolfi and Kiessling, 2014), which may be very different for inshore reefs compared to their further offshore counterparts (Done et al., 2007). Indeed, the majority of U-Th or radiocarbon ages from the fringing reefs along the cross-shelf transect (derived from corals in reef cores and fossil microatolls on the reef flat surface) are older than 2,000 yBP, if not much older (Figure 6.1). This excludes ages derived from moated fossil microatolls (<600 yBP) that grew on a much older reef flat surface (the significance of these moated fossil microatolls is discussed in section “*Reef flat geomorphology - the influence of cyclones*”). Figure 6.1 illustrates that the main period of reef accretion at all sites, including reef flat development, occurred prior to 2,000 yBP and negligible reef accretion has occurred since, as discussed earlier in this chapter (see section 6.2.2). Notably, all reefs were substantially emplaced well before European settlement of Bowen and surrounding catchments ~1860 AD, and were in a low accretion stage long before the records of reef condition captured in historical photographs or contemporary datasets were collected (Figure 6.1).

Thus, although the historical images of Bramston Reef and Stone Island depict outer reef flats with high coral cover and structural diversity in the late 1800s (Saville-Kent, 1893), reef core records indicate that these communities were veneers of coral growth that did not contribute to net reef accretion for several millennia prior to European settlement. Indeed, this is the case for many inshore fringing reefs in the GBR (Smithers et al., 2006; Perry and Smithers, 2011), but long-term reef development histories are rarely considered in assessments of present reef condition, perhaps because long-term data provides too coarse a temporal scale relevant to the

management of reef ecosystems (Pandolfi and Kiessling, 2014). Yet long-term core records can provide a wealth of baseline information about past reef accretion and the timing of reef flat development (Smithers et al., 2006) to contextualise present reef condition and consider future reef trajectories. For example, van Woesik et al. (1999) interpreted that some fringing reefs in the Whitsunday Island group were no longer actively accreting, which they linked to water quality changes since European settlement without any supportive long-term chronological data of reef development. My long-term core data from Middle Island and Stone Island (which are located ~50 – 80 km north of van Woesik et al.'s [1999] sites) reveal that major net reef accretion ceased prior to 4,000 yBP and this reduction in net growth was entirely driven by natural factors (Figure 6.1). Clearly there is a need for a thorough chronostratigraphic examination of van Woesik et al.'s (1999) sites to quantify when reef accretion stalled.

The results of contemporary benthic ecological surveys at each reef (presented in Chapters 2, 3, 4 and 5 and summarised in Table 6.3) revealed variations in present reef condition (reef flat elevation, ecological zonation, and live coral cover) along the cross-shelf transect. These variations are discussed below, along with how the nature of past reef development may have influenced present reef eco-geomorphological zonation. Finally, I consider whether major changes in reef condition have occurred since European settlement, using all presently available data sources (core records, historical records and photographs, and quantitative ecological data), which span multiple timescales.

Reef flat ecological zonation – the influence of past sea level

The backreef surfaces at Holbourne, Middle and Stone Islands were elevated ~1.0 m above lowest astronomical tide (LAT), but at Bramston Reef it was lower at ~0.6 mLAT (Table 6.1). These backreef zones are sub-aerially exposed during low tidal stages today, when the tides fall below mean low water neap (1.3 mLAT) at Holbourne, Middle and Stone Islands, or below mean low water spring (MLWS) level (0.67 mLAT) at Bramston Reef. Higher backreef flats that are exposed at low tides are a common feature of many fringing reefs in the GBR (Hopley et al., 1983; Perry and Smithers, 2010; Lewis et al., 2012) and are usually the result of reef flat development occurring under higher mid-Holocene sea levels (Smithers et al., 2006). Subsequent relative sea-level fall, which occurred between ~5,000 yBP and present (Lewis et al., 2013), has resulted in reef flat exposure during low tides today (Smithers et al., 2006). Indeed, the elevations of fossil microatoll data from Bramston Reef and Stone Island (Appendix 9), indicate that sea level in Edgecumbe Bay began to fall from the +1.0 m highstand around 5,000 yBP and was near the present level by ~2,000 yBP. This finding is consistent with sea-level data for the entire GBR region (Lewis et al., 2013) and for the southern GBR (Harris et

al., 2015), confirming that the elevated backreef zones on the reef flats at Middle and Stone Islands were developed during the highstand (reef flat development at these sites occurred between ~7,000 – 6,000 yBP; Table 6.1, Figure 6.1). Bramston Reef accreted vertically and reached the sea surface by $4,256 \pm 14$ yBP (indicated by a U-Th age from a fossil microatoll on the reef flat surface; Table 6.1) at which time sea-level fall from the highstand towards the present level had commenced (Appendix 9, Lewis et al., 2013), explaining the lower elevation of the emergent backreef at Bramston Reef. The fact that reef emplacement at all sites occurred during periods of higher sea level (+1.0 – 0.6 m) has important implications for interpretations of present reef condition, which are discussed below.

The backreef surfaces are currently too high to support open-water coral growth, which on reef flats of the GBR is generally restricted to below the MLWS tide level (Davies and Montaggioni, 1985; Hopley and Barnes, 1985; Hopley et al., 2007), which equates to 0.67 mLAT in Edgumbe Bay. Considering this MLWS level of 0.67 mLAT and that the elevation of the backreef zone at Bramston Reef is ~0.6 mLAT, it could be expected that the entire Bramston Reef flat, the surface of which is entirely elevation below MLWS, could support live coral cover. However, the maximum elevation for coral growth may be lower on some inshore reefs, such as Bramston Reef, than others. The surfaces of nearshore reef flats (or shoals) on the inshore GBR with high coral cover, for which relatively precise elevation data are known, are generally elevated <0.3 mLAT (Browne et al., 2010; Perry et al., 2014). Indeed, the elevation below which live corals on the reef flat were surveyed in this study was lowest at the inshore sites (0.5 mLAT) compared with further offshore at Middle Island (0.8 mLAT) and Holbourne Island (0.6 mLAT) (Table 6.3). Furthermore, the average elevation of the living rims of *Porites* microatolls (open-water) was slightly lower at the turbid, inshore sites (Bramston Reef; 0.31 mLAT and SI-S; 0.29 mLAT) compared with further offshore in less turbid environments (Holbourne Island; 0.37 mLAT) (Table 6.3). Although these differences in microatoll elevation are relatively small (<0.1 m), these data provide some of the most precise elevations (typically 0.01 – 0.005 m vertical error) of microatoll upper surfaces on the GBR to date. The living rims of *Porites* microatolls on the GBR and elsewhere has been shown to approximate within ~10 cm of MLWS tide level (Chappell et al., 1983; Hopley and Isdale, 1977; Smithers and Woodroffe, 2000) (MLWS is 0.67 mLAT in Edgumbe Bay). My precise elevation data (Table 6.3) show that on the inner- to mid-shelf in this region of the central GBR, this level is lower than previously considered; averaging 0.21 – 0.38 m below MLWS. The reduced upper limit of *Porites* microatoll growth may be related to the calm wave climate of Edgumbe Bay, where wave energy is generally restricted to small (significant wave height <1.0 m) wind waves (Orpin et al., 1999). Additional high precision elevation data are required from a range of

environments throughout the GBR to better constrain the upper limit of *Porites* microatoll growth.

At all sites the backreef flat was dominated by sediment/coral rubble and macroalgae (with the exception of Holbourne Island where macroalgae was scarce) (Table 6.3). This area typically comprised the shoreward 150 – 300 m of each reef flat between 1.3 and 0.6 mLAT (Table 6.3). This dominance of macroalgae and/or sediment on mid-Holocene backreef flats at all sites is a common feature on the GBR (Hopley et al., 2007) and may be a naturally-occurring consequence of past sea-level fall exposing elevated backreef areas (Hopley and Barnes, 1985). However, baseline natural levels of macroalgae on reefs are not well understood (Bruno et al., 2014). High macroalgae cover has been documented on reefs that are exposed to minimal freshwater runoff and direct human impacts (Johansson et al., 2014), while other researchers contend that human-related eutrophic conditions have elevated macroalgae cover on inshore reefs (Fabricius, 2005; De'ath and Fabricius, 2010). Nevertheless, understanding how past sea-level changes influenced reef development histories (and thus reef flat elevation) becomes particularly important for the inshore sites in Edgecumbe Bay, where conclusions about reef condition are based on comparisons between modern and historical photographs of the SI-S reef flat that are not properly referenced with high spatial and elevation accuracy (e.g. Wachenfeld, 1997; Hughes et al., 2010; Bell et al., 2014, see Chapter 3 for a more detailed discussion of this issue). Some of these photographs may be of the elevated (1.0 – 0.8 mLAT) and old (~6,000 yBP) backreef zone.

Ecological surveys of benthic cover at each reef revealed live (open-water) corals growing on the outer reef flat and reef slope, with differences in coral cover between sites along the cross-shelf transect. Generally, reef flat live coral cover was highest at the further offshore sites (the outer reef flat live coral cover averaged 38.1 ± 32.0 , 63.1 ± 20.2 , 0 and $13.9 \pm 19.2\%$ at Holbourne Island, Middle Island, Stone Island and Bramston Reef, respectively, Table 6.3). Clark et al. (2016) conducted ecological surveys at Bramston Reef and Stone Island in 2012 and presented similar results of live coral cover (7.0 ± 4.7 and $0.09 \pm 0.12\%$ at Bramston Reef and Stone Island, respectively). The reef flat live coral cover surveyed at Middle Island (reaching an average of $63.1 \pm 20.2\%$) and Holbourne Island (up to $38.1 \pm 32.0\%$) is comparable to, if not much higher than, other published values for inshore reef flats in the GBR (e.g. ~35% [Perry et al., 2009]; ~7% [Browne et al., 2010]; 5 – 33% [Bull, 1982]) and inshore reef slopes (30 – 40% [Thompson et al., 2013]). Increases in live coral cover with distance from the mainland have been documented on the GBR and are usually related to the detrimental effects of higher sediment and nutrient loads further inshore (van Woosik and Done, 1997; van Woosik et al., 1999; Fabricius et al., 2005; DeVantier et al., 2006). While a similar pattern was observed in

this study for reef flat coral cover, the inshore reef slopes displayed high (but patchy) live coral cover, with mean cover ranging from 3.0 ± 6.6 to $51.3 \pm 19.4\%$ at Bramston Reef, 18.5 ± 23.7 to $46.0 \pm 36.2\%$ at SI-N, and 2.0 ± 5.6 to 100% at Middle Island (Table 6.3). DeVantier et al. (1998) measured similar patchiness and coral cover on the Middle Island reef slope in 1994 – 1995, where they characterised the upper slope as below average hard coral cover, but the lower slope as above average hard coral cover. This finding of high coral cover on the Bramston Reef and SI-N reef slopes supports a growing number of studies that show healthy reef growth is possible in turbid inshore regions (Browne et al., 2010, 2012; Perry et al., 2012; Roff et al., 2015), despite their locations typically being considered marginal for healthy reef growth (Rogers, 1990; Fabricius, 2005). In particular, high coral cover documented at Bramston Reef emphasises that inshore reefs can flourish even in sheltered bay settings, where terrestrial sedimentation has been high throughout the Holocene (refer to section 6.2.2) and water circulation may be poor (Andutta et al., 2013; Brodie et al., 2014).

Reef flat geomorphology - the influence of cyclones

Cyclones largely influenced reef flat zonation and geomorphology at Holbourne and Middle Island fringing reefs. Fringing reef flats located in exposed settings have been shown to exhibit more distinct zonation compared with reefs in more protected environments (Hopley and Barnes, 1985). Early researchers noted the effects of cyclones at Holbourne Island and Middle Island (Agassiz, 1898; Rainford, 1925; Hopley, 1975; Hopley and Isdale, 1977). Indeed the ecological and topographic surveys undertaken in my study indicated that of all sites, the most exposed and further offshore sites (Holbourne and Middle Islands) displayed more pronounced geomorphological evidence of storms/cyclones (e.g. shingle ridges on the reef flat at Holbourne Island, and shingle ridges onshore and basset edges at both sites) (Table 6.3). Ecological zonation was most distinct at Holbourne Island, where areas of the backreef flat were moated at low tidal stages with water 10 – 40 cm deep allowing *Porites* microatolls to grow in the moated pools up to elevation 0.57 – 0.94 m above the average elevation of their modern open-water counterparts (Table 6.3, see also Chapter 5, section 5.5.2).

The majority of fossil microatoll ages from Holbourne and Middle Islands were young; between 1361 and 1984 AD (Figure 6.1) and the corresponding elevations indicate they were moated at the time they were alive (see Chapters 5 and 6 for details). This reveals that cyclones have actively modified the reef flat ecology and geomorphology for at least the past 600 years at Holbourne Island and 250 years at Middle Island. If microatoll data of appropriate ages (mid- to late-Holocene) from open-water (not moated) microatolls were collected at Middle and Holbourne Islands, that data could be compared with the open-water fossil microatoll data from

Bramston Reef and Stone Island (Appendix 9) to examine cross-shelf sea-level patterns (Scoffin and Stoddart, 1978; Chappell et al., 1983). However, the greater exposure of Middle and Holbourne Islands to storms and cyclones means that regular ponding on the reef flat (due to shingle ridge emplacement) occurs at these sites, resulting in the dominance of moated microatoll data. This made it difficult to draw firm conclusions about differences in hydro-isostatic adjustments across the inner- to mid-shelf, which may be more pronounced on the inner-shelf (Chappell et al., 1982; Lambeck and Nakada, 1990). Indeed, the total of 26 young ages obtained from moated fossil microatolls on the reef flats at Middle and Holbourne Islands (Appendix 2 and 7) indicate the importance of considering the effects of moating where past sea-level reconstructions are based on fossil microatoll data.

Changes in reef condition since European settlement

Degradation of reef condition (i.e. declines in live coral cover and structural diversity) at Stone Island since European settlement ~1860 AD is widely reported (Wachenfeld, 1997; Hughes et al., 2010; Bell et al., 2014; Clark et al., 2016), and widely presented as demonstrative of anthropogenically-driven changes in reef condition more broadly in the inshore GBR. Changes in reef condition since European settlement (for all Edgumbe Bay sites) based on information about coral cover and structural diversity from a range of qualitative and quantitative sources are schematically shown in Figure 6.1b, including: historical accounts (Saville-Kent, 1893; Agassiz, 1898; Hedley, 1925; Marshall et al., 1925; Rainford, 1925; Stanley, 1928; Steers, 1937; Richards, 1938; Stephenson et al., 1953; Hopley, 1975); historical photographs (Saville-Kent, 1893; Agassiz, 1898); contemporary ecological surveys (DeVantier et al., 1998; Clark et al., 2016; this thesis); and contemporary photographs (Wachenfeld, 1997; Clark et al., 2016; this thesis). While the data in Figure 6.1b are not precise indicators of coral cover due to the nature of the data sources, they do highlight that temporal gaps of 7 – 100 years exist in the ecological records that are available for each site (denoted by question marks in Figure 6.1b). These gaps, along with the paucity of quantitative ecological data since European settlement at these sites (DeVantier et al., 1998; Clark et al., 2016), means that robust conclusions about changes in reef condition and recovery rates cannot be made. However, at all sites (with the exception of Bramston Reef), historical records depict the complete loss of coral cover on the reef flats, associated with freshwater plumes during cyclones that occurred in 1918 (Hedley, 1925; Marshall et al., 1925; Rainford, 1925). However, Stone Island was the only site along the cross-shelf transect that displayed negligible reef flat coral cover in contemporary surveys (Table 6.3, see also Clark et al., 2016). Indeed, live coral cover was high at the Middle Island reef flat ($63.1 \pm 20.2\%$) and parts of the reef slopes at SI-N ($46.0 \pm 36.2\%$) and Bramston Reef ($51.3 \pm 19.4\%$). Potential reasons for these disparities were outlined in Chapter 3 (see section

3.6.2), where it was concluded that local, site-specific factors were most likely responsible for the poor coral cover at SI-S.

An interesting feature of the inshore reef flats and slopes in Edgcumbe Bay was the patchiness (or spatial inconsistency) of coral cover (see photographs of Bramston Reef in Appendix 1). Contemporary photographs of Bramston Reef (in Appendix 1) were taken less than two years apart (in 2012 [Clark et al., 2016] and 2013/2014), during which time no major disturbance events impacted this region. The two sets of photographs were taken around 900 m alongshore from each other, both on the outer reef flat, but depict a markedly different reef condition. The photographs presented in Clark et al. (2016) show a dominance of dead *in situ* hard corals, while my photographs show live hard and soft coral cover and structural diversity similar to that described and photographed by Saville-Kent (1893) (Chapter 2). Whether this patchiness is a normal (baseline) characteristic of inshore reefs is unknown due to the limited and temporally punctuated data available, however, continual ecological surveys in future work using consistent methods at these inshore sites will provide insights into the patchiness and recovery potential of inshore reefs. There is no doubt that humans have elevated sediment and nutrient loads to the inshore GBR (Kroon et al., 2012; Waters et al., 2014). However, my findings have stressed the value of understanding temporal (including long-term) and spatial variability in reef growth and condition to contextualise present reef condition where human impacts are implicated. The millennial-scale records derived from reef cores at inshore sites in Edgcumbe Bay demonstrates that these reef ecosystems have always been exposed to (and have recovered from) episodic cyclones and sedimentation (Figure 6.1).

7 Conclusions

7.1 Summary of research findings and future directions

The overarching aim of this research was to investigate reef development in detail at four fringing reef locations distributed along a cross-shelf transect extending from the mainland to the mid-shelf in the central Great Barrier Reef (GBR). Reef cores combined with high-precision uranium-thorium (U-Th) ages (mean age error 19 ± 12 years) of coral material were used in conjunction with high-precision elevation data (horizontal and vertical precision typically 0.01 – 0.005 m) to reconstruct the chronostratigraphies of five fringing reefs. The fringing reefs were located at: Bramston Reef; Stone Island South (SI-S); Stone Island North (SI-N); Middle Island; and Holbourne Island. Holocene reef initiation, modes and rates of accretion, palaeo-ecology and past sediment regimes were examined, contributing insights to the baseline knowledge of reef growth, condition and variability. The present ecological benthic cover at each reef was quantified and contextualised in terms of Holocene reef development and historical (centennial-scale) changes. This research provides new knowledge about fringing reef systems on the GBR that can be applied to other reef systems globally, and also revealed knowledge gaps to be addressed in future research.

The five key objectives of this research and associated conclusions and future directions are outlined below:

Objective 1: To determine the timing and location of reef initiation over the cross-shelf transect (Chapters 2 – 5).

The fringing reefs developed in a range of environmental settings, from adjacent to the mainland (Bramston Reef), within an island embayment (SI-N) and attached to island shorelines and headlands in relatively exposed (Holbourne Island and Middle Island) or sheltered (SI-S) locations. The earliest ages for reef initiation varied between sites from $7,873 \pm 17$ yBP (Middle Island) to $5,396 \pm 51$ yBP (Bramston Reef). The pre-Holocene antecedent substrates identified were: unconsolidated terrigenous sands and lag gravels overlaying Pleistocene clay at Bramston Reef; a compacted regolith clay at Middle Island; and granite and weathered last interglacial reef at Holbourne Island. At 5.9 m below the present reef flat surface, this last interglacial reef, aged at $137,778 \pm 608$ yBP, is the shallowest confirmed interglacial reef beneath a Holocene fringing reef in the GBR. Additional chronostratigraphic

records of mid-shelf fringing reef development that extend to the pre-Holocene foundations are required to determine whether all mid-shelf fringing reefs on the GBR developed upon last interglacial reef foundations.

Objective 2: To reconstruct the chronostratigraphy of the fringing reefs along this transect to establish past rates and styles of reef development and any variability over time, including detailed examinations of the palaeo-ecological coral community compositions (Chapters 2 – 5)

The chronostratigraphy of each fringing reef was developed using a total of 42 reef cores combined with 112 U-Th ages. Reef growth rates during the Holocene varied from 2.5 – 9.8 mm/yr at Bramston Reef, 0.3 – 5.0 mm/yr at Stone Island, 3.5 – 7.6 mm/yr at Middle Island and 0.7 – 3.2 mm/yr at Holbourne Island. Different styles or modes of growth were observed, with the traditional ‘up and out’ growth mode being most common. Despite developing according to different growth modes, reef flat development at all sites occurred within ~2,000 years of initiation. The majority of reef flat development occurred by ~6,000 yBP at the further offshore sites (Middle and Holbourne Islands), by ~4,000 yBP at Stone Island, and by ~2,000 yBP at Bramston Reef. Negligible reef flat progradation has occurred since these times at any site, however Bramston Reef experienced seaward progradation for a considerably longer time relative to the other sites, extending into the late-Holocene (~2,000 – 1,000 yBP). Palaeo-ecological analyses of coral material within the cores revealed up to 25 genera at Bramston Reef, 20 – 23 genera at the Stone Island reefs, 15 genera at Middle Island reef and at least 10 genera at Holbourne Island reef. These differences more likely reflect the degree of coral clast preservation, rather than actual palaeo-coral generic diversity. Inshore reefs with higher terrestrial sedimentation likely preserve more accurate records of palaeo-ecological composition than mid-shelf reefs where a lot of coral material was poorly preserved detrital material. Temporal variability in palaeo-ecology was investigated at Bramston Reef and no major changes through time were observed, with the major reef-building coral genera recovered in all cores across the reef, independent of time. New long-term core records of fringing reef growth are required from throughout the GBR to expand the fringing reef development database. In particular, palaeo-ecological studies from the inshore GBR are called for to reveal if inshore reefs are the most suitable for comparisons of past and present coral community composition. Long-term core records would be especially valuable from sites where limited fringing reef accretion potential has been inferred without a long-term understanding of reef development, including in the Whitsunday Island Group (e.g. van Woesik et al., 1999).

Objective 3: To investigate the influence of natural stressors on past reef development (Chapters 2 – 5)

Sea level influenced reef development by controlling when substrates were transgressed during the early-Holocene and the maximum age at which reef growth could be initiated, in addition to constraining vertical accommodation space and reef flat elevations. The influence of late-Holocene relative sea-level fall was evident at all sites, where the backreef flats formed during the mid-Holocene sea-level highstand were elevated up to 1.0 m above the outer reef flat and reef crest. The timing of late-Holocene sea-level fall coincided with a slowing of reef accretion at most sites; the majority of reef flat emplacement occurred prior to this fall at all sites, with the exception of Bramston Reef, where reef flat emplacement occurred under a falling sea-level and rapid reef slope progradation evidently occurred during the late-Holocene. The ability of this mainland-attached reef to accrete into the late-Holocene not only in a muddy, sheltered environment, but also under a falling sea-level, indicates that sea-level fall is unlikely to be the only factor influencing reef accretion potential at other locations.

The impacts of cyclones on Holocene reef development were most evident at Middle Island and Holbourne Island, whereby cyclones stripped the upper and outer reef structures during the mid-Holocene resulting in age gaps in the reef chronostratigraphies of 3,500 – 5,000 years. The stripped material was re-worked and re-distributed across the reef flat, moved downslope or offshore, or deposited onshore in the form of shingle ridges and this process has likely occurred multiple times. Ultimately, episodically high export rates during cyclones may have contributed to reduced net reef accretion at Middle and Holbourne Islands by removing material from the reef structure. However, the reefs at Middle and Holbourne Islands were required to prograde upon steep foundations, in comparison with the shallow, gently sloping foundations underlying the inshore reefs and this may have contributed to reduced progradation in the late-Holocene at the further offshore sites. Recognition of the cyclone stripping process is necessary in interpretations of palaeo-ecological records from coral reefs, because age gaps in reef chronostratigraphies do not necessarily equate to a hiatus in reef growth. A detailed investigation of the age structure of the shingle ridges preserved onshore at Holbourne and Middle Islands would be valuable, to establish past cyclone frequency and intensity, and to confirm that reef growth occurred at these sites during the age gaps recorded in the reef cores.

Terrestrial sedimentation impacts were most pronounced close to the mainland, at Stone Island and Bramston Reef. The chronostratigraphies from these sites reveal that the majority of reef development occurred in terrigenous mud-rich settings, as the cores were dominated by mud-rich facies. Furthermore, at Bramston Reef palaeo-ecological analyses revealed that the coral community composition has not changed through time, with the key reef-building coral genera (including *Acropora*, *Montipora*, *Euphyllia*, *Porites* and *Goniopora*) present throughout the

palaeo-ecological record and identified in the contemporary reef slope survey. This highlights the ability of inshore reefs to initiate and accrete rapidly over the past 5,000 years in sheltered, muddy locations adjacent to the coast. To establish the frequency of freshwater floods and other terrestrial influences in Edgcumbe Bay over the Holocene, and the influence on reef development, coral core records from Edgcumbe Bay would be useful. Combined with geochemical analyses (e.g. McCulloch et al., 2003) or luminescence measurements (Lough et al., 2014), such records may also provide information about if and how water quality indicators in Edgcumbe Bay have changed since European settlement of surrounding catchments.

Objective 4: To describe and quantify the contemporary ecological community composition and structure and determine whether this has changed since European settlement (Chapters 2, 3 and 5)

The emergent backreef flats at all reefs were elevated between 1.0 – 0.6 m above lowest astronomical tide (LAT), and were largely composed of macroalgae, sand and coral rubble (generally each comprising around 20 – 60% cover). Live coral cover was restricted to the lower elevation outer reef flats (0.6 – 0.0 mLAT), where average live coral cover reached $13.9 \pm 19.2\%$ at Bramston Reef (and was highly patchy), $63.1 \pm 20.2\%$ at Middle Island and $38.1 \pm 32.0\%$ at Holbourne Island. Live coral cover on the reef flats at Stone Island was minimal and restricted to a few isolated colonies of *Porites* and *Acropora*. Reef slope coral cover was patchy, particularly at inshore sites where coral cover was interspersed with zones that were dominated by macroalgae and sediment. Nevertheless, there were zones on these inshore reef slopes where high live coral cover was recorded (e.g. up to $51.3 \pm 19.4\%$ at Bramston Reef slope and $46.0 \pm 36.2\%$ at SI-N reef slope). Clearly parts of these inshore reefs can maintain high ecological value.

Due to limited modern data on reef condition at the study sites, determining changes in reef condition since European settlement relies on comparisons between core records, historical records and modern ecological data. However, there is a temporal mismatch between millennial-scale core records, centennial-scale historical records and contemporary data, which reveal decadal trends at most. Nevertheless, the only site where a change in condition was inferred based on the available data was SI-S, which supported very low coral cover at the time of survey. However, this poor reef condition was not observed elsewhere in Edgcumbe Bay, including at SI-N, where the reef slope was characterised by high live coral cover ($46.0 \pm 36.2\%$). Indeed, the condition of Bramston Reef and Middle Island appeared comparable to the late 1800s, as described in historical records. This suggests that localised, site-specific stressors are affecting coral cover on the reef flat at SI-S, and that assertions that a regional decline in

water quality is involved are more difficult to support. Whether the condition of this reef is temporary or reflects a trajectory of decline remains uncertain. Future ecological monitoring at the reefs in Edgumbe Bay, including SI-S, with attention paid to reef flat elevation, is required to generate robust conclusions about reef recovery potential. Additionally, obtaining data on the potential local stressors in the region, including the hydrodynamics in Edgumbe Bay and surrounding Stone Island, would be extremely useful to further understand the reasons behind poor reef condition at SI-S. The importance and value of understanding the long-term reef development history was highlighted in Chapter 3, and similar studies are called for at other sites in the GBR and globally where photographic comparisons show apparent declines in reef condition.

Objective 5: To investigate Holocene reef development and present reef condition across the shelf, to identify variability and similarities across this gradient, and to examine how such patterns reflect the influence of key environmental parameters (Chapter 6)

Holocene reef development was compared over the cross-shelf transect and the following key variations were observed:

- Reef initiation generally occurred earlier and at a greater depth further offshore;
- Different growth modes characterised each site;
- Reef flats were wider further inshore (up to 900 m) and Bramston Reef flat was lower in elevation (~0.6 mLAT) compared with the other sites (~1.0 mLAT);
- Palaeo-ecological coral community diversity was highest at inshore sites (25 genera identified at Bramston Reef compared with ~10 genera at Holbourne Island);
- Accretion rates were higher in muddy inshore reef environments (maximum 9.8 mm/yr at Bramston Reef), where the reef matrix sediments in subtidal core facies typically contained >40 – 50% mud and >30 – 50% terrigenous material.

Despite these variations, all reefs accreted rapidly after initiation and reef flats were emplaced within a 1,000 or 2,000-year period, after which negligible reef flat progradation occurred at any site. Variations in the timing of reef initiation between sites resulted from differences in either a) the depth to the antecedent surface, which typically increased with distance from the shore, or b) the composition of the antecedent surface which varied across-shore, with unconsolidated substrates at Bramston Reef being most difficult for coral colonisation. Sea level and the shape of the underlying substrate influenced accommodation space at each site, and influenced the timing and nature of vertical reef accretion and reef flat progradation. Furthermore, the greater exposure to cyclones of Middle and Holbourne Islands was evident in

the reef chronostratigraphies, while the impacts of terrestrial sedimentation were greater further inshore (at Bramston Reef and Stone Island). The impacts of cyclones largely influenced the present geomorphology and ecology of the reef flats and shorelines at the two further offshore sites.

Future studies investigating mainland-attached reef growth on the GBR are required to determine whether the lag in reef initiation due to substrate constraints interpreted for Bramston Reef is characteristic of similar fringing reefs. The possible interplay between hydrodynamics around a reef and substrate depth or slope may influence how far a reef can prograde seaward, but this was beyond the scope of this thesis and requires further research. Cross-shelf variations in past sea-level changes were not evident, due to the dominance of moated fossil microatolls at Middle and Holbourne Islands, which made it difficult to reconstruct a true Holocene sea-level history. This has important implications for sea-level reconstructions where microatolls are used as a proxy for sea level; the influence of moating on sea-level data must be considered, especially where data are collected from locations that display geomorphic evidence of present and past cyclone activity. Sea-level data are required from open-water fossil microatolls at reefs on the mid-shelf GBR to examine and quantify the influence of hydro-isostasy across the shelf, however, given the cyclone regime at Holbourne Island and Middle Island, such data may be scarce. Detailed age data are required from material within the onshore shingle ridges at Holbourne and Middle Islands to better understand the relative influences of cyclone stripping and sea-level change on reef accretion. An extension of this cross-shelf investigation of fringing reef development to the outer-shelf reefs of the central GBR would provide further comparisons between fringing reefs and platform or barrier reefs and the relative influences of sea-level change, storms and terrestrial sedimentation.

7.2 Concluding remarks

Inshore reefs are clearly different to their mid-shelf and outer-shelf counterparts in many ways. In some ways they may be more resilient to certain stressors; their location close to the mainland means they have been influenced by terrestrial sedimentation throughout their Holocene development. Furthermore, inshore fringing reefs accreted well into the late-Holocene, while those further offshore were characterised by shorter periods of net reef accretion, which slowed thousands of years ago.

This thesis adds to a growing number of studies, which also recognise the potential resilience of inshore fringing reefs. The temporal and spatial diversity in reef development and condition

revealed in this examination of five fringing reefs must be put in the context of the small sample of fringing reefs on the GBR for which reef growth records are currently known. The GBR includes ~758 fringing and nearshore reefs that span ~15 degrees of latitude, and thus there remains much to be learnt about the development, diversity and potential of these reefs which developed well before European settlement in Australia, but provide important ecological, economic and social value today.

References

- Agassiz, A. 1898 A visit to the Great Barrier Reef of Australia in the steamer "Croydon" during April and May, 1896, *Bulletin of the Museum of Comparative Zoology at Harvard College*, 28: 93-148.
- Andutta, F.P., Ridd, P.V. and Wolanski, E. 2013 The age and the flushing time of the Great Barrier Reef waters, *Continental Shelf Research*, 53: 11-19.
- Anthony, K.R.N. and Fabricius, K.E. 2000 Shifting roles of heterotrophy and autotrophy in coral energetics under varying turbidity, *Journal of Experimental Marine Biology and Ecology*, 252: 221-253.
- Bainbridge, Z.T., Wolanski, E., Alvarez-Romero, J.G., Lewis, S.E. and Brodie, J.E. 2012 Fine sediment and nutrient dynamics related to particle size and floc formation in a Burdekin River flood plume, Australia. *Marine Pollution Bulletin*, 65: 236-248.
- Baker, A.C., Glynn, P.W. and Riegl, B. 2008 Climate change and coral reef bleaching: An ecological assessment of long-term impacts, recovery trends and future outlook, *Estuarine, Coastal and Shelf Science*, 80: 435-471.
- Bartram, G. 1972 The dam that grew...and grew...into a lake, *The Australian Women's Weekly*, Accessed at <http://trove.nla.gov.au/ndp/del/article/51274151?searchTerm=%2522Stone%20Island%2522%20AND%20%2522bowen%2522%20AND%20%2522dam%2522&searchLimits>. Accessed on 10 February 2016.
- Bell, P.R.F. and Elmetri, I. 1995 Ecological indicators of large-scale eutrophication in the Great Barrier Reef lagoon, *Ambio*, 24(4): 208-215.
- Bell, P.R.F., Elmetri, I. and Lapointe B.E., 2014 Evidence of large-scale chronic eutrophication in the Great Barrier Reef: Quantification of chlorophyll *a* thresholds for sustaining coral reef communities, *Ambio*, 43(3): 361-376.
- Bellwood, D.R., Hughes, T.P., Folke, C. and Nystrom, M. 2004 Confronting the coral reef crisis, *Nature*, 429: 827-833.
- Bird, E.C.F. 1971 The fringing reefs near Yule Point, North Queensland, *Australian Geographic Studies*, 9: 107-115.
- Blanchon, P. and Jones, B. 1997 Hurricane control on shelf-edge reef architecture around Grand Cayman, *Sedimentology*, 44: 479-506.
- Blanchon, P., Jones, B. and Kalbfleisch, W. 1997 Anatomy of a fringing reef around Gran Cayman: storm rubble, not coral framework, *Journal of Sedimentary Research*, 67(1): 1-16.
- BOM 2016a, Bureau of Meteorology, <http://www.bom.gov.au/cyclone/faq/index.shtml#definitions>. Accessed on 27 February 2016.
- BOM 2016b, Bureau of Meteorology, <http://www.bom.gov.au/australia/tides/#!/qld-abbot-point>. Accessed on 12 February 2016.
- Bowen Independent, 1916 Pleasure resorts, Bowen Independent pp. 2, Accessed at <http://trove.nla.gov.au/ndp/del/article/196356917?searchTerm=%22Stone%20Island%22%20AND%20%22goats%22&searchLimits=>. Accessed on 10 February 2016.
- Bowen Independent, 1934 Spitfire survey of Port Denison, Bowen Independent pp. 1, Accessed at <http://trove.nla.gov.au/ndp/del/article/193100480?searchTerm=%22Stone%20Island%22%20AND%20%22sheep%22&searchLimits=>. Accessed on 10 February 2016.

- Braithwaite, C.J.R., Montaggioni, L.F., Camoin, G.F., Dalmaso, H., Dullo, W.C. and Mangini, A. 2000 Origins and development of Holocene coral reefs: a revisited model based on reef boreholes in the Seychelles, Indian Ocean, *International Journal of Earth Sciences*, 89: 431-445.
- Braithwaite, C.J.R. et al. 2004 The Great Barrier Reef: the chronological record from a new borehole, *Journal of Sedimentary Research*, 74(2): 298-310.
- Brodie, J. and Waterhouse, J. 2012 A critical review of environmental management of the 'not so Great' Barrier Reef, *Estuarine, Coastal and Shelf Science*, 104-105: 1-22.
- Brodie, J., Ariel, E., Thomas, C., O'Brien, D. and Berry, K. 2014 Links between water quality and marine turtle health, A technical report to the World Wildlife Fund, Centre for Tropical Water & Aquatic Ecosystem Research (TropWATER).
- Brodie, J. et al. 2012 Terrestrial pollutant runoff to the Great Barrier Reef: An update of issues, priorities and management responses, *Marine Pollution Bulletin*, 65: 81-100.
- Bronk Ramsey, C. 2009 Bayesian analysis of radiocarbon dates, *Radiocarbon*, 51: 337-360.
- Browne, N.K., Smithers, S.G. and Perry, C.T. 2010 Geomorphology and community structure of Middle Reef, central Great Barrier Reef, Australia: an inner-shelf turbid zone reef subject to episodic mortality events, *Coral Reefs*, 29: 683-689.
- Browne, N.K., Smithers, S.G. and Perry, C.T. 2012 Coral reefs of the turbid inner-shelf of the Great Barrier Reef, Australia: An environmental and geomorphic perspective on their occurrence, composition and growth, *Earth-Science Reviews*, 115: 1-20.
- Browne, N.K., Smithers, S.G. and Perry, C.T. 2013 Spatial and temporal variations in turbidity on two inshore reefs on the Great Barrier Reef, Australia, *Coral Reefs*, 32: 195-210.
- Bruno, J.F. and Selig, E.R. 2007 Regional decline of coral cover in the Indo-Pacific: timing, extent, and subregional comparisons, *PloS One*, 2(8): e711. doi:10.1371/journal.pone.0000711.
- Bruno, J.F., Sweatman, H., Precht, W.F., Selig, E.R. and Schutte, V.G.W. 2009 Assessing evidence of phase shifts from coral to macroalgal dominance on coral reefs, *Ecology*, 90(6): 1478-1484.
- Bruno, J.F., Precht, W.F., Vroom, P.S., and Aronson, R.B. 2014 Coral reef baselines: how much macroalgae is natural?, *Marine Pollution Bulletin*, 80: 24-29.
- Budd, A.F., Fukami, H., Smith, N.D. and Knowlton, N. 2012 Taxonomic classification of the reef coral family Mussidae (Cnidaria: Anthozoa: Scleractinia), *Zoological Journal of the Linnean Society*, 166: 465-529.
- Buddemeier, R.W. and Hopley, D. 1988 Turn-ons and turn-offs: causes and mechanisms of the initiation and termination of coral reef growth, *Proceedings of the Sixth International Coral Reef Symposium* (Townsville, Australia), pp. 253-261.
- Buddemeier, R.W. and Smith, S.V. 1988 Coral reef growth in an era of rapidly rising sea level: predictions and suggestions for long-term research, *Coral Reefs*, 7: 51-56.
- Bull, G.D. 1982 Scleractinian coral communities of two inshore high island fringing reefs at Magnetic Island, North Queensland, *Marine Ecology Progress Series*, 7: 267-272.
- Burke, L., Reytar, K., Spalding, M. and Perry, A. 2011 *Reefs at risk revisited*. World Resources Institute, Washington, DC.
- Cabioch, G., Montaggioni, L.F. and Faure, G. 1995 Holocene initiation and development of New Caledonian fringing reefs, SW Pacific, *Coral Reefs*, 14: 131-140.

- Carleton, J.H. and Done, T.J. 1995 Quantitative video sampling of coral reef benthos: large-scale application, *Coral Reefs*, 14: 35-46.
- Chappell, J. 1980 Coral morphology, diversity and reef growth, *Nature*, 286: 249-252.
- Chappell, J., Chivas, A., Wallensky, E., Polach, H. and Aharon, P. 1983 Holocene palaeo-environmental changes central to north Great Barrier Reef inner zone, *BMR Journal of Australian Geology and Geophysics*, 8: 223-235.
- Chappell, J., Rhodes, E.G., Thom, B.G. and Wallensky, E. 1982 Hydro-isostasy and the sea-level isobase of 5500 B.P. in North Queensland, Australia, *Marine Geology*, 49: 81-90.
- Cheal, A.J. et al. 2010 Coral-macroalgal phase shifts or reef resilience: links with diversity and functional roles of herbivorous fishes on the Great Barrier Reef, *Coral Reefs*, 29: 1005-1015.
- Chivas, A., Chappell, J., Polach, H., Pillans, B. and Flood, P. 1986 Radiocarbon evidence for the timing and rate of island development, beach-rock formation and phosphatization at Lady Elliot Island, Queensland, Australia, *Marine Geology*, 69: 273-287.
- Clark, T.R. et al. 2012 Spatial variability of initial $^{230}\text{Th}/^{232}\text{Th}$ in modern *Porites* from the inshore region of the Great Barrier Reef, *Geochimica et Cosmochimica Acta*, 78: 99-118.
- Clark, T.R., Roff, G., Zhao, J., Feng, Y., Done, T.J. and Pandolfi, J.M. 2014a Testing the precision and accuracy of the U-Th chronometer for dating coral mortality events in the last 100 years, *Quaternary Geochronology*, 23: 35-45.
- Clark, T.R. et al. 2016 Historical photographs revisited: a case study for dating and characterizing recent loss of coral cover on the inshore Great Barrier Reef, *Scientific Reports*, 2: DOI: 10.1038/srep19285.
- Clark, T.R. et al. 2014b Discerning the timing and cause of historical mortality events in modern *Porites* from the Great Barrier Reef, *Geochimica et Cosmochimica Acta*, 138: 57-80.
- Commonwealth of Australia (Geoscience Australia) 2015 <http://www.ga.gov.au/scientific-topics/positioning-navigation/geodesy/auspos>. Accessed on 29 February, 2016.
- Connell, J.H., Hughes, T.P. and Wallace, C.C. 1997 A 30-year study of coral abundance, recruitment, and disturbance at several scales in space and time, *Ecological Monographs*, 67(4): 461-488.
- Cooper, T.F., Uthicke, S., Humphrey, C. and Fabricius, K.E. 2007 Gradients in water column nutrients, sediment parameters, irradiance and coral reef development in the Whitsunday Region, central Great Barrier Reef, *Estuarine, Coastal and Shelf Science*, 74: 458-470.
- Darwin, C.R. 1842 *The Structure and Distribution of Coral Reefs*. London, Smith Elder and Co.
- Dawson, J.L., Smithers, S.G., and Hua, Q. 2014 The importance of large benthic foraminifera to reef island sediment budget and dynamics at Raine Island, northern Great Barrier Reef, *Geomorphology*, 222: 68-81.
- Davies, P.J. and Montaggioni, L.F. 1985 Reef growth and sea-level change: the environmental signature, *Proceedings of the Fifth International Coral Reef Congress*, Tahiti, 3: 477-511.
- Davies, P.J., Marshall, J.F. and Hopley, D. 1985 Relationships between reef growth and sea level in the Great Barrier Reef, *Proceedings of the Fifth International Coral Reef Congress*, Tahiti, 3: 95-103.
- De'ath, G., Fabricius, K. 2010 Water quality as a regional driver of coral biodiversity and macroalgae on the Great Barrier Reef, *Ecological Applications*, 20(3): 840-850.
- De'ath, G., Fabricius, K.E., Sweatman, H. and Puotinen, M. 2012 The 27-year decline of coral cover on

- the Great Barrier Reef and its causes, *Proceedings of the National Academy of Sciences*, 65: 1-5.
- Dechnik, B., Webster, J.M., Davies, P.J., Braga, J.C. and Reimer, P.J. 2015 Holocene “turn-on” and evolution of the southern Great Barrier Reef: revisiting cores from the Capricorn Bunker Group, *Marine Geology*, 363: 174-190.
- DeVantier, L.M., Turak, E., Done, T.J. and Davidson, J. 1997 The effects of cyclone Sadie on coral communities of nearshore reefs in the central Great Barrier Reef. In: *Cyclone Sadie Flood Plumes in the Great Barrier Reef Lagoon: Composition and Consequences*. GBRMPA, Workshop series no. 22: 65-85.
- DeVantier, L.M., De’ath, G., Done, T.J. and Turak, E. 1998 Ecological assessment of a complex natural system: a case study from the Great Barrier Reef, *Ecological Applications*, 8(2): 480-496.
- DeVantier, L.M., De’ath, G., Turak, E., Done, T.J. and Fabricius, K.E. 2006 Species richness and community structure of reef-building corals on the nearshore Great Barrier Reef, *Coral Reefs*, 25: 329-340.
- Devlin, M., Waterhouse, J., Taylor, J. and Brodie, J. 2001 Flood plumes in the Great Barrier Reef: Spatial and temporal patterns in composition and distribution, *Great Barrier Reef Marine Park Authority Research Publication No. 68*.
- Devlin, M.J. et al. 2012 Mapping the pollutants in surface riverine flood plume waters in the Great Barrier Reef, Australia, *Marine Pollution Bulletin*, 65: 224-235.
- Diaz-Pulido, G., Harii, S., McCook, L.J. and Hoegh-Guldberg, O. 2010 The impact of benthic algae on the settlement of a reef-building coral, *Coral Reefs*, 29: 203-208.
- Done, T.J. 1992 Effects of tropical cyclone waves on ecological and geomorphological structures on the Great Barrier Reef, *Continental Shelf Research*, 12(78): 859-872.
- Done, T.J. 2011 Coral Reefs, Definition, in Hopley, D. ed. *Encyclopedia of Modern Coral Reefs – Structure, Form and Process*, Springer, The Netherlands, 261-267.
- Done, T., Turak, E., Wakeford, M., DeVantier, L., McDonald, A. and Fisk, D. 2007 Decadal changes in turbid-water coral communities at Pandora Reef: Loss of resilience or too soon to tell? *Coral Reefs*, 26: 789-805.
- Druffel, E.R.M. and Griffin, S. 2004 *Southern Great Barrier Reef Coral Radiocarbon Data*. IGBP PAGES/World Data Center for Paleoclimatology, Data Contribution Series #2004-093, NOAA/NCDC Paleoclimatology Program, Boulder CO, USA.
- Easton, W.H. and Olson, E.A. 1976 Radiocarbon profile of Hanauma Reef, Oahu, Hawaii, *Geological Society of America Bulletin*, 87: 711-719.
- Etienne, S. and Terry J.P. 2012 Coral boulders, gravel tongues and sand sheets: Features of coastal accretion and sediment nourishment by Cyclone Tomas (March 2010) on Taveuni Island, Fiji, *Geomorphology*, 175-176: 54-65.
- Fabricius, K.E. 2005 Effects of terrestrial runoff on the ecology of corals and coral reefs: review and synthesis, *Marine Pollution Bulletin*, 50: 125-146.
- Fabricius, K.E., De’ath, G., McCook, L., Turak, E. and Williams, D.McB. 2005 Changes in algal, coral and fish assemblages along water quality gradients on the inshore Great Barrier Reef, *Marine Pollution Bulletin*, 51: 384-398.
- Fabricius, K.E., De’ath, G., Puotinen, M.L., Done, T., Cooper, T.F. and Burgess, S.C. 2008 Disturbance gradients on inshore and offshore coral reefs caused by a severe tropical cyclone, *Limnology and Oceanography*, 53(2): 690-704.

- Fabricius, K.E., Okaji, K. and De'ath, G. 2010 Three lines of evidence to link outbreaks of the crown-of-thorns seastar *Acanthaster planci* to the release of larval food limitation, *Coral Reefs*, 29: 593-605.
- Fallon, S.J., McCulloch, M.T. and Alibert, C. 2003 Examining water temperature proxies in *Porites* corals from the Great Barrier Reef: a cross-shelf comparison, *Coral Reefs*, 22: 389-404.
- Fink, D. et al. 2004 The ANTARES AMS facility at ANSTO, *Nuclear Instruments and Methods in Physics Research B*, 223-224: 109–115.
- Forsyth, A.J., Nott, J. and Bateman, M.D. 2010 Beach ridge plain evidence of a variable late-Holocene tropical cyclone climate, North Queensland, Australia, *Palaeogeography, Palaeoclimatology, Palaeoecology*, 297: 707-716.
- Foster, N.L., Box, S.J. and Mumby, P.J. 2008 Competitive effects of macroalgae on the fecundity of the reef-building coral *Montastraea annularis*, *Marine Ecology Progress Series*, 367: 143-152.
- Gagan, M.J., Sandstrom, M.W. and Chivas, A.R. 1987 Restricted terrestrial carbon input to the continental shelf during Cyclone Winifred: implications for terrestrial runoff to the Great Barrier Reef province, *Coral Reefs*, 6: 113-119.
- Gagan, M.K. et al. 1998 Temperature and surface-ocean water balance of the mid-Holocene tropical western Pacific, *Science*, 279: 1014-1018.
- Gardner, T.A., Côté, I.M., Gill, J.A., Grant, A., Watkinson, A.R., 2003 Long-term regional-wide declines in Caribbean corals, *Science*, 301: 958-960.
- Great Barrier Reef Marine Park Authority (GBRMPA) 2013 *Don basin assessment: Burdekin dry tropics natural resource management section*, GBRMPA, Townsville.
- Great Barrier Reef Marine Park Authority (GBRMPA) 2014 *Great Barrier Reef Outlook Report*, GBRMPA, Townsville.
- Gibbs, R.J., Matthews, M.D. and Link, D.A. 1971 The relationship between sphere size and settling velocity, *Journal of Sedimentary Petrology*, 41(1): 7-18.
- Gilmour, J.P., Smith, L.D., Heyward, A.J., Baird, A.H. and Pratchett, M.S. 2013 Recovery of an isolated coral reef system following severe disturbance, *Science*, 340: 69-71.
- Graham, N.A.J., Nash, K.L. and Kool, J.T. 2011 Coral reef recovery dynamics in a changing world, *Coral Reefs*, 30: 283-294.
- Haig, J., Nott, J. and Reichart, G.J. 2014 Australian tropical cyclone activity lower than at any time over the past 550-1,500 years, *Nature*, 505: 667-671.
- Harmelin-Vivien, M.L. 1994 The effects of storms and cyclones on coral reefs: a review, *Journal of Coastal Research*, Special Issue 12: 211-231.
- Harris, D.L., Webster, J.M., Vila-Concejo, A., Hua, Q., Yokoyama, Y. and Reimer, P.J. 2015 Late Holocene sea-level fall and turn-off of reef flat carbonate production: rethinking bucket fill and coral reef growth models, *Geology*, 43: 175-178.
- Harvey, N., Davies, P.J. and Marshall, J.F. 1979 Seismic refraction – a tool for studying coral reef growth, *BMR Journal of Australian Geology and Geophysics*, 4: 141-147.
- Hayne, M., and Chappell, J. 2001 Cyclone frequency during the last 5000 years at Curacoa Island, north Queensland, Australia, *Palaeogeography, Palaeoclimatology, Palaeoecology*, 168: 207-219.
- Hayward, A.B. 1982 Coral reefs in a clastic sedimentary environment: fossil (Miocene, S.W. Turkey) and modern (recent, Red Sea) analogues, *Coral Reefs*, 1: 109-114.

- Hedley, C. 1925 The natural destruction of a coral reef, *Transactions of the Royal Geographical Society of Australasia (Queensland), Reports of the Great Barrier Reef Committee*, 1: 35-40.
- Hoegh-Guldberg, O. 2014 Coral reefs in the Anthropocene: persistence or the end of the line? In: Waters, C.N., Zalasiewicz, J.A., Williams, M., Ellis, M.A. and Snelling, A.M. eds. *A stratigraphical basis for the Anthropocene*, Geological Society, London, Special Publications, 395: 167-183.
- Hoegh-Guldberg, O. et al. 2007 Coral reefs under rapid climate change and ocean acidification, *Science*, 318: 1737-1742.
- Hopley, D. 1975 Contrasting evidence for Holocene sea levels with special reference to the Bowen-Whitsunday area of Queensland. In: Douglas, I., Hobbs, J.E. and Pigram, J.J. eds. *Geographical essays in honour of Gilbert J. Butland*. University of New England, Armidale, 51-84
- Hopley, D. 1982 *Geomorphology of the Great Barrier Reef: Quaternary Development of Coral Reefs*, New York: John Wiley-Interscience.
- Hopley, A. and Barnes, R. 1985 Structure and development of a windward fringing reef, Orpheus Island, Palm Group, Great Barrier Reef, *Proceedings of the Fifth International Coral Reef Congress*, Tahiti, 3: 141-146.
- Hopley, D. and Isdale, P.J. 1977 Coral micro atolls, tropical cyclones and reef flat morphology: a north Queensland example, *Search*, 8: 79-81.
- Hopley, D., McLean, R.F., Marshall, J., Smith, A.S. 1978 Holocene-Pleistocene boundary in a fringing reef: Hayman Island, North Queensland, *Search*, 9: 323-325.
- Hopley, D., Slocombe, A.M., Muir, F. and Grant, C. 1983 Nearshore fringing reefs in North Queensland, *Coral Reefs*, 1: 151-160.
- Hopley, D., Smithers, S. and Parnell, K. 2007 *The Geomorphology of the Great Barrier Reef: Development, Diversity and Change*, Cambridge University Press, Cambridge.
- Hubbard, D.K., Miller, A.I. and Scaturro, D. 1990 Production and cycling of calcium carbonate in a shelf-edge reef system (St. Croix, U.S. Virgin Islands): Applications to the nature of reef systems in the fossil record, *Journal of Sedimentary Petrology*, 60(3): 335-360.
- Hubbard, D.K., Parsons, K.M., Bythell, J.C. and Walker, N.D. 1991 The effects of Hurricane Hugo on the reefs and associated environments of St. Croix, U.S. Virgin Islands – a preliminary assessment, *Journal of Coastal Research*, 8: 33-48.
- Hughes, T.P. 1994 Catastrophes, phase shifts, and large-scale degradation of a Caribbean coral reef, *Science*, 265: 1547-1551.
- Hughes, T.P. and Connell, J.H. 1999 Multiple stressors on coral reefs: a long-term perspective, *Limnology and Oceanography*, 44: 932-940.
- Hughes, T.P., Bellwood, D.R., Baird, A.H., Brodie, J., Bruno, J.F. and Pandolfi, J.M. 2011 Shifting baselines, declining coral cover, and the erosion of reef resilience: comment on Sweatman et al. (2011), *Coral Reefs*, 30: 653-660.
- Hughes, T.P., Graham, N.A.J., Jackson, J.B.C., Mumby, P.J. and Steneck, R.S. 2010 Rising to the challenge of sustaining coral reef resilience, *Trends in Ecology and Evolution*, 25: 633-642.
- Hughes, T.P. et al. 2007 Phase shifts, herbivory, and the resilience of coral reefs to climate change, *Current Biology*, 17: 360-365.
- Insalaco, E. 1999 Facies and palaeoecology of Upper Jurassic (Middle Oxfordian) coral reefs in England, *Facies*, 40: 81-100.

- Jackson, J.B.C. et al. 2001 Historical overfishing and the recent collapse of coastal ecosystems, *Science*, 293: 629-638.
- Johansson, C.L., Bellwood, D.R. and Depczynski, M. 2010 Sea urchins, macroalgae and coral reef decline: a functional evaluation of an intact reef system, Ningaloo, Western Australia, *Marine Ecology Progress Series*, 414: 65-74.
- Johns, K.A., Osborne, K.O. and Logan, M. 2014 Contrasting rates of coral recovery and reassembly in coral communities on the Great Barrier Reef, *Coral Reefs*, 33: 553-563.
- Johnson, D.P. and Risk, M.J. 1987 Fringing reef growth on a terrigenous mud foundation, Fantome Island, central Great Barrier Reef, Australia, *Sedimentology*, 34: 275-287.
- Johnson, D., Cuff, C. and Rhodes, E. 1984 Holocene reef sequences and geochemistry, Britomart Reef, central Great Barrier Reef, Australia, *Sedimentology*, 31: 515-529.
- Jones, A.M. and Berkelmans, R. 2014 Flood impacts in Keppel Bay, southern Great Barrier Reef in the aftermath of cyclonic rainfall, *PloS ONE*, 9: e84739. doi:10.1371/journal.pone.0084739.
- Jupiter, S. et al. 2008 Linkages between coral assemblages and coral proxies of terrestrial exposure along a cross-shelf gradient on the southern Great Barrier Reef, *Coral Reefs*, 27: 887-903.
- Kan, H., Nakashima, Y. and Hopley, D. 1997 Coral communities during structural development of a fringing reef flat, Hayman Island, the Great Barrier Reef, *Proceedings of the 8th International Coral Reef Symposium*, Panama City, Panama, 1: 465-470.
- Kelley, R. 2009 *Indo Pacific Coral Finder*, BYO Guides, Townsville.
- Kench, P.S. and Mclean, R.F. 1997 A comparison of settling and sieve techniques for the analysis of bioclastic sediments, *Sedimentary Geology*, 109: 111-119.
- Kennedy, D.M. and Woodroffe, C.D. 2002 Fringing reef growth and morphology: a review, *Earth-Science Reviews*, 57: 255-277.
- Kittinger, J.N. et al. 2011 Historical reconstruction reveals recovery in Hawaiian coral reefs, *PloS One*, 6(10): e25460. doi:10.1371/journal.pone.0025460.
- Kleypas, J.A. 1996 Coral reef development under naturally turbid conditions: fringing reefs near Broad Sound, Australia, *Coral Reefs*, 15: 153-167.
- Kleypas, J.A. and Hopley, D. 1992 Reef development across a broad continental shelf, southern Great Barrier Reef, Australia, *Proceedings of the Seventh International Coral Reef Symposium*, Guam, 2: 1129-1141.
- Kleypas, J.A., Buddemeier, R.W. and Gattuso, J.P. 2001 The future of coral reefs in an age of global change, *International Journal of Earth Sciences*, 90: 426-437.
- Kohler, K.E. and Gill, S.M. 2006 Coral Point Count with Excel extensions (CPCe): A visual basic program for the determination of coral and substrate coverage using random point count methodology, *Computers and Geosciences*, 32: 1259-1269.
- Kroon, F.J. et al. 2012 River loads of suspended solids, nitrogen, phosphorus and herbicides delivered to the Great Barrier Reef lagoon, *Marine Pollution Bulletin*, 65: 167-181.
- Lambeck, K. and Nakada, M. 1990 Late Pleistocene and Holocene sea-level change along the Australian coast, *Palaeogeography, Palaeoclimatology, Palaeoecology*, 89: 143-176.
- Larcombe, P. and Woolfe, K.J. 1999a Increased sediment supply to the Great Barrier Reef will not increase sediment accumulation at most coral reefs, *Coral Reefs*, 18: 163-169.

- Larcombe, P. and Woolfe, K.J. 1999b Terrigenous sediments as influences upon Holocene nearshore coral reefs, central Great Barrier Reef, Australia, *Australian Journal of Earth Sciences*, 46: 141-154.
- Larcombe, P., Costen, A. and Woolfe, K.J. 2001 The hydrodynamic and sedimentary setting of nearshore coral reefs, central Great Barrier Reef shelf, Australia: Paluma Shoals, a case study, *Sedimentology*, 48: 811-835.
- Larcombe, P., Carter, R.M., Dye, J., Gagan, M.K. and Johnson, D.P. 1995a New evidence for episodic post-glacial sea-level rise, central Great Barrier Reef, Australia, *Marine Geology*, 127: 1-44.
- Larcombe, P., Ridd, P.V. and Wilson, A.P. 1995b Factors controlling suspended sediment on inner-shelf coral reefs, Townsville, Australia, *Coral Reefs*, 14: 163-171.
- Leonard, N.D. et al. 2016 Holocene sea level instability in the southern Great Barrier Reef, Australia: high-precision U-Th dating of fossil microatolls, *Coral Reefs*, DOI 10.1007/s00338-015-1384-x.
- Lewis, S., Brodie, J. and Ledee, E. 2006 The spatial extent of delivery of terrestrial materials from the Mackay Whitsunday region in the Great Barrier Reef lagoon, *Australian Centre for Tropical Freshwater Research Report 06/14*.
- Lewis, S.E., Wust, R.A.J., Webster, J.M. and Shields, G.A. 2008 Mid-late Holocene sea-level variability in eastern Australia, *Terra Nova*, 20: 74-81.
- Lewis, S.E., Sloss, C.R., Murray-Wallace, C.V., Woodroffe, C.D. and Smithers, S.G. 2013 Post-glacial sea-level changes around the Australian margin: a review, *Quaternary Science Reviews*, 74: 115-138.
- Lewis, S.E. et al. 2012 Development of an inshore fringing coral reef using textural, compositional and stratigraphic data from Magnetic Island, Great Barrier Reef, Australia, *Marine Geology*, 299-302: 18-32.
- Lewis, S.E., Wust, R.A.J., Webster, J.M., Collins, J., Wright, S.A. and Jacobsen, G. 2015 Rapid relative sea-level fall along north-eastern Australia between 1200 and 800 cal. Years BP: An appraisal of the oyster evidence, *Marine Geology*, 370: 20-30.
- Lirman, D. and Fong, P. 2007 Is proximity to land-based sources of coral stressors an appropriate measure of risk to coral reefs? An example from the Florida Reef Tract, *Marine Pollution Bulletin*, 54: 779-791.
- Liu, E.T. et al. 2014 High-precision U-Th dating of storm-transported coral blocks on Frankland Islands, northern Great Barrier Reef, Australia, *Palaeogeography, Palaeoclimatology, Palaeoecology*, 414: 68-78.
- Lough, J.M. and Barnes, D.J. 2000 Environmental controls on growth of the massive coral *Porites*, *Journal of Experimental Marine Biology and Ecology*, 245: 225-243.
- Lough, J.M., Lewis, S.E. and Cantin, N.E. 2015 Freshwater impacts in the central Great Barrier Reef: 1648-2011, *Coral Reefs*, 34(3): 739-751.
- Lough, J.M. et al. 2014 Evidence for suppressed mid-Holocene northeastern Australian monsoon variability from coral luminescence, *Palaeoceanography*, 29: 581-594.
- Maragos, J.E., Evans, C. and Holthus, P. 1985 Reef corals in Kaneohe Bay six years before and after termination of sewage discharges (Oahu, Hawaiian Archipelago), *Proceedings of the 5th International Coral Reef Congress*, Tahiti, 4: 189-194.
- Marshall, J.F. 1983 Submarine cementation in a high-energy platform reef: One Tree Reef, southern Great Barrier Reef, *Journal of Sedimentary Research*, 53(4): 1133-1149.

- Marshall, J.F. and Davies, P.J. 1984 Last interglacial reef growth beneath modern reefs in the southern Great Barrier Reef, *Nature*, 307: 44-46.
- Marshall, P., Richards, H.C. and Walkom, A.B. 1925 Recent emergence at Holbourne Island, Great Barrier Reef, *Reports of the Great Barrier Reef Committee*, 4: 35.
- Martin, J.M., Braga, J.C., Rivas, P. 1989 Coral successions in Upper Tortonian reefs in SE Spain, *Lethaia*, 22: 271-286.
- Masse, J.P. and Montaggioni, L.F. 2001 Growth history of shallow water carbonates: control of accommodation on ecological and depositional processes, *International Journal of Earth Sciences*, 90: 452-469.
- McCook, L.J., Jompa, J. and Diaz-Pulido, G. 2001 Competition between corals and algae on coral reefs: a review of evidence and mechanisms, *Coral Reefs*, 19: 400-417.
- McCulloch, M., Fallon, S., Wyndham, T., Hendy, E., Lough, J. and Barnes, D. 2003. Coral record of increased sediment flux to the inner Great Barrier Reef since European settlement, *Nature*, 421: 727-730.
- McIntyre-Tamwoy, S. 2004 'My Barrier Reef': exploring the Bowen community's attachment to the Great Barrier Reef, *Historic Environment*, 17(3): 19-28.
- Moberg, F. and Folke, C. 1999 Ecological goods and services of coral reefs, *Ecological Economics*, 29: 215-233.
- Montaggioni, L.F. 2005 History of Indo-Pacific coral reef systems since the last glaciation: development patterns and controlling factors, *Earth-Science Reviews*, 71: 1-75.
- Muhs, D.R., Simmons, K.R. and Steinke, B. 2002 Timing and warmth of the Last Interglacial period: new U-series evidence from Hawaii and Bermuda and a new fossil compilation for North America, *Quaternary Science Reviews*, 21: 1355-1383.
- Murray-Wallace, C.V. and Belperio, A.P. 1991 The last interglacial shoreline in Australia – A review, *Quaternary Science Reviews*, 10: 441-461.
- Murray-Wallace, C.V. and Woodroffe, C.D. 2014 *Quaternary sea-level changes: a global perspective*, Cambridge University Press, Cambridge.
- Neumann, A.C. and MacIntyre, I. 1985 Reef response to sea level rise: keep-up, catch-up or give-up, *Proceedings of the Fifth International Coral Reef Congress (Tahiti)*, 3: 105-110.
- Nott, J. and Forsyth, A. 2012 Punctuated global tropical cyclone activity over the past 5,000 years, *Geophysical Research Letters*, 39: DOI: 10.1029/2012GL052236.
- Nott, J. and Hayne, M. 2001 High frequency of 'super-cyclones' along the Great Barrier Reef over the past 5,000 years, *Nature*, 413: 508-512.
- Nott, J., Haig, J., Neil, H. and Gillieson, D. 2007 Greater frequency variability of landfalling tropical cyclones at centennial compared to seasonal and decadal scales, *Earth and Planetary Science Letters*, 255: 367-372.
- Nott, J., Smithers, S., Walsh, K. and Rhodes, E. 2009 Sand beach ridges record 6000 year history of extreme tropical cyclone activity in northeastern Australia, *Quaternary Science Reviews*, 28: 1511-1520.
- Orpin, A.R., Ridd, P.V. and Stewart, L.K. 1999 Assessment of the relative importance of major sediment-transport mechanisms in the central Great Barrier Reef lagoon, *Australian Journal of Earth Sciences*, 46: 883-896.

- Packett, R., Dougall, C., Ellis, R., Waters, D. and Carroll, C. 2014 Modelling reductions of pollutant loads due to improved management practices in the Great Barrier Reef catchments – Mackay Whitsunday NRM Region, Technical Report, Volume 5, *Queensland Department of Natural Resources and Mines*, Rockhampton, Queensland.
- Palmer, S.E., Perry, C.T., Smithers, S.G. and Gulliver, P. 2010 Internal structure and accretionary history of a nearshore, turbid-zone coral reef: Paluma Shoals, central Great Barrier Reef, Australia, *Marine Geology*, 276: 14-29.
- Pandolfi, J.M. 2015 Incorporating uncertainty in predicting the future response of coral reefs to climate change, *Annual Review of Ecology, Evolution, and Systematics*, 46: 281-303.
- Pandolfi, J.M. and Jackson, J.B.C. 2006 Ecological persistence interrupted in Caribbean coral reefs, *Ecology Letters*, 9: 818-826.
- Pandolfi, J.M. and Kiessling, W. 2014 Gaining insights from past reefs to inform understanding of coral reef response to global climate change, *Current Opinion in Environmental Sustainability*, 7: 52-58.
- Pandolfi, J.M. and Minchin, P.R. 1995 A comparison of taxonomic composition and diversity between reef coral life and death assemblages in Madang Lagoon, Papua New Guinea, *Palaeogeography, Palaeoclimatology, Palaeoecology*, 119: 321-341.
- Pandolfi, J.M. et al. 2003 Global trajectories of the long-term decline of coral reef ecosystems, *Science*, 301: 955-958.
- Partain, B.R. and Hopley, D. 1989 Morphology and development of the Cape Tribulation fringing reefs, Great Barrier Reef, Australia, *Great Barrier Reef Marine Park Authority Technical Memorandum 21*, 1-45.
- Pastorak, R.A. and Bilyard, G.R. 1985 Effects of sewage pollution on coral-reef communities, *Marine Ecology Progress Series*, 21: 175-189.
- Perry, C.T. 2001 Storm-induced coral rubble deposition: Pleistocene records of natural reef disturbance and community response, *Coral Reefs*, 20: 171-183.
- Perry, C.T. and Smithers, S.G. 2006 Taphonomic signatures of turbid-zone reef development: Examples from Paluma Shoals and Lugger Shoal, inshore central Great Barrier Reef, Australia, *Palaeogeography, Palaeoclimatology, Palaeoecology*, 242: 1-20.
- Perry, C.T. and Smithers, S.G. 2010 Evidence for the episodic “turn on” and “turn off” of turbid-zone coral reefs during the late Holocene sea-level highstand, *Geology*, 38: 119-122.
- Perry, C.T. and Smithers, S.G. 2011 Cycles of coral reef ‘turn-on’, rapid growth and ‘turn-off’ over the past 8500 years: a context for understanding modern ecological states and trajectories, *Global Change Biology*, 17: 76-86.
- Perry, C.T., Smithers, S.G. and Gulliver, P. 2013 Rapid vertical accretion on a ‘young’ shore-detached turbid zone reef: offshore Paluma Shoals, central Great Barrier Reef, Australia, *Coral Reefs*, 32(4): 1143-1148.
- Perry, C.T., Smithers, S.G., Gulliver, P. and Browne, N.K. 2012 Evidence of very rapid reef accretion and reef growth under high turbidity and terrigenous sedimentation, *Geology*, 40(8): 719-722.
- Perry, C.T., Smithers, S.G. and Johnson, K.G. 2009 Long-term coral community records from Lugger Shoal on the terrigenous inner-shelf of the central Great Barrier Reef, Australia, *Coral Reefs*, 28: 941-948.
- Perry, C.T., Smithers, S.G., Kench, P.S. and Pears, B. 2014 Impacts of Cyclone Yasi on nearshore,

- terrigenous sediment-dominated reefs of the central Great Barrier Reef, Australia, *Geomorphology*, 222: 92-105.
- Perry, C.T., Smithers, S.G., Palmer, S.E., Larcombe, P. and Johnson, K.G. 2008 1200 year palaeoecological record of coral community development from the terrigenous inner shelf of the Great Barrier Reef, *Geology*, 36(9): 691-694.
- Perry, C.T., Smithers, S.G., Roche, R.C. and Wassenburg, J. 2011 Recurrent patterns of coral community and sediment facies development through successive phases of Holocene inner-shelf reef growth and decline, *Marine Geology*, 289: 60-71.
- Pratchett, M.S., Caballes, C.F., Rivera-Posada, J.A. and Sweatman, H.P.A. 2014 Limits to understanding and managing outbreaks of crown-of-thorns starfish (*Acanthaster* spp.), *Oceanography and Marine Biology: An Annual Review*, 52: 133-300.
- Puotinen, M.L., Done, T.J. and Skelly, W.C. 1997 *An atlas of tropical cyclones in the Great Barrier Reef region, 1969-1997*, CRC Reef Research Centre Technical Report No. 19, Townsville, 201 pp.
- Purdy, E.G. 1974 Reef configuration: cause and effect, in Laporte, L.F. ed. *Reefs in Time and Space*, SEPM special publication 13, 9-76.
- Queensland Government (1997) Wave data recording program, Abbot Point Region, for the years 1977 to 1996, *Conservation Data Report No. W06.2*, 17 pp.
- Rainford, E.H. 1925 Destruction of the Whitsunday group fringing reefs, *Australian Museum Magazine*, 2: 175-177.
- Reimer, P.J. et al. 2013 IntCal13 and MARINE13 radiocarbon age calibration curves 0–50000 years calBP, *Radiocarbon*, 55: 4.
- Reymond, C.E., Roff, G., Chivas, A.R., Zhao, J.X. and Pandolfi, J.M. 2013 Millennium-scale records of benthic foraminiferal communities from the central Great Barrier Reef reveal spatial differences and temporal consistency, *Palaeogeography, Palaeoclimatology, Palaeoecology*, 374: 52-61.
- Richards, H.C. 1938 *Some problems of the Great Barrier Reef*, University of Queensland Papers, Department of Geology, 1: 68-85.
- Risk, M.J. 2014 Assessing the effects of sediments and nutrients on coral reefs, *Current Opinion in Environmental Sustainability*, 7: 108-117.
- Roche, R.C., Perry, C.T., Johnson, K.G., Sultana, K., Smithers, S.G. and Thompson, A.A. 2011 Mid-Holocene coral community data as baselines for understanding contemporary reef ecological states, *Palaeogeography, Palaeoclimatology, Palaeoecology*, 299: 159-167.
- Roche, R.C. et al. 2014 Mid-Holocene sea surface conditions and riverine influence on the inshore Great Barrier Reef, *The Holocene*, 24(8): 885-897.
- Rodriguez-Ramirez, A., Grove, C.A., Zinke, J., Pandolfi, J.M. and Zhao, J.X. 2014 Coral luminescence identifies the Pacific Decadal Oscillation as a primary driver of river runoff variability impacting the southern Great Barrier Reef, *PloS One*, 9(1): e84305. doi:10.1371/journal.pone.0084305.
- Roff, G. et al. 2012 Palaeoecological evidence of a historical collapse of corals at Pelorus Island, inshore Great Barrier Reef, following European settlement, *Proceedings of the Royal Society of Biological Sciences*, 280: 1-10.
- Roff, G., Zhao, J.X. and Pandolfi, J.M. 2015 Rapid accretion of inshore reef slopes from the central Great Barrier Reef during the late Holocene, *Geology*, 43(4): 343-346.

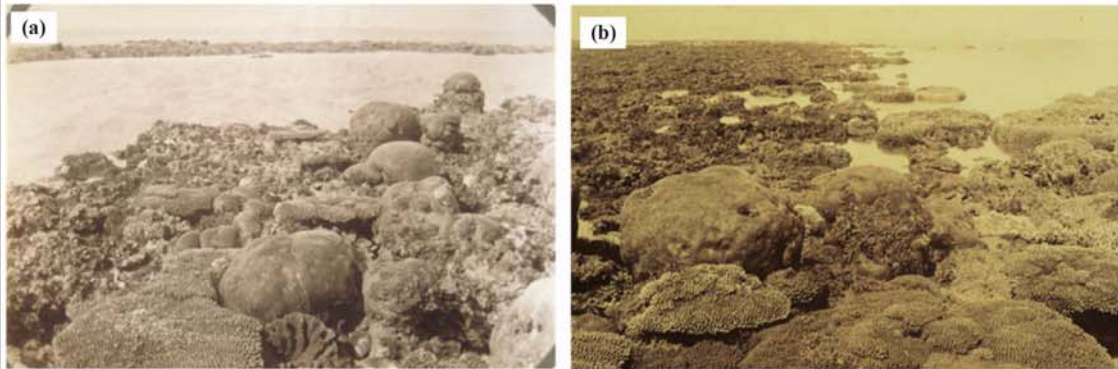
- Rogers, C.S. 1990 Responses of coral reefs and reef organisms to sedimentation, *Marine Ecology Progress Series*, 62: 185-202.
- Ryan, E.J., Smithers, S.G., Lewis, S.E., Clark, T.R. and Zhao, J.X. 2016 Chronostratigraphy of Bramston Reef reveals a long-term record of fringing reef growth under muddy conditions in the central Great Barrier Reef, *Palaeogeography, Palaeoclimatology, Palaeoecology*, 441: 734-747.
- Santodomingo, N. et al. 2015 A diverse patch reef from turbid habitats in the Middle Miocene (East Kalimantan, Indonesia), *Palaios*, 30: 128-149.
- Saville-Kent, W. 1893 *The Great Barrier Reef of Australia*, Allen Press, London.
- Scoffin, T.P. 1993 The geological effects of hurricanes on coral reefs and the interpretation of storm deposits, *Coral Reefs*, 12: 203-221.
- Scoffin, T.P. and Stoddart, D.R. 1978 The nature and significance of microatolls, *Philosophical Transactions of the Royal Society of London Series B, Biological Sciences*, 284: 99-122.
- Simpson, R.H. and Reihl, H. 1981 *The Hurricane and its Impact*, Louisiana State University Press, Baton Rouge.
- Smithers, S.G. 2011 Fringing Reefs, in Hopley, D. ed. *Encyclopedia of Modern Coral Reefs –Structure, Form and Process*, Springer, The Netherlands, 430-44.
- Smithers, S. and Larcombe, P. 2003 Late Holocene initiation and growth of a nearshore turbid-zone coral reef: Paluma Shoals, central Great Barrier Reef, Australia, *Coral Reefs*, 22: 499-505.
- Smithers, S.G. and Woodroffe, C.D. 2000 Micro-atolls as sea-level indicators on a mid-ocean atoll, *Marine Geology*, 168: 61-78.
- Smithers, S.G., Hopley, D. and Parnell, K.E. 2006 Fringing and nearshore coral reefs of the Great Barrier Reef: Episodic Holocene development and future prospects, *Journal of Coastal Research*, 22(1): 175-187.
- Stanley, G.A.V. 1928 The physiography of the Bowen district and of the northern isles of the Cumberland Group, *Reports of the Great Barrier Reef Commission*, 2: 1-51.
- Steen, R.M. 1972 History of the Port of Bowen: from a paper read to the Bowen Historical Society, *Bowen Independent*, Bowen.
- Steers, J.A. 1937 The coral islands and associated features of the Great Barrier Reefs, *The Geographic Journal*, 89: 1-28.
- Stephenson, W., Endean, R. and Bennett, I. 1958 An ecological survey of the marine fauna of Low Isles, Queensland, *Australian Journal of Marine and Freshwater Research*, 9: 261-329.
- Stuiver, M. and Reimer, P.J. 1993 Extended 14C database and revised CALIB radiocarbon calibration program, *Radiocarbon* 35: 215-230.
- Suchanek, T.H., Colin, P.L., McMurtry, G.M. and Suchanek, C.S. 1986 Bioturbation and redistribution of sediment radionuclides in Enewetak Atoll lagoon by callianassid shrimp: biological aspects, *Bulletin of Marine Science*, 38(1): 144-154.
- Sweatman, H., Delean, S. and Syms, C. 2011 Assessing loss of coral cover on Australia's Great Barrier Reef over two decades, with implications for longer-term trends, *Coral Reefs*, 30: 521-531.
- Sweatman, H. and Syms, C. 2011 Assessing loss of coral cover on the Great Barrier Reef: A response to Hughes et al. (2011), *Coral Reefs*, 30: 661-664.

- The State of Queensland, 2015 *Water Monitoring Information Portal* <https://water-monitoring.information.qld.gov.au>, Accessed on 13 February 2016.
- Thom, B.G., Orme, G.R. and Polach, H.A. 1978 Drilling investigation of Bewick and Stapleton islands, *Philosophical Transactions of the Royal Society, London A*, 291: 37-54.
- Thompson, A.A. and Dolman, A.M. 2010 Coral bleaching: one disturbance too many for near-shore reefs of the Great Barrier Reef, *Coral Reefs*, 29: 637-648.
- Thompson, A., Costello, P., Davidson, J., Schaffelke, B., Uthicke, S. and Liddy, M. 2013 Reef Rescue Marine Monitoring Program, *Report of AIMS Activities – Inshore coral reef monitoring 2012*, Report for Great Barrier Reef Marine Park Authority, Australian Institute of Marine Science, Townsville.
- Thornborough, K.J. and Davies, P.J. 2011 Reef flats, in in Hopley, D. ed. *Encyclopedia of Modern Coral Reefs – Structure, Form and Process*, Springer, The Netherlands, 869-876.
- Thurstan, R.H. et al. 2015 Filling historical data gaps to foster solutions in marine conservation, *Ocean and Coastal Management*, 115: 31-40.
- Toth, L.T. et al. 2012 ENSO drove 2500-year collapse of eastern Pacific coral reefs, *Science*, 337: 81-84.
- Tudhope, A.W. and Scoffin, T.P. 1994 Growth and structure of fringing reefs in a muddy environment, South Thailand, *Journal of Sedimentary Research*, 64: 752-764.
- van Woerik, R., and Done, T.J. 1997 Coral communities and reef growth in the southern Great Barrier Reef, *Coral Reefs*, 16: 103-115.
- van Woerik, R., DeVantier, L.M. and Glazebrook, J.S. 1995 Effects of Cyclone 'Joy' on nearshore coral communities of the Great Barrier Reef, *Marine Ecology Progress Series*, 128: 261-270.
- van Woerik, R., Tomascik, T. and Blake, S. 1999 Coral assemblages and physico-chemical characteristics of the Whitsunday Islands: evidence of recent community changes, *Marine Freshwater Research*, 50: 427-440.
- Veron, J.E.N 1986 *Coral Reefs of Australia and the Indo-Pacific*, Australian Institute of Marine Science, Townsville.
- Wachenfeld, D. 1997 Long-term trends in the status of coral reef flat benthos: the use of historical photographs, in *Proceedings of the State of the Great Barrier Reef World Heritage Area Workshop: 27-29 November 1995*, Townsville, Queensland, eds. D. Wachenfeld, J. Oliver and K. Davis, Great Barrier Reef Marine Park Authority, Townsville: 134-148.
- Waterhouse, J., Brodie, J., Lewis, S. and Mitchell, A. 2012 Quantifying the sources of pollutants in the Great Barrier Reef catchments and the relative risk to reef ecosystems, *Marine Pollution Bulletin*, 65: 394-406.
- Waters, D.K. et al. 2014 *Modelling reductions of pollutant loads due to improved management practices in the Great Barrier Reef Catchments – Whole of GBR*, Volume 1, Department of Natural Resources and Mines, Technical Report (ISBN: 978-1-7423-0999).
- Webb, G.E., Nothdurft, L.D., Zhao, Z.X., Opdyke, B. and Price, G. 2016 Significance of shallow core transects for reef models and sea-level curves, Heron Reef, Great Barrier Reef, *Sedimentology*, DOI 10.1111/sed.12266.
- Webster, J.M. and Davies, P.J. 2003 Coral variation in two deep drill cores: significance for the Pleistocene development of the Great Barrier Reef, *Sedimentary Geology*, 159: 61-80.
- Wilkinson, C. 2008 *Status of Coral Reefs of the World: 2008*, Global Coral Reef Monitoring Network and Reef and Rainforest Research Centre, Townsville, Australia.

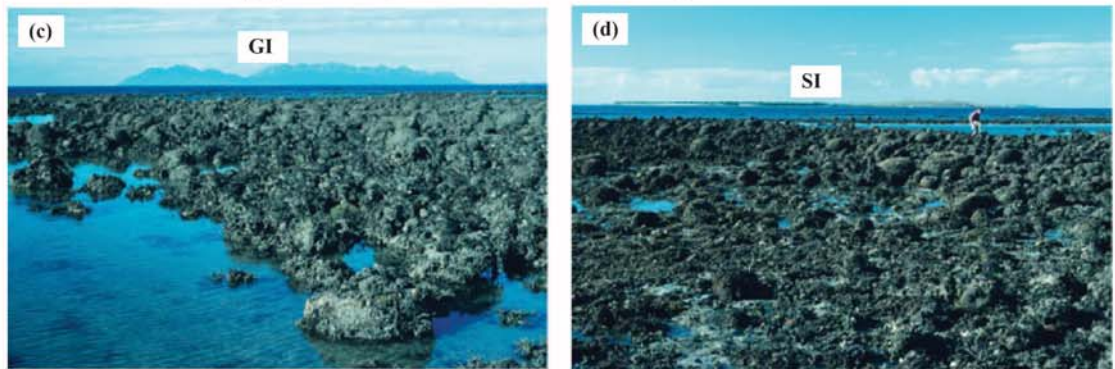
- Wilson, M.E.J. and Lokier, S.W. 2002 Siliciclastic and volcanoclastic influences on equatorial carbonates: insights from the Neogene of Indonesia, *Sedimentology*, 49: 583-601.
- Wolanski, E., Fabricius, K., Spagnol, S. and Brinkman, R. 2005 Fine sediment budget on an inner-shelf coral-fringed island, Great Barrier Reef of Australia, *Estuarine, Coastal and Shelf Science*, 65: 153-158.
- Wolff, N.H., Wong, A., Vitolo, R., Stolberg, K., Anthony, K.R.N. and Mumby, P.J. 2016 Temporal clustering of tropical cyclones on the Great Barrier Reef and its ecological importance, *Coral Reefs*, DOI 10.1007/s00338-016-1400-9.
- Woodroffe, S.A. 2009 Testing models of mid to late Holocene sea-level change, North Queensland, Australia, *Quaternary Science Reviews*, 28: 2474-2488.
- Woodroffe, C.D. and Webster, J.M. 2014 Coral reefs and sea-level change, *Marine Geology*, 352: 248-267.
- Woodroffe, C.D., Kennedy, D.M., Hopley, D., Rasmussen, C.E. and Smithers, S.G. 2000 Holocene reef growth in Torres Strait, *Marine Geology*, 170: 331-346.
- Yu, K. et al. 2012 High-precision U-series ages of transported coral blocks on Heron Reef (southern Great Barrier Reef) and storm activity during the past century, *Palaeogeography, Palaeoclimatology, Palaeoecology*, 337-338: 23-36.
- Zhao, J.X., Hu, K., Collerson, K.D. and Xu, H.K. 2001 Thermal ionization mass spectrometry U-series dating of a hominid site near Nanjing, China, *Geology*, 29(1): 27-30.
- Zhou, H., Zhao, J.X., Qing, W., Feng, Y. and Tang, J. 2011 Speloethem-derived Asian summer monsoon variations in Central China, 54-46 ka, *Journal of Quaternary Science*, 26(8): 781-790.

Appendices

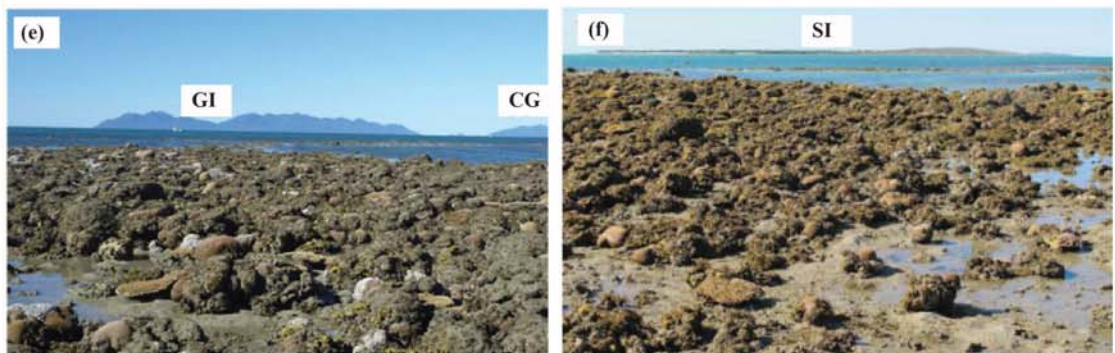
Bramston Reef c. 1890 (Photographer: W. Saville-Kent (1893))



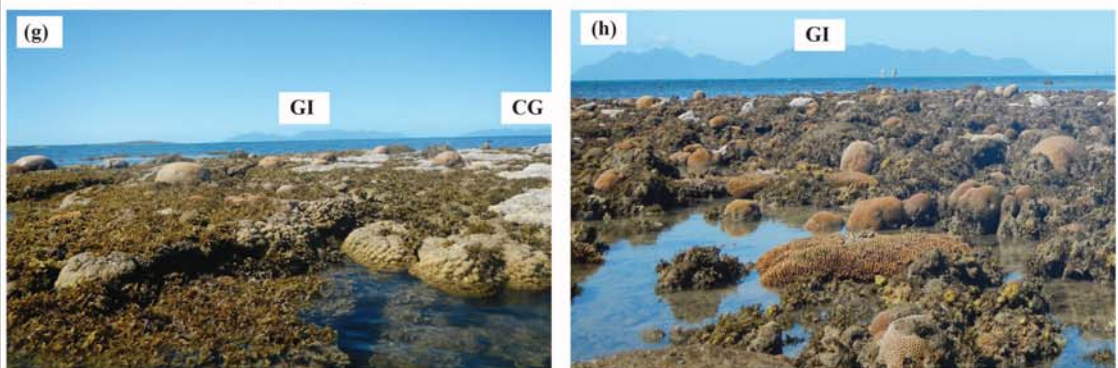
Bramston Reef 1994 (Photographer: A. Elliot, ©Commonwealth of Australia, GBRMPA)



Bramston Reef 2012 (Photographer: N. Leonard, from Clark et al. 2016)



Bramston Reef 2014 (Photographer: E. Ryan)



Bramston Reef c. 1890 (Photographer: W. Saville-Kent (1893))



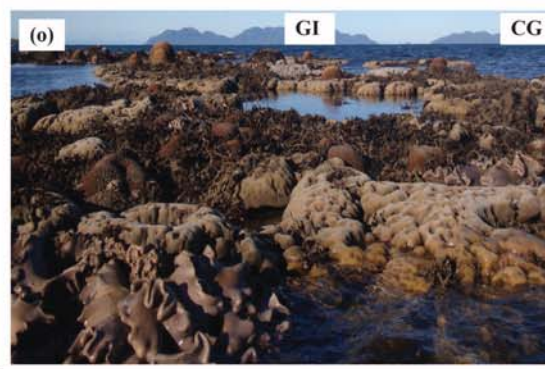
Bramston Reef 1994 (Photographer: A. Elliot, ©Commonwealth of Australia, GBRMPA)

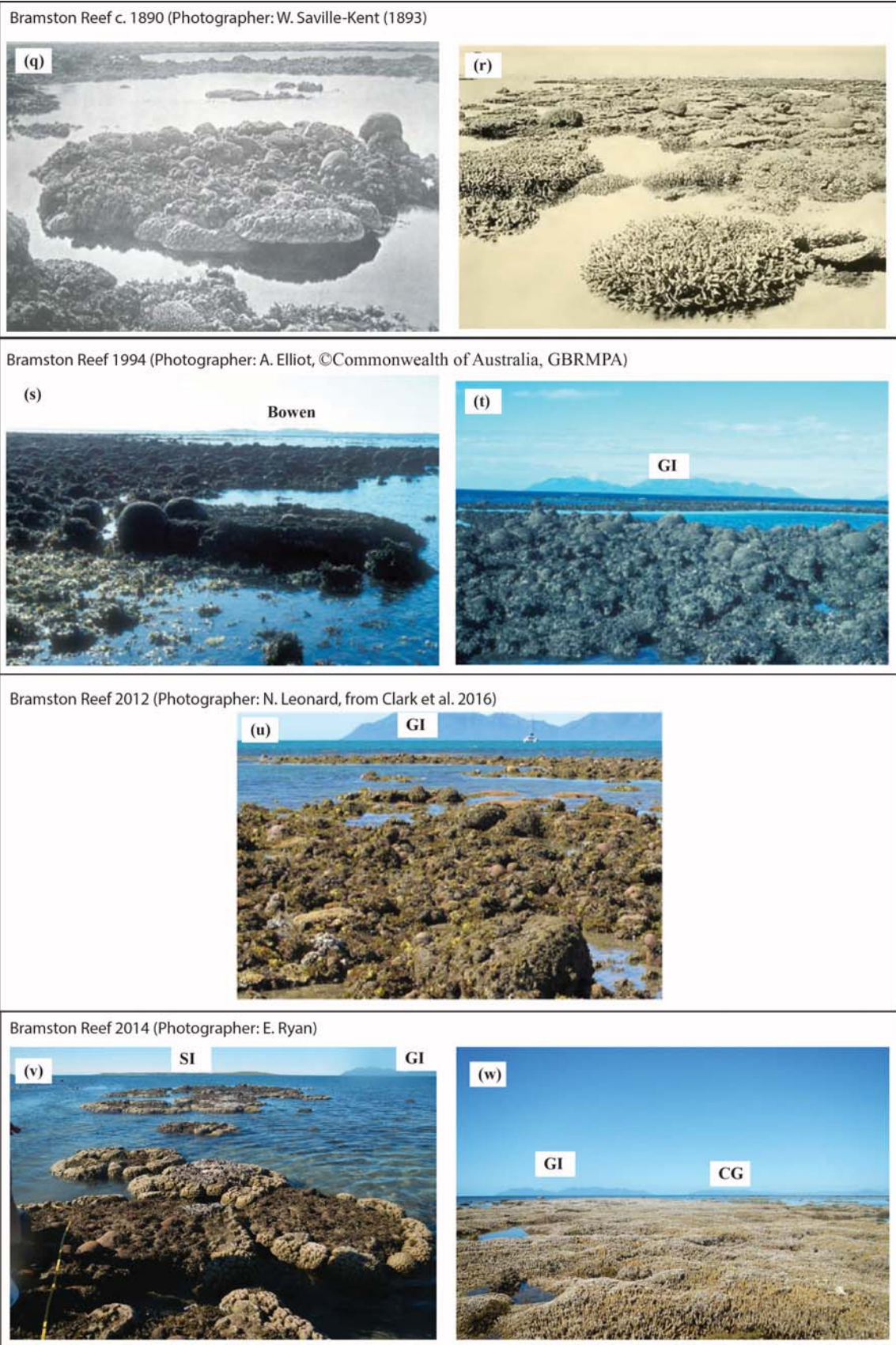


Bramston Reef 2012 (Photographers: H. Markham (m) and N. Leonard (n), from Clark et al. 2016)



Bramston Reef 2014 (Photographer: E. Ryan)





Appendix 1. Collection of photographs from Bramston Reef flat: circa 1890 (Saville-Kent, 1893) (a, b, i, j, q, r) showing live coral, including faviids, *Acropora*, *Porites*, soft corals and macroalgae; 1994 (©Commonwealth of Australia, GBRMPA) (c, d, k, l, s, t) showing very little live coral cover; 2012 (Clark et al., 2016) (e, f, m, n, u) showing dead corals, live corals

including *Acropora* and faviids, and algae; 2014 (g, h, o, p, v, w) showing live coral, including *Acropora*, *Porites* (including large microatolls), faviids, *Montipora*, soft corals, and macroalgae. Gloucester Island (GI), Cape Gloucester (CG), Stone Island (SI), Mount Bramston (Mt. B) and Mount Gordon (Mt. G) are shown in the horizon for reference. Elevations of the 2014 photographs are given in Appendix 10.

Appendix 2. Multicollector inductively coupled plasma mass spectrometer uranium-thorium (U-Th) data from microatoll and core samples from Bramston Reef, Stone Island, Middle Island and Holbourne Island, central Great Barrier Reef.

Sample Name*	Sample genus	Sample weight (g)	U (ppm)	²³² Th (ppb)	(²³⁰ Th/ ²³² Th)	(²³⁰ Th/ ²³⁸ U)	(²³⁴ U/ ²³⁸ U)	uncorr. ²³⁰ Th Age (ka)	corr. ²³⁰ Th Age (ka)†	corr. Initial (²³⁴ U/ ²³⁸ U)	Age (years BP=1950)
BR-FMA-1	<i>Porites</i>	0.1693	3.0083 ± 0.0014	1.5947 ± 0.0053	200.58 ± 1.19	0.035043 ± 0.000173	1.1483 ± 0.0011	3.377 ± 0.017	3.363 ± 0.017	1.1498 ± 0.0011	3298 ± 17
BR-FMA-2	<i>Porites</i>	0.16925	2.6599 ± 0.0008	11.7957 ± 0.0189	26.03 ± 0.11	0.038041 ± 0.000145	1.1454 ± 0.0013	3.681 ± 0.015	3.591 ± 0.023	1.1470 ± 0.0013	3526 ± 23
BR-FMA-3	<i>Porites</i>	0.17837	3.2648 ± 0.0014	0.4103 ± 0.0013	1076.71 ± 4.64	0.044599 ± 0.000136	1.1456 ± 0.0011	4.327 ± 0.014	4.320 ± 0.014	1.1474 ± 0.0012	4256 ± 14
BR-FMA-4	<i>Porites</i>	0.16773	2.7771 ± 0.0014	7.1218 ± 0.0138	46.42 ± 0.17	0.039231 ± 0.000127	1.1464 ± 0.0011	3.794 ± 0.013	3.740 ± 0.017	1.1480 ± 0.0011	3676 ± 17
BR-FMA-5	<i>Porites</i>	0.163	3.0144 ± 0.0017	17.3090 ± 0.0302	23.97 ± 0.07	0.045366 ± 0.000119	1.1455 ± 0.0013	4.403 ± 0.013	4.289 ± 0.026	1.1474 ± 0.0013	4224 ± 26
BR-FMA-6	<i>Porites</i>	0.16963	2.6651 ± 0.0014	14.4766 ± 0.0199	21.15 ± 0.08	0.037872 ± 0.000140	1.1453 ± 0.0009	3.664 ± 0.014	3.555 ± 0.026	1.1470 ± 0.0010	3491 ± 26
BR-FMA-7	<i>Porites</i>	0.17713	3.0085 ± 0.0019	23.7788 ± 0.0493	13.84 ± 0.05	0.036058 ± 0.000100	1.1454 ± 0.0013	3.486 ± 0.011	3.330 ± 0.033	1.1470 ± 0.0013	3266 ± 33
BR-FMA-8	<i>Porites</i>	0.17175	2.8827 ± 0.0014	3.6430 ± 0.0046	93.07 ± 0.29	0.038763 ± 0.000114	1.1439 ± 0.0012	3.757 ± 0.012	3.728 ± 0.013	1.1454 ± 0.0012	3664 ± 13
BR-FMA-9	<i>Porites</i>	0.19533	3.1318 ± 0.0011	1.7810 ± 0.0036	189.66 ± 0.65	0.035547 ± 0.000099	1.1475 ± 0.0010	3.429 ± 0.010	3.414 ± 0.011	1.1490 ± 0.0011	3350 ± 11
BR-FMA-11	<i>Porites</i>	0.15522	2.8553 ± 0.0013	25.8184 ± 0.1307	11.29 ± 0.08	0.033647 ± 0.000184	1.1469 ± 0.0013	3.245 ± 0.018	3.067 ± 0.040	1.1485 ± 0.0013	2686 ± 28
BR-FMA-11	<i>Porites</i>	0.15522	2.8553 ± 0.0013	25.8184 ± 0.1307	11.29 ± 0.08	0.033647 ± 0.000184	1.1469 ± 0.0013	3.245 ± 0.018	3.067 ± 0.040	1.1485 ± 0.0013	3003 ± 40
BR-FMA-12	<i>Porites</i>	0.17108	3.1487 ± 0.0013	8.4324 ± 0.0150	40.30 ± 0.16	0.035567 ± 0.000129	1.1468 ± 0.0010	3.433 ± 0.013	3.378 ± 0.017	1.1483 ± 0.0010	3314 ± 17
BR-P1-40	<i>Favites</i>	0.16692	2.6736 ± 0.0013	2.1952 ± 0.0138	81.78 ± 0.62	0.022130 ± 0.000094	1.1473 ± 0.0009	2.123 ± 0.009	2.102 ± 0.010	1.1482 ± 0.0009	2038 ± 10
BR-P2-160	<i>Turbinaria</i>	0.04757	2.9613 ± 0.0014	8.6778 ± 0.3818	58.54 ± 2.62	0.056537 ± 0.000487	1.1440 ± 0.0015	5.521 ± 0.049	5.461 ± 0.051	1.1463 ± 0.0015	5396 ± 51
BR-P3-200	<i>Acropora</i>	0.23003	3.5446 ± 0.0017	3.5610 ± 0.0067	133.03 ± 0.41	0.044045 ± 0.000109	1.1480 ± 0.0008	4.263 ± 0.011	4.239 ± 0.012	1.1498 ± 0.0008	4175 ± 12
BR-P3-170	<i>Turbinaria</i>	0.18443	3.2207 ± 0.0018	3.1058 ± 0.0065	143.99 ± 0.55	0.045763 ± 0.000149	1.1499 ± 0.0010	4.425 ± 0.015	4.402 ± 0.016	1.1518 ± 0.0011	4338 ± 16
BR-P4-143	<i>Fungia</i>	0.16724	2.8345 ± 0.0014	0.9970 ± 0.0023	421.50 ± 1.45	0.048863 ± 0.000129	1.1463 ± 0.0011	4.746 ± 0.014	4.734 ± 0.014	1.1483 ± 0.0011	4670 ± 14
BR-P6-340	<i>Favites</i>	0.16775	2.3071 ± 0.0007	4.0900 ± 0.0069	78.64 ± 0.40	0.045947 ± 0.000219	1.1480 ± 0.0009	4.450 ± 0.022	4.411 ± 0.023	1.1499 ± 0.0009	4346 ± 23
BR-P6-190	<i>Fungia</i>	0.17904	2.3559 ± 0.0010	0.5361 ± 0.0008	531.73 ± 2.00	0.039881 ± 0.000139	1.1459 ± 0.0011	3.860 ± 0.014	3.850 ± 0.014	1.1475 ± 0.0011	3786 ± 14
BR-P6-75	<i>Acropora</i>	0.1652	3.2633 ± 0.0016	0.4266 ± 0.0010	797.42 ± 3.18	0.034360 ± 0.000114	1.1468 ± 0.0010	3.315 ± 0.012	3.308 ± 0.012	1.1482 ± 0.0011	3244 ± 12
BR-P7-290	<i>Favites</i>	0.17795	2.7183 ± 0.0016	0.2332 ± 0.0007	904.36 ± 3.87	0.025572 ± 0.000082	1.1472 ± 0.0015	2.457 ± 0.009	2.450 ± 0.009	1.1482 ± 0.0015	2386 ± 9
BR-P7-210	<i>Calaustrea</i>	0.21947	2.5525 ± 0.0008	1.0453 ± 0.0016	180.72 ± 0.66	0.024391 ± 0.000081	1.1473 ± 0.0011	2.342 ± 0.008	2.329 ± 0.009	1.1483 ± 0.0011	2265 ± 9
BR-P7-180	<i>Montipora</i>	0.16637	3.2433 ± 0.0016	6.7739 ± 0.0108	31.42 ± 0.14	0.021630 ± 0.000093	1.1457 ± 0.0013	2.078 ± 0.009	2.033 ± 0.013	1.1466 ± 0.0014	1969 ± 13
BR-P8-75	<i>Fungia</i>	0.18084	2.3928 ± 0.0007	1.2241 ± 0.0022	86.13 ± 0.48	0.014522 ± 0.000077	1.1471 ± 0.0014	1.389 ± 0.008	1.373 ± 0.008	1.1477 ± 0.0014	1309 ± 8

BR-P8-170	<i>Platygyra</i>	0.19031	2.6415 ± 0.0013	0.2231 ± 0.0006	572.93 ± 3.07	0.015947 ± 0.000073	1.1462 ± 0.0016	1.527 ± 0.007	1.520 ± 0.008	1.1468 ± 0.0016	1456 ± 8
SI-S-P1-58	<i>Montipora</i>	0.21575	3.1467±0.0026	19.4274±0.0199	34.34±0.07	0.0699±0.0001	1.1431±0.0008	6.869±0.015	6.746±0.029	1.1460±0.0008	6681±29
SI-S-P1-160	<i>Echinophyllia?</i>	0.16562	2.9049±0.0015	6.4259±0.0063	99.32±0.22	0.0724±0.0001	1.1438±0.0008	7.122±0.016	7.075±0.018	1.1468±0.0008	7010±18
SI-S-P1-205	<i>Acropora</i>	0.21053	3.0082±0.0016	4.9554±0.0056	137.20±0.27	0.0745±0.0001	1.1454±0.0009	7.323±0.014	7.287±0.016	1.1485±0.0009	7222±16
SI-S-P3-140	<i>Montipora</i>	0.19953	3.1606±0.0016	12.2095±0.0172	57.45±0.13	0.0731±0.0001	1.1446±0.0009	7.191±0.015	7.113±0.022	1.1477±0.0010	7048±22
SI-S-P5-230	<i>Acropora?</i>	0.20736	3.9607±0.0027	24.8726±0.0302	34.51±0.10	0.0714±0.0002	1.1457±0.0009	7.010±0.020	6.886±0.032	1.1487±0.0009	6821±32
SI-S-P5-270	<i>Acropora?</i>	0.17518	3.1187±0.0018	13.6891±0.0091	49.90±0.11	0.0722±0.0002	1.1460±0.0008	7.085±0.017	6.996±0.024	1.1491±0.0008	6931±24
SI-S-P5-305	<i>Galaxea</i>	0.16176	3.3103±0.0018	3.7376±0.0051	192.51±0.52	0.0716±0.0002	1.1475±0.0011	7.020±0.018	6.994±0.019	1.1505±0.0011	6929±19
SI-S-P5-340	<i>Astreopora</i>	0.16991	2.8840±0.0018	10.6622±0.0171	60.40±0.18	0.0736±0.0002	1.1466±0.0013	7.224±0.021	7.148±0.026	1.1497±0.0013	7083±26
SI-S-P6-243	<i>Fungia</i>	0.24719	3.1007±0.0018	4.1694±0.0042	141.86±0.35	0.0629±0.0001	1.1460±0.0009	6.146±0.016	6.116±0.017	1.1485±0.0009	6051±17
SI-S-P6-320	<i>Acropora</i>	0.15603	3.4518±0.0032	16.5770±0.0158	41.45±0.07	0.0656±0.0001	1.1442±0.0010	6.431±0.013	6.335±0.023	1.1470±0.0010	6270±23
SI-S-P6-348	<i>Acropora</i>	0.19332	3.8507±0.0019	14.2128±0.0393	55.14±0.19	0.0671±0.0001	1.1467±0.0009	6.564±0.015	6.490±0.021	1.1495±0.0009	6425±21
SI-S-P6-370	<i>Goniastrea?</i>	0.16593	2.7815±0.0017	10.3483±0.0111	61.31±0.14	0.0752±0.0002	1.1460±0.0010	7.388±0.017	7.312±0.023	1.1491±0.0010	7247±23
SI-S-P9-90	<i>Acropora</i>	0.18877	3.4118±0.0013	16.3489±0.0135	29.25±0.06	0.0462±0.0001	1.1456±0.0011	4.485±0.010	4.389±0.022	1.1476±0.0011	4324±22
SI-S-P9-170	<i>Porites?</i>	0.21903	2.8464±0.0018	1.1778±0.0014	336.86±0.79	0.0459±0.0001	1.1447±0.0011	4.463±0.011	4.450±0.011	1.1466±0.0012	4385±11
SI-N-P1-120	<i>Turbinaria</i>	0.1513	3.7116±0.0023	9.5592±0.0091	77.19±0.18	0.0655±0.0001	1.1449±0.0011	6.419±0.016	6.366±0.019	1.1476±0.0011	6301±19
SI-N-P1-137	<i>Acropora</i>	0.15099	3.3960±0.0019	4.7758±0.0053	115.53±0.28	0.0535±0.0001	1.1459±0.0010	5.213±0.013	5.182±0.014	1.1481±0.0010	5117±14
SI-N-P2-255	<i>Dipsastraea?</i>	0.15749	2.4786±0.0015	13.9761±0.0158	37.78±0.08	0.0702±0.0001	1.1442±0.0010	6.896±0.014	6.783±0.026	1.1472±0.0010	6718±26
SI-N-P2-290	<i>Cyphastrea</i>	0.21055	2.6844±0.0008	4.2976±0.0041	133.36±0.27	0.0704±0.0001	1.1441±0.0010	6.913±0.014	6.877±0.016	1.1470±0.0011	6812±16
SI-N-P3-153	<i>Turbinaria</i>	0.1553	3.3376±0.0023	4.9700±0.0055	115.97±0.29	0.0569±0.0001	1.1456±0.0008	5.551±0.014	5.519±0.016	1.1479±0.0009	5454±16
SI-N-P3-243	<i>Acropora</i>	0.18981	3.3703±0.0014	15.7033±0.0346	46.18±0.14	0.0709±0.0002	1.1439±0.0006	6.970±0.017	6.877±0.025	1.1469±0.0006	6812±25
SI-N-P4-87	<i>Hydnophora</i>	0.17439	2.9422±0.0015	11.3488±0.0113	39.43±0.10	0.0501±0.0001	1.1472±0.0009	4.867±0.012	4.788±0.020	1.1493±0.0010	4723±20
SI-N-P5-55	<i>Montastrea?</i>	0.16615	2.7145±0.0015	8.4770±0.0080	44.72±0.12	0.0460±0.0001	1.1443±0.0010	4.473±0.013	4.408±0.018	1.1462±0.0010	4343±18
SI-N-P5-155	<i>Acropora</i>	0.19371	3.2528±0.0018	4.9628±0.0099	114.54±0.39	0.0576±0.0002	1.1455±0.0008	5.620±0.017	5.586±0.018	1.1479±0.0008	5521±18
SI-N-P5-280	<i>Galaxea</i>	0.15815	3.0829±0.0019	5.3853±0.0052	126.84±0.27	0.0730±0.0001	1.1465±0.0006	7.167±0.015	7.129±0.017	1.1496±0.0006	7064±17
SI-N-P5-220	<i>Montipora</i>	0.16677	3.3881±0.0015	18.5639±0.0239	35.78±0.09	0.0646±0.0001	1.1436±0.0011	6.333±0.015	6.224±0.026	1.1463±0.0011	6159±26
SI-S-FMA-1	<i>Porites</i>	0.1556	3.0897±0.0017	4.1796±0.0035	104.75±0.27	0.0467±0.0001	1.1475±0.0009	4.527±0.012	4.497±0.014	1.1494±0.0009	4432±14
SI-S-FMA-2	<i>Porites</i>	0.2076	2.7754±0.0015	2.2285±0.0026	151.06±0.44	0.0400±0.0001	1.1450±0.0008	3.872±0.011	3.852±0.012	1.1466±0.0008	3787±12

SI-S-FMA-3	<i>Porites</i>	0.17588	2.8840±0.0009	6.1024±0.0110	96.77±0.26	0.0675±0.0001	1.1431±0.0014	6.628±0.016	6.582±0.019	1.1458±0.0014	6518±19
SI-S-FMA-4	<i>Porites</i>	0.16906	3.0751±0.0018	5.2987±0.0071	122.11±0.39	0.0693±0.0002	1.1427±0.0010	6.818±0.021	6.780±0.023	1.1455±0.0010	6716±23
SI-S-FMA-5	<i>Porites</i>	0.17473	3.4858±0.0013	0.3191±0.0006	2058±5.2	0.0621±0.0001	1.1422±0.0012	6.090±0.013	6.084±0.013	1.1447±0.0013	6020±13
SI-S-FMA-6	<i>Porites</i>	0.16148	2.8541±0.0017	8.1953±0.0144	73.18±0.22	0.0693±0.0002	1.1431±0.0013	6.807±0.020	6.747±0.23	1.1459±0.0014	6683±23
SI-S-FMA-7	<i>Porites</i>	0.16971	2.9055±0.0012	5.9842±0.0184	90.33±0.39	0.0613±0.0002	1.1437±0.0010	6.002±0.020	5.958±0.022	1.1462±0.0011	5894±22
SI-S-FMA-8	<i>Porites</i>	0.24771	2.9610±0.0014	6.9935±0.0089	87.92±0.24	0.0684±0.0002	1.1449±0.0010	6.713±0.018	6.663±0.021	1.1478±0.0011	6599±21
SI-S-FMA-9	<i>Porites</i>	0.16688	3.0193±0.0013	26.6601±0.0332	25.52±0.07	0.0743±0.0002	1.1394±0.0011	7.341±0.021	7.167±0.040	1.1425±0.0011	7103±40
SI-S-FMA-10	<i>Porites</i>	0.21337	2.8451±0.0021	2.0915±0.0043	288.51±0.94	0.0699±0.0002	1.1448±0.0009	6.861±0.019	6.842±0.020	1.1477±0.0009	6777±20
SI-S-FMA-11	<i>Porites</i>	0.16964	2.6623±0.0019	4.3082±0.0044	132.76±0.26	0.0708±0.0001	1.1446±0.0009	6.954±0.014	6.918±0.016	1.1476±0.0010	6853±16
SI-S-FMA-12	<i>Porites</i>	0.23411	2.7961±0.0012	8.8096±0.0080	64.68±0.15	0.0672±0.0002	1.1456±0.0007	6.581±0.016	6.516±0.020	1.1484±0.0007	6451±20
SI-S-FMA-13	<i>Porites</i>	0.16273	2.8711±0.0021	11.6698±0.0128	51.79±0.13	0.0694±0.0002	1.1438±0.0010	6.815±0.017	6.732±0.024	1.1466±0.0010	6667±24
SI-N-FMA-14	<i>Porites</i>	0.1689	2.7336±0.0016	29.7643±0.0356	13.63±0.04	0.0489±0.0001	1.1453±0.0010	4.754±0.013	4.540±0.045	1.1475±0.0010	4475±45
SI-N-FMA-15	<i>Porites</i>	0.18224	2.7080±0.0015	1.8490±0.0022	100.60±0.37	0.0226±0.0001	1.1462±0.0009	2.174±0.008	2.156±0.009	1.1472±0.0009	2091±9
SI-N-FMA-16	<i>Porites</i>	0.1687	2.6780±0.0014	10.8745±0.0106	16.87±0.08	0.0226±0.0001	1.1478±0.0011	2.165±0.010	2.083±0.019	1.1488±0.0011	2018±19
MI-FMA-1	<i>Porites</i>	0.17665	3.1819 ± 0.0012	1.5715 ± 0.0173	435.91 ± 4.19	0.070956 ± 0.000168	1.1440 ± 0.0012	6.973 ± 0.019	6.959 ± 0.019	1.1469 ± 0.0012	6895 ± 19
MI-FMA-2	<i>Porites</i>	0.17096	2.8067 ± 0.0014	4.7207 ± 0.0073	3.41 ± 0.04	0.001890 ± 0.000020	1.1472 ± 0.0012	0.180 ± 0.002	0.143 ± 0.008	1.1473 ± 0.0012	78 ± 8
MI-FMA-3	<i>Porites</i>	0.17204	3.0201 ± 0.0013	1.7019 ± 0.0036	18.06 ± 0.16	0.003354 ± 0.000029	1.1452 ± 0.0013	0.320 ± 0.003	0.304 ± 0.004	1.1453 ± 0.0013	240 ± 4
MI-FMA-4	<i>Porites</i>	0.16562	2.8905 ± 0.0016	0.5016 ± 0.0011	30.73 ± 0.52	0.001758 ± 0.000029	1.1468 ± 0.0009	0.167 ± 0.003	0.159 ± 0.003	1.1469 ± 0.0009	95 ± 3
MI-FMA-5	<i>Porites</i>	0.17453	2.8086 ± 0.0010	2.5323 ± 0.0051	5.90 ± 0.07	0.001754 ± 0.000021	1.1443 ± 0.0008	0.167 ± 0.002	0.145 ± 0.005	1.1444 ± 0.0008	81 ± 5
MI-FMA-6	<i>Porites</i>	0.21671	2.6435 ± 0.0011	0.7088 ± 0.0016	20.00 ± 0.30	0.001768 ± 0.000027	1.1450 ± 0.0009	0.168 ± 0.003	0.158 ± 0.003	1.1451 ± 0.0009	94 ± 3
MI-FMA-7	<i>Porites</i>	0.15135	2.9265 ± 0.0013	1.8049 ± 0.0027	8.54 ± 0.13	0.001736 ± 0.000027	1.1466 ± 0.0013	0.165 ± 0.003	0.149 ± 0.004	1.1467 ± 0.0013	84 ± 4
MI-FMA-8	<i>Porites</i>	0.19911	3.0088 ± 0.0017	2.4795 ± 0.0049	12.56 ± 0.10	0.003411 ± 0.000027	1.1444 ± 0.0010	0.325 ± 0.003	0.305 ± 0.005	1.1446 ± 0.0010	241 ± 5
MI-FMA-9	<i>Porites</i>	0.17186	3.0207 ± 0.0013	1.9607 ± 0.0159	14.09 ± 0.17	0.003015 ± 0.000028	1.1441 ± 0.0010	0.288 ± 0.003	0.271 ± 0.004	1.1443 ± 0.0010	206 ± 4
MI-FMA-10	<i>Porites</i>	0.17564	2.8426 ± 0.0015	1.6544 ± 0.0024	13.95 ± 0.16	0.002677 ± 0.000031	1.1457 ± 0.0013	0.255 ± 0.003	0.239 ± 0.004	1.1458 ± 0.0013	175 ± 4
MI-P1-200	<i>Acropora</i>	0.15535	3.2997 ± 0.0020	26.8893 ± 0.0234	28.53 ± 0.05	0.0766 ± 0.0001	1.1446 ± 0.0011	7.545 ± 0.016	7.385 ± 0.035	1.1479 ± 0.0011	7320 ± 35
MI-P1-150	<i>Isopora?</i>	0.1534	3.0438 ± 0.0017	14.4597 ± 0.0144	47.39 ± 0.11	0.0742 ± 0.0002	1.1437 ± 0.0010	7.305 ± 0.017	7.210 ± 0.026	1.1468 ± 0.0010	7145 ± 26
MI-P2-55	<i>Pavona</i>	0.17066	3.7599 ± 0.0015	19.9783 ± 0.0202	41.05 ± 0.10	0.0719 ± 0.0002	1.1458 ± 0.0012	7.057 ± 0.017	6.952 ± 0.027	1.1488 ± 0.0012	6887 ± 27
MI-P2-110	<i>Dipsastraea</i>	0.17661	2.6802 ± 0.0012	25.4699 ± 0.0267	23.76 ± 0.06	0.0744 ± 0.0002	1.1442 ± 0.0011	7.324 ± 0.018	7.137 ± 0.041	1.1475 ± 0.0011	7072 ± 41

MI-P2-160	?	0.15531	3.9771 ± 0.0031	24.9074 ± 0.0270	36.22 ± 0.07	0.0748 ± 0.0001	1.1434 ± 0.0013	7.364 ± 0.016	7.240 ± 0.029	1.1466 ± 0.0013	7175 ± 29
MI-P4-145	<i>Porites</i>	0.15008	3.2282 ± 0.0018	7.8353 ± 0.0110	95.04 ± 0.27	0.0760 ± 0.0002	1.1455 ± 0.0010	7.478 ± 0.021	7.427 ± 0.023	1.1487 ± 0.0010	7362 ± 23
MI-P6-100	<i>Hydnophora?</i>	0.19221	2.9347 ± 0.0014	8.7262 ± 0.0081	72.72 ± 0.15	0.0713 ± 0.0001	1.1444 ± 0.0010	7.003 ± 0.015	6.941 ± 0.019	1.1473 ± 0.0010	6876 ± 19
MI-P5-250	<i>Acropora</i>	0.15785	3.4156 ± 0.0020	81.3308 ± 0.0610	10.69 ± 0.02	0.0839 ± 0.0002	1.1424 ± 0.0008	8.305 ± 0.017	7.844 ± 0.093	1.1463 ± 0.0008	7779 ± 93
MI-P7-95	<i>Acropora</i>	0.1592	3.2160 ± 0.0019	8.5709 ± 0.0100	20.63 ± 0.09	0.0181 ± 0.0001	1.1465 ± 0.0008	1.737 ± 0.008	1.681 ± 0.014	1.1473 ± 0.0008	1616 ± 14
MI-P8-70	<i>Acropora</i>	0.16275	3.1938 ± 0.0018	5.1999 ± 0.0046	33.38 ± 0.14	0.0179 ± 0.0001	1.1461 ± 0.0008	1.717 ± 0.007	1.682 ± 0.010	1.1468 ± 0.0008	1617 ± 10
MI-P8-200	<i>Acropora?</i>	0.1551	3.7846 ± 0.0024	5.5028 ± 0.0041	139.32 ± 0.36	0.0668 ± 0.0002	1.1463 ± 0.0011	6.536 ± 0.018	6.504 ± 0.019	1.1490 ± 0.0011	6439 ± 19
MI-D1-36	<i>Porites</i>	0.17184	2.8051 ± 0.0011	10.3322 ± 0.0108	11.67 ± 0.05	0.0142 ± 0.0001	1.1468 ± 0.0008	1.355 ± 0.006	1.280 ± 0.016	1.1474 ± 0.0009	1215 ± 16
MI-D1-450	<i>Dipsastraea?</i>	0.17332	3.2377 ± 0.0018	2.6943 ± 0.0025	293.75 ± 0.55	0.0806 ± 0.0001	1.1431 ± 0.0010	7.958 ± 0.016	7.938 ± 0.017	1.1464 ± 0.0011	7873 ± 17
MI-D1-710	?	0.18929	4.2148 ± 0.0038	34.5816 ± 0.0564	29.18 ± 0.07	0.0789 ± 0.0002	1.1423 ± 0.0014	7.794 ± 0.020	7.634 ± 0.037	1.1456 ± 0.0014	7569 ± 37
MI-D1-100	?	0.15401	2.5297 ± 0.0019	4.2254 ± 0.0071	24.97 ± 0.16	0.0137 ± 0.0001	1.1457 ± 0.0011	1.316 ± 0.008	1.278 ± 0.011	1.1463 ± 0.0011	1213 ± 11
HI-P1-10	<i>Porites</i>	0.15454	2.8663 ± 0.0012	35.0528 ± 0.0372	2.13 ± 0.02	0.0086 ± 0.0001	1.1462 ± 0.0008	0.821 ± 0.007	0.582 ± 0.048	1.1468 ± 0.0008	517 ± 48
HI-P1-110	<i>Favites?</i>	0.16045	2.7212 ± 0.0015	2.0712 ± 0.0022	291.30 ± 0.78	0.0731 ± 0.0002	1.1446 ± 0.0009	7.184 ± 0.019	7.165 ± 0.020	1.1476 ± 0.0010	7100 ± 20
HI-P3-35	<i>Dipsastraea</i>	0.15431	3.1142 ± 0.0020	9.3400 ± 0.0097	67.33 ± 0.16	0.0665 ± 0.0001	1.1448 ± 0.0009	6.523 ± 0.016	6.461 ± 0.020	1.1476 ± 0.0009	6396 ± 20
HI-P3-145	<i>Porites?</i>	0.15847	3.4105 ± 0.0020	6.0905 ± 0.0083	125.81 ± 0.33	0.0740 ± 0.0002	1.1449 ± 0.0009	7.281 ± 0.019	7.243 ± 0.020	1.1480 ± 0.0009	7178 ± 20
HI-P4-60	<i>Dipsastraea</i>	0.15511	3.4990 ± 0.0020	7.1010 ± 0.0078	96.88 ± 0.24	0.0648 ± 0.0001	1.1449 ± 0.0009	6.346 ± 0.016	6.303 ± 0.018	1.1475 ± 0.0009	6238 ± 18
HI-P4-105	<i>Acropora</i>	0.16358	3.5527 ± 0.0023	5.7588 ± 0.0057	124.31 ± 0.33	0.0664 ± 0.0002	1.1454 ± 0.0009	6.505 ± 0.018	6.470 ± 0.019	1.1481 ± 0.0009	6406 ± 19
HI-P5-20	?	0.15672	4.3009 ± 0.0018	15.6908 ± 0.0186	12.72 ± 0.04	0.0153 ± 0.0001	1.1469 ± 0.0009	1.464 ± 0.005	1.391 ± 0.015	1.1476 ± 0.0009	1326 ± 15
HI-D1-60	<i>Porites</i>	0.16189	2.7820 ± 0.0022	0.8230 ± 0.0011	39.61 ± 0.31	0.0039 ± 0.0000	1.1460 ± 0.0011	0.368 ± 0.003	0.357 ± 0.004	1.1461 ± 0.0012	292 ± 4
HI-D1-640	<i>Platygyria?</i>	0.16035	2.6411 ± 0.0017	0.3855 ± 0.0004	1604.12 ± 3.94	0.0772 ± 0.0002	1.1456 ± 0.0013	7.593 ± 0.020	7.585 ± 0.020	1.1487 ± 0.0014	7520 ± 20
HI-D1-800	?	0.17577	3.0853 ± 0.0024	2.5875 ± 0.0029	250.50 ± 0.68	0.0692 ± 0.0002	1.1467 ± 0.0009	6.783 ± 0.019	6.762 ± 0.019	1.1496 ± 0.0009	6697 ± 19
HI-D4-110	?	0.15665	2.3437 ± 0.0016	0.2959 ± 0.0005	687.76 ± 2.6	0.0286 ± 0.0001	1.1461 ± 0.0011	2.756 ± 0.010	2.748 ± 0.010	1.1472 ± 0.0011	2683 ± 10
HI-D3-37	<i>Porites</i>	0.16156	2.6681 ± 0.0018	0.2676 ± 0.0005	104.00 ± 0.83	0.0034 ± 0.0000	1.1456 ± 0.0011	0.328 ± 0.003	0.321 ± 0.003	1.1457 ± 0.0011	256 ± 3
HI-D3-330	<i>Favites</i>	0.15349	2.9891 ± 0.0016	0.8949 ± 0.0011	761.91 ± 1.61	0.0752 ± 0.0001	1.1433 ± 0.0013	7.407 ± 0.016	7.396 ± 0.016	1.1463 ± 0.0013	7331 ± 16
HI-D3-350	<i>Acropora</i>	0.16783	3.6183 ± 0.0020	3.8074 ± 0.0035	220.67 ± 0.42	0.0765 ± 0.0001	1.1451 ± 0.0012	7.532 ± 0.016	7.508 ± 0.017	1.1483 ± 0.0012	7443 ± 17
HI-D2-10	<i>Porites</i>	0.15721	2.9391 ± 0.0018	4.2492 ± 0.0043	7.35 ± 0.05	0.0035 ± 0.0000	1.1455 ± 0.0013	0.334 ± 0.002	0.301 ± 0.007	1.1457 ± 0.0013	236 ± 7
HI-D2-620	?	0.05713	1.4915 ± 0.0009	83.7686 ± 0.1063	44.04 ± 0.09	0.8152 ± 0.0015	1.1121 ± 0.0011	138.91 ± 0.59	137.84 ± 0.61	1.1673 ± 0.0016	137778 ± 608
HI-FMA-1	<i>Porites</i>	0.22481	2.9284 ± 0.0013	4.4440 ± 0.0109	9.57 ± 0.06	0.004787 ± 0.000030	1.1456 ± 0.0012	0.457 ± 0.003	0.423 ± 0.007	1.1458 ± 0.0012	359 ± 7

HI-FMA-2	<i>Porites</i>	0.20076	2.8052 ± 0.0011	5.7741 ± 0.0218	10.79 ± 0.07	0.007317 ± 0.000041	1.1468 ± 0.0012	0.698 ± 0.004	0.654 ± 0.010	1.1472 ± 0.0012	589 ± 10
HI-FMA-3	<i>Porites</i>	0.18129	2.7744 ± 0.0018	2.0148 ± 0.0021	13.16 ± 0.11	0.0031 ± 0.0000	1.1466 ± 0.0008	0.300 ± 0.003	0.281 ± 0.005	1.1468 ± 0.0008	216 ± 5
HI-FMA-4	<i>Porites</i>	0.16514	2.9699 ± 0.0020	1.5833 ± 0.0021	16.84 ± 0.12	0.0030 ± 0.0000	1.1476 ± 0.0009	0.281 ± 0.002	0.266 ± 0.004	1.1478 ± 0.0009	202 ± 4
HI-FMA-5	<i>Porites</i>	0.20117	2.9353 ± 0.0019	2.0755 ± 0.0027	8.17 ± 0.10	0.0019 ± 0.0000	1.1470 ± 0.0008	0.181 ± 0.002	0.163 ± 0.004	1.1471 ± 0.0008	98 ± 4

Ratios in parentheses are activity ratios calculated from atomic ratios using decay constants of Cheng et al. (2000). All values have been corrected for laboratory procedural blanks. All errors reported as 2σ. Uncorrected ²³⁰Th age was calculated using Isoplot/EX 3.0 program (Ludwig, 2003), where ka denotes thousand years.

*For the sample nomenclature, BR-P1-40 refers to Bramston Reef (SI-S = Stone Island South; SI-N = Stone Island North; MI = Middle Island; HI = Holbourne Island), percussion core (D = drill core), core one, 40 cm downcore where the coral sample was dated. BR-FMA-1 refers to Bramston Reef fossil microatoll sample one. †²³⁰Th ages corrected using a model two-component correction value based on the equation from Clark et al. (2014):

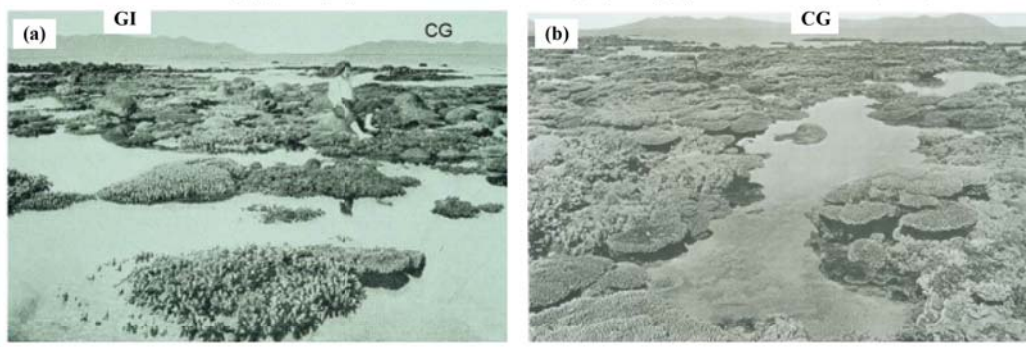
$$\left(\frac{^{230}\text{Th}}{^{232}\text{Th}}\right)_{\text{mix}} = \left(\left(\frac{^{232}\text{Th}_{\text{live}}}{^{232}\text{Th}_{\text{dead}}}\right) \times \left(\frac{^{230}\text{Th}}{^{232}\text{Th}}\right)_{\text{live}}\right) + \left(\left(\frac{^{232}\text{Th}_{\text{dead}} - ^{232}\text{Th}_{\text{live}}}{^{232}\text{Th}_{\text{dead}}}\right) \times \left(\frac{^{230}\text{Th}}{^{232}\text{Th}}\right)_{\text{sed}}\right)$$

where ²³²Th_{dead} is the measured ²³²Th value (ppb) in the non-living coral sample. ²³²Th_{live} is the mean measured ²³²Th value (ppb) determined to be 0.95 ppb and ²³⁰Th/²³²Th_{live} represents or approximates the isotopic composition of the hydrogenous component in the dead coral skeleton with an atomic value of 5.85 × 10⁻⁶ ± 20% (which corresponds to an activity value of 1.08 ± 20%) based on live *Porites* corals collected from the Palm Islands region (Clark et al., 2014) which is of a similar setting to the reefs in this study. ²³⁰Th/²³²Th_{sed} is the detrital component represented by a mean atomic value of 3.53 × 10⁻⁶ ± 20% (which corresponds to an activity value of 0.61 ± 20%) from isochron derived initial ²³⁰Th/²³²Th values obtained from dead *Porites* coral skeletons collected from the Palm Islands region (Clark et al., 2014).

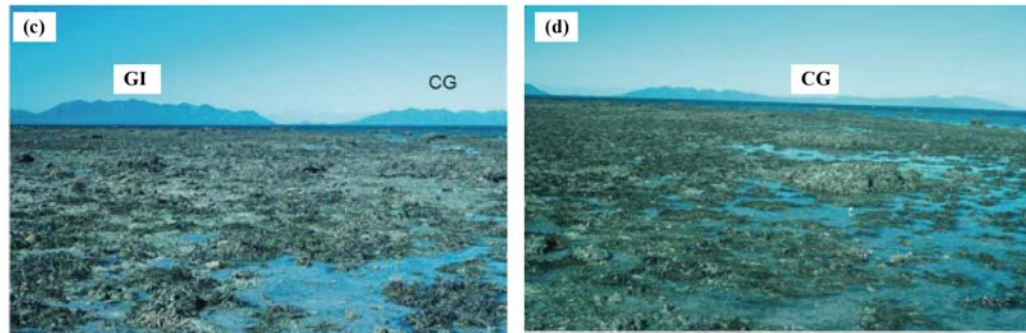
References

- Ludwig, K.R. 2003 *Users Manual for Isoplot/Ex version 3.0: A Geochronological Toolkit for Microsoft Excel*, Berkeley Geochronology Centre Special Publication No.3, Berkeley.
- Cheng, H., Edwards, R.L., Hoff, J., Gallup, C.D., Richards, D.A. and Asmerom, Y. 2000 The half-lives of uranium-234 and thorium-230, *Chemical Geology*, 169: 17-33.
- Clark, T.R. et al. 2014 Discerning the timing and cause of historical mortality events in modern *Porites* from the Great Barrier Reef, *Geochimica et Cosmochimica Acta*, 138: 57-80.

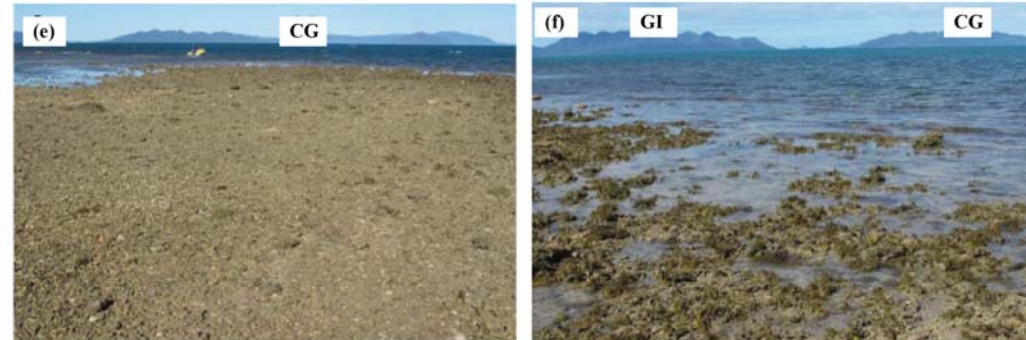
Stone Island Reef c.1915 (a) and 1890 (b) (Photographer of [b]: W. Saville-Kent, 1893)



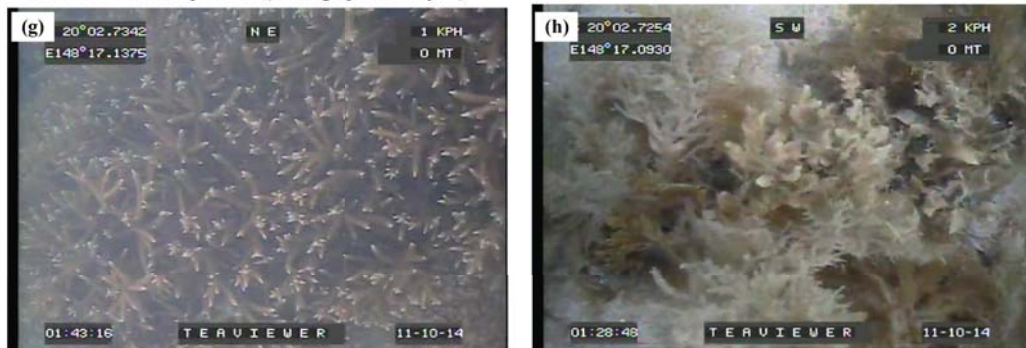
Stone Island Reef 1994 (Photographer: A. Elliot, ©Commonwealth of Australia, GBRMPA)



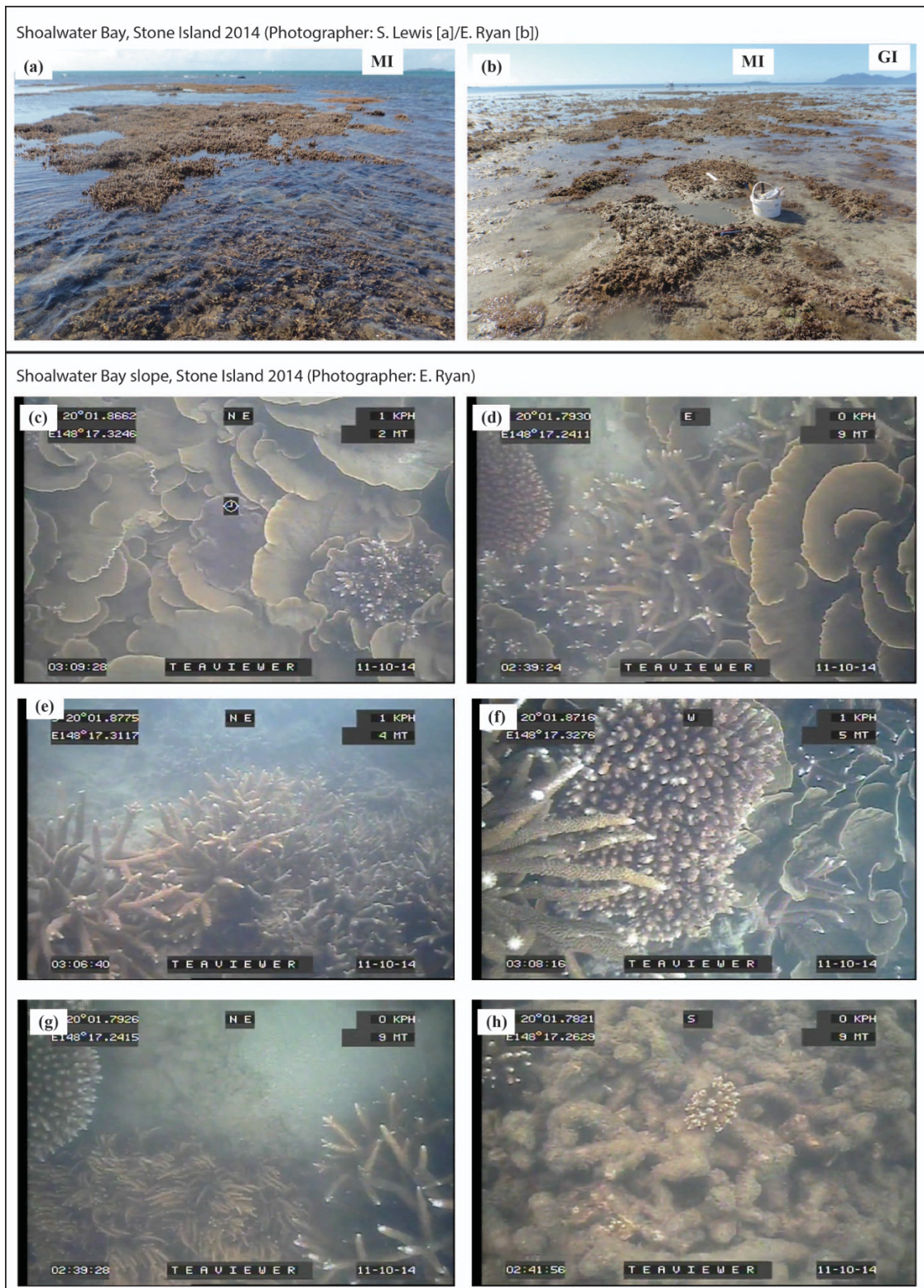
Stone Island Reef 2012 (Photographer: N Leonard, from Clark et al. 2016)



Stone Island Reef slope 2014 (Photographer: E.Ryan)

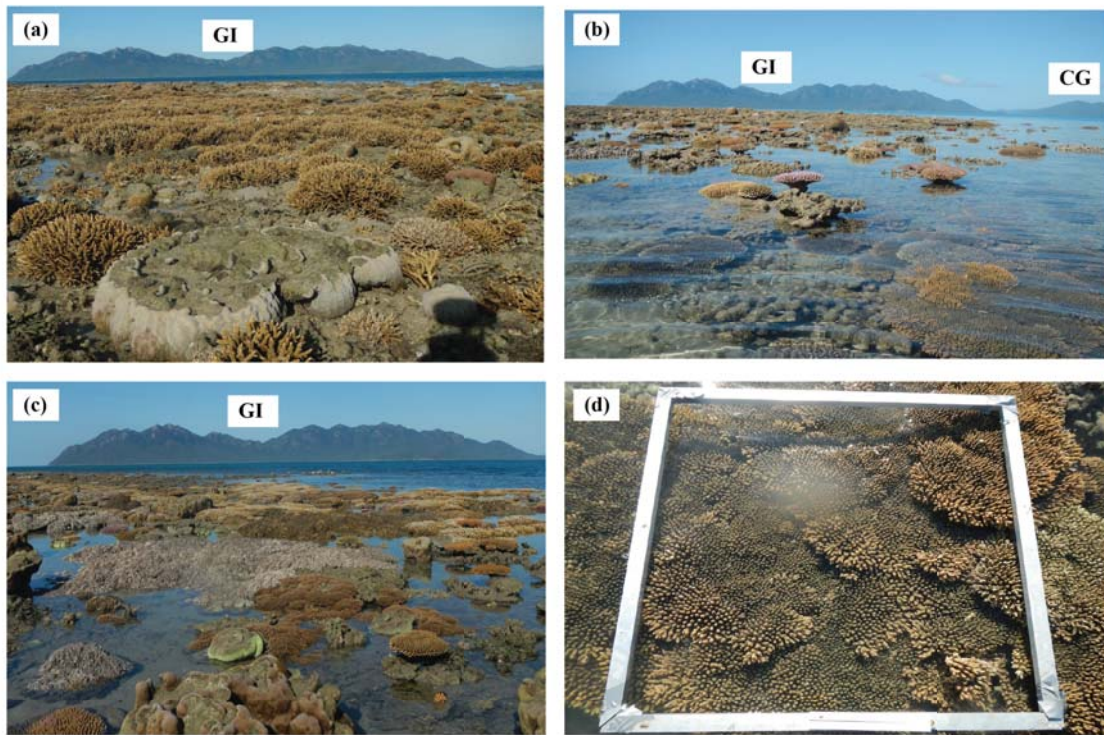


Appendix 3. Photographs from Stone Island South. (a) c. 1915 (from Clark et al., 2016); (b) 1890 (Saville-Kent, 1893) showing live coral of *Acropora*, *Montipora*, *Goniastrea*, *Fungia* and *Turbinaria*; (c, d) 1994 (©Commonwealth of Australia, GBRMPA) showing macroalgae; (e, f) 2012 (Clark et al., 2016) showing macroalgae. Gloucester Island (GI) and Cape Gloucester (CG) are in the horizon; (g, h) 2014 photographs extracted from video footage of the reef slope showing occasional live *Acropora*, and high macroalgae cover (typical of the reef slope).

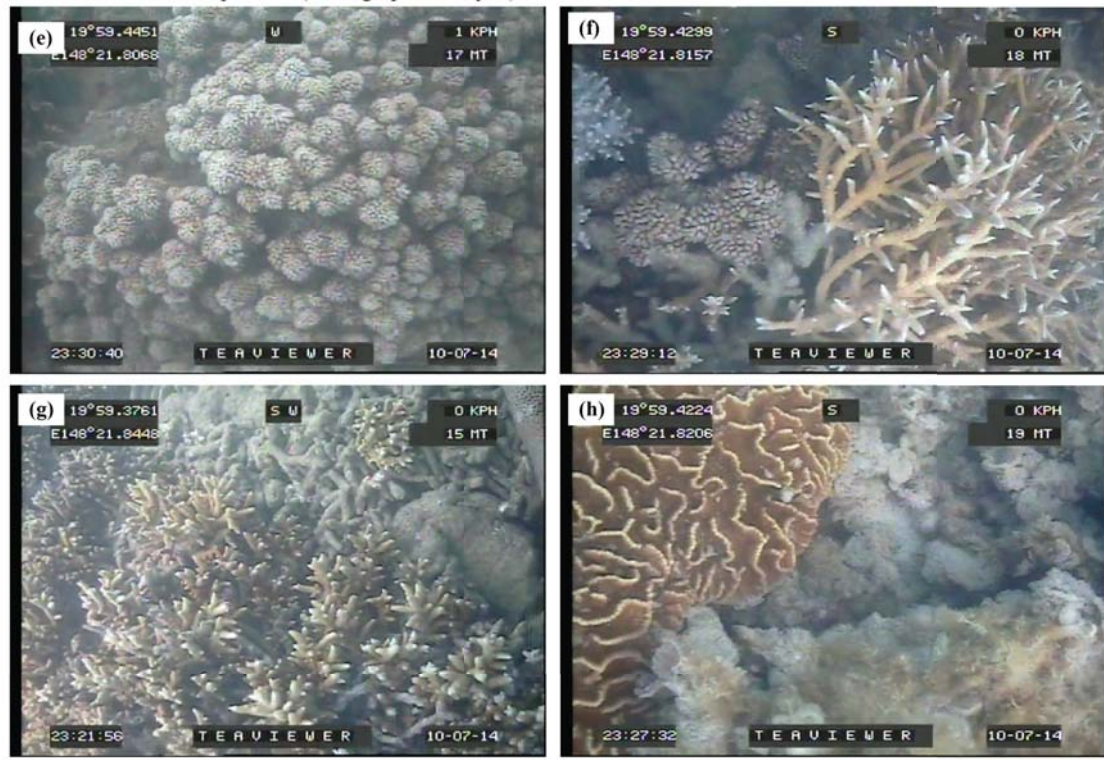


Appendix 4. Photographs from Stone Island North in 2014 (a) living *Montipora* at the outer reef flat exposed during low tide; (b) sand and macroalgae, typical of the outer reef flat; (c – h) images extracted from video footage of the reef slope showing live coral cover, of *Acropora*, foliaceous, encrusting and plate corals, and coral rubble colonised by live coral recruits (h). Elevations of (a) and (b) are given in Appendix 10.

Middle Island Reef Flat 2013 (Photographer: E.Ryan)



Middle Island Reef Slope 2014 (Photographer: E.Ryan)



Appendix 5. Photographs from Middle Island reef. (a – d) 2013 showing high reef flat live coral cover at low tide, including branching *Acropora*, *Montipora*, massive *Porites* microatolls and faviids; (e – h) 2014 images extracted from video footage of the reef slope, showing live coral cover, including *Galaxea* (e), branching *Acropora* (f, g) and foliaceous coral/macroalgae (h). Elevations of (a – d) are given in Appendix 10.

Appendix 6. Date (calendar years AD), name, details and location of recorded cyclones that have passed over or in close proximity to Bowen, Queensland since 1867.

Date of cyclone	Cyclone name	Details of cyclone	Location of coastal crossing	Reference
1867, 6 March		Gale winds at Bowen		Windworker*; Casey (1992)^
1870, Jan		Floods in Bowen		Windworker*
1873, 1 Feb		Heaviest flood since Bowen was settled		Casey (1992)
1874, 24 Jan		Heavy and sudden flood in the Don River		Casey (1992)
1875, 24 April		Euri Creek and Don River flooded		Casey (1992)
1884, 9 Feb		Cyclone report		Casey (1992)
1888		Cyclone East of Mackay		Windworker*
1911		Yongala wrecked, high Don River flood		Windworker*, Casey (1992)
1915		Bowen damaged		Windworker*
1917		Heavy rain and gales, Bowen		Windworker*
1918, Jan		3.6 m storm surge in Mackay	Just North of Mackay	BOM^; Windworker*
1918, March		Huge storm and flooding	Innisfail	BOM^; Hopley and Isdale (1977); Stanley (1928); Hedley (1925); Rainford (1925)
1938		Floods	Bowen	Windworker*
1951		Major Burdekin River flood	Southeast Gulf region	Windworker*
1954		Heavy flooding	South of Townsville	Windworker*
1958		2 m storm surge	Bowen	Windworker*
1959	Connie	Severe wind damage at Bowen		Windworker*
1970, 17 Jan	Ada	Passed through Whitsunday group. Severe flooding Mackay to Bowen	Airlie Beach	BOM^
1971 10-16 Feb	Gertie	Passed offshore from Bowen, moved close to Holbourne Island		BOM^; Puotinen et al. (1997)
1974	Una		Just South of Townsville	Puotinen et al. (1997)
1974	Vera	Passed offshore from Bowen		Puotinen et al. (1997)
1976	Dawn	Headed down coast over Bowen		Puotinen et al. (1997)
1977, 6-10 March	Otto	Aggravated already serious floods between Cairns and Ingham	Near Bowen	BOM^
1979 13 Feb-6 March	Kerry	Passed by Bowen		BOM^
1980, 7-8 Jan	Paul	One of the highest Don River floods. Came from North over land		BOM^
1988, 21 Feb-1 March	Charlie		Upstart Bay	BOM^
1989, 1-5 April	Aivu	Severe local flooding	Between Townsville and Bowen	BOM^
1990, March	Ivor		Near to Bowen	Done (1992); BOM^; Puotinen et al. (1997)
1996, 26-29 Jan	Celeste	Moved close to Holbourne Island	Came close to Bowen	BOM^; Puotinen et al. (1997)
2006, 17-21 March	Larry		Near Innisfail	BOM^
2009, 4-11 March	Hamish	Passed offshore islands		BOM^
2010, 8-21 March	Ului		Airlie Beach	BOM
2011, 22-31 Jan	Anthony		Bowen	BOM

* from <http://www.windworker.com.au/qldcyclones.htm>

^ from <http://www.bom.gov.au/cyclone/history/index.shtml>

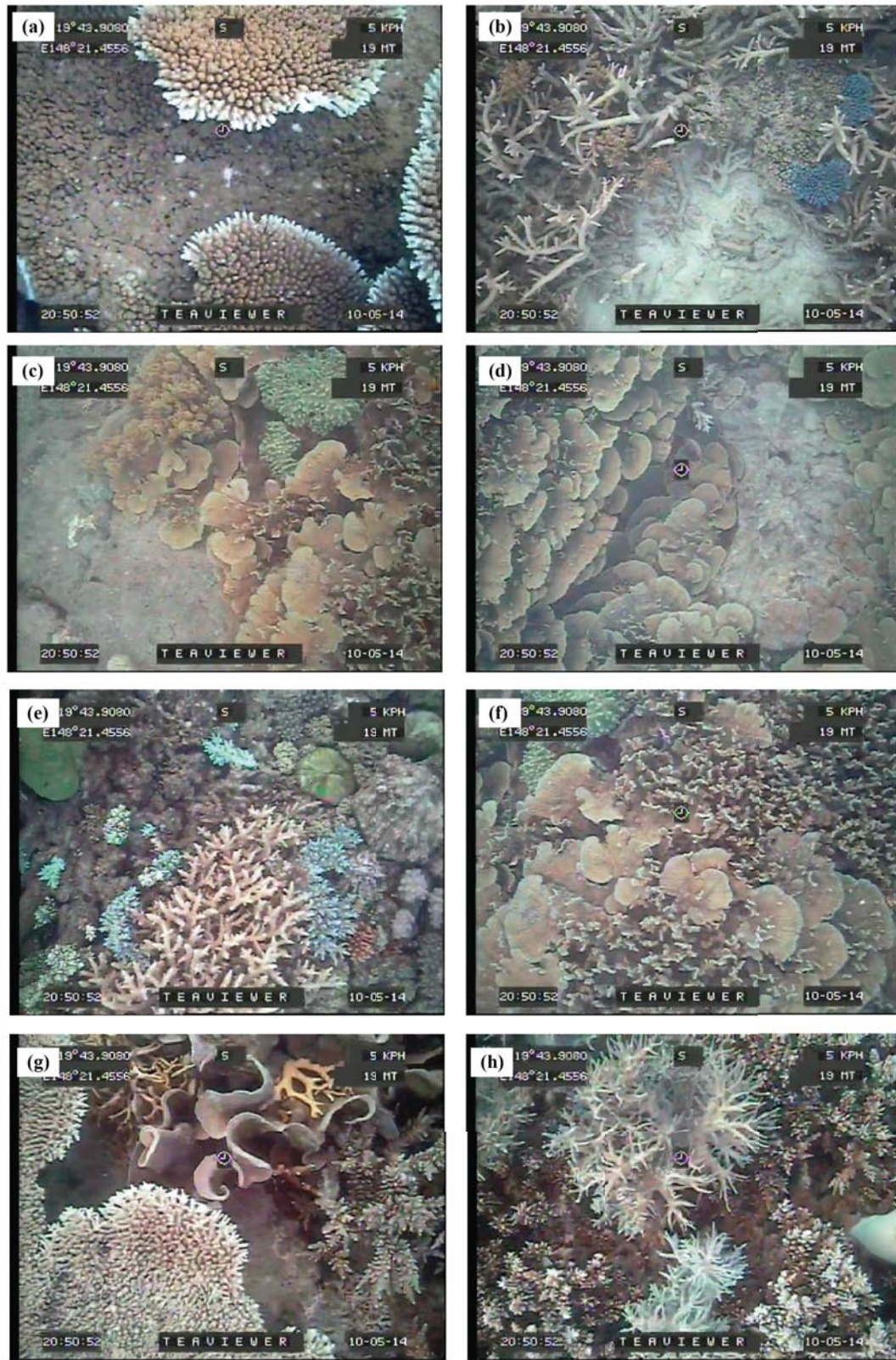
Reference list for Appendix 6

- Casey, P.N. 1992 Records of cyclones and floods from the Bowen newspapers. Bowen Historical Society, Bowen.
- Done, T.J. 1992 Effects of tropical cyclone waves on ecological and geomorphological structures on the Great Barrier Reef, *Continental Shelf Research*, 12: 859-872.
- Hedley, C. 1925 The natural destruction of a coral reef, Transactions of the Royal Geographical Society of Australasia (Queensland), *Reports of the Great Barrier Reef Committee*, 1: 35-40.
- Hopley, D. and Isdale, P.J. 1977 Coral micro atolls, tropical cyclones and reef flat morphology: a north Queensland example, *Search*, 8: 79-81.
- Puotinen, M.L., Done, T.J. and Skelly, W.C. 1997 An atlas of tropical cyclones in the Great Barrier Reef region, 1969-1997, CRC Reef Research Centre Technical Report No. 19, Townsville, 201 pp.
- Rainford, E.H. 1925 Destruction of the Whitsunday group fringing reefs, *Australian Museum Magazine*, 2: 175-177.
- Stanley, G.A.V. 1928 The physiography of the Bowen district and of the northern isles of the Cumberland Group, *Reports of the Great Barrier Reef Commission*, 2: 1-51.

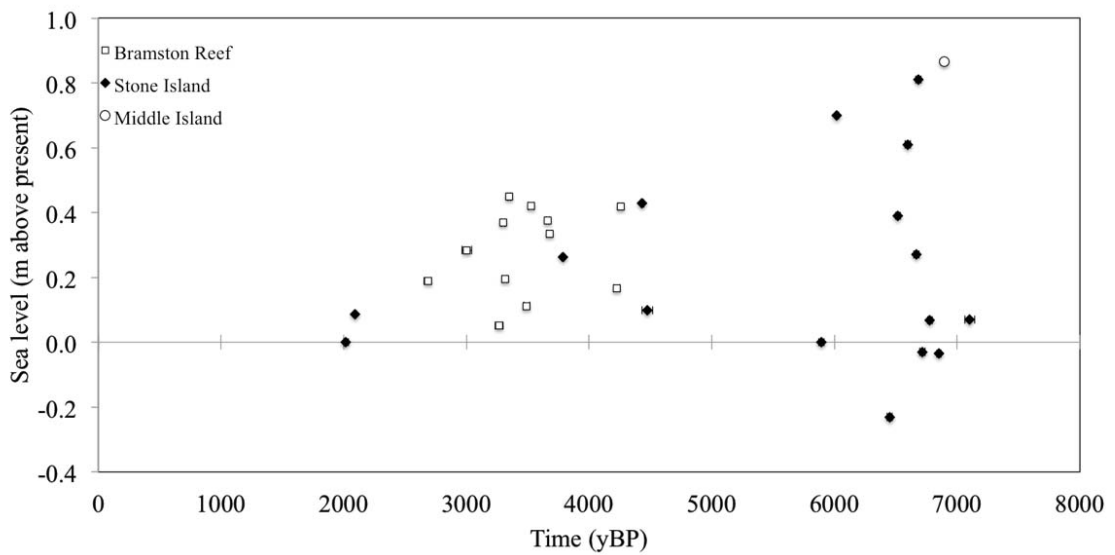
Appendix 7. Radiocarbon (^{14}C) accelerator mass spectrometry ages of *Porites* fossil microatoll samples from Holbourne Island.

Sample name	Lab ID	$\delta^{13}\text{C}$ (‰)		pMC		^{14}C Age (BP)		Calibrated Age (cal yBP)		
		mean	1 σ	mean	1 σ	mean	1 σ	2 σ range	median	
HI-FMA6	OZR271	-2.0	0.1	91.52	0.28	710	25	452	269	356
HI-FMA7	OZR272	-0.9	0.1	95.27	0.32	390	30	128	-9	41
HI-FMA8	OZR273	-1.4	0.1	91.99	0.28	670	25	446	154	319
HI-FMA9	OZR274	-2.4	0.1	94.96	0.33	415	30	188	-9	49
HI-FMA10	OZR275	-0.1	0.1	94.85	0.33	425	30	223	-9	53
HI-FMA11	OZR276	-1.9	0.2	111.82	0.41	Modern		-19	-44	-24
HI-FMA12	OZR277	-1.6	0.1	112.86	0.33	Modern		-21	-40	-34
HI-FMA13	OZR278	-1.4	0.1	93.84	0.28	510	25	245	0	131
HI-FMA14	OZR279	-1.3	0.2	102.95	0.29	Modern		-13	-15	-14
HI-FMA15	OZR280	-1.5	0.1	114.20	0.31	Modern		-23	-37	-29
HI-FMA16	OZR281	-1.1	0.1	111.91	0.36	Modern		-19	-42	-24
HI-FMA17	OZR282	-1.3	0.3	94.08	0.27	490	25	235	-3	105

Holbourne Island Reef Slope 2014 (Photographer: E.Ryan)



Appendix 8. Collection of photographs from Holbourne Island reef slope taken in 2014 by E.Ryan using an underwater drop camera showing various live coral morphologies including plate (a, g), branching (b, e, h), foliaceous, (c – d, f), free-living (e).



Appendix 9. Fossil microatoll sea-level data from Bramston Reef, Stone Island and Middle Island, central Great Barrier Reef, showing age of the fossil microatoll (calibrated years before present [yBP], where present is 1950 AD) with 2σ (varying from 9 to 45 years) and the elevation relative to modern counterparts (elevation precision is $\sim 0.01 - 0.005$ m).

Appendix 10. Table showing the elevations of reef flat photographs presented in this thesis relative to lowest astronomical tide (LAT). Reef flat surface elevation is given, unless where possible, the top of living coral elevation is also given and denoted by [^]. Note reef slope photographs are not included because elevations are approximate.

Photograph	Page number	Site and location	Elevation relative to LAT (m)
Plate 1	1	Middle Island outer reef flat	~0.5
Plate 3	43	SI-S outer reef flat	0.0, 0.3 [^]
Plate 4	74	Holbourne Island backreef moat	0.9 [^]
Figure 2.2	25	Bramston Reef outer reef flat	-0.4, 0.3 [^]
Figure 2.6h	36	Bramston Reef outer reef flat	~0.2
Figure 3.1c	47	SI-S outer reef flat	0.1
Figure 3.1d	47	SI-S outer reef flat	0.1 – 0.2
Figure 3.5	58	SI-S Zone 1 (backreef flat)	1.0
Figure 3.5	58	SI-S Zone 3 (mid-reef flat)	1.0
Figure 3.5	58	SI-S Zone 5 (outer reef flat)	~0.0
Figure 3.5	58	SI-N Zone 2 (backreef flat)	1.0
Figure 3.5	58	SI-N Zone 5 (mid-reef flat)	~0.7
Figure 3.5	58	SI-N Zone 5 (outer reef flat)	~0.1
Figure 3.5	58	Middle Island Zone 1 (backreef flat)	0.9
Figure 3.5	58	Middle Island Zone 2 (mid-reef flat)	0.8
Figure 3.5	58	Middle Island Zone 3 (outer reef flat)	0.7
Figure 3.5	58	SI-S Zone 4 (outer reef flat)	~0.1
Figure 3.5	58	SI-N Zone 5 (outer reef flat)	~0.1
Figure 3.5	58	Middle Island Zone 3 (outer reef flat)	~0.5
Figure 4.2	79	Middle Island backreef (basset edge)	~1.2 – 1.4
Figure 5.2a	104	Holbourne Island backreef flat	1.2
Figure 5.2b	104	Holbourne Island backreef flat	~0.9
Figure 5.2c	104	Holbourne Island backreef flat	~1.1
Figure 5.2d	104	Holbourne Island basset edge	~1.2
Figure 5.2e	104	Holbourne Island mid-reef flat	~0.5
Figure 5.2f	104	Holbourne Island outer reef flat	0.2 [^]
Appendix 1g	160	Bramston Reef outer reef flat	0.3 [^]
Appendix 1h	160	Bramston Reef outer reef flat	~0.2 – 0.3
Appendix 1o	161	Bramston Reef outer reef flat	0.4 [^]
Appendix 1p	161	Bramston Reef outer reef flat	0.3 [^]
Appendix 1v	162	Bramston Reef outer reef flat	0.4 [^]
Appendix 1w	162	Bramston Reef outer reef flat	~0.2
Appendix 4a	170	SI-N outer reef flat	0.1 [^] – 0.2 [^]
Appendix 4b	170	SI-N outer reef flat	~0.1
Appendix 5a	171	Middle Island outer reef flat	0.5 [^]
Appendix 5b	171	Middle Island outer reef flat	~0.5
Appendix 5c	171	Middle Island outer reef flat	~0.5
Appendix 5d	171	Middle Island outer reef flat	~0.3 [^]